UNIVERSITY OF LONDON THESIS

Degree PhD Year 2008 Name of Author CARROLL, CHRISTOPHER, JOHN.

Regulation of cardiac ischaemia/reperfusion injury or hypertrophy by interferon-gamma and cardiotrophin-1 signalling pathways

Christopher J Carroll

Medical Molecular Biology Unit

Institute of Child Health

University College London

A thesis submitted for the Degree of Doctor of Philosophy in the University of London

2008

ProQuest LLC
789 East Eisenhower Parkway
P.O. Box 1346
Ann Arbor, MI 48106-1346

Abstract

Cardiac ischaemia/reperfusion (I/R)-injury and hypertrophy are two causes of heart failure. The molecular pathways that regulate these processes include those that are stimulated by the cytokines, interferon-gamma (IFNγ) and cardiotrophin-1 (CT-1). This thesis describes the investigation of components of the IFNγ or CT-1 signalling pathways and their regulation of I/R-injury or hypertrophy.

The transcription factor, signal transducer and activator of transcription 1 (STAT1), is the primary mediator of the IFNγ signalling pathway and promotes apoptosis of cardiac cells following I/R-injury or stimulation with IFNγ. It is unclear what contribution the caspase-8 and caspase-9 apoptotic pathways have in STAT1 mediated I/R-injury and IFNγ induced apoptosis. Therefore, to investigate this relationship, constructs conditionally overexpressing specific caspase inhibitors were used to generate transgenic mice with inactivated caspase -8 or -9 pathways.

STAT1 and the transcription factor p53 proteins are known to associate and this interaction has been demonstrated to be necessary for the maximal activation of distinct p53 target genes. STAT1 and p53 double knockout mice were generated to further investigate the role of these proteins in I/R-injury. A proteomic approach was used to identify proteins regulated by STAT1 and/or p53 in the heart where the expression of the cytokine, interleukin-6, was regulated by STAT1 and p53.

The CT-1 cytokine has cardioprotective and hypertrophic effects. CT-1 expression is induced by another cardioprotective cytokine, urocortin. The mechanism by which urocortin protects the heart from I/R-injury is not fully understood, however, prevention of mitochondrial damage has been shown to be involved. In this study the protective effect of urocortin was shown to involve the mitochondrial permeability transition pore. Furthermore, the hypertrophic effect of CT-1 in cultured cardiac cells has been shown to be dependent on induction of heat shock protein 56 (hsp56). Transgenic mice overexpressing hsp56 were generated to test the cardioprotective and hypertrophic effects of hsp56 *in vivo*. Taken together, the data presented here demonstrate clearly that a number of key molecules regulate cardiac (patho)physiology *in vivo*. Targeting these signalling pathways may provide novel routes for therapeutic intervention in heart disease.

Publications

SOOND, S. M., **CARROLL, C.**, TOWNSEND, P. A., SAYAN, E., MELINO, G., BEHRMANN, I., KNIGHT, R. A., LATCHMAN, D. S. & STEPHANOU, A. (2007) STAT1 regulates p73-mediated Bax gene expression. *FEBS Lett,* 581, 1217-26.

TOWNSEND, P. A., DAVIDSON, S. M., CLARKE, S. J., KHALIULIN, I., **CARROLL, C. J.**, SCARABELLI, T. M., KNIGHT, R. A., STEPHANOU, A., LATCHMAN, D. S. & HALESTRAP, A. P. (2007) Urocortin prevents mitochondrial permeability transition in response to reperfusion injury indirectly, by reducing oxidative stress. *Am J Physiol Heart Circ Physiol.*

DAVIDSON, S. M., TOWNSEND, P. A., **CARROLL, C.**, YUREK-GEORGE, A., BALASUBRAMANYAM, K., KUNDU, T. K., STEPHANOU, A., PACKHAM, G., GANESAN, A. & LATCHMAN, D. S. (2005) The transcriptional coactivator p300 plays a critical role in the hypertrophic and protective pathways induced by phenylephrine in cardiac cells but is specific to the hypertrophic effect of urocortin. *Chembiochem,* 6, 162-70.

LAWRENCE, K. M., KABIR, A. M., BELLAHCENE, M., DAVIDSON, S., CAO, X. B., MCCORMICK, J., MESQUITA, R. A., **CARROLL, C. J.**, CHANALARIS, A., TOWNSEND, P. A., HUBANK, M., STEPHANOU, A., KNIGHT, R. A., MARBER, M. S. & LATCHMAN, D. S. (2005) Cardioprotection mediated by urocortin is dependent on PKCepsilon activation. *Faseb J,* 19, 831-3.

JAMSHIDI, Y., ZOURLIDOU, A., **CARROLL, C. J.**, SINCLAIR, J. & LATCHMAN, D. S. (2004) Signal-transduction pathways involved in the hypertrophic effect of hsp56 in neonatal cardiomyocytes. *J Mol Cell Cardiol,* 36, 381-92.

LAWRENCE, K. M., TOWNSEND, P. A., DAVIDSON, S. M., **CARROLL, C. J.**, EATON, S., HUBANK, M., KNIGHT, R. A., STEPHANOU, A. & LATCHMAN, D. S. (2004) The cardioprotective effect of urocortin during ischaemia/reperfusion involves the prevention of mitochondrial damage. *Biochem Biophys Res Commun,* 321, 479-86.

LAWRENCE, K. M., SCARABELLI, T. M., TURTLE, L., CHANALARIS, A., TOWNSEND, P. A., **CARROLL, C. J.**, HUBANK, M., STEPHANOU, A., KNIGHT, R. A. & LATCHMAN, D. S. (2003) Urocortin protects cardiac myocytes from ischemia/reperfusion injury by attenuating calcium-insensitive phospholipase A2 gene expression. *Faseb J,* 17, 2313-5.

Acknowledgements

I would like to thank my supervisors Professor David Latchman and Dr Paul Townsend for their guidance throughout my PhD. I am especially grateful to Professor Latchman for allowing me to undertake a PhD in his group and for his and Dr Townsend's comments and corrections of this thesis. I would also like to thank Maruschka Malacos and Dr Paul Riley for advice and suggestions during my PhD.

Professor Chris Proud and Professor Andrew Halestrap and their groups are thanked for their teaching of cardiac myocyte preparations and Langendorff perfusion respectively. Dr Naushaad Suleman is especially thanked for his teaching and assistance with Langendorff perfusion.

I am extremely grateful to Drs David Faulkes, Sean Davidson and James Diss for their help and supervision with numerous molecular biological methods, discussions and their support throughout my PhD. Furthermore, I cannot overstate how appreciative I am of how approachable they always were and for their time that they have sacrificed. I would also like to thank Dr James McCormick for his thorough teaching of proteomic techniques.

I would also like to the thank the following members of David Latchman's group who have at some point provided help and discussion, and for their friendship and support; Liz, Ros, Shazia, Mattia, Kevin and Sean. John Estridge is thanked for lending an ear, daily, and for making a calm and pleasant working environment.

Finally, I would like to thank Anastasia Lambrianides, whose constant encouragement and support has enabled me to realise the completion of this thesis.

Declaration

The author carried out the work in this thesis unless otherwise stated.

Table of Contents

List of Figures

List of Tables

Abbreviations

A-II	Angiotensin II
Ach	Acetylcholine
αhCRH	Alpha-helical corticotrophin releasing hormone
AIF	Apoptosis inducing factor
Akt	Protein kinase B
αMHC	Alpha-myosin heavy chain
AMCM	Adult mouse ventricular myocytes
AMID	AIF-homologous Mitochondrion-associated Protein
ANF	Atrial natriuretic factor
ANT	Adenine nucleotide translocase
Apaf-1	Apoptosis protease activating factor-1
AR	Androgen receptor
ARVC	Adult rat ventricular myocytes
ATP	Adenosine 5'-triphosphate
Bcl-2	B-cell lymphoma-2
BEL	Bromoenol lactone
β-MHC	Beta-myosin heavy chain
BNP	Brain natriuretic factor
BSA	Bovine serum albumin
C9s	Caspase-9 short
cAMP	Cyclic AMP
CAD	Caspase-activated deoxyribonuclease
CARD	Caspase recruitment domain
CBP	CREB-binding protein
cDNA	Complementary DNA
CHF	Congestive heart failure
CHO	Chinese hamster ovary
CLC	Cardiotrophin like protein
CMV	Cytomegalovirus
CNTF	Ciliary neurotrophic factor
CREB	cAMP response binding protein
CRH	Corticotrophin releasing hormone
CRM	Chromosomal regional maintenance

CyP40	Cyclophilin 40
CyP-D	Cyclophilin D
CT-1	Cardiotrophin-1
$\Delta m\Psi$	Mitochondrial membrane potential
DD	Death domain
DED	Death effector domain
DOG	2-deoxyglucose
DMSO	Dimethyl sulfoxide
DNA	Deoxyribonucleic acid
dNTPs	Deoxynucleotide triphosphates
DOC	Deoxycholate
DP	Diastolic pressure
dP	Developed pressure
DTT	Dithiothreitol
EDP	End diastolic pressure
EGCG	Epigallocatechin-3-gallate
ELISA	Enzyme-linked immunosorbent assay
EPAS-1	Endothelial PAS domain protein-1
ER	Oestrogen receptor
ERK	Extracellular regulated kinase
FADD	Fas-associated death domain
FAK	Focal adhesion kinase
FKBP	FK506 binding protein
FLIP	Cellular flice-like inhibitory protein
GAS	Gamma activated sequence
gp130	Glycoprotein 130
GPRC	G-protein coupled receptor
GTN	Glyceryl trinitrate
HDAC	Histone deacetylase
Hq	Harlequin
HSV	Herpes simplex virus
IEF	Isoelectric focusing
IFNγ	Interferon gamma
IL-6	Interleukin-6
IL-6R	Interleukin-6 receptor
ICV	Intracerebroventicular

IPC	Ischaemic preconditioning
$iPLA_2$	Calcium insensitive phospholipase 2
ISGF3	IFN-stimulated response element
I/R	Ischaemia/reperfusion
IV	Intravenous
JAK	Janus kinase
K_{ATP}	ATP-sensitive potassium channel
Kir	Potassium inward rectifying
KIR	Kinase inhibitory region
LDH	Lactate dehydrogenase
LIF	Leukaemia inhibitory factor
LMP2	Low molecular mass polypeptide 2
LPC	Lysophosphatidylcholine
LPS	Lipopolysaccharide
LVDP	Left ventricular developed pressure
LVH	Left ventricular hypertrophy
MAPK	Mitogen activated protein kinase
MALDI-TOF	Matrix assisted laser desorption ionization- time of flight
Mdm2	Murine double minute 2
MEF	Mouse embryonic fibroblasts
MEK	MAPK kinase
MHC	Major histocompatibility complex
MKP-1	MAPK phosphatase 1
MPTP	Mitochondrial permeability transition pore
mRNA	Messenger ribonucleic acid
LDH	Lactate dehydrogenase
LPC	Lysophosphatidylcholine
LPS	Lipopolysaccharide
NES	Nuclear export signal
NF	Nuclear factor
NFAT	Nuclear factor of activated T cells
NMCM	Neonatal mouse cardiac myocytes
NLS	Nuclear localisation signal
NPC	Nuclear pore complex
NRCM	Neonatal rat cardiac myocytes
OSM	Oncostatin M

PAGE	Polyacrylamide gel electrophoresis
PAK2	p21-activated kinase 2
PARP	Poly ADP-ribose polymerase
PCR	Polymerase chain reaction
PE	Phenylephrine
PFT	Pifithrin-alpha
PI3K	Phosphatidylinositol-3-OH kinase
PKC	Protein kinase C
PPIase	Peptidyl-prolyl *cis-trans* isomerase
PR	Progesterone receptor
PRG3	p53-responsive gene 3
RISK	Reperfusion injury salvage kinase
RNA	Ribonucleic acid
ROS	Reactive oxygen species
RTK	Receptor tyrosine kinase
SCP	Stresscopin
SfA	Sanglifehrin A
SH2	Src-homology-2
SOD	Superoxide dismutase
SRP	Stresscopin related peptide
STAT	Signal transducer and activator of transcription
TAD	Transactivation domain
tetO	Tetracycline operon
tetR	Tetracycline repressor
TMRM	Tetramethyl rhodamine methyl ester
TNF	Tumour necrosis factor
TPR	Tetracopeptide repeat
Trp53	Transformation related protein 53
tTA	Tetracycline transactivator
TTC	Triphenyltetrazolium chloride
Ucn	Urocortin

CHAPTER ONE

Introduction

CHAPTER ONE

Introduction

Diseases of the heart and circulatory system are the main cause of death in the UK and account for over 208,000 deaths each year (www.heartstats.org), and heart failure represents the fastest growing subclass of cardiovascular disease over the past decade (Heineke and Molkentin, 2006). Cardiac ischaemia/reperfusion injury and hypertrophy are two causes of heart failure and are regulated by complex intracellular signalling pathways. Therefore, elucidation of these pathways involved is required to enable the generation of effective therapies for the causes of heart failure.

In this introduction, the structure and function of the normal working heart, ischaemia/reperfusion injury and hypertrophy, and the principal experimental systems used in laboratory based cardiovascular research will be described first. Then, the basic principles of signal transduction and apoptotic cell death, a feature of cardiac disease, will be described. Evidence for the role of apoptosis in ischaemia/reperfusion injury and the signalling pathways involved in ischaemia/reperfusion-induced apoptosis, and hypertrophy, will then be discussed. This is followed by further discussion on the role of the interferon-gamma and cardiotrophin-1 signalling pathways in the regulation ischaemia/reperfusion injury or hypertrophy.

1.1 The cardiovascular system

Animal cells require a supply of oxygen and nutrients, which they metabolise to produce usable energy in the form of adenosine 5'-triphosphate (ATP). In animals with specialised tissues, the supply of oxygen and nutrients is carried in the blood. The blood is transported through vessels known as vasculature, and the beating heart maintains the circulation of the blood throughout these vessels.

The mammalian heart is a four-chambered organ consisting of the left and right ventricles and atria. During the contraction phase of the heartbeat, termed systole, blood is ejected from the ventricles of the heart into the arteries as blood from the

veins fill the atria. When the heart relaxes, the diastole phase, blood from the atria fills the ventricles. The blood is circulated from the heart to tissues via the arterial system and returns via the venous system. Oxygenated blood from the lungs is received by the left atrium via the pulmonary vein and is ejected from the left ventricle into the aorta, the major artery that feeds systemic circulation. The aorta divides into the arteries that direct flow to all parts of the body. In order to reach all the cells packed within tissues the arteries branch into smaller vessels that comprise the microcirculation. Arteries branch into arterioles and these in turn branch into even smaller vessels, the capillaries. The capillaries are the smallest of the blood vessels and it is from the capillaries that oxygen and nutrients are exchanged for carbon dioxide and waste products of metabolism with nearby cells. In the heart there is at least one capillary adjacent to each cell (Davidson and Duchen, 2007). Deoxygenated blood from the capillaries enters the venous system of blood vessels. Blood travels from capillaries to venules to veins and then to the superior or inferior vena cava, the major veins that return blood to the heart from the systemic circulation. Deoxygenated blood from the systemic circulation enters the right atrium and fills the right ventricle during relaxation. The right ventricle supplies the deoxygenated blood to the lungs via the pulmonary circulation where the blood is oxygenated in the capillaries of the lungs. The principles for pulmonary circulation are similar to those for systemic circulation. Oxygenated blood is returned to the left atrium via the pulmonary vein thereby to complete the circulation.

1.1.1 Heart cells

Cardiomyocytes are specialised cells of the heart muscle tissue, or myocardium, which contract to form the heartbeat and move blood though the body. Cardiomyocytes constitute approximately 75% of the total volume of the myocardium (Brilla et al., 1991). The remainder consists of pacemaker and conducting cells, blood vessels and extracellular space. The contractile proteins of cardiomyocytes are organised into contractile units, known as sarcomeres, which are grouped in bundles to form myofibrils. Cardiomyocytes are joined together by connective tissue made of collagen to form myofibres.

Ventricular myocytes are responsible for ejecting blood from the heart and propelling it around the body and their anatomy is different to myocytes in the atrium, pacemaker and conducting tissue. Ventricular cardiomyocytes are cylindrical in

shape, measuring approximately 10 to 25 μm in diameter and 50 to 100 μm in length (reviewed by Opie, 2004). Each cell is bound by a plasma membrane known as the sarcolemma that invaginates to form a tubular network called T-tubules that are linked to the sarcoplasmic reticulum, which allows the flow of calcium that is involved in contraction and relaxation. Myocytes are packed with longitudinally arranged myofibrils, which are the structures responsible for the cross-striated appearance of myocytes when viewed under the light microscope. Some myocytes are multinucleated and highly abundant in mitochondria, the organelles where oxygen dependent energy metabolism takes place, which are interspersed between the myofibrils and beneath the sarcolemma (reviewed by Opie, 2004).

1.1.2 The sarcomere

The sarcomere is the fundamental unit of contraction in myocytes (Figure 1.1) The sarcomere contains overlapping thin and thick filaments comprised of actin and myosin respectively. During contraction, the thin and thick filaments of the sarcomere slide along each other, thus pulling together the two poles of the sarcomere. The structures of the sarcomere are referred to as bands or lines, which were assigned because of the patterns of the sarcomere when observed in electron microscopic images. The ends of the sarcomere are the Z lines (also called Z bands or Z discs) to which the actin filaments are joined by elastic filaments made of the protein titin. The actin thin filaments stretch part way towards the centre of the sarcomere. The middle of the sarcomere is the M line from which the myosin thick filaments are bound and extend part way towards the Z lines and overlap with the actin thin filaments. The dark region where actin and myosin filaments overlap is the anisostropic, or A band, and the lighter regions either side where there are only actin thin filaments are the isotropic, or I bands. In the centre of the A band is the H zone where there are only myosin thick filaments appearing as light regions, which are attached to proteins in the dark M line in the centre. Cross-bridge cycling is the process by which actin and myosin interact to contract and relax the sarcomere, a process that is regulated by proteins of the troponin family. Contraction is initiated by an increase in cellular calcium released from the sarcoplasmic reticulum, which happens in response to a wave of electricity that reaches the ventricular myocytes from the conducting cells. Relaxation occurs as the interaction of actin and myosin is displaced, an action that is dependent on ATP.

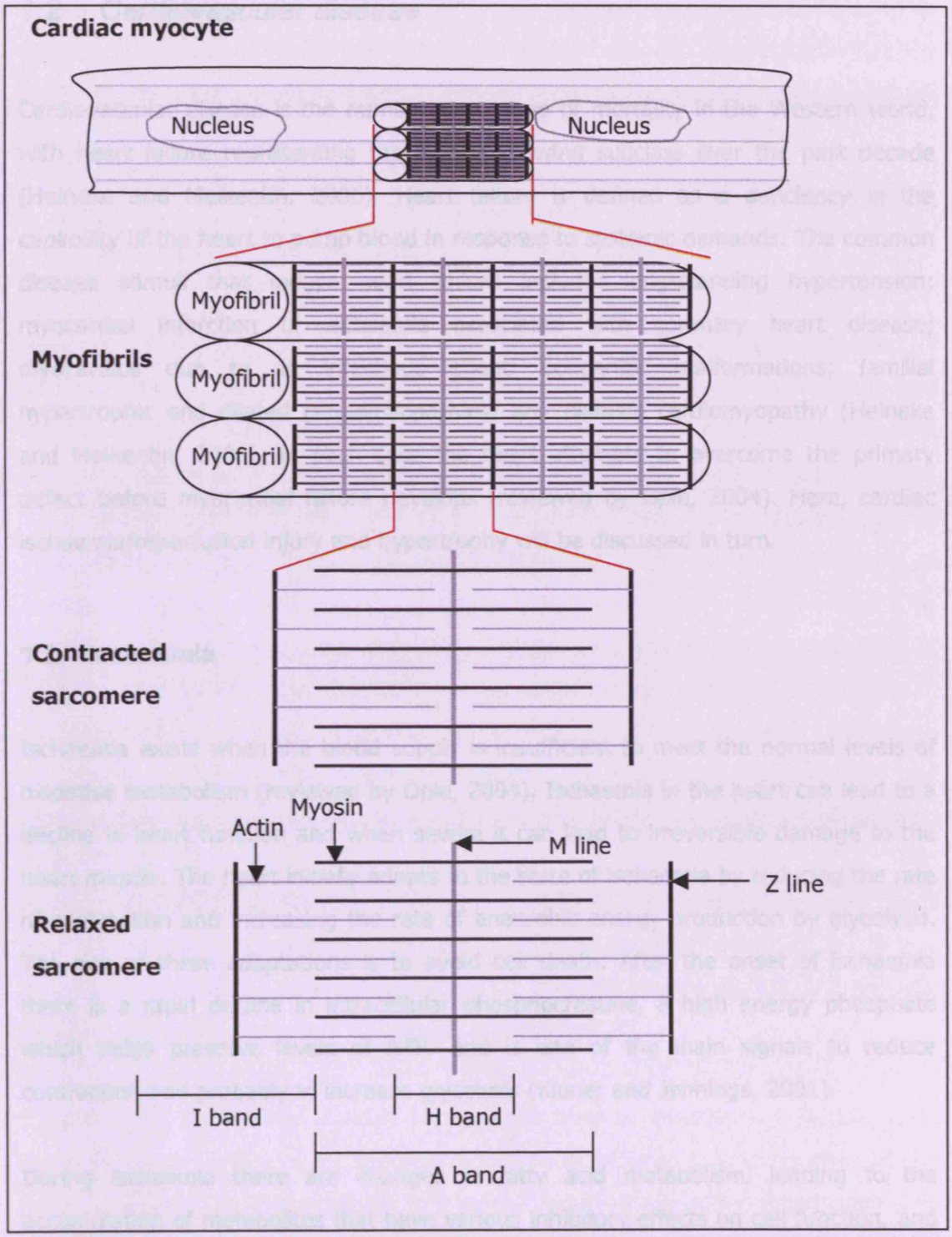

Figure 1.1 Contractile units of the cardiac myocyte. Myofibrils run longitudinally throughout the length of the cardiac myocyte. Sarcomeres are the basic contractile unit consisting of the contractile proteins actin (thin filament) and myosin (thick filament). Contraction and relaxation occurs through interaction of the thin and thick filaments. I (inostropic) band, A (anisotropic) band, H band and Z (Zuckung) line are the names given to the sarcomeric structures when viewed under electron microscopy.

1.2 Cardiovascular disease

Cardiovascular disease is the number one cause of mortality in the Western world, with heart failure representing the fastest growing subclass over the past decade (Heineke and Molkentin, 2006). Heart failure is defined as a deficiency in the capability of the heart to pump blood in response to systemic demands. The common disease stimuli that induce heart failure include: long-standing hypertension; myocardial infarction or ischaemia associated with coronary heart disease; myocarditis due to an infectious agent; congenital malformations; familial hypertrophic and dilated cardiomyopathies; and diabetic cardiomyopathy (Heineke and Molkentin, 2006). In each case the heart attempts to overcome the primary defect before myocardial failure develops (reviewed by Opie, 2004). Here, cardiac ischaemia/reperfusion injury and hypertrophy will be discussed in turn.

1.2.1 Ischaemia

Ischaemia exists when the blood supply is insufficient to meet the normal levels of oxidative metabolism (reviewed by Opie, 2004). Ischaemia in the heart can lead to a decline in heart function and when severe it can lead to irreversible damage to the heart muscle. The heart initially adapts to the state of ischaemia by reducing the rate of contraction and increasing the rate of anaerobic energy production by glycolysis. The aim of these adaptations is to avoid cell death. After the onset of ischaemia there is a rapid decline in intracellular phosphocreatine, a high energy phosphate which helps preserve levels of ATP, and is one of the main signals to reduce contraction and probably to increase glycolysis (Kloner and Jennings, 2001).

During ischaemia there are changes in fatty acid metabolism, leading to the accumulation of metabolites that have various inhibitory effects on cell function, and an increase in phospholipase mediated breakdown of phospholipids into products that may adversely affect membranes (reviewed by Opie, 2004). The levels of calcium increase and as ATP decreases the energy-requiring sodium pumps fail with consequent increases in sodium and loss of potassium. There is an accumulation of CO_2 and protons in ischaemic tissue that decreases the pH from the normal value of approximately 7.0 to 6.5 (Cross et al., 1995).

Myocardial ischaemia may manifest itself in contractile failure, chest pain known as angina, shortness of breath and electrocardiographic changes. Myocardial infarction (MI) is the event went ischaemic tissue becomes irreversibly damaged with consequent cell death of ventricular myocytes.

1.2.2 Ischaemia/reperfusion injury

Reperfusion is necessary for salvaging the ischaemic myocardium, however, a paradox exists in that reperfusion can result in enhanced levels of tissue injury and increased infarct size (Eefting et al., 2004). The events that occur when the ischaemic myocardium is reperfused include a fall in diastolic pressure (DP), reduced developed pressure (dP), states of myocardial dysfunction known as stunning and hibernation, arrhythmias and cell death. These events are collectively known as ischaemia/reperfusion (I/R)-injury or simply, reperfusion injury (Opie, 1989). I/R-injury triggers a cascade of key pathogenic cellular events such as a massive influx of calcium, mitochondrial damage and rapid depletion of high-energy stores, leading to both necrotic and apoptotic cell death (Scarabelli et al., 2002). Cell death after injury, and the form that it takes, is largely dependent on levels of intracellular ATP and other high-energy phosphates (Leist and Nicotera, 1997). For example, viable cells have an ADP:ATP ratio of <0.11, apoptotic cells a ratio between 0.11 and 1.0 and necrotic cells a ratio up to 15 (Bradbury et al., 2000). The degree of myocyte death and severity of haemodynamic consequences are major determinants of the clinical outcome of I/R-injury, and therapies for MI must improve both cell survival and promote mechanical recovery (Scarabelli et al., 2002).

Evidence that reperfusion causes damage has been demonstrated in studies that have shown the extent of the damage can be reduced when therapy is given at the point of reperfusion. For example, in a canine model of I/R injury, when adenosine was given at reperfusion there was significant reduction in the infarct sizes compared to hearts that were not given adenosine (Olafsson et al., 1987).

The most common cause of myocardial ischaemia is coronary artery disease, also known as atherosclerosis, and the main risk factors for atherosclerosis are high cholesterol, hypertension and tobacco smoking. Atherosclerosis is an inflammatory disease that renders the endothelium of arterial vasculature susceptible to the uptake of inflammatory cells and lipoprotein molecules thereby creating a lesion that is a

mixture of inflammation and fat (Ross, 1999). Atherogenesis is the process that refers to the development of these lesions, also known as atheromatous plaques. As a lesion develops, there is narrowing of the lumen of the artery thereby reducing the blood flow. Partial obstruction is not usually sufficient to cause MI. However, when a lesion ruptures, and becomes unstable, this precipitates a thrombus (blood clot) at the site of the lesion resulting in complete obstruction of the flow of blood. The region of cardiac tissue supplied by an occluded coronary artery is described as the area at risk.

1.2.3 Oxidative stress in I/R-injury

Free radicals are highly reactive chemical species with unpaired electrons in their outer orbitals. Those derived from oxygen, such as superoxide anion ($\cdot O_2$-) and hydroxyl (·OH-), are called reactive oxygen species (ROS). ROS are mainly derived from mitochondria as by-products of oxidative phosphorylation. ROS are involved in biological processes, for example, nitric oxide (·NO) is a signalling molecule that regulates vascular tone. However, excessive production of ROS causes damage to lipids, proteins and DNA (Esposito et al., 1999, Melov et al., 1999).

ROS are generated when oxygen is reintroduced to ischaemic tissue. ROS mediated reperfusion injury has been reported in a number of tissues including the heart (Becker, 2004). In early reperfusion of the heart a 'burst' of ROS generation has been observed (Bolli et al., 1989a, Wang et al., 1998). In a canine model of I/R injury, reperfusion mediated generation of ROS contributed to reperfusion injury (Bolli et al., 1989b).

The generation of ROS are normally kept in check by endogenous free radical scavengers. Such scavengers include the enzymes superoxide dismutase (SOD) and glutathione reductase, and also non-enzymatic scavengers such as vitamin A. The experimental use of free radical scavengers in models of I/R-injury lends further support to the role of oxidative stress in I/R-injury. The free radical scavenger, epigallocatechin-3-gallate (ECGC), is a constituent of green tea and has been shown to protect cultured neonatal rat cardiac myocyte cells from I/R injury (Townsend et al., 2004b).

1.2.4 Mitochondrial damage in I/R-injury

In cardiac myocytes the primary role of mitochondria is to provide sufficient ATP through oxidative phosphorylation to meet the high-energy demands of the beating heart. When inhibition of oxidative phosphorylation occurs in ischaemia, glycolysis alone is unable provide sufficient ATP, leading to heart dysfunction. Mitochondrial damage may occur under stressful conditions leading to loss of the mitochondrial membrane potential ($\Delta m\Psi$), resulting in cell death.

The mitochondrial permeability transition pore (MPTP) is a non-specific pore in the mitochondrial inner membrane of which the core components are the adenine nucleotide translocase (ANT) and cyclophilin D (CyP-D) (Halestrap et al., 2004). Under normal conditions the pore is closed, however, in stressful conditions such as reperfusion there is opening of the pore. Normally the inner mitochondrial membrane is only permeable to a few selected metabolites and ions, however, all molecules under 1.5 kDa may pass freely through an open MPTP (Crompton, 1999). When the MPTP opens, the permeability barrier of the inner mitochondrial membrane becomes disrupted with two major consequences. Opening of the pore allows passage to small molecular weight solutes but not proteins, and this results in an osmotic pressure that causes the mitochondria to swell. Swelling causes the outer membrane to rupture with release of proteins such as cytochrome c and apoptosis inducing factor (AIF), which are involved in apoptosis. Secondly, the inner membrane becomes freely permeable to protons which causes uncoupling of oxidative phosphorylation from ATP synthesis thereby reducing the available supply of ATP in the cell (Halestrap et al., 2004). If the pore remains open the cell will undergo irreversible damage resulting in necrotic cell damage and even if it closes it may undergo apoptosis since there was release of proapoptotic molecules such as cytochrome c and AIF (Halestrap et al., 2004).

The principal factor responsible for MPTP opening is mitochondrial calcium overload, especially when this is accompanied by oxidative stress, adenine nucleotide depletion, elevated phosphate concentrations, and mitochondrial depolarisation (Halestrap et al., 2004). These are exactly the conditions that exist in reperfusion and there is evidence that MPTP opening is important in the transition from reversible to irreversible reperfusion injury (Crompton, 1999). Inhibitors of MPTP opening have demonstrated that reperfusion injury is mediated by the opening of

this pore. Sanglifehrin A (SfA), an inhibitor of MPTP opening, was able to reduce reperfusion injury in the isolated rat heart (Clarke et al., 2002).

Tetramethyl rhodamine methyl ester (TMRM) and mitotracker are fluorescent dyes used experimentally in isolated cardiac myocytes to measure changes in the mitochondrial potential as an index of MPTP opening and mitochondrial damage. TMRM and mitotracker have a net positive charge and accumulate in the negative environment of healthy mitochondria. However, opening of MPTP and concomitant reduction in membrane potential results in loss of TMRM or mitotracker. In the isolated perfused heart model, the mitochondrial entrapment of a radioactive marker, [^{3}H]2-deoxyglucose (^{3}H-DOG), is used to measure MPTP opening.

1.2.5 Cardiac hypertrophy

Cardiac hypertrophy is the process by which the ventricular myocytes and consequently the heart become larger in response to the increased wall tension caused by volume or pressure stress, mutations of sarcomeric proteins or loss of myocardial cells following I/R-injury. This results in left ventricular hypertrophy (LVH) and is characterised by an increase in thickness and mass of the left ventricular wall, which can normalise the wall tension. This compensatory response of the heart to increased workload is initially a mechanism that is physiologically normal in athletes, however, sustained hypertrophy in response to disease stimuli may increase the risk of cardiomyocyte loss and heart failure.

Sustained increases in haemodynamic function that are caused by either physiological or pathological stimuli eventually lead to changes in the heart/body weight ratio (reviewed by Opie, 2004). Different pathological stimuli cause distinctive forms of myocyte hypertrophy. Volume overload hypertrophy results in chamber dilation and cells have increased length due to addition of sarcomeric units in series. The elongation observed in volume overload hypertrophy is defined as eccentric hypertrophy. Chronic volume overload hypertrophy can result in irreversible loss of cardiac function. This type of hypertrophy is distinct to that caused by pressure overload where addition of sarcomeric units is not observed (Wollert et al., 1996). An increased pressure load causes a thicker myocyte and is defined as concentric hypertrophy. There are also differences observed between physiological and pathological induced hypertrophy. Exercise-induced hypertrophy is not normally

associated with accumulation of collagen in the myocardium and only a small increase in ventricular wall thickness is observed (Iemitsu et al., 2001).

Adult cardiomyocyte hypertrophy is characterised by increased cell size, enhanced protein synthesis and a higher organisation of the sarcomere. A key feature of hypertrophy is the activation of the foetal gene program. In response to haemodynamic load there are increases in immediate-early genes such as *c-fos*, *c-myc* and *c-jun* (reviewed by Opie, 2004), which are genes that are activated rapidly in response to certain stimuli and have been shown to regulate growth. The expression of atrial natriuretic factor (ANF) and brain natriuretic factor (BNP) are also induced. There are changes in relative quantities of isoforms of sarcomeric proteins. For example, there is a relative decrease in the alpha form of myosin heavy chain (αMHC) and a relative increase in the beta form (βMHC).

The generation of ATP in the adult myocardium depends on the mitochondrial oxidation of long-chain fatty acids. Cardiac hypertrophy is associated with a reduction of fatty acid oxidation and metabolic reversion of the heart to increased glucose utilization, which is also a characteristic feature of the foetal heart (Depre et al., 1998).

Although the hypertrophic response of the heart to pathological stimuli has been generally considered to be a compensatory response that becomes pathological, more recent evidence suggests that this initial response is not beneficial and that the entire process is maladaptive. For example, in surgically induced pressure overload in mice, inhibition of hypertrophy had no effect on haemodynamic function (Hill et al., 2000). Therefore, this raises the hopes that therapeutic inhibition of hypertrophy would not interfere with a necessary function of hypertrophy in response to pathological stimuli.

1.3 Experimental systems for studying heart disease

There are three commonly used experimental systems in the investigation of heart function and disease; cultured cardiac cells (*in vitro*), the isolated perfused mammalian heart known as Langendorff perfusion (*ex vivo*) and in live animals (*in vivo*). Those studies that demonstrate their findings *in vivo* are often considered to

be more significant than those demonstrated *ex vivo*, and *ex vivo* more significant than *in vitro.* The generally held belief is that *in vivo* experimentation is conducted in the natural context of the organism whereas *ex vivo* and *in vitro* systems are artificial ones. However, for various reasons all these systems are commonly used. For example, experiments in cultured cells are easier, cheaper and do not require the same licensing as working with animals. Moreover, one adult rodent heart or several rodent neonatal hearts provides enough cells to conduct many different experimental conditions compared to one in each *in vivo* or *ex vivo* experiment.

Experiments *in vitro* may be conducted in freshly isolated ("primary") cardiac myocytes or in immortalised cardiac myocyte cell lines. Two commonly used immortalised cell lines used are the H9c2 and CLEM cell lines derived from rat. Immortalised cell lines represent the most practical cardiac model, as they are readily available and relatively easy to maintain. However, freshly isolated myocytes are the preferred *in vitro* model, as immortalised cell lines have lost certain characteristics of cardiac myocytes, notably the terminal differentiated phenotype of adult cardiac myocytes. Of particular concern with immortalised cell lines would be the profile of activated genes in dividing cells and the effect this will have on investigating diseases that involve cell death because the protein products of these growth-promoting genes often promote resistance to cell death.

Primary cultures of human cardiac myocytes may be prepared from biopsies. However, as the possibility to obtain biopsies is limited the possibility of thorough investigation is difficult. Primary cultures of cardiac myocytes are most commonly isolated from neonatal mouse, rat or rabbit species. The neonatal rat cardiac myocyte (NRCM) preparation is probably the most commonly used *in vitro* cardiac model. However, since the advent of transgenic mice the use of neonatal mouse cardiac myocyte (NMCM) cells is increasing.

A preparation of cardiac myocytes from neonatal rodents is often chosen instead of adults because they are comparatively simple to prepare. However, the phenotypical differences that exist between adult and neonatal cells make it difficult to interpret predominantly adult related conditions such as ischaemia when conducted in neonatal cells. For example, unlike adult cells, neonatal cells have been shown to grow and regenerate as they can readily maintain and assemble myofibrils (Rothen-Rutishauser et al., 1998). Calcium handling has been shown to be different between

neonatal and adult cardiac myocytes; the immature myocardium has a reduced ability to sequester calcium and produces smaller L-type calcium currents (Maginot et al., 1998). There is also lower phosphodiesterase activity in NRCM cells (Picq et al., 1995), which implies differences in cyclic nucleotide signalling. Thus, although neonatal cardiac myocyte cultures are an important system many studies often extend their investigations into adult rat ventricular cells (ARVC) or adult mouse ventricular cells (AMVC).

The isolated perfused mammalian heart was developed by Oscar Langendorff in 1897, hence it is also known as Langendorff perfusion. Crystalloid perfusates are delivered to the heart by retrograde perfusion via a canula inserted in the ascending aorta. The Langendorff perfusion model was first applied in the study of heart biology and later on to test the effects of cardiovascular drugs and single gene alterations on heart function and to identify novel therapies to protect the heart from ischaemia and other insults (Skrzypiec-Spring et al., 2007). Limitations of the Langendorff model include the absence of normal neurohumoral influences and neuronal regulation. However, the isolated perfused heart is sometimes preferred to an *in vivo* approach, as it allows assessment of the direct effect of cardioprotective agents in the absence of interfering peripheral haemodynamic and neurohumoral alterations (Scarabelli et al., 2002).

In vivo experimentation is the gold standard for assessing the effect of drugs in cardiovascular function and disease. The most commonly used *in vivo* model of I/R-injury is conducted in the rat or mouse, whereby ischaemia is induced by ligature of the left coronary artery and subsequently released to allow reperfusion.

Transgenic mice are used to assess the role of any given gene product in cardiovascular function and disease. This may be achieved by targeted deletion of specific genes to generate "knockout" mice or by introduction of specific mutations to generate "knock-in" mice. Alternatively, transgenes are introduced to mice to over-express specific genes. Transgenic animals may then be used for *in vivo* experiments or cardiomyocytes or whole hearts may be isolated for *in vitro* or *ex vivo* experimentation respectively.

Some transgenic systems may be more sophisticated, whereby the expression of the transgene may be regulated temporally and/or spatially. The tetracycline (Tet)-

inducible system facilitates regulated expression of foreign genes in cultured mammalian cells (Gossen and Bujard, 1992), *in vivo* (Fishman et al., 1994) and in transgenic animals (Passman and Fishman, 1994). The Tet-inducible system is based on the regulatory elements of the Tn*10*-specified tetracycline-resistance operon in *E.coli*, in which transcription of resistance-mediating genes is negatively regulated by the tetracycline repressor (*tet*R). In the presence of tetracycline, the *tet*R does not bind to its operators located within the promoter region of the operon, enabling transcription of resistance genes (Figure 1.2A). By combining *tet*R with the C-terminal domain of VP16 from herpes simplex virus (HSV), which is known to be a strong transactivator, a hybrid transactivator known as the tetracycline transactivator (tTA) was generated that stimulates minimal promoters fused to the tetracycline operator (*tet*O) sequences (Gossen and Bujard, 1992) (Figure 1.2B). These promoters are virtually silent in the presence of low concentrations of tetracycline or derivatives of tetracycline (e.g. doxycycline), which prevents the tetracycline–controlled tTA from binding to *tet*O sequences. Thus, this system is known as the Tet-off system. A variant of the Tet-off system is the Tet-on system. The tTA protein used in the Tet-on system differs from the Tet-Off transactivator by four amino acids. The Tet-on transactivator binds the *tetO* and induces gene expression only when bound by tetracyclines (Figure 1.2C).

By using a tTA expression plasmid and a tTA responder plasmid in which a gene of interest is inserted, tetracycline regulated expression was achieved in cultured cells and subsequently *in vivo* (Fishman et al., 1994). Furthermore, by using tissue specific promoters to drive expression of the tTA, transgenic mice can be generated in which expression of tTA target genes can be restricted to selected tissues (Figure 1.3). The generation of transgenic mice expressing tTA under the control of a rat α myosin heavy chain promoter (αMHC-tTA mice) restricts expression of the tTA in the heart only. Thus, when mated with mice harbouring tTA responsive transgenes, only the progeny inheriting both transgenes will express the target gene, and expression will be restricted to those cells that would normally express αMHC, cardiac myocytes (Passman and Fishman, 1994, Redfern et al., 2000).

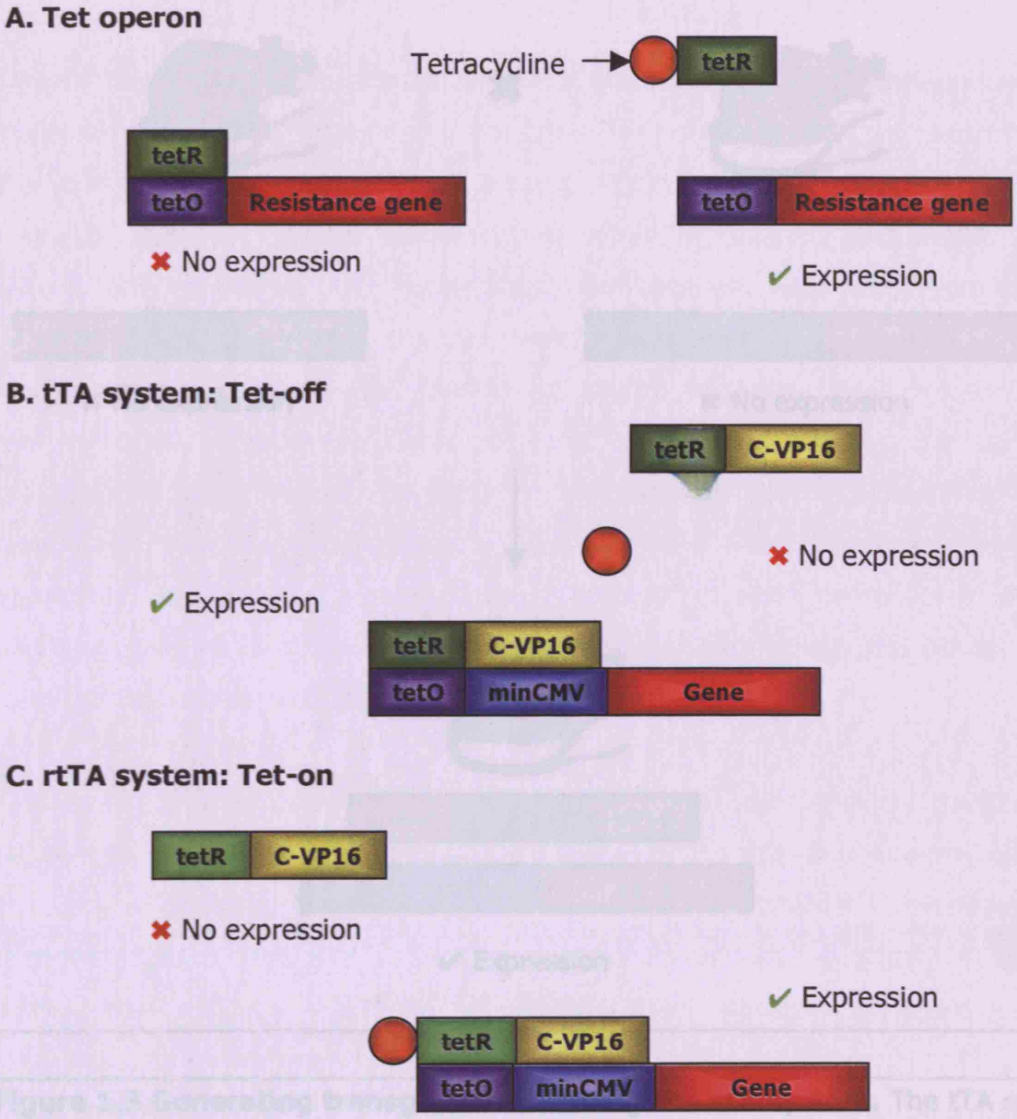

Figure 1.2 The Tet-inducible system. (A) The Tet-inducible system is based on the Tet operon from *E.coli*. The tet repressor (tetR) protein binds the Tet operon and inhibits the expression of the tetracycline resistance gene. Tetracycline binds tetR and alters its conformation, preventing it from binding the tetO and thereby allowing expression of the tetracycline resistance gene. (B) The tTA system (Tet-off): the tTA protein is a hybrid of tetR and the C-terminal domain of the VP16 transcriptional transactivator from herpes simplex virus. The tTA protein stimulates minimal promoter sequences, such as the cytomegalovirus promoter (CMV), fused to the *tetO* and induces gene expression. Tetracycline binds tTA and inhibits expression. (C) The rtTA system (Tet-on): a mutant of tTA, rtTA, differs in sequence to tTA at four amino acids. In this system, Tet-on, tetracycline binds to and alters the conformation of rtTA, enabling it to bind *tetO* and induce gene expression.

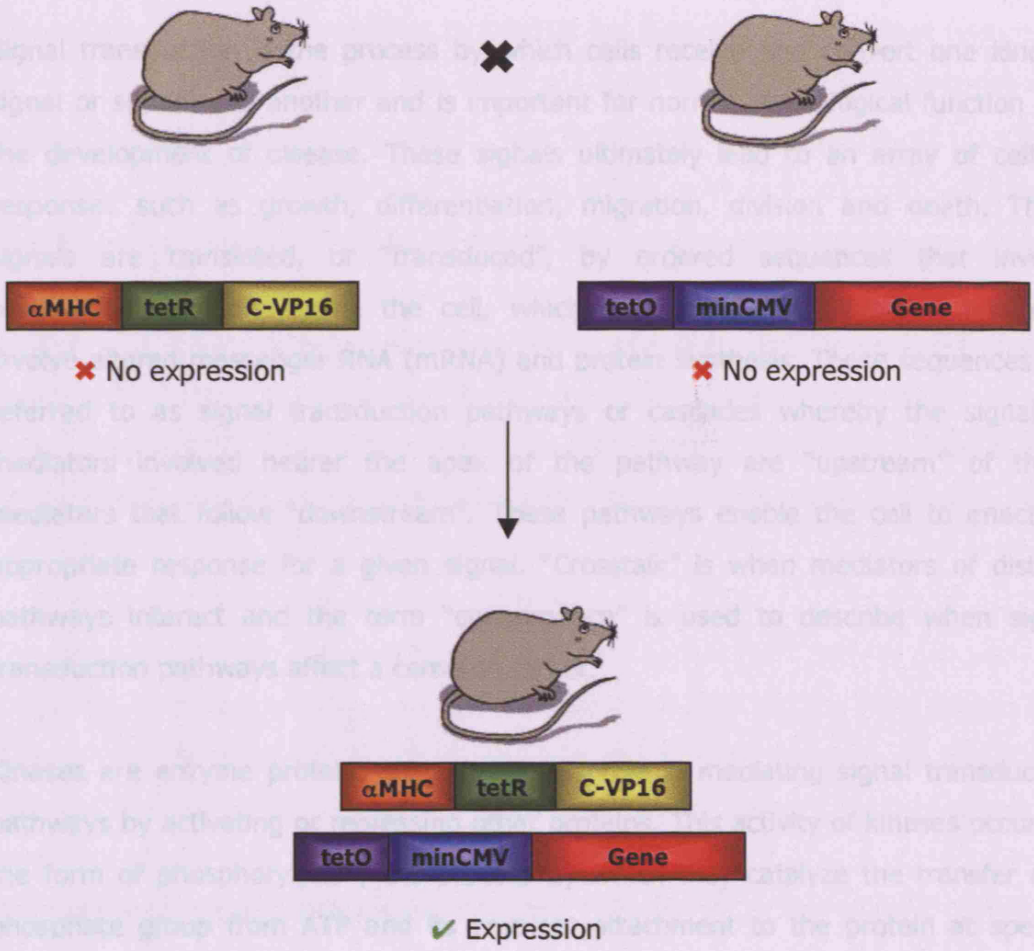

Figure 1.3 Generating transgenic mice using the tTA system. The tTA system (or rtTA system) in transgenic mice is a binary system requiring two distinct transgenics to be produced. The Tet-mouse carries the tTA transgene. The Tet-responder mouse carries the transgene for the gene of interest to be expressed, which is fused to the *tetO*-minCMV promoter. These mice are bred with each other to produce compound transgenic mice carrying both transgenes. These mice will express tTA, which will induce expression of the Tet-responsive transgene. Expression will be inhibited in mice given tetracycline, or derivatives of tetracyclines. In the rtTA system, compound transgenic mice will only express the Tet-responsive transgene when given tetracycline, or its derivatives. Regulation of spatial expression in the tTA system is achieved by choosing an appropriate promoter for the expression of the tTA gene in a particular tissue. The promoter of the αMHC gene is used restrict expression of tTA and responder transgene to the heart.

1.4 Signal transduction

Signal transduction is the process by which cells receive and convert one kind of signal or stimuli into another and is important for normal physiological function and the development of disease. These signals ultimately lead to an array of cellular responses such as growth, differentiation, migration, division and death. These signals are translated, or "transduced", by ordered sequences that involve biochemical reactions inside the cell, which are mediated by proteins and may involve altered messenger RNA (mRNA) and protein synthesis. These sequences are referred to as signal transduction pathways or cascades whereby the signalling mediators involved nearer the apex of the pathway are "upstream" of those mediators that follow "downstream". These pathways enable the cell to enact an appropriate response for a given signal. "Crosstalk" is when mediators of distinct pathways interact and the term "convergence" is used to describe when signal transduction pathways affect a common target.

Kinases are enzyme proteins that play a key role in mediating signal transduction pathways by activating or repressing other proteins. This activity of kinases occurs in the form of phosphorylation, the process by which they catalyze the transfer of a phosphate group from ATP and its covalent attachment to the protein at specific amino acid residues. Cascades of kinases exist whereby upstream kinases phosphorylate downstream kinases. Transphosphorylation is the process of a protein being phosphorylated by a kinase. However, kinases may also phosphorylate themselves, thereby undergoing autophosphorylation. Stimulation of signal transduction pathways may result in phosphorylation of transcription factors, proteins that bind deoxyribonucleic acid (DNA) and regulate the synthesis of mRNA for specific genes. Altered synthesis of mRNA may lead to altered levels of the corresponding protein in the cell. Enhancing the quantity of a specific protein in the cell may result in increasing the effect of a particular function performed by that protein, and vice versa for reducing the quantity of a protein. Although some signalling pathways require synthesis of new proteins to produce the intended effect, some pathways require only existing proteins in the cell to execute the intended signal.

Signals that mediate communication between cells usually take the form of small molecules that bind cell surface-receptors, specific proteins in the plasma membrane

of the cell, and initiate downstream events inside the cell. For example, neurotransmitters such as acetylcholine (ACh) are chemical messengers that signal from one neuronal cell to another by binding ion channels, proteins that form pores in the plasma membrane and allow passage of specific ions in order to propagate an action potential (Kistler et al., 1982). Cytokines such as tumour necrosis factor α (TNFα) and peptide hormones such as insulin are small proteins that bind plasma membrane receptors and regulate a variety of cellular events including activation of inflammatory cells and metabolism of glucose respectively. However, steroids represent a type of extracellular signalling molecule that crosses the plasma membrane of the cell because of their lipophilic and hydrophobic nature. Steroids locate their specific intracellular receptor, usually a transcription factor kept inactive by proteins known as chaperones, inside the cytoplasm or nucleus of the cell (Beato et al., 1996).

The endocrine system represents the organs of the body that synthesise signalling molecules, termed hormones, which are secreted systemically and may reach all the tissues in the body via the blood. However, signalling molecules may be synthesised and excreted by cells that then act locally on other cells, a process known as paracrine signalling, or they may act on the cell from which it was secreted in what is then described as autocrine signalling.

Cell surface receptors are transmembrane proteins that consist of extracellular and intracellular domains. Binding of a molecule, or ligand, to a cell-surface receptor stimulates a series of events in the cell, with different types of receptor stimulating different intracellular responses. Three major types of cell-surface receptors are; receptors that themselves act as ion channels; receptors that themselves act as enzymes or are closely associated with cytoplasmic enzymes; and G-protein coupled receptors (GPCRs).

Receptor tyrosine kinases (RTKs) are transmembrane proteins with a ligand binding extracellular domain and an intracellular kinase domain. Ligand binding of the receptor initiates an interaction between two identical receptors to form a dimer. Dimer formation results in autophosphorylation of tyrosine residues within the cytoplasmic tyrosine kinase domains of RTKs causing their conformation to change. This results in the kinase domain of the receptor being activated, initiating a

signalling cascade of phosphorylation of downstream cytoplasmic molecules (Li and Hristova, 2006).

GPCRs are a family of membrane proteins composed of seven-transmembrane domains, and are linked to a guanine nucleotide binding protein (G-protein). GPCRs represent the largest category of plasma membrane receptors including adrenergic receptors, olfactory receptors and opioid receptors. Ligand binding of the receptor will alter its conformation and will activate the bound G-protein. The activated G-protein will dissociate from the receptor and diffuse along the inner plasma membrane to interact with downstream proteins. These proteins are either ion channels or enzymes that mediate the next step in the pathway. These enzymes catalyze the generation of "second messengers" that relay the message from the plasma membrane to inside the cell. G_s-protein (subscript s denotes stimulatory) activates the enzyme adenylyl cyclase, which catalyzes the conversion of adenosine triphosphate (ATP) to cyclic 3',5'-adenosine monophosphate, called simply cyclic AMP (cAMP). Inside the cell cAMP binds to and activates cAMP-dependent kinase, which is known to phosphorylate several other kinases in pathways that lead to many different cellular responses.

1.5 Cell death

Cell death is an important feature of normal physiology and disease and occurs in different forms, the best understood being necrosis (oncosis) and apoptosis, although there is growing evidence for a third form of cell death known as autophagy. Necrosis is a rapid and irreversible process that occurs when cells are severely damaged. The characteristic morphology of necrosis includes swelling of the cell and its organelles, disruption of mitochondria, membrane rupture, and cell lysis (Searle et al., 1982). The contents released from the lysed cell act as a stimulus for inflammation with macrophage infiltration, fibroblast activation, and ultimately scar formation. Apoptosis is a mechanism of cell death morphologically distinct from necrosis with accompanying biochemical hallmarks that are unique to apoptotic cell death. These morphological characteristics include cell shrinkage, chromatin condensation, DNA fragmentation, membrane blebbing and formation of apoptotic bodies (Kerr et al., 1972). Biochemical techniques for the detection of characteristic features of apoptosis have been developed and are commonly used experimentally

for identifying apoptosis and the signalling pathways that contribute to this form of cell death. For example, Terminal transferase dUTP nick end labelling (TUNEL) is a method commonly used for detecting DNA fragmentation (Gavrieli et al., 1992). Another commonly used method is annexin V labelling of phosphatidylserine (PS), a phospholipid found within the plasma membrane of the cell. Annexin V is a phospholipid binding protein with high affinity for PS. PS is not normally exposed to the extracellular environment. However, an early event in apoptosis is the externalisation of PS, enabling its detection by annexin V.

Apoptosis represents a mode of cell death that, unlike necrosis, is highly regulated by signal transduction pathways. Apoptosis is important in normal physiology, notably development, and is now recognised to contribute to the pathology of many diseases. Prevention of cell death is a desirable effect in diseases for which loss of non-renewable tissue is a pathogenic factor. Thus, dissection of the apoptotic signalling pathways involved in disease is required to provide a better understanding of this process and how these pathways may be targeted therapeutically.

1.5.1 Apoptotic signalling pathways

Apoptosis has been found to be largely dependent on a family of proteases called caspases. However, there are also caspase independent mechanisms involved in apoptosis such as those involving apoptosis inducing factor (AIF) (Joza et al., 2001).

Caspases are cysteine proteases that were first implicated in apoptosis with the discovery that CED-3, the product of a gene required for cell death in the nematode *Caenorhabditis elegans*, is related to mammalian interleukin-1β-converting enzyme (ICE or caspase-1) (Miura et al., 1993, Thornberry et al., 1992). The 'c' refers to a cysteine protease mechanism, whereas 'aspase' reflects their ability to cleave after aspartic acid (Alnemri et al., 1996). To date, fourteen members of the caspase (ICE-related protease) family have been identified, and although caspase-1 has no obvious role in cell death several other members of this protease family have distinct roles in inflammation and apoptosis (Thornberry and Lazebnik, 1998).

Caspases are similar in their amino acid sequence, structure and substrate specificity (Nicholson and Thornberry, 1997). They are all expressed as precursor enzymes (30 to 50 kDa) that contain three domains; an NH_2-terminal (prodomain of variable

length), a large subunit (~20kDa), and a small subunit (~10kDa). Activation occurs as a result of proteolytic cleavage between domains, followed by association of the large and small subunits to form a heterodimer. The crystal structures of caspase-1 and caspase-3 have been determined and in both cases two heterodimers associate to form a tetramer with two catalytic sites that appear to function independently (Walker et al., 1994, (Rotonda et al., 1996).

Two features of the precursor protein are key to the mechanism of activation of these enzymes; their cleavage sites and the NH_2-terminal domain. All domains are derived from the proenzyme by cleavage at caspase consensus sites enabling activation by themselves and each other. Granzyme B, a serine protease, is the only other protein known to cleave caspases other than caspases themselves (Waterhouse and Trapani, 2002). Caspases are among the most specific of proteases, with an almost absolute requirement for cleavage after aspartic acid. The NH_2-terminal domain is highly variable in sequence and length and determines where caspases function in the apoptotic cascade. Long prodomain caspases such as caspase-8 and caspase-9 are initiator caspases and exert their activity not on cell death directly, but by activating short prodomain caspases. Short prodomain caspases such as caspase-3 cleave numerous substrates that may result in apoptosis, and are termed effector caspases.

There are two well-characterized and distinctly different apoptotic signalling pathways. These are the extrinsic death-receptor dependent pathway (Figure 1.4) and the intrinsic mitochondrial dependent pathway (Figure 1.5). These pathways signal via distinct initiator caspases that then activate common effector caspases, which cleave target substrates resulting in disassembly of the cell (Boldin et al., 1996).

Death receptors are a family of eight plasma membrane receptors that belong to the tumour necrosis factor (TNF) superfamily of receptors. The death receptor pathway involves the binding of extracellular death signal proteins such as TNF-1α and Fas ligand to their cognate cell surface receptors. This leads to intracellular association of proteins that interact through a conserved region known as the death domain (DD), one example of which is Fas-associated death domain (FADD) protein that binds to the Fas receptor. FADD then recruits procaspase-8 through the death effector domain (DED) resulting in autoprocessing of procaspase-8 molecules that then activate downstream caspases such as caspase-3.

The intrinsic mitochondrial dependent pathway for caspase activation involves mitochondrial derived cytochrome c and apoptosis protease activating factor-1 (Apaf-1) protein mediated activation of caspase-9. Apoptotic stimuli that permeabilise the outer mitochondrial membrane facilitate the release of cytochrome c into the cytoplasm, enabling it to bind to Apaf-1. This complex, which also involves binding of dATP to Apaf-1, recruits procaspase-9 through its caspase recruitment domain (CARD) to complete the structure known as the apoptosome. At the apoptosome, procaspase-9 is cleaved to produce active caspase-9, which then cleaves procaspase-3 to produce the active form (Li et al., 1997).

In addition to caspases -8 and -9, more recent studies also indicate an initiator role for caspase-2 (Lassus et al., 2002, Robertson et al., 2002). These findings suggest that in some cells caspase-9 may not be the initiator caspase in stress-mediated apoptosis because caspase-2 is required upstream of mitochondria for the release of cytochrome c and other apoptotic factors (Read et al., 2002).

The substrates targeted for cleavage by caspases and the subsequent contributions made to apoptotic cell death are varied. One class of substrates are those that are activated by caspase cleavage, which include the caspases themselves. However, caspases also inactivate proteins that protect living cells from apoptosis. One target for cleavage is I^{CAD}/DFF45 (Enari et al., 1998), which is an inhibitor of the nuclease responsible for the fragmentation of DNA, CAD (caspase-activated deoxyribonuclease). CAD and its inhibitor exist as a complex in non-apoptotic cells, however, during apoptosis the inhibitor is inactivated by caspases, leaving CAD free to function as a nuclease. Another example of protein inactivation that leads to apoptosis is that of poly (ADP-ribose) polymerase (PARP), one of the earlier discovered substrates of caspases that is an early marker of apoptosis (Lazebnik et al., 1994). PARP-1 protects the genome by responding to DNA damage and facilitating DNA repair and loss of PARP-1 results in chromatin condensation and DNA fragmentation (Shall and de Murcia, 2000).

Other targets for caspases that contribute to apoptosis include direct disassembly of cell structures. For example, caspases mediate the destruction of nuclear lamina, a rigid structure that underlies the nuclear membrane and is involved in chromatin organisation (Takahashi et al., 1996). Head-to-tail polymers of intermediate filament

proteins called lamins form lamina. During apoptosis, lamins are cleaved at a single site by caspases, causing lamina to collapse and contribute to chromatin condensation (Thornberry and Lazebnik, 1998). Caspases also disrupt cell structures indirectly by cleaving several proteins involved in cytoskeleton regulation, including gelsolin (Kothakota et al., 1997), focal adhesion kinase (FAK) (Wen et al., 1997), and p21-activated kinase 2 (PAK2) (Rudel and Bokoch, 1997).

There are many anti-apoptotic proteins that exert their activity by disrupting the caspase pathways. This effect is quite often mediated by proteins competing with caspases for binding sites in caspase adaptor molecules. Many of these proteins are splice variants of caspases themselves that lack the catalytic domain that is required for cleavage and therefore compete with the active form. Others are products of distinct genes that contain the binding domains found in caspases and compete in a similar manner. Caspase-9 short (C9s) is a splice variant of caspase-9 that lacks the central large subunit that contains the catalytic site. The variant C9s competes with its full length counterpart for binding APAF-1 in the apoptosome but because it does not contain the catalytic site apoptosis is reduced because of the reduction in active caspase-9 binding APAF-1 (Srinivasula et al., 1999). Cellular flice-like inhibitory protein (c-FLIP or FLIP) bears sequence homology to caspase-8 and inhibits caspase-8 mediated apoptosis. c-FLIP contains the DED found in caspase-8 that is required for recruitment to the Fas adaptor molecule FADD. Binding of c-FLIP to FADD results in a reduction of caspase-8 processing and a subsequent reduction in apoptosis (Scaffidi et al., 1999).

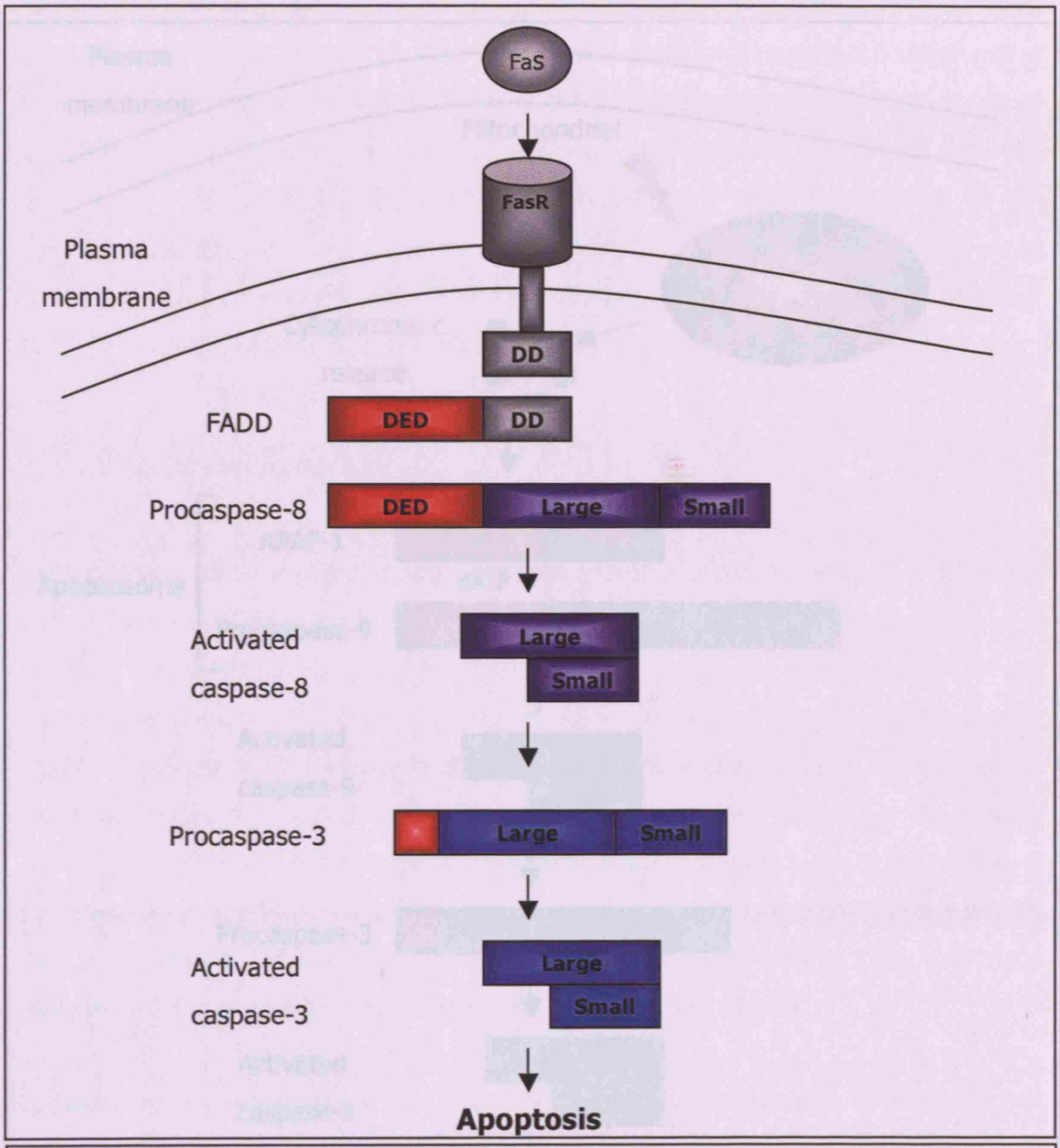

Figure 1.4 The extrinsic (death-receptor) apoptotic signalling pathway. Death receptor binding of cognate ligand, such as Fas/FasL, leads to activation of the extrinsic apoptotic signalling pathway. Fas/FasL binding results in recruitment of the adaptor protein, fas-associated death domain protein (FADD), through the death domains (DD) of FADD and the intracellular part of Fas receptor. Procaspase-8 is then recruited to the FasR/FADD complex and associates with FADD through death effector domains (DED). Autoproteolysis of procaspase-8 results in cleavage of the prodomain containing the DED domain, the large and small subunits. Association of the large and small subunits form the active caspase-8 protein, which then cleaves caspase-3. Caspase-3 cleavage results in association of its large and small subunits and formation of the active caspase-3 protein. Activated caspase-3 then cleaves substrates leading cell death.

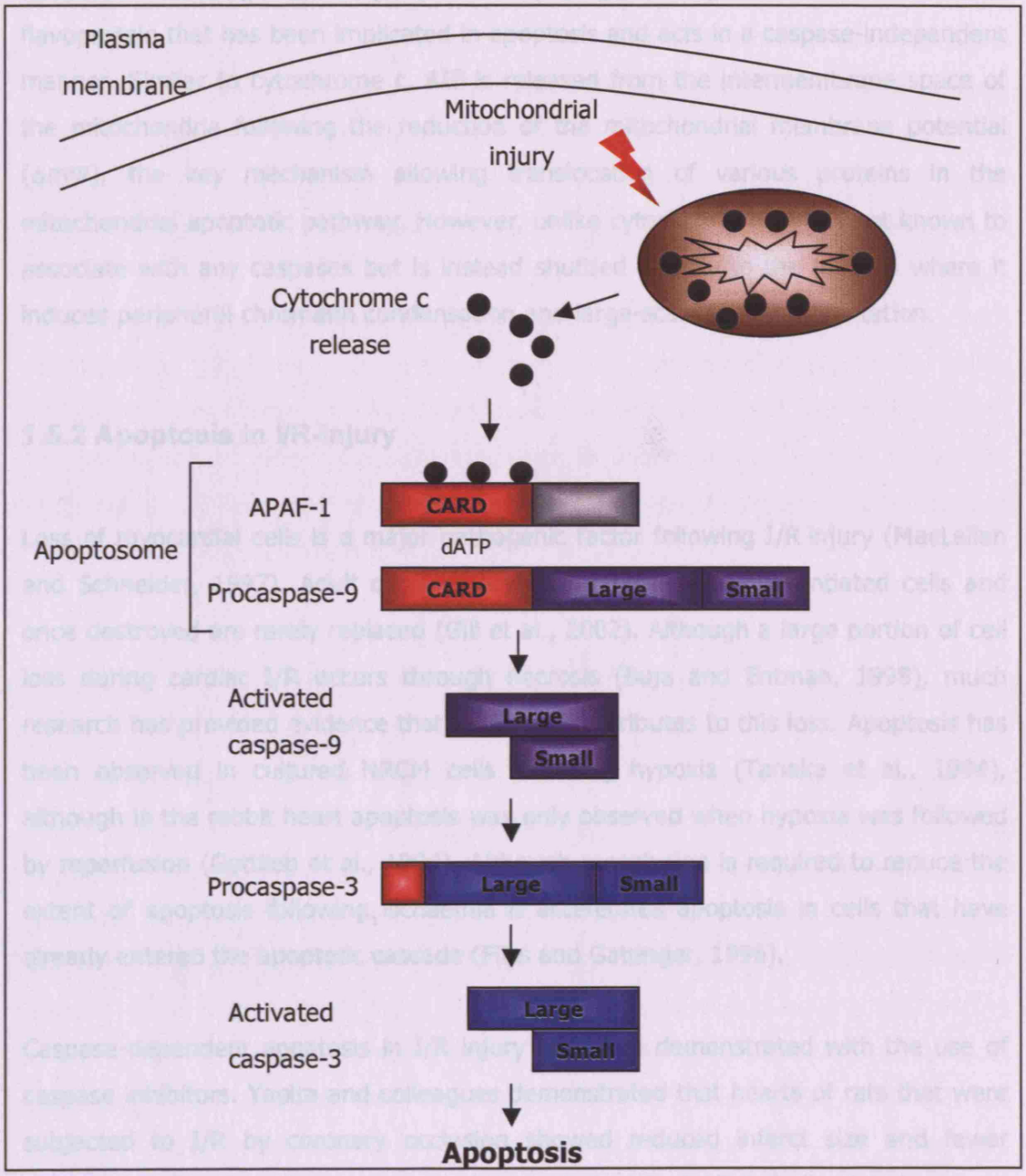

Figure 1.5 The intrinsic (mitochondrial) apoptotic signalling pathway. Mitochondrial injury that results in release of cytochrome c activates the intrinsic apoptotic signalling pathway. Association of apoptosis activating factor (APAF-1) and procaspase-9 through their caspase recruitment domains (CARD), cytochrome c and dATP form the apoptosome. Formation of the apoptosome results in autoproteolysis of procaspase-9 and cleavage of the prodomain containing the CARD domain, the large and small subunits. Association of the large and small subunits form the active caspase-9 protein, which then cleaves caspase-3. Caspase-3 cleavage results in association of its large and small subunits and formation of the active caspase-3 protein. Activated caspase-3 then cleaves substrates leading cell death.

Apoptosis inducing factor (AIF) is a phylogenetically ancient mitochondrial flavoprotein that has been implicated in apoptosis and acts in a caspase-independent manner. Similar to cytochrome c, AIF is released from the intermembrane space of the mitochondria following the reduction of the mitochondrial membrane potential ($\Delta m\Psi$), the key mechanism allowing translocation of various proteins in the mitochondrial apoptotic pathway. However, unlike cytochrome c, AIF is not known to associate with any caspases but is instead shuttled directly to the nucleus where it induces peripheral chromatin condensation and large-scale DNA fragmentation.

1.5.2 Apoptosis in I/R-injury

Loss of myocardial cells is a major pathogenic factor following I/R injury (MacLellan and Schneider, 1997). Adult cardiomyocytes are terminally differentiated cells and once destroyed are rarely replaced (Gill et al., 2002). Although a large portion of cell loss during cardiac I/R occurs through necrosis (Buja and Entman, 1998), much research has provided evidence that apoptosis contributes to this loss. Apoptosis has been observed in cultured NRCM cells following hypoxia (Tanaka et al., 1994), although in the rabbit heart apoptosis was only observed when hypoxia was followed by reperfusion (Gottlieb et al., 1994). Although reperfusion is required to reduce the extent of apoptosis following ischaemia it accelerates apoptosis in cells that have already entered the apoptotic cascade (Fliss and Gattinger, 1996).

Caspase-dependent apoptosis in I/R injury has been demonstrated with the use of caspase inhibitors. Yaoita and colleagues demonstrated that hearts of rats that were subjected to I/R by coronary occlusion showed reduced infarct size and fewer apoptotic cells when the rats were also treated with zVAD-fmk (a global caspase inhibitor) (Yaoita et al., 1998). However, specific caspase inhibitors have enabled a better understanding of the caspase pathways involved in I/R injury. For example, use of specific chemical and genetic inhibitors have been used to examine the relative contributions of initiator caspases in apoptosis of cardiac myocytes during ischaemia versus reperfusion injury (Stephanou et al., 2001a). Data from this study suggests that ischaemia induces apoptosis through the mitochondrial mediated caspase-9 pathway and reperfusion-induced cell death is additionally mediated via the death receptor mediated caspase-8 pathway.

The roles of caspases in apoptosis have been assessed using transgenic mice. Heart-targeted over-expression of caspase-3 in mice increases infarct size and depresses cardiac function (Condorelli et al., 2001). These transgenic mice, which constitutively express caspase-3 under the rat α-myosin heavy chain promoter, had depression of cardiac function and abnormal nuclear and myofibrillar ultra-structural damage. When subjected to I/R, the hearts of these mice also showed increased infarct size.

Several lines of caspase-deficient mice have been generated that exhibit cell death abnormalities (Bergeron et al., 1998, Kuida et al., 1998, Woo et al., 1998). These knockouts do not exhibit a global suppression of cell death, but rather tissue- and cell type-specific or stimulus-dependent defects of apoptosis (Kuida et al., 1998). The preferential apoptosis defects suggest that different sets of caspases are involved in separate cell death pathways *in vivo*.

1.5.3 Additional regulation of apoptosis in I/R-injury

Stressful conditions such as ischaemia and reperfusion induce apoptosis via the death receptor or mitochondrial pathways. However, extracellular molecules acting on other cell surface receptors activate intracellular signalling pathways that modulate these apoptotic programmes. Multiple signalling pathways are activated in ischaemia and/or reperfusion and some of these pathways may promote cell death whereas others are involved in cell survival. A number of studies have implicated the mitogen activated protein kinase (MAPK) pathway as a survival pathway in both cardiac cells (Adderley and Fitzgerald 1999, Maulik 1996, Sheng 1997) and other cell types (Allen 1999, Cano and Mahadevan 1995, Cobb and Goldsmith 1995, Downward 1998, Schaeffer and Weber 1999, Xia 1995). Extracellular regulated kinase (ERK), one sub-family of MAP kinases, is composed of the kinases p42 and p44; their names denote their size in kilodaltons. Phosphorylation and activation of p42/p44 MAPK is mediated by MAP kinases MEK (MAPK kinase) 1/2. The MEK1/2-p42/p44 cascade can mediate cellular protection when activated in I/R (Yue et al., 2000). Activation of the phosphatidylinositol-3-OH kinase (PI3K)-protein kinase B (Akt) signalling cascade has also been shown to confer protection against I/R injury (Matsui et al., 1999, Matsui et al., 2001). Activation of the pro-survival pathways MEK1/2-ERK1/2 and PI3K-Akt in I/R has been named the reperfusion injury salvage kinase (RISK) pathway (Hausenloy and Yellon, 2004). However, activation of the p38 MAPK signalling

cascade has been demonstrated to promote apoptotic cell death in I/R injury (Ma et al., 1999).

The targets of these signalling cascades may be components of apoptotic pathways such as caspases. For example, caspase-9 is phosphorylated by ERK2 resulting in its inhibition and promotion of cell survival (Allan et al., 2003). Cell surface receptor and kinase cascade mediated regulation of apoptosis may occur through regulation of other intracellular proteins that influence cell death, such as the B-cell lymphoma-2 (Bcl-2) family of proteins. The Bcl-2 family includes pro- and anti apoptotic members that regulate mitochondrial membrane permeabilisation. Cardiac over-expression of the proapoptotic protein Bcl-2 attenuates apoptosis and protects against myocardial I/R injury in transgenic mice (Chen et al., 2001). Langendorff perfused hearts from these mice showed improved recovery compared to hearts from wild-type mice following I/R. When Bcl-2 transgenic mice were subjected to coronary artery occlusion followed by reperfusion, transgenic hearts had significantly fewer TUNEL positive myocytes than hearts from non-transgenic littermates. However, phosphorylation of Bcl-2 by p38 MAPK has been demonstrated to inhibit its anti-apoptotic potential (De Chiara et al., 2006)

Although ischaemia is essentially a damaging stimulus, short episodes of ischaemia are able to protect against a subsequent more lethal dose of ischaemia, a concept known as ischaemic preconditioning (IPC). IPC was first described by Murry and colleagues (Murry et al., 1986) and is one of the most powerful and consistent protectors against severe ischaemia (reviewed by Opie, 2004). The protection conferred by IPC against subsequent ischaemia was found to last for 2-3 hours. However, a second window of protection occurring between 1-3 days after the initial IPC episode has been described (Marber and Yellon, 1996).

Adenosine is an endogenous trigger of classical IPC, which activates its G-coupled receptor to transmit the signal to protein kinase C (PKC), which then leads to activation of the mitochondrial ATP-sensitive potassium channel (K_{ATP}) (Przyklenk et al., 1996, Speechly-Dick et al., 1995). Opening of mitochondrial K_{ATP} channels have been proposed to protect the mitochondria from calcium overload during I/R (Murata et al., 2001).

1.6 Hypertrophic signalling pathways

Multiple signalling pathways have been shown to regulate the stimulation of hypertrophic growth. Two key pathways involved are the calcium-calcineurin pathway and the angiotensin II (A-II) pathways. Increases in intracellular calcium and binding of calmodulin lead to activation of calcineurin, an essential mediator in the growth response to pressure overload (Shimoyama et al., 1999). Calcineurin is a serine-threonine phosphatase that dephosphorylates transcription factors of the NFAT (nuclear factor of activated T-cells) family. Dephosphorylation of NFAT family proteins unmasks their nuclear localisation signals (NLS), which results in their translocation to the nucleus and gene induction. The role of the calcineurin/NFAT pathway in hypertrophy has been demonstrated in transgenic mice. Transgenic mice expressing constitutively active calcineurin develop enlarged hearts that leads to heart failure (Molkentin et al., 1998). A-II is released from the heart in response to mechanical strain (Amedeo Modesti et al., 2002). A-II binds its cognate membrane receptor to induce hypertrophy via multiple signalling pathways including the MAPK pathway (Ruwhof and van der Laarse, 2000).

The MAPK signalling pathway is involved in mediating hypertrophic signals, including those elicited by A-II stimulation. Over-expression of MAPK phosphatase 1 (MKP-1), which inhibits different MAPK signalling pathways, blocked both agonist-induced hypertrophy *in vitro* and pressure overload-associated hypertrophy *in vivo* (Bueno et al., 2001). MEK5 is involved in transducing hypertrophic signals that result in eccentric cardiomyocyte hypertrophy, which occurs in response to volume-overload induced myocyte growth (Nicol et al., 2001).

Alpha1A-adrenergic agonists stimulate cardiac myocyte hypertrophy. Phenylephrine (PE) is a potent hypertrophic drug that binds the alpha1A-adrenergic receptor. Transduction of the PE signal involves activation of ERK1/2, p38 MAPK and Akt. Hypertrophy induced by PE in NRCM cells has been demonstrated to be dependent on the ability of ERK1/2 to phosphorylate the transcription coactivator p300 and the highly related cAMP response binding protein (CREB)-binding protein (CBP) (Gusterson et al., 2002). The role of p300 as a transcriptional coactivator is found for basal and non-constitutive cardiac transcription factors. It has histone acetylase transferase (HAT) activity, which modifies associated transcription factors and chromatin by acetylation, thereby relaxing chromatin structure and promoting gene

activation. Inhibition of p300 attenuates PE induced hypertrophy in NRCM cells (Gusterson et al., 2003) and mice deficient in p300 have reduced expression of αMHC and α-actinin resulting in structural defects (Yao 1998).

Enzymes known as histone deacetylases (HDACs) inhibit the HAT activity exhibited by transcriptional co-activators such as p300 thereby inhibiting physiological responses such as hypertrophy, which are dependent on *de novo* mRNA synthesis. HDACs inhibit hypertrophy through direct association with myocyte enhancer factor 2 (MEF2), a transcription factor that positively regulates hypertrophic signalling pathways including the calcineurin pathway (Zhang et al., 2002). Several other signalling pathways have been shown to be involved in mediating hypertrophic signals. Various PKC isoforms have been implicated in mediating hypertrophy. For example, transgenic mice overexpressing PKC-β develop cardiac hypertrophy, which results in sudden death (Bowman et al., 1997).

There is evidence to suggest that physiological and pathological hypertrophy differ at the molecular level. Iemitsu and colleagues found the mRNA expression levels for some hypertrophy-associated genes differed between spontaneously hypertensive and exercised rats (Iemitsu et al., 2001). Therefore, it is important to further characterise hypertrophic signalling pathways and understand how pathological and physiological pathways differ in order to help identify the most suitable molecules to be targeted for therapy.

Thus far, some of the best understood signalling pathways that regulate I/R-injury and hypertrophy have been described. The role of the interferon-gamma and cardiotrophin-1 signalling pathways in the regulation of cardiac I/R-injury and hypertrophy will now be discussed.

1.7 Interferon gamma signalling pathway

Interferon gamma (IFNγ) belongs to a small family of cytokines named interferons (IFNs) that are secreted by cells of the immune system and have antiviral and antiproliferative effects. They were originally discovered by their ability to interfere with viral replication, hence the name interferon. IFNs are classified into three groups based on their amino acid sequence and recognition of cell-surface receptors. There are six type I IFNs and IFNγ is the only type II interferon. Recently, a third type of IFN was identified, named IFN-lambda (IFNλ) (Ank et al., 2006).

IFNγ is a peptide with a molecular mass of 17 kDa. Two molecules of IFNγ interact to form a homodimer before binding its receptor. The IFNγ receptor is expressed in nearly all cell types (Bach et al., 1997). The receptor consists of two polypeptides known as the alpha and beta chains or IFNGR-1 and IFNGR-2, which are 90 kDa and 65 kDa respectively. The IFNγ homodimer binds the IFNGR-1 chain but it does not interact directly with IFNGR-2, although IFNGR-2 is thought to stabilise IFNγ and IFNGR-1 interaction (Ank et al., 2006).

The intracellular signalling cascade following IFN stimulation is mediated by the Janus kinase–signal transducer and activator of transcription (JAK-STAT) pathway (Darnell et al., 1994). Most STAT-activating cytokine receptors do not have intrinsic tyrosine kinase activity, however, their intracellular domains are closely associated with the tyrosine kinases known as Janus kinases (JAKs,) of which there are four members; JAK1, JAK2, JAK3 and TYK2 (Aaronson and Horvath, 2002). Binding of IFNγ to its transmembrane receptor results in trans- and auto- phosphorylation of the intracellular IFNγ receptor bound tyrosine kinases JAK1 and JAK2 (Ihle, 1995).

JAK phosphorylation of IFN receptors creates docking sites on the receptor for latent transcription factors known as signal transducers and activators of transcription (STAT) proteins. Phosphorylation of STAT proteins by JAKs on activating tyrosine residues leads to homo- and hetero- dimerisation. STAT dimers then translocate to the nucleus where they bind their target promoters and act to enhance or repress gene transcription. STAT activation and translocation is a rapid process, occurring within minutes of receptor stimulation (Barry et al., 2007).

1.8 Signal transducer and activator of transcription 1

The signal transducer and activator of transcription 1 (STAT1) protein is a transcription factor that belongs to the family of STATs, which have been shown to play a role in development, cell growth, proliferation and apoptotic cell death (Stephanou and Latchman, 2003). To date, there are seven STAT family members that have been identified and are encoded by distinct genes (STAT1, STAT2, STAT3, STAT4, STAT5α, STAT5β, STAT6) (Stephanou and Latchman, 2003, Murray, 2007). There are 24 exons in the STAT1 gene and the protein is expressed in two distinct isoforms, STAT1α (91 kDa) and STAT1β (84 kDa), which are generated by alternative splicing (Schindler et al., 1992). STATs have a highly conserved structure consisting of amino terminal, coiled coil, DNA binding, linker, Src-homology-2 (SH2) and carboxyl transactivation domain (TAD) (Figure 1.6)

1.8.1 Activation of STAT1

IFNγ binding of the IFNGR-1 chain of the IFNγ receptor results in phosphorylation of the intracellular domain, which creates a docking site for STAT1 (Greenlund et al., 1994) (Figure 1.7). When STAT1 is recruited to the IFNγ receptor interaction occurs via their SH2 domains. JAK phosphorylation and activation of STAT1 occurs at tyrosine residue Y701 in the transactivation domain (Shuai et al., 1993). Additional regulation of STAT function occurs by serine phosphorylation within the TAD (Decker and Kovarik, 2000). STAT1 transcriptional activity is enhanced by IFNγ independent serine phosphorylation at residue S727 and it has been demonstrated that this is mediated by p38 MAPK and PKCδ (Kovarik et al., 1999, Uddin et al., 2002, DeVries et al., 2004). Serine phoshorylation may enhance transcriptional activity by the recruitment of co-factors. For example, serine phosphorylation of STAT3 has been shown to influence recruitment of the co-factor p300/CBP (Schuringa et al., 2001). The STAT1β isoform lacks 38 amino acids encompassing the TAD, including the S727 residue, and has been shown to be transcriptionally inactive and exerts a dominant-negative effect on gene activation by STAT1α (Baran-Marszak et al., 2004).

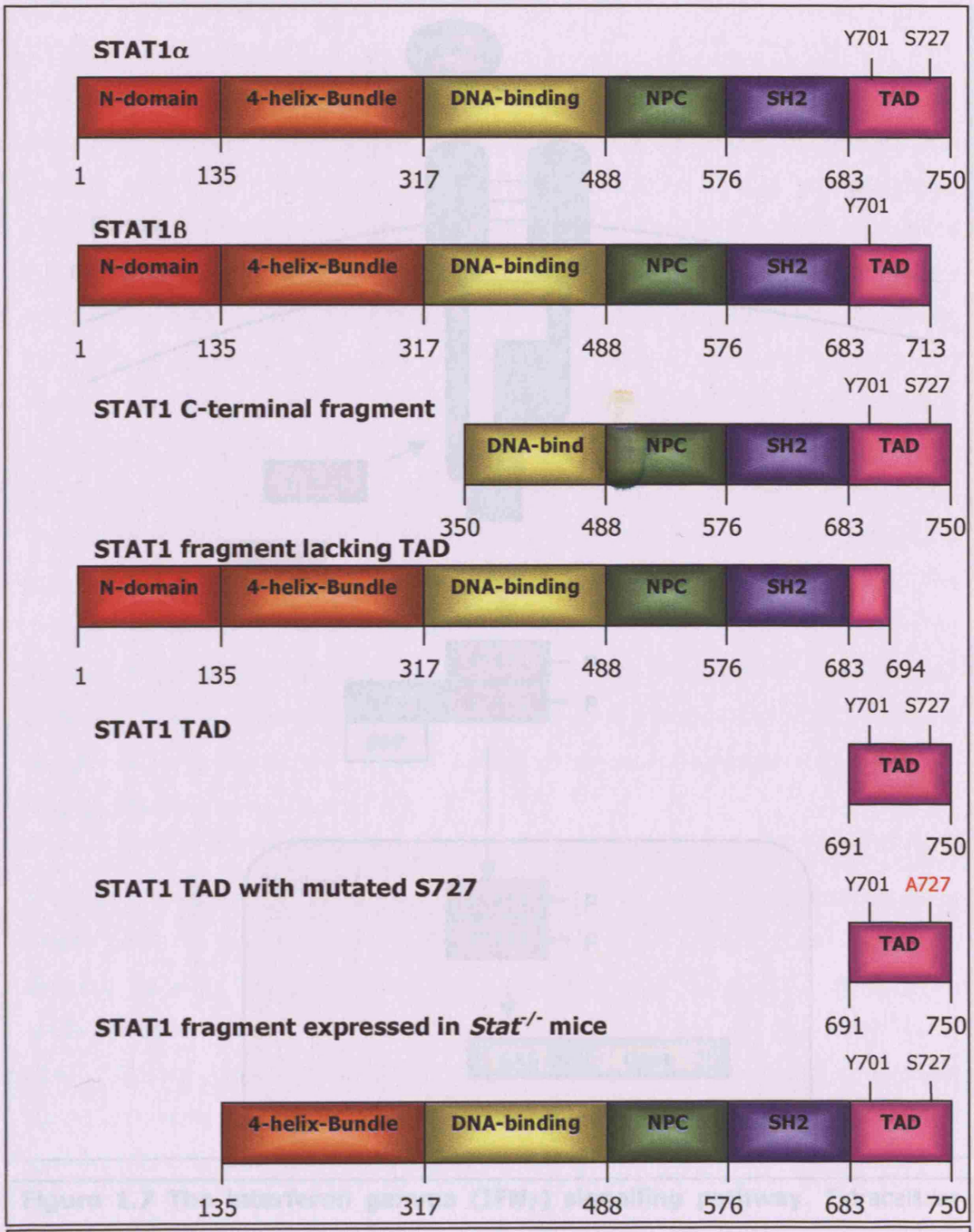

Figure 1.6 The structure of STAT1 and experimental mutants. The 91 kDa STAT1α protein is composed of the N-terminal, 4-Helix-Bundle (linker domain), DNA-binding, nuclear pore complex (NPC), Src-homology-2 (SH2) and transactivation domains (TAD). STAT1β is 84 KDa and lacks the last 37 amino acids of STAT1α including the serine 727 site. STAT1 C-terminal fragment, STAT1 fragment lacking TAD, STAT1 TAD and STAT1 TAD with serine 727 mutated to alanine are experimental mutants of STAT1. The STAT1 fragment expressed in *Stat1*$^{-/-}$ mice is a truncated protein of 72 KDa.

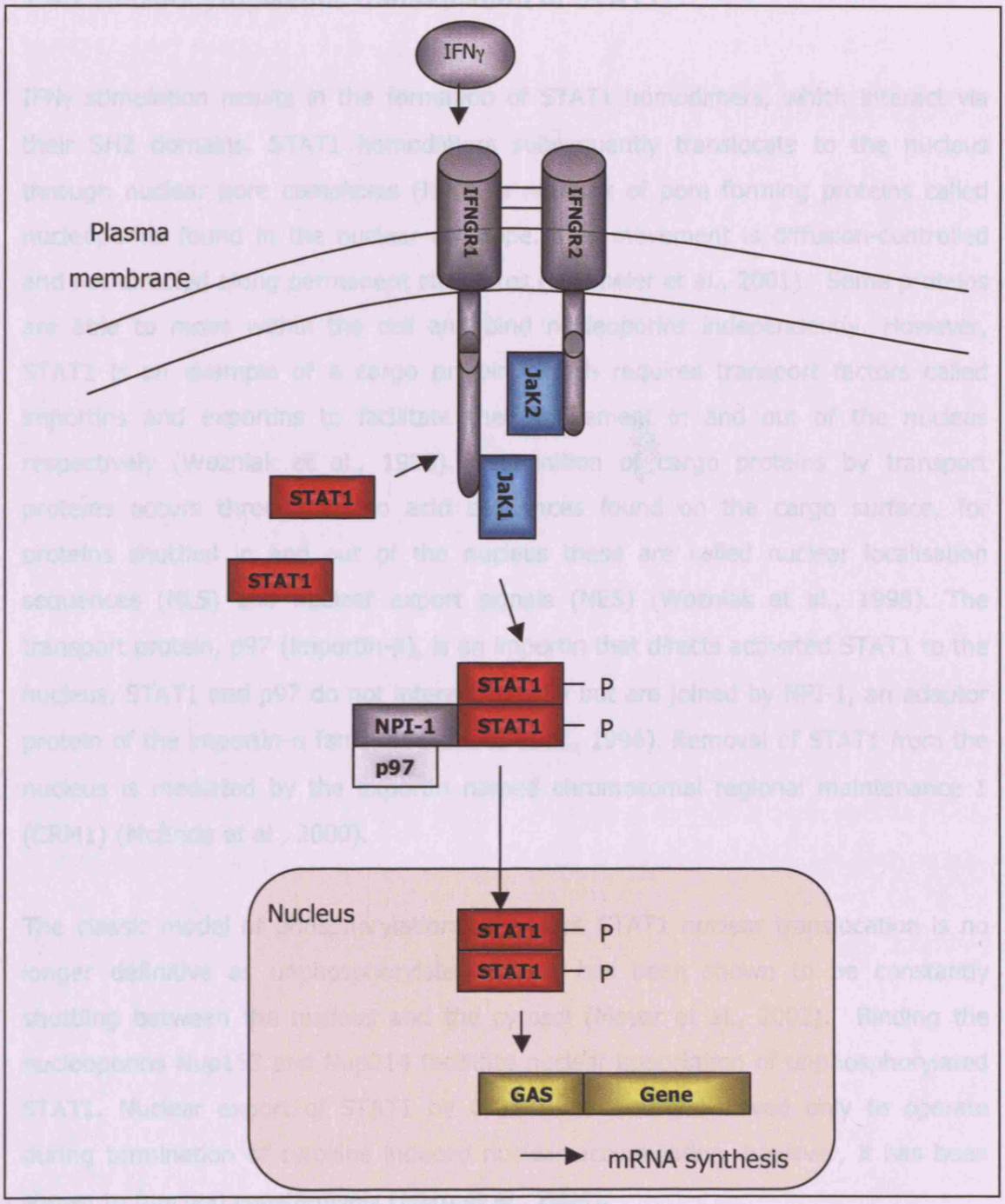

Figure 1.7 The interferon gamma (IFNγ) signalling pathway. Extracellular binding of IFNγ and the IFNGR-1 chain of the IFNγ pathway activates the intracellular Janus Kinase/Signal transducer and activator of transcription (JAK/STAT) pathway. Ligand binding results in tyrosine phosphorylation of the intracellular domains of the receptor by Jak1 and Jak2, resulting in the recruitment of STAT1 to the receptor, which is also phosphorylated by Jak1 and Jak2. Phosphorylated STAT1 molecules form dimers and are imported to the nucleus by p97, which interacts with the STAT1 dimer via NPI-1. STAT1 dimers induce synthesis of genes with gamma-activated sequences (GAS) in their promoters.

1.8.2 Nucleocytoplasmic translocation of STAT1

IFNγ stimulation results in the formation of STAT1 homodimers, which interact via their SH2 domains. STAT1 homodimers subsequently translocate to the nucleus through nuclear pore complexes (NPC), a network of pore forming proteins called nucleoporins found in the nuclear envelope. This movement is diffusion-controlled and not directed along permanent structures (Lillemeier et al., 2001). Some proteins are able to move within the cell and bind nucleoporins independently. However, STAT1 is an example of a cargo protein, which requires transport factors called importins and exportins to facilitate their movement in and out of the nucleus respectively (Wozniak et al., 1998). Recognition of cargo proteins by transport proteins occurs through amino acid sequences found on the cargo surface, for proteins shuttled in and out of the nucleus these are called nuclear localisation sequences (NLS) and nuclear export signals (NES) (Wozniak et al., 1998). The transport protein, p97 (importin-β), is an importin that directs activated STAT1 to the nucleus. STAT1 and p97 do not interact directly but are joined by NPI-1, an adaptor protein of the importin-α family (Sekimoto et al., 1996). Removal of STAT1 from the nucleus is mediated by the exportin named chromosomal regional maintenance 1 (CRM1) (McBride et al., 2000).

The classic model of phosphorylation dependent STAT1 nuclear translocation is no longer definitive as unphosphorylated STAT1 has been shown to be constantly shuttling between the nucleus and the cytosol (Meyer et al., 2002). Binding the nucleoporins Nup153 and Nup214 facilitate nuclear importation of unphosphorylated STAT1. Nuclear export of STAT1 by CRM1 was initially believed only to operate during termination of cytokine induced nuclear accumulation, however, it has been shown to function constitutively (Marg et al., 2004).

1.8.3 STAT1 gene transactivation

Over 200 genes are known to be regulated by IFNγ (Boehm et al., 1997). These include major histocompatibility complex (MHC) genes, transcription factors, selectins, selectin ligands, chemokines, chemoattractants, integrins, cellular adhesion molecules, immunoglobulins, cytokines, cytokine receptors, tyrosine kinases and apoptosis-related genes (Boehm et al., 1997). STAT1 homodimers bind DNA in the

promoter region of genes through the STAT1 DNA-binding domain. STAT1 homodimers recognise an 8- to 10-base pair inverted repeat element with a consensus sequence of 5'-TT(N_{4-6})AA-3', which is called a gamma activated sequence (GAS) element (Aaronson and Horvath, 2002).

STAT1 may be also be activated by type I IFNs. Type I stimulation results in the heterodimerisation of STAT1 and STAT2. The STAT1/STAT2 dimer binds the protein interferon regulatory factor 9 (IRF9) to from a transcription-promoting complex known as interferon-stimulated gene factor 3 (ISGF3). This complex recognises a distinct DNA sequence in gene promoters, the IFN-stimulated response element (ISGF3), with the sequence 5'-AGTTTN$_3$TTTCC-3'.

1.8.4 Inhibition of STAT1 activity

Several different protein families mediate negative regulation of STATs in distinct ways. These negative regulators are essential for proper homeostasis of the immune response (Yoshimura et al., 2007). Suppressors of cell signalling (SOCS) proteins bind receptor sites and/or JAK catalytic sites in such a way as to block further STAT-protein activation (Yasukawa et al., 2000). SOCS1 can inhibit JAK tyrosine activity through a kinase inhibitory region (KIR) found in SOCS proteins. A fragment corresponding to the KIR of SOCS1 has been shown to inhibit JAK2 mediated phosphorylation of STAT1 (Waiboci et al., 2007).

A similar mechanism of inhibition exists for activated STATs, which are negatively regulated in the nucleus by protein inhibitor of activated stats (PIAS) proteins. PIAS proteins interact with only those STAT proteins that are tyrosine phosphorylated and block them from DNA binding (Greenhalgh and Hilton, 2001). For example, PIAS1 was shown to specifically inhibit gene activation by STAT1 (Liu et al., 1998).

Another mechanism of inhibition of activated STATs is carried out by tyrosine phosphatases. Phosphatases are enzymes that dephosphorylate proteins thereby reversing the effect of kinases. Dephosphorylation of STATs is mediated by phosphatases found in the cytosol and the nucleus. STAT1 has been shown to be inhibited by the nuclear phosphatase TC45 (ten Hoeve et al., 2002).

1.8.5 Roles of STAT1

STAT1 is essential for mediating the immunoregulatory effects of IFNγ. Mutations in genes encoding either chains of the IFNγ receptor and STAT1 have been shown to result in enhanced susceptibility to mycobacterial infections (Newport et al., 1996, Jouanguy et al., 1996, Dupuis et al., 2001). Recently, humans with homozygous mutations in the alpha chain of the IFNγ receptor were described (Noordzij et al., 2007). Defects in the IFNγ receptor-dependent signalling pathway were observed in these individuals. One became ill after Bacillus vaccination and subsequently died while the other suffered several infection episodes. The role of the IFNγ/STAT1 pathway in host defence has also been demonstrated in mice. Transgenic mice that are deficient in either chains of the IFNγ receptor have defects in their immune response, demonstrating that the receptor is necessary for killing intracellular pathogens, such as mycobacterium, by macrophages (Huang et al., 1993, Dalton et al., 1993). Transgenic mice lacking functional STAT1 are unresponsive to IFNγ and are susceptible to viral disease (Durbin et al., 1996, Meraz et al., 1996). Furthermore, mice deficient in the STAT1 inhibitor, SOCS1, are hypersensitive to lipopolysaccharide (LPS), a component of the outer membrane of gram-negative bacteria and a potent stimulator of IFNγ (Nakagawa et al., 2002).

The antiproliferative and pro-apoptotic effects of IFNs largely rely on STAT1 in promoting apoptotic death (Kim and Lee, 2007). The mechanism by which STAT1 mediates antiproliferation of tumours has been shown to occur at the level of the immune system. For example, the inhibition of tumour formation by IFNα in mice is dependent on STAT1 activating natural killer (NK) cells and not directly inducing apoptosis within the malignant cell (Lesinski et al., 2003). However, there is evidence showing that STAT1 is more intimately involved in regulating cell fate. For example, STAT1 activation has been shown to have prognostic significance in breast cancer; patients with high STAT1 activation had longer overall and relapse-free survival (Widschwendter et al., 2002). Furthermore, apoptotic cell death induced with chemotherapeutic agents in cancerous cells is modulated by STAT1 (Thomas et al., 2004). Moreover, activation and expression of caspases in IFNγ-induced apoptosis in various cell types is dependent on STAT1 (Chin et al., 1997).

1.8.6 Regulation of cardiac I/R-injury by STAT1

STAT1 has been implicated as a pro-apoptotic factor in the heart and in isolated cardiac cells subjected to I/R. Stephanou and colleagues made a number of observations regarding STAT1 and its role in cardiac I/R-injury (Stephanou et al., 2000). They showed that STAT1 is tyrosine phosphorylated at residue Y701 during simulated ischaemia and is maintained following reperfusion in NRCM cells, and following simulated I/R-injury in the isolated intact heart. Similarly, IFNγ also induced STAT1 tyrosine phosphorylation and apoptosis of NRCM cells. Furthermore, over-expression of STAT1 using an expression construct introduced into NRCM cells by transient transfection rendered them more susceptible to apoptosis following the simulated I/R cycle. Moreover, inhibiting STAT1 with an antisense construct reduced ischaemia-induced cell death in NRCM cells. Stephanou and colleagues also found that STAT1 induced cell death involved activation of caspase-1. Both STAT1 over-expression and IFNγ treatment or ischaemia activated the caspase-1 promoter in NRCM cells as determined by a luciferase reporter assay.

STAT1 up-regulates the expression of the Fas receptor and its ligand in NRCM cells and in the isolated intact heart following I/R-injury (Stephanou et al., 2001b). In this regard, it is interesting that hearts from transgenic mice lacking functional FasR show a considerable reduction in cell death following I/R-injury compared to control hearts (Lee et al., 2003). In addition to the earlier finding that STAT1 is tyrosine phosphorylated following I/R, it has also been demonstrated that serine phosphorylation at residue S727 also occurs, and is necessary for I/R induced expression of FasR/FasL and apoptosis in NRCM cells (Stephanou et al., 2001b). Phosphorylation of S727 appeared to be accomplished by p38 MAPK activation during I/R, since it can be blocked both by a chemical inhibitor of p38 MAPK, SB203580, and by a dominant negative form of MKK6, the upstream activator of p38 MAPK (Stephanou et al., 2001b).

Furthermore, by mutating phosphorylation sites in STAT1, it was shown that the induction of FasR/FasL gene expression and apoptosis is dependent on serine phosphorylation at residue S727 of STAT1 but tyrosine phosphorylation of residue 701 is not required (Stephanou et al., 2001b). The finding that STAT1 induces expression of the FasR/FasL and apoptosis in the absence of tyrosine phosphorylation may seem incompatible with the classic signalling pathway in which

STAT1 is tyrosine phosphorylated and subsequently translocates to the nucleus. However, this may be partly explained by the finding that a proportion of the cell's STAT1 is constantly shuttled between the cytosol and the nucleus independently of tyrosine phosphorylation (Meyer et al., 2002). The constitutive expression of the low molecular mass polypeptide 2 (LMP2) has been shown to be mediated by a complex of unphosphorylated STAT1 and IRF-1 (Chatterjee-Kishore et al., 2000). Evidence that constitutive expression of genes is promoted by DNA–binding of unphosphorylated STAT1 on tyrosine 701 lends further support for the theory that STAT1 transcriptional activity does not require tyrosine phosphorylation.

The mechanism by which STAT1 is activated in response to I/R is unknown. IFNγ expression has been detected in lymphocytes and NK cells only, thus precluding autocrine/paracrine stimulation by IFNγ in isolated cultures of cardiac myocytes. Moreover, STAT phosphorylation has been observed in the rat heart within the first few minutes of reperfusion and therefore it is unlikely *de novo* synthesis of cytokines is the source of stimulation (McCormick et al., 2006). It has been postulated that the generation of ROS, which occurs at the onset of reperfusion, may be responsible for activating tyrosine and serine kinases in the cell by an unknown mechanism (Barry et al., 2007). Indeed, myocardial protection from I/R-injury by antioxidants is associated with a decrease in STAT phosphorylation. Epigallocatechin-3-gallate (EGCG), a polyphenol extract from green tea, inhibited I/R induced STAT1 phosphorylation and was associated with reduced infarct sizes in the isolated intact rat heart and reduced apoptotic death of isolated cardiac myocytes (Townsend et al., 2004b). The free radical scavenger tempol has been shown to reduce infarct size and STAT phosphorylation in the rat heart *in vivo* (McCormick et al., 2006).

1.8.7 STAT1 functions as a transcriptional co-activator

STAT1 can influence gene regulation and apoptosis by interacting with other transcription factors and enhancing the regulatory effects of those transcription factors it binds with. Transcriptional regulators that have been discovered to bind STAT1 include CBP/p300, MCM5 and BRCA1 (Zhang et al., 1996, Zhang et al., 1998, Ouchi et al., 2000).

One of the two reported STAT1 deficient mouse mutants expresses a truncated STAT1 protein of 72 kDa, and given the design of the targeting vector, this product

is mostly likely derived from an internal methionine that initiates at position 135 (Meraz et al., 1996) (Figure 1.6). However, the product was found to be expressed at relatively low levels compared to the wild type STAT1 protein in mice and when the mutant protein was over-expressed in isolated mouse kidney fibroblasts it was found to be functionally inactive in response to IFNγ (Meraz et al., 1996). Although the other mouse model has not been shown to express any STAT1 species, there is a similarity in the phenotypes of the two mouse models in that they both have compromised immune systems and have a reduced sensitivity to IFNγ (Meraz et al., 1996, Durbin et al., 1996). Unexpectedly, isolated myocytes and the intact heart from mice containing the truncated STAT1 protein are more sensitive to I/R-injury when compared to wild type littermates (Stephanou et al., 2002).

The finding that there is increased susceptibility to cardiac I/R injury in *Stat1*$^{-/-}$ mice harbouring the truncated STAT1 protein seems to be counterintuitive as STAT1 is considered to be a predominantly pro-apoptotic factor and has been shown to induce apoptosis in cardiac I/R injury (Stephanou et al., 2000, Stephanou et al., 2001b). However, this unexpected result is supported by studies demonstrating that N-terminal deletion mutants of STAT1 are capable of mediating stress-induced apoptosis. Janjua and colleagues demonstrated that N-terminal deletion mutants of STAT1, including mutants lacking the DNA-binding domain, when over-expressed in cells lacking endogenous STAT1 were sufficient for stress-induced apoptosis (Janjua et al., 2002). Furthermore, those mutants that lacked the DNA-binding domain were capable of inducing apoptosis, suggesting STAT1 may act as transcriptional co-activator. Moreover, over-expression of the TAD enhanced stress-induced apoptosis. Similar effects were found in cardiac cells; NRCM cells transfected with the TAD of STAT1 were more susceptible to I/R injury compared to cells transfected with wild type STAT1 (Stephanou et al., 2002). The above-mentioned studies demonstrate that N-terminal STAT1 deletion mutants, including those lacking the DNA-binding domain are sufficient for inducing apoptotic death and that the TAD enhances apoptosis.

Although the overall structure of STATs is quite conserved within the coiled-coiled domain, the DNA-binding domain, the linker domain, the SH2 domain, and the TAD, the amino-terminal domain is less conserved among STATs and suggests this part of the protein may be involved in mediating specific responses (Stephanou, 2004). Deletion of the N-terminal domain in the mutant STAT1 protein found in *Stat1*$^{-/-}$ mice

may have meant loss of regulatory elements that would normally mediate its inactivation, or interaction with transcription factors.

Another point to consider is that even though N-terminal deletion mutants of STAT1 are sufficient for inducing stress, the mutant protein in *Stat1*$^{-/-}$ mice was found to be functionally inactive and *Stat1*$^{-/-}$ mice are immunocompromised (Meraz et al., 1996). Functional inactivity was measured only in responses to IFNγ- and pathogen-induced expression of classical STAT1 regulated genes and immune defects. However, I/R-induced activation of STAT1 and apoptosis in the heart is likely to be mediated via a different pathway and its functional role as a co-activator may be masked when only measuring the activity of genes to which it directly transactivates.

The effects of N-terminal deletion mutants of STAT1 and especially the unexpected truncated protein in the *Stat1*$^{-/-}$ mouse may be considered to be an artificial system. However, physiological relevance exists. Interestingly, it has been shown that STAT1 is cleaved by caspase-3 at position 694, which will ultimately release the C-terminal STAT1 TAD (King and Goodbourn, 1998). Caspase-3 mediated release of the TAD may act as a positive feedback mechanism in apoptosis.

STAT1 interacts with the transcription factor p53, an interaction that is required for maximal activation of p53 responsive genes and apoptosis in cells subjected to DNA damage (Townsend et al., 2004a). Activation of the p53 target genes Bax and Noxa was reduced in cells deficient in STAT1 following treatment with DNA-damaging agents. In cells containing STAT1, induction of Bax and Noxa was abolished when the p53 responsive element in the promoters of these genes was disrupted, thereby demonstrating that the reduction in activity was not a direct result of STAT1 mediated transcription but by an indirect mechanism that involves p53 (Townsend et al., 2004a).

The role of p53 in the regulation of I/R-injury is unclear, however, the expression and activation of p53 is induced in experimental models of different forms of heart disease that involve apoptosis. For example, rapid ventricular pacing in dogs induces heart failure and is associated with apoptotic cell death of ventricular myocytes and enhanced expression and activity of p53 (Leri et al., 1998). ARVC cells exposed to simulated hyperglycaemia underwent apoptosis and was associated with increased activation of p53 (Fiordaliso et al., 2001).

NRCM cells exposed to hypoxia for 48 h resulted in apoptosis, as determined by intranucleosomal DNA cleavage, and increased p53 protein accumulation and transactivation activity (Long et al., 1997). Furthermore, apoptosis was induced in NRCM cells infected with a replication-defective adenovirus expressing human p53, whereas apoptosis was not observed in cells infected with control virus lacking an insert (Long et al., 1997). The expression of p53 mRNA and protein is up-regulated in reperfusion of ischaemic myocardium of Langendorff perfused rat (Maulik et al., 2000, Xie et al., 2000). p53 induces cardiac rupture after MI in mice by positively regulating apoptosis in the area around the infarct (Matsusaka et al., 2006). Moreover, transgenic mice homozygous or heterozygous knockout for the p53 gene had a significantly better survival rate and a lower incidence of left ventricular rupture than wild type mice following MI (Matsusaka et al., 2006).

However, not all studies are in agreement that I/R-injury involves p53. An *in vivo* model of I/R injury, induced by occlusion of the left coronary artery, demonstrated that mice deficient in p53 were equally susceptible to I/R-injury and apoptosis when compared to wild type littermates (Bialik et al., 1997). Similar results were also found for NMCM cells and the isolated intact heart from mice deficient in p53 compared to wild type littermates (Bialik et al., 1997, Webster et al., 1999). These studies that used knockout mice appeared to have dismissed p53 involvement in cardiac I/R injury. However, more recent studies have once again implicated p53 has a regulator of reperfusion induced apoptosis (reviewed by Crow, 2006).

Findings from transgenic studies of p53-related proteins support the contention that p53 is a mediator of cardiac I/R injury. The Bcl-2 family member, Bax, is a proapoptotic protein that is positively regulated by p53. Genetic ablation of the Bax gene in mice resulted in increased resistance to I/R-injury over wild type littermates, as determined by improved functional recovery and reduced necrosis and apoptosis (Hochhauser et al., 2003). The PUMA gene is a transcriptional target of p53 and mediates p53-dependent and independent apoptosis. Langendorff perfused hearts from *PUMA*$^{-/-}$ mice are more resistant than hearts from wild type mice to I/R injury (Nickson et al., 2007, Toth et al., 2006a). Murine double minute 2 (Mdm2) is an E3 ubiquitin ligase that regulates the degradation and activity of proteins including p53. Over-expression of Mdm2 in NRCM cells conferred protection from I/R-induced apoptosis, whereas inhibition of Mdm2 resulted in elevated p53 levels and promoted I/R-induced apoptosis (Toth et al., 2006b). Consistent with this latter finding,

decreased expression of Mdm2 in a genetic mouse model was accompanied by decreased functional recovery of the heart following I/R-injury that was simulated by Langendorff perfusion (Toth et al., 2006b).

Pharmacological inhibition of p53 reduces the extent of I/R injury. Pifithrin-alpha (PFT), a p53 inhibitor, improves cardiac functional recovery and attenuates p53-mediated apoptosis *in vivo* in the rat subjected to cardiac I/R by ligation of the left coronary artery (Liu et al., 2006). Inhibition of p53 with PFT has also been shown to lower the threshold of isoflurane-induced cardioprotection during early reperfusion in rabbits (Venkatapuram et al., 2006). Activation of p53 in I/R injury has been suggested to be via caspase-3/MEKK1 dependent pathway (Zebrowski et al., 2006). MEKK1 is a MAPK that undergoes proteolytic cleavage by caspase-3, in both in vitro and in vivo models of ischaemic injury, to produce a pathological kinase fragment that promotes phosphorylation and activation of p53 by an unknown mechanism (Zebrowski et al., 2006).

The role of STAT1 in the regulation of I/R-injury is not well understood. The evidence from studies in cultured cardiac cells suggests that it acts independently of IFNγ, although the pathways downstream of STAT1 may be similar to when STAT1 is induced by IFNγ. Furthermore, the regulation may involve interaction with p53, and this should be investigated further.

Another regulator of I/R-injury is the extracellular ligand Cardiotrophin-1, and in contrast to STAT1, it elicits cardioprotective effects rather than death-inducing ones. The pathways mediating Cardiotrophin-1 induced effects include the JAK-STAT pathway and specifically STAT3. Cardiotrophin-1 is also a stimulator of hypertrophy, and the signalling pathways involved in the regulation of hypertrophy and I/R-injury by Cardiotrophin-1 will now be discussed.

1.9 Cardiotrophin-1 and heat shock protein 56

1.9.1 Cardiotrophin-1

Cardiotrophin-1 (CT-1) is a 201 amino acid peptide that belongs to the interleukin-6 (IL-6)-type family of cytokines that comprises IL-6, IL-11, leukaemia inhibitory factor (LIF), cardiotrophin like protein (CLC), ciliary neurotrophic factor (CNTF) and oncostatin M (OSM) (Heinrich et al., 2003). IL-6-type cytokines activate genes involved in differentiation, survival, apoptosis and proliferation (Heinrich et al., 2003). IL-6-type cytokines bind cell surface receptor complexes containing the common signal transducing receptor chain glycoprotein 130 (gp130). The signal transducing receptor, gp130, is the most promiscuous of cytokine receptors, and is involved in transducing signals from all IL-6 type cytokines (Muller-Newen, 2003). The intracellular branch of the gp130-transducing signal is mediated by the JAK/STAT pathway.

The receptors involved in the recognition of IL-6-type cytokines can be divided into two groups, the non-signalling α receptors (IL-6Rα, IL-11Rα and CNTFRα) and the signal transducing receptors (gp130, LIFR and OSMR). The intracellular domains of the transducing subunits are associated with JAKs and are tyrosine phosphorylated following cytokine stimulation. Each cytokine binds a particular combination of receptor complex that contains at least one gp130 molecule. IL-6, IL-11 and OSM cytokines bind to their specific α receptor subunits. The cytokine and α receptor complex initiates the recruitment and binding of the signalling receptor subunit. An α receptor subunit has also been proposed to exist for CT-1 (Robledo et al., 1997). IL-6 and IL-11 signalling is mediated by homodimers of gp130 and OSM signalling is mediated by homodimers of gp130 or a heterodimer of gp130 and OSMR. For CT-1 and in the remainder of the IL-6-type cytokines (LIF, CNTF and CLC), signalling is mediated by a heterodimer of gp130 and LIFR (Heinrich et al., 2003) (Figure 1.8).

CT-1 was discovered due to its ability to induce cardiac myocyte hypertrophy *in vitro*, as determined by an increase in cell size and induction of ANF secretion (Pennica et al., 1995). The hypertrophic effect of CT-1 was supported in a subsequent *in vivo* study in which CT-1 was administered to mice by intraperitoneal injection every day for a fortnight (Jin et al., 1996). In this study there were increases in heart-to-body

weight ratios of CT-1 treated mice compared to mice treated with a control substance.

CT-1 mRNA expression has been detected in numerous tissues including the heart and brain in adult mice and humans (Pennica et al., 1995, Pennica et al., 1996). The expression of CT-1 is increased both in human and experimental forms of heart failure. CT-1 mRNA expression has been shown to be increased in the ventricles of humans with cardiomyopathies and circulating levels of CT-1 are increased in humans with chronic heart failure (Zolk et al., 2002, Talwar et al., 1999). CT-1 and gp130 expression is augmented in both left and right ventricles following MI in the rat (Aoyama et al., 2000). The expression of CT-1 is increased in a canine model of CHF and this precedes the activation of BNP (Jougasaki et al., 2000, Jougasaki et al., 2003). Interestingly, increased myocardial CT-1 gene expression precedes pathological heart failure in hypertensive rats, suggesting it is acting upstream in this pathway (Ishikawa et al., 1999).

Growth promoting factors are often also agents that confer resistance to stress and this is true for CT-1. Sheng and colleagues observed that treatment with CT-1 was able to enhance survival of cultured NRCM cells from cell death induced by serum starvation (Sheng et al., 1996). Moreover, NRCM cells pretreated with CT-1 were protected against a subsequent exposure to heat shock or simulated ischaemia (Stephanou et al., 1998). This effect was associated with the ability of CT-1 to induce accumulation of heat shock proteins (hsps) hsp70 and hsp90, whose expression has been previously shown to protect NRCM cells against both thermal and ischaemic stress (Heads et al., 1994, Heads et al., 1995, Cumming et al., 1996).

The cardioprotection conferred by CT-1 from ischaemic damage *in vitro* suggested that it might be used to minimise the effect of ischaemic damage in the human heart (Latchman, 2000). The finding that CT-1 exerts its protective effect by lessening the degree of apoptosis induced by serum removal or ischaemic stress supported such a possibility (Sheng et al., 1996, Stephanou et al., 1998). Further investigation revealed that CT-1 has a protective effect in NRCM cells when added after the ischaemic period at the onset of reoxygenation (Brar et al., 2001a). This effect was observed both in assays of total cell death and assays specifically measuring apoptotic cell death, such as TUNEL labelling or annexin V staining.

Studies in neonatal cells provided preliminary data suggesting that there was a potential therapeutic use of CT-1. However, as I/R-injury is predominantly an adult disease, the need to investigate the effect of this cytokine in an adult model was of importance. ARCM cells and the Langendorff perfused rat heart were protected from I/R-injury when CT-1 was given prior to ischaemia or more importantly at the onset of reoxygenation/reperfusion, when the use of such protective agents would be clinically relevant in I/R-injury (Liao et al., 2002).

The JAK/STAT pathway mediates IL-6-type signalling. However, activation of additional signalling pathways are also induced by IL-6-type cytokines, including CT-1, by binding their receptor (Hirano et al., 1997). Furthermore, there is divergence downstream in the cardioprotective and hypertrophic signalling pathways, suggesting that one effect of CT-1 can potentially be manipulated without interrupting the other, thus harnessing the cardioprotective effect CT-1 and eliminating the deleterious hypertrophic effect. Dissecting the signalling pathways via which CT-1 signals to achieve cardioprotection and hypertrophy facilitates two possibilities; the therapeutic use of CT-1 or similar acting molecules in reperfusion injury and the inhibition of endogenous CT-1 or the pathways it activates to prevent the transition of hypertrophy to heart failure.

CT-1 induced activation of the p42/p44 MAPK pathway has been observed, and results in the threonine phosphorylation of the nuclear factor (NF)-IL-6 (C/EBPβ) transcription factor, allowing it to activate gene transcription (Sheng et al., 1996, Nakajima et al., 1993). CT-1 mediated protection from I/R injury is dependent on its ability to activate the p42/p44 MAPK pathway. Pharmacological inhibition of the p42/p44 MAPK pathway with PD98059 resulted in a blocking of the cardioprotective effect of CT-1 from I/R-induced death of NRCM cells, ARCM cells and in the Langendorff perfused rat heart (Brar et al., 2001a, Liao et al., 2002).

Receptor binding of CT-1 also results in the activation of the PI3-kinase/Akt pathway and is important for cardioprotection. NRCM cells treated with CT-1 results in phosphorylation of Akt (Kuwahara et al., 2000). NRCM cells treated with LY294002, an inhibitor of the PI3K/Akt pathway, attenuated cell death induced by serum withdrawal (Kuwahara et al., 2000). Again, inhibition of the PI3K pathway with LY294002 or wortmannin, demonstrated that the PI3K pathway mediates the

protection conferred by CT-1 in NRCM cells from I/R induced death (Brar et al., 2001b).

Although induced by stress, many hsps are highly expressed in unstressed cells with their synthesis being further enhanced in response to stressful stimuli. For example, hsp90 (each hsp is named on the basis of its mass in kilodaltons) is one of the most abundant proteins in unstressed cells accounting for approximately 1% of the total protein in mammalian cells (Latchman, 2001a). Thus, it is not surprising that hsps have functional roles that are required in normal cells, although they are needed to a greater extent in stressed cells.

Heat shock protein 56 (hsp56) has been implicated as a mediator of the hypertrophic response induced by CT-1 (Figure 1.8). Hsps were first identified as a result of their expression being induced in cells exposed to heat. However, it has been demonstrated that induction of hsps occurs not only in response to heat but also to a variety of stimuli including ischaemia, and they have therefore been referred to as "stress proteins" (Latchman, 2001a). Many hsps have a role in ensuring the correct folding and unfolding of proteins, a function known as chaperoning, and are thus also referred to as chaperone proteins. This function is particularly important in cells exposed to stress when incorrect folding and aggregation of proteins may occur with pathological consequences.

1.9.2 Heat shock protein 56

Hsp56 is an immunophilin, the name ascribed to proteins that bind immunosuppressive drugs such as FK506 (tacrolimus) and cyclosporin. Hsp56 belongs to the family of FK506-binding proteins (FKBPs) and is also known as FKBP52 (Yem et al., 1992, Davies and Sanchez, 2005). Hsp56 has peptidyl-prolyl *cis-trans* isomerase (PPIase) activity (also known as rotamase activity), which is a chaperoning function that catalyzes the conversion of prolyl-peptide bonds from trans- to cis-proline, often a rate-limiting step in protein folding (Schiene and Fischer, 2000). FK506 reduces PPIase activity by binding the smaller immunophilin FKBP12, a complex that inhibits the phosphatase enzyme calcineurin, an important signalling molecule required for T-lymphocyte signal transduction and activation (Liu et al., 1991). However, the role of hsp56 in binding with FK506 is unclear, as the interaction does not inhibit calcineurin (Lebeau et al., 1994).

The structure of hsp56 is composed of four distinct domains. Domains I and II contain a functional site for PPIase activity and a PPIase-like region (Chambraud et al., 1993). Domain III harbours three tetracopeptide repeat (TPR) elements that mediate interactions with other TPR containing proteins. A putative binding site for calmodulin is found in domain IV (Davies and Sanchez, 2005). Expression studies in the rat have demonstrated that hsp56 is highly expressed in thymus, liver, and spleen, with low levels in lung and muscle (Ruff et al., 1992). Hsp56 is located in the cytoplasm and the nucleus (Ruff et al., 1992, Czar et al., 1994).

Hsp56 is a component of steroid receptor complexes, where it interacts with the heat shock protein hsp90 via tetracopeptide repeat domains shared by the two proteins. Hsp90 associates with steroid receptors and keeps them in the inactive form in the cytoplasm until stimulation of the receptor by the corresponding steroid. Upon steroid and receptor interaction, hsp90 dissociates from the receptor enabling the receptor to translocate to the nucleus and activate gene transcription. Steroid receptor complexes consist of a receptor monomer, an hsp90 dimer, the co-chaperone p23, and one of four cochaperones that contain a TPR domain. The TPR cochaperones include two FKBP family members, hsp56/FKBP52 and FKBP51, a member of the cyclosporin-binding immunophilin cyclophilin 40 (CyP40) or the protein phosphatase PP5 (Tranguch et al., 2005).

Hsp56 was first discovered as a component of the progesterone receptor (PR) complex (Nakao et al., 1985, Sanchez et al., 1990) In addition, hsp56 has also been found to be in steroid complexes for the oestrogen (ER), androgen (AR) and glucocorticoid receptors (Renoir et al., 1990, Tai et al., 1986). Possibly the most important physiological role played by hsp56 is in mediating steroid hormone signalling in reproduction. Progesterone and oestrogen are the primary regulators of uterus preparation for embryo implantation, a process dependent on hsp56. Female transgenic mice deficient in the hsp56 gene, *FKBP4*$^{-/-}$, have complete implantation failure due to lack of attainment of uterine receptivity (Tranguch et al., 2005). Male *FKBP4*$^{-/-}$ mice have several defects in tissues that are consistent with androgen insensitivity (Cheung-Flynn et al., 2005).

In addition to binding FK506 and its role in steroid receptor signalling hsp56 has now been implicated in mediating the hypertrophic response induced by CT-1. Railson

and colleagues demonstrated that hsp56 is induced by CT-1 and mediates its hypertrophic effect (Railson et al., 2001). Increased synthesis of hsp56 mRNA and protein was detected in NRCM cells treated with CT-1. Moreover, over-expression of hsp56 in NRCM cells, achieved by transformation with a viral or plasmid expression vector for hsp56, was sufficient for inducing hypertrophy as determined by an increase in cell size and protein to DNA ratio. In NRCM cells transfected with the plasmid expression vector for hsp56, the hypertrophic effect was abrogated with an hsp56 antisense expression construct. The hypertrophic effect of hsp56 is the first time such an effect for a heat shock protein had been demonstrated. The effect was also specific to hsp56 as no hypertrophy was observed in cells in which hsp27, hsp70 or hsp90 was over-expressed.

Jamshidi and colleagues demonstrated that the hypertrophic effect of hsp56 is dependent on several well-characterized signal transduction pathways (Jamshidi et al., 2004). Pharmacological inhibition of the JAK/STAT, PI3K/Akt or MEK signalling pathways abrogated the hypertrophic effect induced by hsp56 over-expression in NRCM cells, as determined by an increase in cell size and activity of a luciferase reporter of the ANF promoter that was co-transfected with hsp56.

CT-1 mRNA expression has been shown to be induced by Urocortin, a peptide related to corticotrophin releasing hormone that has cardioprotective and hypertrophic effects. The role of Urocortin in cardioprotection from I/R-injury will be discussed further.

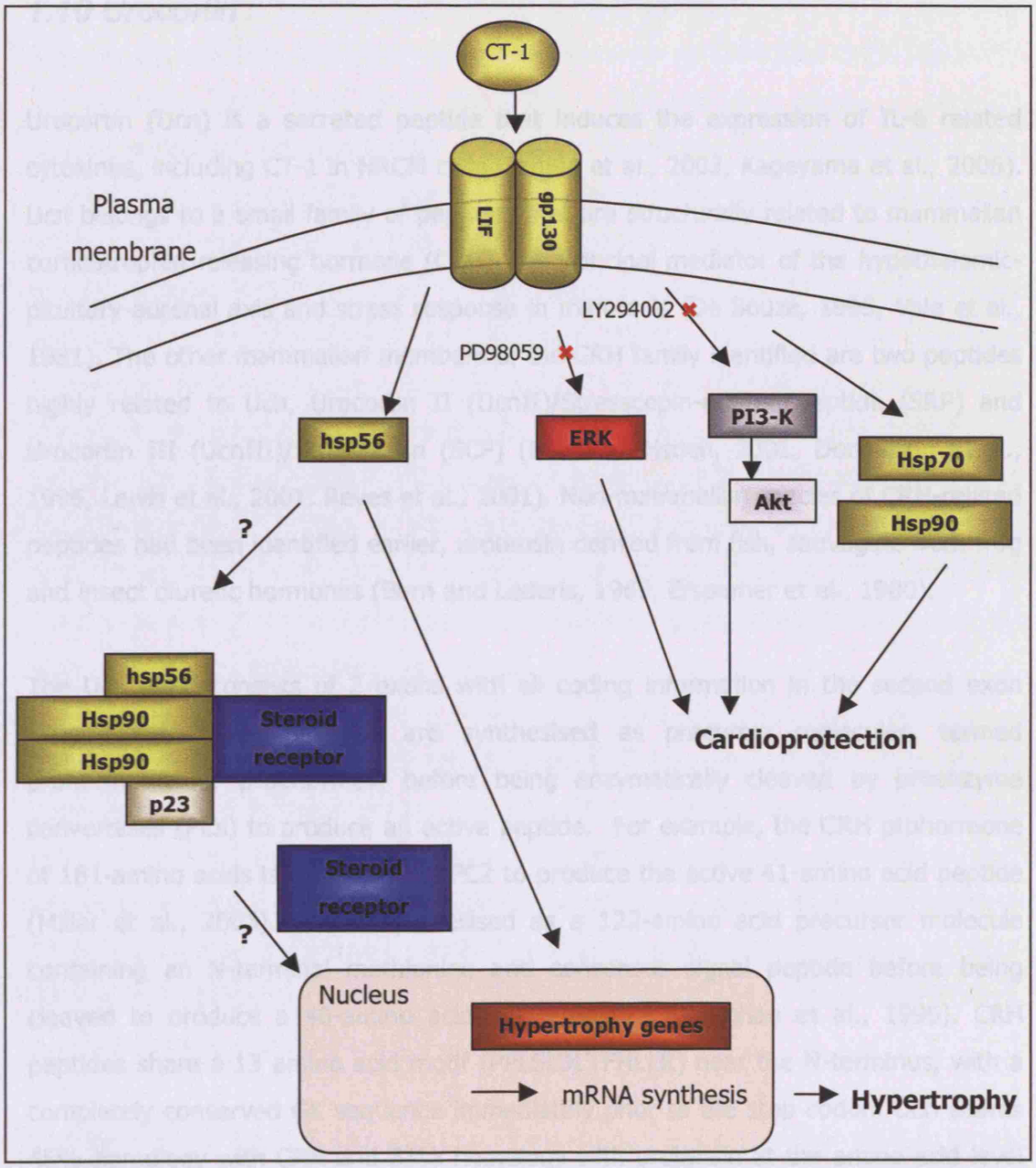

Figure 1.8 The cardiotrophin-1 (CT-1) signalling pathway. Binding of CT-1 to its receptor, a heterodimer of leukaemia inhibitory factor (LIF) and gp130 subunits, induces cardioprotective and hypertrophic signalling pathways in cardiac myocytes. Cardioprotective pathways of CT-1 signal via the ERK and PI3-K/Akt signalling pathways, which are inhibited by the pharmacological agents PD98059 and LY294002, respectively. CT-1 mediated cardioprotection is also dependent on the induction of hsp70 and hsp90 accumulation. CT-1 induces hypertrophy, including induction of mRNA synthesis of hypertrophic molecules such as ANF, and is dependent on its ability to induce hsp56. The hsp56 protein is known to associate with steroid receptor complexes although it is not known if this is important for CT-1 mediated effects

1.10 Urocortin

Urocortin (Ucn) is a secreted peptide that induces the expression of IL-6 related cytokines, including CT-1 in NRCM cells (Janjua et al., 2003, Kageyama et al., 2006). Ucn belongs to a small family of peptides that are structurally related to mammalian corticotrophin releasing hormone (CRH), the principal mediator of the hypothalamic-pituitary-adrenal axis and stress response in mammals (De Souza, 1995, Vale et al., 1981). The other mammalian members of the CRH family identified are two peptides highly related to Ucn, Urocortin II (UcnII)/Stresscopin-related peptide (SRP) and Urocortin III (UcnIII)/Stresscopin (SCP) (Hsu and Hsueh, 2001, Donaldson et al., 1996, Lewis et al., 2001, Reyes et al., 2001). Non-mammalian species of CRH-related peptides had been identified earlier, urotensin derived from fish, sauvagine from frog and insect diuretic hormones (Bern and Lederis, 1969, Erspamer et al., 1980).

The Ucn gene consists of 2 exons with all coding information in the second exon (Zhao 1998). CRH peptides are synthesised as precursor molecules, termed prohormones or proenzymes, before being enzymatically cleaved by proenzyme convertases (PCs) to produce an active peptide. For example, the CRH prohormone of 181-amino acids is converted by PC2 to produce the active 41-amino acid peptide (Miller et al., 2003). Ucn is synthesised as a 122-amino acid precursor molecule containing an N-terminal methionine and consensus signal peptide before being cleaved to produce a 40-amino acid active peptide (Vaughan et al., 1995). CRH peptides share a 13 amino acid motif (PPLSIDLTFHLLR) near the N-terminus, with a completely conserved GK sequence immediately prior to the stop codon. Ucn shares 45% homology with CRH and 63% homology with urotensin at the amino acid level (Vaughan et al., 1995). CRH family members are evolutionary conserved; homology between human and mouse is 100% for CRH and 95% for Ucn (Coste et al., 2002).

Ucn was the second mammalian member of the CRH family discovered when it was identified by screening a rat midbrain cDNA library with a probe derived from urotensin (Vaughan et al., 1995). Histological analysis of the midbrain region demonstrated that Ucn is highly expressed in the Edinger-Westphal nucleus and the lateral superior olive, both of which do not express CRH (Vaughan et al., 1995). Although originally identified in the brain, Ucn has been found to be expressed in the placenta, lymphocytes and the heart (Petraglia et al., 1996, Bamberger et al., 1998,

Okosi et al., 1998). Synthetic Ucn stimulates adrenocorticotrophin (ACTH) secretion from rat pituitary cells in primary culture and *in vivo* in rat (Vaughan et al., 1995).

Cell signalling by the CRH family is mediated by binding two types of G-protein coupled seven transmembrane receptor, CRH-R1 and CRH-R2, which are coupled to adenylate cyclase (Lawrence and Latchman, 2006). Alternative RNA splicing gives rise to subtypes of CRH receptors. To date, there are eight CRH-R1 and four CRH-R2 isoforms identified (Lawrence and Latchman, 2006). In COSM6 cells transiently transfected with expression constructs for CRH-R1 and CRH-R2 receptors, it was demonstrated that CRH-R2 receptors bind Ucn with higher affinity than CRH-R1 and Ucn was ten fold more potent at inducing intracellular cAMP in cells expressing CRH-R2 (Vaughan et al., 1995). In the same study, Ucn binding to CRH-R2 was forty times stronger than CRH. CRH-R1 shows no appreciable binding to UCN II or III but binds UCN and CRH with similar potency (Hsu and Hsueh, 2001, Donaldson et al., 1996, Lewis et al., 2001, Reyes et al., 2001).

CRH-R1 receptors are generally found in the CNS whereas CRH-R2 receptors are more widespread in the periphery and discretely located in the CNS. Although this distinctly different distribution is true for rodents, it is not so well defined in humans (Coste et al., 2002). In rodents, CRH-R1 receptors are highly expressed on ACTH containing cells of the anterior pituitary and are responsible for mediating pituitary-adrenal activation. They are also found in brain regions including the cerebral cortex, cerebellum, hippocampus, brain stem and hypothalamus.

Endogenous inhibition of CRH and Ucn signalling is mediated by CRH binding protein (CRH-BP). CRH-BP is a 37 kDa secreted glycoprotein that is known to bind CRH and Ucn with high affinity, thus preventing them from stimulating CRH receptors (Westphal and Seasholtz, 2006). Molecules that inhibit CRH have been developed for potential clinical use in treating undesirable effects of CRH on the nervous system, such as depression and anxiety (Lawrence and Latchman, 2006). These molecules tend to be antagonists of CRH receptors and can be used experimentally to elucidate the roles that CRH family members play in disease pathways. For example, the synthetic peptides, alpha helical CRH (αhCRH) and astressin, are non-selective CRH receptor antagonists. However, selective inhibition of CRH receptor can be achieved with R278995 and CRA0405, which are antagonists of the CRH-R1 and CRH-R2 receptors respectively (Lawrence and Latchman, 2006).

CRH-R2 receptors are the only type of CRH receptor found in the heart, the alpha form in man and the beta form in the rat (Chen et al., 1993, Stenzel et al., 1995, Perrin et al., 1995, Kishimoto et al., 1995). CRH has been shown to stimulate adenylate cyclase activity in cardiac myocytes (Heldwein et al., 1996). Given that CRH-R2 receptors are the only CRH receptor found in the heart and that Ucn has a higher affinity for this receptor than CRH, it suggests Ucn may have important physiological effects in the heart and has led to the idea that CRH-R2 may be a natural receptor for Ucn (Latchman, 2001b).

The CRH family of peptides have effects on the nervous, cardiovascular and immune systems. Injection of Ucn can produce enhanced anxiety and activity as well as an appetite suppressing effect in the mouse and rat that is more potent than CRH (Spina et al., 1996). The distribution of CRH receptors in different sites of the brain suggests the effects of Ucn on anxiety are mediated via CRH-R1 and appetite via CRH-R2 (Lovenberg et al., 1995). CRH stimulates T and B cell proliferation *in vitro*, when applied exogenously CRH and Ucn can reduce inflammation (Turnbull et al., 1996).

CRH peptides mediate central and peripheral regulation of cardiovascular function. Intracerebroventicular (ICV) administration of CRH elicits cardiovascular responses similar to effects of stress, increasing heart rate, cardiac output, and mean arterial pressure, which depend on an intact sympathetic nervous system (Fisher et al., 1983). However, intravenous (IV) delivery was shown to induce a marked decrease in mean arterial pressure accompanied by reflex tachycardia due to vasodilation in specific beds (Lenz et al., 1985). Direct peripheral actions were subsequently demonstrated in isolated heart preparations. Perfusion of CRH in the isolated heart resulted in a sustained increase in coronary blood flow, a positive inotropic effect, and rapid release of ANF (Grunt et al., 1992, Grunt et al., 1993). IV administration of Ucn also induced a reduction in mean arterial pressure and increased cardiac contractility in rodents, although it is possible that the decrease in blood pressure contributed to the increase in cardiac contractility (Vaughan et al., 1995, Parkes et al., 1997, Terui et al., 2001). However, Ucn induced an increase in cardiac in contractility in sheep, in addition to increased cardiac output and coronary flow, and this was not accompanied with hypotension (Parkes et al., 1997). The expression of Ucn II and III mRNA in certain brain regions and the finding that delivery of Ucn II in the CNS activates several brain regions important in autonomic function suggests

these peptides may mediate central regulation of cardiovascular function (Coste et al., 2002).

CRH and Ucn mRNAs are expressed in the rodent heart and Ucn protein has been detected in all four chambers of the human heart (Muglia et al., 1994, Okosi et al., 1998, Kageyama et al., 2000, Nishikimi et al., 2000, Kimura et al., 2002). Ucn II has been shown to be highly expressed in the human and mouse heart whereas Ucn III is virtually absent in the mouse heart (Hsu and Hsueh, 2001, Lewis et al., 2001). Interestingly, this pattern of Ucn II and Ucn III mRNA expression is reversed in cardiac myocytes from rat, with expression of Ucn III mRNA but no Ucn II mRNA observed (Chanalaris et al., 2003).

Studies in transgenic mice deficient in CRH-R2 demonstrate the importance of this receptor in mediating the regulation of cardiovascular function by the CRH family of peptides. *CRH-R2*$^{-/-}$ mice have increased arterial pressure compared to wild type mice, which is not lowered with systemic administration of Ucn (Coste et al., 2000). It has been postulated that Ucn affects arterial pressure through activation of CRH-R2 in vascular beds because the rapid fall in peripheral resistance is the primary cause of hypotension associated with CRH peptides in rodents (Coste et al., 2002). This is indeed possible, as CRH-R2 expression has been reported in cardiac arterioles and in a vascular smooth muscle cell line (Chalmers et al., 1995, Perrin et al., 1995, Kageyama et al., 2000).

1.10.1 Urocortin protects from I/R injury

Ucn has been shown to be a cardioprotective agent, reducing the effects of I/R induced death or injury. Ucn mRNA expression increases in NRCM cells following heat shock or ischaemia (Okosi et al., 1998, Brar et al., 1999). Treatment with Ucn protected NRCM cells from a subsequent dose of simulated lethal ischaemia as measured by the uptake of trypan blue and LDH release (Okosi et al., 1998). The protective effect of exogenous Ucn in NRCM cells was shown to be superior to that of CRH and urotensin (Brar et al., 1999). Furthermore, Ucn is released into the culture medium of NRCM cells following ischaemia (Brar et al., 1999). When another culture of NRCM cells were incubated in this conditioned medium they were protected from ischaemia (as measured by trypan blue uptake and LDH release), an effect that was abolished with αhCRH (Brar et al., 1999). These findings demonstrate that stress induced production of Ucn protects NRCM cells in an autocrine/paracrine manner.

Furthermore, the cardioprotective effect of Ucn may, at least in part, be dependent on its ability to induce the expression of CT-1.

The induction of the Ucn gene in ischaemia may be mediated by the transcription factors C/EBP, NF-IL6/NF-IL6β and NF-κβ. MAP kinase signalling pathways are activated in ischaemia and NF-IL6 and NF-IL6β are substrates of MAP kinase phosphorylation (Nakajima et al., 1993).The expression and activity of NF-IL6, NF-IL6β and the p65 subunit of NF-κβ are induced by hypoxia or ischaemia (Yan et al., 1997, Brar et al., 1999). Moreover, the Ucn gene contains a consensus site for C/EBP transcription factors and the CRH gene has been shown to be transcriptionally regulated by NF-IL6 and NF-IL6β in neuronal and lymphoblastoid cells (Stephanou et al., 1997).

Like CT-1, Ucn protects NRCM cells and the intact heart from simulated I/R injury when given at reperfusion (Brar et al., 2000). Whereas previous experiments in NRCM cells had demonstrated Ucn protected against total cell death, in this study Brar and colleagues used TUNEL and annexin V assays in NRCM cells to show that Ucn was specifically inhibiting apoptosis, which was contributing to cell death following simulated I/R (Brar et al., 2000). Ucn was also shown to protective when given at reperfusion in an *in vivo* rat model of I/R (Schulman et al., 2002). In order to demonstrate that reduced infarct sizes in the *in vivo* rat model was not a secondary effect of the reduction in arterial pressure induced by Ucn, glyceryl trinitrate (GTN) was infused to mimic the hypotensive effect of Ucn. Infusion of GTN did not reduce infarct sizes.

The protective effect of Ucn in the Langendorff perfused rat heart has also been measured in terms of improved functional recovery following I/R. Scarabelli and colleagues observed improvements of developed pressure (DP) and diastolic pressure (dP) ranging from partial to complete recovery depending on when Ucn was delivered (Scarabelli et al., 2002). Ucn delivery prior to ischaemia and during reperfusion resulted in complete recovery of DP and dP. However, when given only prior to ischaemia there was normalization of DP and partial restoration of dP. When given at reperfusion there was progressive but partial recovery of DP and dP. Improvements in cardiac function were accompanied by reduced necrotic and apoptotic cell death, as determined by reduced CPK release and caspase-3 activity. This reduction in cell death was observed whether Ucn was delivered prior to

ischaemia or at reperfusion. However, improvements in ATP and creatine phosphate stores were observed when Ucn was given prior to ischaemia but not when given only at reperfusion.

Cardiopulmonary bypass, cardioplegic arrest and subsequent reperfusion expose the heart to an iatrogenic (meaning caused by medical treatment) I/R injury (IRI) (Scarabelli et al., 2004). Different cardioplegic techniques (crystalloid, cold blood and warm blood cardioplegia) have been developed to prevent this injury (Mauney and Kron, 1995). However, protection is inadequate, especially in surgical procedures requiring prolonged cardiac arrest (Scarabelli et al., 2004). Cardiac myocyte survival in human heart biopsies subjected to IRI is associated with Ucn expression (Scarabelli et al., 2004). Only viable cells expressed Ucn whereas it was not detected in TUNEL positive cardiac myocytes. This study suggests that Ucn improves cardiac myocyte survival following I/R injury.

1.10.2 Cardioprotective signalling pathways of Urocortin

Members of the CRH family activate p42/p44 MAPK enzymes (Figure 1.9). For example, CRH has been shown to activate p42/p44 MAPK in the Chinese hamster ovary (CHO) cell line transfected with CRH-R1 and CRH-R2 receptors (Rossant et al., 1999). Ucn was shown to activate p42/p44- but not p38- or JNK- MAPK in NRCM cells (Brar et al., 2000). Ucn induced activation of p42/p44 MAPK is necessary for mediating its protective effect. Blocking p42/p44 MAPK activation with the MEK inhibitor PD98059 or dominant negative mutants of p42/p44 MAPK resulted in loss of the protective effect of Ucn in NRCM cells following I/R, even when Ucn was given at reperfusion (Brar et al., 2000). Similar results have been demonstrated in the Langendorff perfused and *in vivo* rat heart. Schulman and colleagues demonstrated that administering Ucn for the first 20 minutes of reperfusion in the Langendorff perfused rat heart was cardioprotective (Schulman et al., 2002). However, when PD98059 was also added with Ucn in the first 20 minutes of reperfusion the cardioprotective effect was abolished. In the same study, using an *in vivo* rat model of I/R, Ucn delivered just before reperfusion was cardioprotective. However, when PD98059 was injected intravenously 3 minutes prior to reperfusion, the cardioprotective effect of Ucn was inhibited.

Activation of the p42/p44 MAPK pathway is necessary for the increased expression of hsp90 observed in NRCM cells treated with Ucn (Brar et al., 2002a). Increased

expression of hsp90 following Ucn treatment is not a result of increased transcription, as the increase was not blocked by actinomycin D, an inhibitor of transcription. However, increased synthesis of proteins is necessary for cardioprotection mediated by Ucn. Cycloheximide, a translational inhibitor blocks Ucn mediated protection from ischaemia induced death in NRCM cells (Brar et al., 2002a). Thus, increased hsp90 expression may be a result of increased hsp90 mRNA stability and/or modified transport to the cytoplasm. However, the role of hsp90 in Ucn signalling is unclear, as earlier studies have seemingly dismissed a protective role for hsp90 in I/R-injury (Heads et al., 1995, Cumming et al., 1996). These studies do not satisfactorily preclude hsp90 as a protective agent from I/R-injury, whether by its over-expression or as a mediator of Ucn induced protection. For instance, there is more than one isoform of hsp90 and those studies that found hsp90 was not protective used over-expression of the beta isoform (hsp90β). Expression of the alpha isoform (hsp90α) has been shown to be induced in reperfused hearts and might potentially be protective from I/R-injury (Nishizawa et al., 1996). Possibly, hsp90 does not protect from I/R-injury when over-expressed. However, Ucn may induce other proteins that are required for hsp90 mediated protection, an effect that may not be observed by hsp90 over-expression alone.

Phosphorylation of Akt is observed in cardiac myocytes treated with Ucn in a PI3K dependent manner. Ucn induced phosphorylation of Akt in NRCM cells was inhibited with the PI3K inhibitors, Wortmannin and LY294002 (Brar et al., 2002b). This was the first study to demonstrate that a peptide of the CRH family can induce Akt via the PI3K pathway. Moreover, Wortmannin and LY294002 attenuated the reduction in I/R-induced necrotic and apoptotic death observed in NRCM and ARVC cells treated with Ucn. Inhibition of PI3K and Akt by over-expression of dominant-negative mutants of these two kinases in NRCM cells also resulted in the loss of Ucn mediated cardioprotection from I/R-induced death.

The findings of some studies suggest that the mechanism by which Ucn elicits cardioprotection is one similar to that of ischaemic preconditioning (IPC). This idea is supported by those studies demonstrating that Ucn is cardioprotective in cultured myocytes when ischaemia is simulated either immediately or when delayed after Ucn treatment, thus mimicking the effects of immediate and delayed IPC respectively. The cardioprotective effect of Ucn in the Langendorff perfusion model can only be investigated when ischaemia is simulated shortly after Ucn treatment as the heart

retains function when perfused *ex vivo* for only a few hours. As there are no such reports *in vivo*, what is known about the cardioprotective of Ucn treatment when ischaemia is delayed is based on studies in cultured cardiac myocytes.

Lawrence and colleagues used Affymetrix gene chips to screen genes whose expression is modulated by Ucn in NRCM cells and found significant increases in two mediators of preconditioning that are involved in cardioprotection; PKCε and the K_{ATP} channel subunit potassium inward rectifying (Kir) 6.1 (Kir6.1) (Lawrence et al., 2002, Lawrence et al., 2005). Increases in mRNA levels following Ucn treatment correlated with increases in the corresponding proteins in NRCM cells and the Langendorff perfused rat heart.

A number of studies have implicated K_{ATP} channels in mediating survival pathways in I/R-injury, in particular preconditioning (Scarabelli et al., 2002, Takano et al., 2000, Takashi et al., 1999). The Kir6.1 subunit is located predominantly in the inner mitochondrial membrane (Suzuki et al., 1997). Simulated I/R also induces the expression of Kir6.1 in NRCM cells and the Langendorff perfused rat heart, however, treatment with αhCRH blocked either Ucn or I/R induced expression of Kir6.1 (Lawrence et al., 2002, Lawrence et al., 2005). Chromakalim, a K_{ATP} channel opener, provided cardioprotection that was similar to Ucn, whereas the protective effect of Ucn was blocked with Tolbutamide, an inhibitor of K_{ATP} channel opening (Lawrence et al., 2002, Lawrence et al., 2005) . Although Tolbutamide is generally considered to be a sarcolemmal K_{ATP} blocker, interference of K_{ATP} mitochondrial channels has been reported and it is generally believed that it is opening of the mitochondrial channel that is responsible for the protective effect of preconditioning (Takano et al., 2000). Therefore, Lawrence and colleagues used 5-HD to specifically inhibit mitochondrial K_{ATP} channels and found that this inhibited Ucn mediated protection. Furthermore, inhibition of Kir6.1 with a dominant negative mutant enhanced I/R induced death (Lawrence et al., 2002, Lawrence et al., 2005).

Translocation of PKCε from a cytosolic fraction to a membrane rich fraction rich in mitochondria was observed in NRCM cells and the Langendorff perfused heart exposed to Ucn for 10 minutes, an effect that was blocked by αhCRH and a specific inhibitor peptide of PKCε (Lawrence et al., 2005). Specific localisation of PKCε in the mitochondria was demonstrated by immunoflourescence in NRCM cells showing co-localisation of PKCε and the mitochondrial specific marker dye, Mitotracker.

Moreover, preventing mitochondrial translocation of PKCε resulted in loss of the protective effect of Ucn from I/R-injury (Lawrence et al., 2005).

Gordon and colleagues demonstrated that Ucn protected ARCM cells from simulated ischaemia when Ucn was present during the ischaemic episode, as determined by release of LDH and CK enzymes into the culture medium (Gordon et al., 2003). The cardioprotective effect of Ucn was comparable with adenosine, which is thought to be a trigger for PKC activation and the classical preconditioning cascade. ARCM cells were treated with Ucn for 5 minutes with 10 minutes of recovery or 20 minutes with 20 hours of recovery prior to ischaemia. These treatment protocols were designed to mimic classical and delayed preconditioning and both were found to be protective. Moreover, the PKC inhibitor chelerythrine and the K_{ATP} channel blocker 5-HD were able to attenuate the cardioprotective effect of Ucn.

In the Affymetrix gene chip study conducted by Lawrence and colleagues, the expression of some genes decreased with Ucn treatment, notably the gene for the calcium insensitive phospholipase 2 ($iPLA_2$) enzyme (Lawrence et al., 2003). This was confirmed by RT-PCR and a decrease in the corresponding protein was also observed by Western blotting. Interestingly, simulated I/R-injury also induced a decrease in $iPLA_2$. Moreover, the I/R induced decrease in $iPLA_2$ was abrogated in the presence of αhCRH, suggesting that the release of Ucn following I/R is responsible for the reduction in $iPLA_2$. There was a concomitant reduction in the iPLA2 substrate lysophosphatidylcholine (LPC) in Ucn treated cells with lower levels of iPLA2. However, I/R caused a large increase in LPC concentration, which was significantly lowered by Ucn treatment. Thus, as iPLA2 expression decreases in I/R, there is most likely an increase in its activity for the resulting increase in LPC accumulation. LPC accumulation is toxic for the cell. Bromoenol lactone (BEL) is an inhibitor of LPC and was shown to inhibit cell death of NRCM cells and improve the functional recovery of the Langendorff perfused rat heart following simulated I/R-injury. The protective effect of BEL was not additive when given in combination with Ucn, suggesting that the two agents protected via a common mechanism.

The roles played by PKCε, Kir6.1 and iPLA2 in Ucn mediated protection involve interaction with mitochondria and prevention of mitochondrial damage. The Kir6.1 subunit has been shown to be the diazoxide (a potassium channel opening drug) sensitive and mitochondrially localised form (Gross and Fryer, 1999, Cui et al., 2001).

The iPLA2 substrate LPC can modulate K_{ATP} channels and PKCε, and PKCε can interact with K_{ATP} channels and iPLA2 (Eddlestone, 1995, Steer et al., 2002). PKCε translocates to mitochondrial membranes and interact with mitochondrial proteins including MPTP (Baines et al., 2003). The loss of $\Delta\Psi_m$ in NRCM cells following I/R, as measured by a reduction in TMRM, was abrogated by Ucn, the K_{ATP} channel opener chromakalim or the LPC inhibitor BEL (Lawrence et al., 2004). Ucn mediated protection was abrogated by a PKCε inhibitor peptide and the inhibitor peptide or the K_{ATP} channel blocker 5-HD caused greater damage than I/R alone (Lawrence et al., 2004). Furthermore, partial restoration of ATP and CK levels at the end of both ischaemia and reperfusion suggests Urocortin acts on the mitochondria to maintain the respiratory transport chain, thus preventing mitochondrial injury (Scarabelli et al., 2002).

In addition to being a cardioprotective agent, Ucn is also a hypertrophic one. Hypertrophy is associated with peptides such as Ucn, which are potent stimulants of contractile function and that signal through cAMP (Miyakoda 1987). Experiments in NRCM cells have demonstrated that Ucn stimulates release of ANF and BNP (Ikeda et al., 1998). Moreover, LVH is associated with higher expression of Ucn mRNA and Ucn treatment also induces an increase in ARVC cell size and NRCM cell size with an accompanying increase in the protein to DNA ratio (Nishikimi et al., 2000, Railson et al., 2002). Ucn induces an increase in intracellular cAMP with concomitant increases in collagen DNA synthesis in fibroblasts (Nishikimi et al., 2000). Thus, Ucn may be involved in processes such as scar formation and collagen deposition that occur during ventricular remodelling of the failing heart.

The ability to induce hypertrophy seemingly precludes Ucn or similarly acting molecules from clinical use. However, it has been demonstrated that the signalling pathways that mediate the hypertrophic effect of Ucn are distinct from the ones that are involved in its cardioprotective effect. Blocking the p42/p44 MAPK pathway inhibits Ucn mediated protection but not Ucn induced hypertrophy (Railson et al., 2002,). Furthermore, Ucn induced hypertrophy requires activation of the transcriptional coactivator p300, although its role in Ucn mediated protection is not known (Railson et al., 2002, Davidson et al., 2005). The results from these studies suggest that analogues of Ucn, or similarly acting molecules, that lack its ability to stimulate the hypertrophic signalling pathway could be synthesised and used in therapy of I/R-injury.

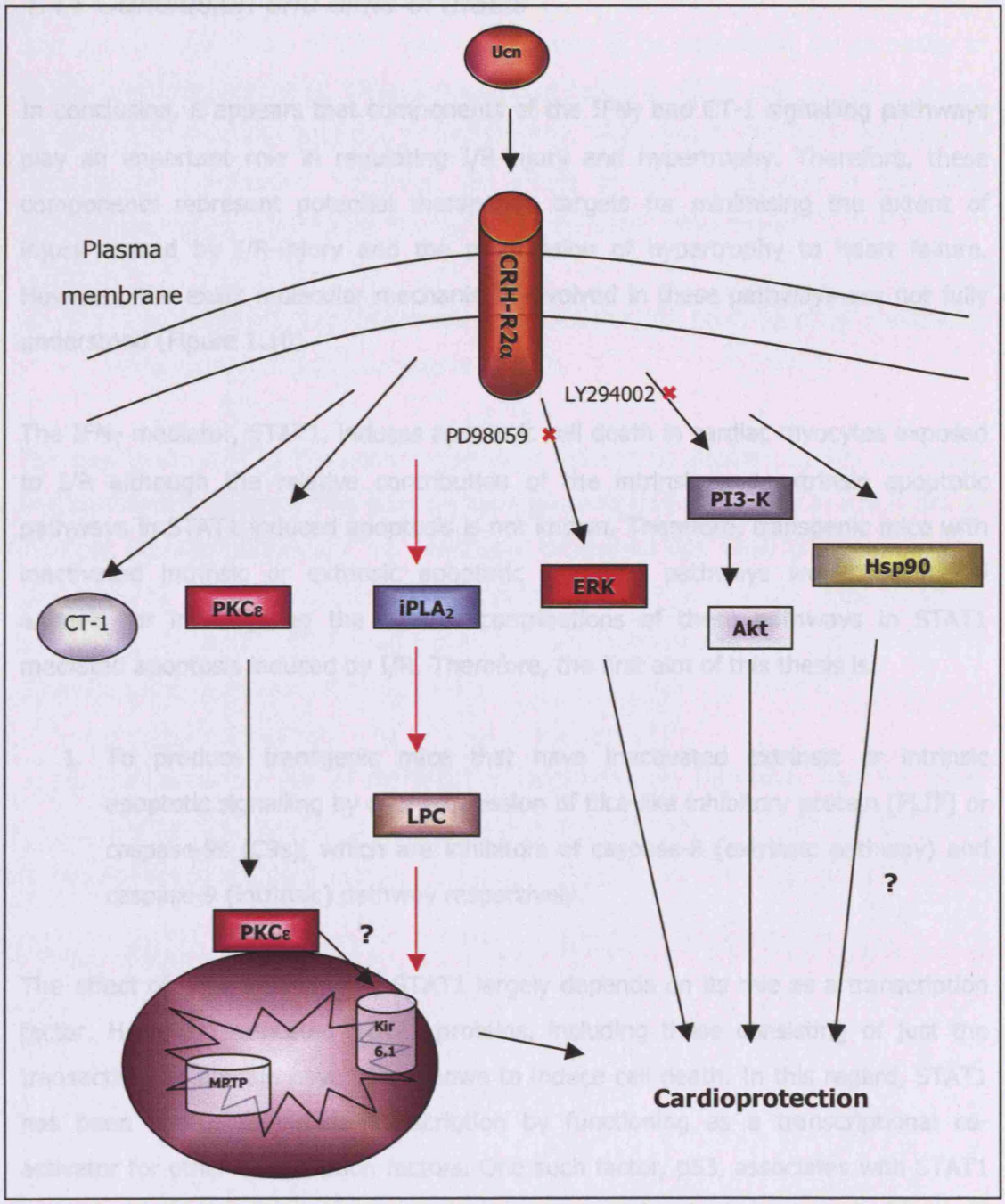

Figure 1.9 The cardioprotective signalling pathways of Urocortin (Ucn). Ucn binds the corticotrophin receptor 2α (CRH-R2α) in the heart and stimulates signalling pathways that mediate protection from I/R injury. Cardioprotection is mediated by the ERK and PI3-K/Akt signalling pathways. Ucn mediated protection also involves protection of the mitochondria through activation of PKCε, increasing Kir6.1, decreasing $iPLA_2$ and the inhibition of mitochondrial permeability transition pore (MPTP) from opening.

1.11 Conclusion and aims of thesis

In conclusion, it appears that components of the IFNγ and CT-1 signalling pathways play an important role in regulating I/R-injury and hypertrophy. Therefore, these components represent potential therapeutic targets for minimising the extent of injury caused by I/R-injury and the progression of hypertrophy to heart failure. However, the exact molecular mechanisms involved in these pathways are not fully understood (Figure 1.10).

The IFNγ mediator, STAT1, induces apoptotic cell death in cardiac myocytes exposed to I/R although the relative contribution of the intrinsic and extrinsic apoptotic pathways in STAT1 induced apoptosis is not known. Therefore, transgenic mice with inactivated intrinsic or extrinsic apoptotic signalling pathways would be model animals for investigating the relative contributions of these pathways in STAT1 mediated apoptosis induced by I/R. Therefore, the first aim of this thesis is:

1. To produce transgenic mice that have inactivated extrinsic or intrinsic apoptotic signalling by over-expression of flice-like inhibitory protein (FLIP) or caspase-9s (C9s), which are inhibitors of caspase-8 (extrinsic pathway) and caspase-9 (intrinsic) pathway respectively.

The effect of gene induction by STAT1 largely depends on its role as a transcription factor. However, truncated STAT1 proteins, including those consisting of just the transactivation domain have been shown to induce cell death. In this regard, STAT1 has been shown to induce transcription by functioning as a transcriptional co-activator for other transcription factors. One such factor, p53, associates with STAT1 and this interaction has been shown to be necessary for the induction of p53 target genes. A commercially available strain of STAT1 deficient mice is IFNγ insensitive but hearts from these mice are more sensitive to I/R injury compared to those from wild types. However, these mice express a truncated STAT1 protein lacking the N-terminal domain (1-135 amino acids). Therefore, the second aim of this thesis is:

2. To test if the increased sensitivity of hearts from *Stat1*$^{-/-}$ mice to I/R injury is dependent on an interaction between p53 and the truncated STAT1 protein expressed in these mice, and to identify other proteins regulated in the process using a proteomic approach.

The hypertrophic effect of CT-1 has been shown to be dependent on its ability to induce expression of hsp56. Over-expression of hsp56 in NRCM cells has been shown to be sufficient for the induction of hypertrophy. Thus, hsp56 may be a mediator of pathological hypertrophy. However, the effect of hsp56 induction in the adult mammalian heart is not known. Therefore the third aim of this thesis:

3. To assess the hypertrophic effect of hsp56 in the adult heart by generating transgenic mice that over-express hsp56.

The expression of CT-1 has been shown to be induced by another, further upstream, cardioprotective peptide. This peptide, Ucn, protects from I/R-injury in the heart via multiple signalling pathways. Ucn mediated protection has been shown to involve protection of the mitochondria and inhibition of the MPTP in NRCM cells. However, the effect of Ucn on MPTP opening in the adult mammalian heart is not known. Therefore, the fourth aim of this thesis is:

4. To assess the role of the MPTP in Ucn mediated protection from I/R injury and cell death in the Langendorff perfused adult rat heart and isolated ARVC cells.

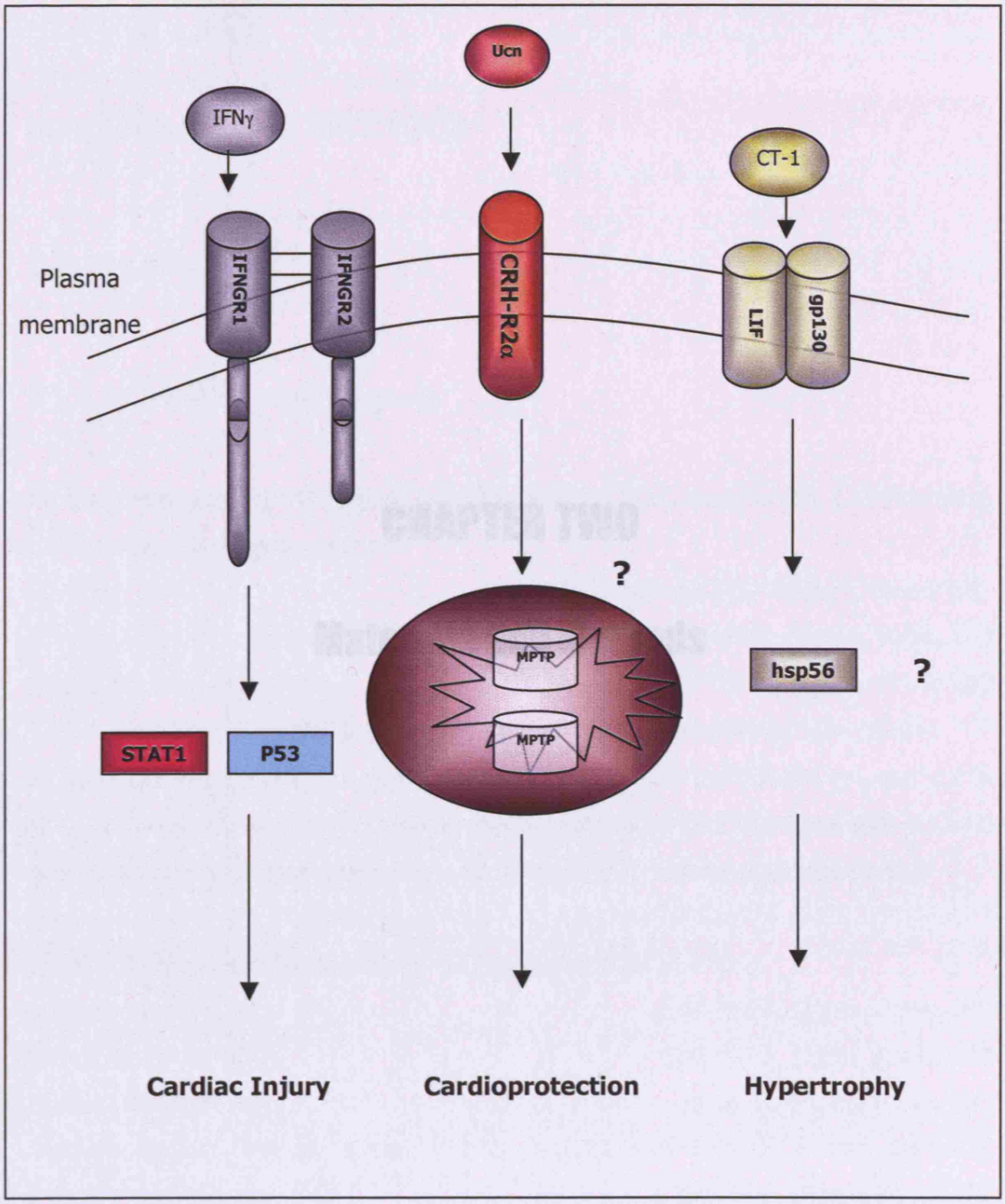

Figure 1.10 The regulation of cardiac injury, cardioprotection and hypertrophy by IFNγ, Ucn and CT-1 signalling pathways. The role of STAT1/p53, MPTP and hsp56 in these pathways is unclear. The aims of thesis will attempt to elucidate these mechanisms.

CHAPTER TWO

Materials and Methods

CHAPTER TWO

MATERIALS AND METHODS

2.1 Materials

2.1.1 Chemicals and reagents

All chemicals used in this project were supplied by BDH, Lutterworth, Leicestershire, UK with the following exceptions:

Alcohols (Hayman Ltd, Witham, Essex, UK)
Dimethyl Sulfoxide (DMSO) (#D-5879, Sigma, Poole, UK)
Trypan Blue solution (0.4%) (#T8154, Sigma, Poole, UK)
5-bromo-4-chloro-3-indolyl-β-D-galactopyranoside in dimethylformamide (X-gal)

All solid chemicals were dissolved in ddH_2O, adjusted to the correct pH with 0.1 M HCL, glacial acetic acid or 0.1M NaOH and autoclaved or filter sterilised with 0.22 μm syringe driven filter units (Millipore, Bedford, MA, USA) unless otherwise stated.

Deoxynucleoside Triphosphates (dNTPs)- 100 mM (pH 7.5) set of dATP, dCTP, dGTP and dTTP (Promega, Southampton, UK) were stored at -20 °C.

Deoxycholate (DOC) (#D-5670, Sigma, Poole, UK)
Dithiothreitol (DTT) (#D-9779, Sigma, Poole, UK)
Nonidet P-40 (NP-40) (#I3021, Sigma, Poole, UK)
Protease inhibitor cocktail tablets (#11-836-153-001, Roche, Germany)
Bovine serum albumin (BSA) (#A7030, Sigma, Poole, UK)
Urocortin (#U6631, Sigma, Poole, UK)
Interleukin-6 (#I9646, Sigma, Poole, UK)

2.1.2 General materials and equipment

15 ml and 50 ml sterile tubes (#91015T, Helena Biosciences, Sunderland, U.K)
Bijou tubes (#39740, Bibby Sterilin Ltd, Staffordshire, U.K)
1.5 ml and 0.5 ml microfuge tubes (Anachem, Luton, Bedfordshire, U.K)
1.7 ml siliconised microfuge tubes (#T3406, Sigma, Poole, U.K)

Centrifuges: (Kendro Laboratory Products Ltd, Herts, U.K)
Sorvall Biofuge *Pico* (and refrigerated version *Fresco*),
Sorvall RT-7 Plus and RC26 Plus
PCR Cycler Machine (Eppendorf Mastercycler, Hamburg, Germany)
Centricon-YM30 centrifugal concentrators (Amicon Bioseparations, Millipore, UK)
Spectrophotometer (BioRad laboratories, CA, USA)

2.1.3 Enzymes

AseI (#R0526, New England Biolabs (NEB), Hertfordshire, UK)
BglII (#R6081, Promega, Southampton, UK)
PstI (#R6111, Promega, Southampton, UK)
PvuII (#R6331, Promega, Southampton, UK)
BamHI (NEB, Hertfordshire, UK)
EcoRI (#R6017, Promega, Southampton, UK)
Proteinase K (#P-6556, Sigma, Poole, UK)
Taq DNA Polymerase (#M1665, Promega, Southampton, UK)

All enzymes were stored at -20°C.

2.1.4 Reaction buffers

a) Buffer E- for restriction enzyme *BamHI* (Promega, Southampton, UK)
- 60 mM Tris-HCl (pH 7.5)
- 1 M NaCl
- 60 mM $MgCl_2$
- 10 mM DTT

b) Buffer H- for restriction enzyme *EcoRI* (Promega, Southampton, UK)
- 900 mM Tris-HCl (pH 7.5)
- 500 mM NaCl
- 100 mM $MgCl_2$

c) Buffer K- for restriction enzyme *AseI* (Promega, Southampton, UK)

- 100 mM Tris-HCl (pH 7.4)
- 1.5 M KCl
- 100 mM $MgCl_2$

d) Thermophilic DNA Polymerase 10x Buffer B supplied with separate $MgCl_2$ (Promega, Southampton, UK)

- 20 mM Tris-HCl (pH 8.0 at 25°C)
- 100 mM KCl
- 0.1 mM EDTA
- 1 mM DTT
- 50% glycerol
- 0.5% Tween 20
- 0.5% NP-40

e) Super Script II 5x First strand cDNA synthesis buffer (Invitrogen, UK)

-250 mM Tris-HCl (pH 8.3 at room temperature)
- 375 mM KCl
- 15 mM $MgCl_2$
- 0.1 M DTT

All reaction buffers were stored at -20 °C.

2.1.5 Antibodies

Primary antibodies used in this study are shown in Table 2.1. Secondary peroxidase-conjugated goat immunoglobulins were from Dako (Glostrup, Denmark). Secondary Alexa Fluor fluorescent antibodies were from Invitrogen.

Primary Antibody	Manufacturer	Catalogue Number
β-Actin (I-19)	Santa Cruz	sc-1616
Caspase-9 short (Ab-1)	Oncogene	PC475
Desmin (Y-20)	Santa Cruz	sc-7559
FLIP	Alexis	ALX-804-428
β–Galactosidase	Abcam	ab616
GAPDH	Chemicon	AB1932
hsp56 (N-17)	Santa Cruz	sc-1803
Interleukin-6 (M-19)	Santa Cruz	sc-1265
$p53^{S15}$ phospho	Calbiochem	PC386
STAT1 (E-23)	Santa Cruz	sc-346
$STAT1^{Y701}$ phospho	Zymed	33-3400
Tet Repressor	Mo Bi Tec	TET03

Table 2.1 Primary antibodies

2.1.6 Agarose gei electrophoresis materials and buffers

Agarose and low melting point agarose were supplied by Gibco BRL, Life Technologies, Paisley, Scotland, UK.

Molecular weight markers:

- 2-Log DNA Mw marker (New England Biolabs, UK)

Loading Buffer:

- 25 mg xylene cyanole, 30% glycerol

2.1.7 General buffers and solutions

a) Tris Acetate EDTA (TAE buffer)

A stock solution of 50 times working strength TAE buffer was made by dissolving the following components in 1L of distilled water:

- 242 g/L Tris base
- 57.1 ml glacial acetic acid
- 100 ml 0.5M EDTA (pH 8.0)

Dilution to a working strength gave a final concentration of 40 mM Tris acetate and 1 mM EDTA.

b) Tris-EDTA (TE buffer) (pH 7.5)

- 10 mM Tris-HCl (pH 7.5)
- 1 mM EDTA

c) Phosphate buffered saline (PBS) (pH 7.4)

One PBS tablet (Gibco, Paisley, UK) was added per 500 ml distilled water.

To make PBS/0.1% Tween, 1 ml "Tween 20" detergent was added to 1L PBS.

2.1.8 Specific buffers and solutions

a) Plasmid DNA purification from bacterial cultures

The following buffers were supplied with Qiagen (Crawley, West Sussex, UK) plasmid purification kits:

- Buffer P1 (Resuspension Buffer)	50 mM Tris-HCl (pH 8.0)
	10 mM EDTA
	100 µg/ml RNase A
- Buffer P2 (Lysis Buffer)	200 mM NaOH
	1% SDS
- Buffer P3 (Neutralisation Buffer)	3 mM potassium acetate (pH 5.5)
- Buffer QBT (Equilibration Buffer)	750 mM NaCl
	50 mM MOPS (pH 7.0)
	15% isopropanol
	0.15% Triton ®X-100
- Buffer QC (Wash Buffer)	1 M NaCl
	50 mM MOPS (pH 7.0)
	15% isopropanol
- Buffer QF (Elution Buffer for maxiprep kit)	1.25 M NaCl
	50mM MOPS (pH 7.0)
	15% isopropanol
- Buffer N3 (Neutralisation Buffer)	3 mM potassium acetate (pH 5.5)
- Buffer EB (Elution buffer for miniprep kit)	10 mM Tris-HCl (pH 8.5)

b) Buffers for production of competent DH5α *E.coli* cells:

Transformation buffer 1:	10 mM MES (pH 5.8)
	100 mM $RbCl_2$
	10 mM $CaCl_2$

	50 mM $MnCl_2$
Transformation buffer 2:	10 mM PIPES (pH 6.5)
	75 mM $CaCl_2$
	10 mM $RbCl_2$
	15% v/v glycerol

c) Tail digestion buffer

-100 mM Tris pH 8
-5 mM EDTA pH 8
-200 mM NaCl
-0.2% SDS
-0.5 mg/ml proteinase K

Peroxidase-Conjugated Goat Anti-Mouse Immunoglobulins (P0447, Dako, Glostrup, Denmark)

2.1.9 Bacterial Strains

- *E. coli* of strain DH5α was supplied by Gibco, Paisley, U.K.

2.1.10 Bacterial growth media

Media were made in ddH_20 and sterilised by autoclaving.
Luria-Bertani (LB) medium:
- 1% (w/v) Bacto-tryptone (Duchefa, Haarlem, The Netherlands)
- 0.5% (w/v) Bacto-yeast extract (Duchefa, Haarlem, The Netherlands)
- 1% (w/v) Sodium chloride

The pH was adjusted to pH 7.0 using NaOH.
For LB agar plates 1.5% (w/v) agar (Duchefa, Haarlem, The Netherlands) was added to the LB medium.

2.1.11 Growth media and solutions for maintenance of eukaryotic cells

-Dulbecco's Modified Eagle Medium (DMEM) (41966-029, Invitrogen, Paisley, UK)
Supplemented with:
10% (v/v) Foetal bovine serum (FBS) (10099-133, Invitrogen, Paisley, UK)
580 µg/ml L-glutamine (25030-024, Invitrogen, Paisley, UK)
10000U/ml penicillin/10000U/ml streptomycin (15140-122, Invitrogen, Paisley, UK)

- Hank's Balanced Salt solution, containing no magnesium and no calcium (HBSS) (14175- 053, Invitrogen, Paisley, UK)
- Trypsin-EDTA (1x) in HBSS w/o CA&MG, liquid - 0.25% Trypsin 1mM EDTA•4Na (25200-056, Invitrogen, Paisley, UK)

2.1.12 Plasmid expression constructs

The plasmid expression vectors used in this study are shown in Table 2.2. The pBIG-C9s expression vector was constructed by Dr. A Stephanou (Stephanou et al., 2002) (figure 2.1). The C9s cDNA insert was sub-cloned from the pcDNA3-C9s expression construct generated by Dr. D Seol (Seol and Billiar, 1999). Human C9s was obtained by PCR from a human liver cDNA library using the following primers: forward primer 5'-ATGGACGAAGCGGATCGGCGGC-3' and reverse primer 5'-TTATGATGTTTTAAAGAAAAGTTTTTTC-3'. The product was then cloned into pcDNA3 (Seol and Billiar, 1999).

Dr D Faulkes constructed the pCAGGs-hsp56 expression vector (figure 2.2). Human hsp56 was PCR cloned using the following primers: forward primer 5'-GGCTCTAGAGCCGCCATGACAGCCGAGGAGATG-3' and reverse primer 5'-CCGCTCGAGCTATGCTTCTGTCTCCAC-3. The PCR was performed with Advantage polymerase mix (Clontech) and cloned in the pGEM-T-easy vector. The hsp56 cDNA was cloned into pCAGGs using *NotI*/*XhoI* excision into *XhoI* cut vector.

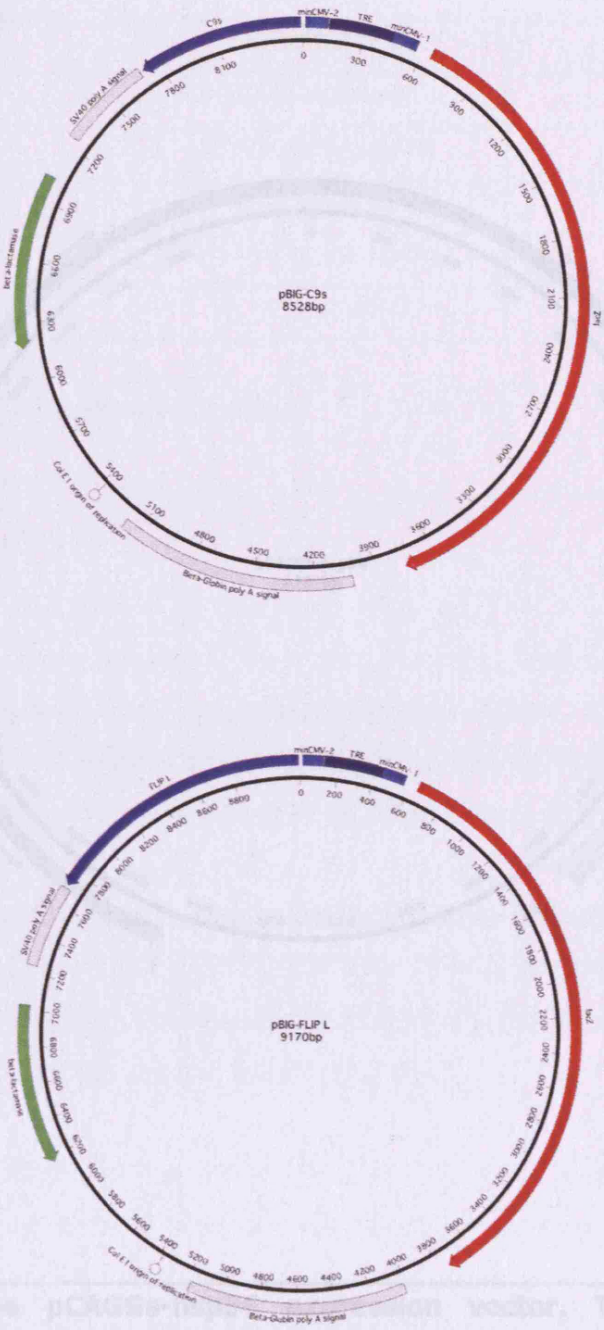

Figure 2.1. The pBIG-C9s and pBIG-FLIP expression vectors. The pBIG expression vector contains a bi-directional Tet responsive element (TRE) fused to minimal CMV promoters. These promote expression of the adjoining *lacZ* gene and inserted cDNA of C9s or FLIP, downstream of which are poly-adenylation signals. The vector also contains the ampicillin resistance gene that encodes for the protein beta-lactamase.

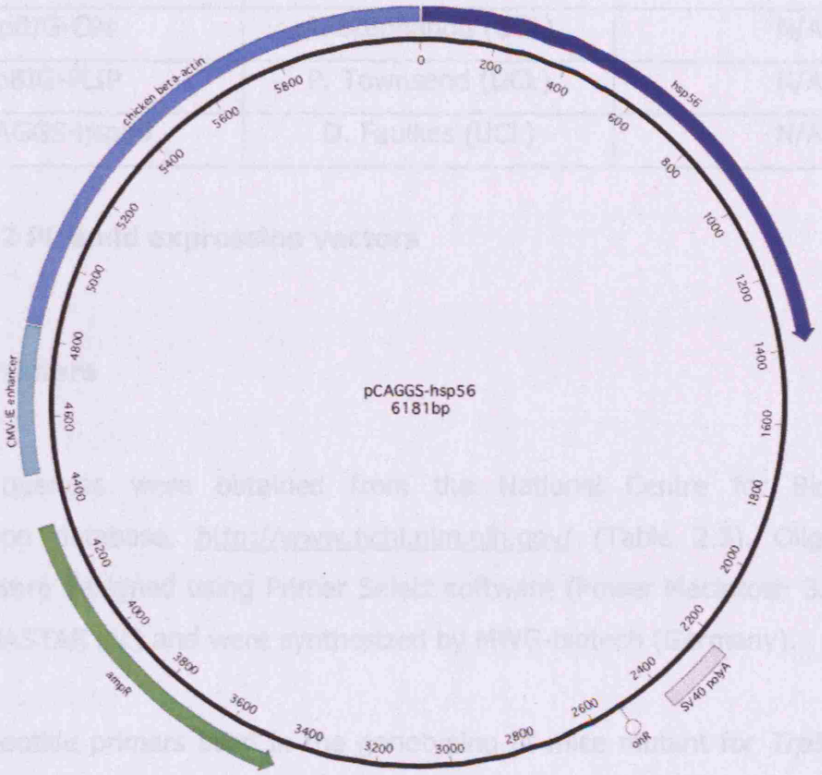

Figure 2.2. The pCAGGs-hsp56 expression vector. The pCAGGs-hsp56 expression vector contains a chicken β-actin promoter that promotes expression of the inserted hsp56 cDNA, downstream of which is a poly-adenylation signal. The vector also contains the ampicillin resistance gene that encodes for the protein beta-lactamase.

Expression Vector	Source	Catalogue Number
pTet-Off	BD Biosciences	K1620-A
pBIG	BD Biosciences	6150-1
pCAGGs	NIH Aids Research	10463
pBIG-C9s	A. Stephanou (UCL)	N/A
pBIG-FLIP	P. Townsend (UCL)	N/A
pCAGGS-hsp56	D. Faulkes (UCL)	N/A

Table 2.2 Plasmid expression vectors

2.1.13 Primers

Gene sequences were obtained from the National Centre for Biotechnology Information database, http://www.ncbi.nlm.nih.gov/ (Table 2.3). Oligonucleotide primers were designed using Primer Select software (Power Macintosh 3.11 ©1994-1997, DNASTAR inc) and were synthesized by MWG-biotech (Germany).

Oligonucleotide primers used in the genotyping of mice mutant for *Trp53* (p5314F, p53E5R and OPT-21) or *Stat1* (STAT1F, STAT1R, STAT1KOF and STAT1KOR) were designed by Taconic (USA). Primers used in the genotyping of *αMHC-tTA* transgenic mice were designed by the Jackson Laboratory (USA).

Primer pairs used in real-time RT-PCR (Table 2.3) were designed so that they spanned at least one intron in order to avoid amplification of contaminating genomic DNA or would amplify differentially sized genomic products that could be distinguished from cDNA amplification products. The exon and intron boundaries of sequences were determined using the UCSC Genome Bioinformatics database, http://genome.ucsc.edu/.

Gene	Gene Symbol	Species	Accession Number
β-Actin	*Actb*	*Mus musculus*	NM_007393
Atrial natriuretic factor (ANF)	*Nppa*	*Mus musculus*	K02781
Brain natriuretic peptide (BNP)	*Nppb*	*Mus musculus*	NM_008726
(MHC) Class II transactivator	*C2ta*	*Mus musculus*	NM_007575
Caspase-9 short (C9s) isoform	*CASP9*	*Homo sapiens*	AF110376
FBJ osteosarcoma oncogene (c-fos)	*Fos*	*Mus musculus*	NM_010234
FLICE-like inhibitory protein long (FLIP-L) isoform	*CFLAR*	*Homo sapiens*	U97074
Glyceraldehyde-3-phosphate dehydrogenase (GAPDH)	*Gapdh*	*Mus musculus*	M32599
Heat shock protein 56 (hsp56)	*FKBP4*	*Homo sapiens*	NM_002014
Serum/glucocorticoid regulated kinase	*Sgk*	*Mus musculus*	NM_011361
Interleukin 6 (IL-6)	*Il6*	*Mus musculus*	NM_031168
Interferon regulatory factor 1 (IRF-1)	*Irf1*	*Mus musculus*	NM_008390
β2-microglobulin	*B2m*	*Mus musculus*	NM_009735
Beta myosin heavy chain (β-MHC)	*Myh7*	*Mus musculus*	NM_080728
p53	*Trp53*	*Mus musculus*	X01237

Table 2.3 NCBI gene accession numbers

Primer Name	Primer Sequence 5'-3'	Annealing Temperature and Amplicon Size
p5314F	ACA CAC CTG TAG CTC CAG CAC	60 °C
p53E5R	AGC GTC TCA CGA CCT CCG TC	WT 520 bp
OPT-21	GTG TTC CGG CTG TCA GCG CA	KO 730 bp
STAT1F	CTA CCA GAG TAT CTG CCT AGA C	60 °C
STAT1R	CCT CTC AAC CTT CCT GAC ACC	325 bp
STAT1565F	GGA GTG TTT TCT AAG GCA G	57 °C
Meraz 3'2 R	GCA TCG CCT TCT ATC GCC	450 bp
C9s F	GTC AGG CTC TTC CTT TGT TC	58 °C
C9s R	GGT CTT TCT GCT CGA CAT CA	225 bp
FLIP F	GGG CCA GCG ATG AAG AAT GTG G	58 °C
FLIP R	GGA TGG TGA GCT GTG AGA CTG C	135 bp
oIMR0015	CAA ATG TTG CTT GTC TGG TG	60 °C
oIMR0016	GTC AGT CGA GTG CAC AGT TT	450 bp
oIMR0856	CGC TGT GGG GCA TTT TAC TTT AG	60 °C
oIMR0857	CAT GTC CAG ATC GAA ATC GTC	200 bp
hsp56 F	GCC TAC GGT TCA GCA GGC A	58 °C
hsp56 R	TCA TCT CCC AAG ACT CCT TG	451 bp

Table 2.4 Oligonucleotide primers for genotyping

Primer Name	Primer Sequence 5'-3'	Annealing Temperature and Amplicon Size
β-Actin F	AGA TCA CCC AGA TCA TGT TTG AG	60 °C
β-Actin R	AGG TCC AGA CGC AGG ATG	187 bp
ANF F	AGG CCA TAT TGG AGC AAA TCC T	66 °C
ANF R	TGC TTC CTC AGT CTG CTC ACT C	151 bp
BNP F	CTG TTT CTG CTT TTC CTT TAT CTG	67 °C
BNP R	CTG GGC CAT TTC CTC CGA CTT T	138bp
CIIta F	GAC AGC CAG CCA GGA CTT CT	61 °C
CIIta R	GGG GCC CAA CGC AAA CTC	341bp
c-fos F	GCG CAG AGC ATC GGC AGA AG	68 °C
c-fos R	GAG AAG GGG CAG GGT GAA GG	375bp
GAPDH F	AAT GTG TCC GTC GTG GAT CTG A	67 °C
GAPDH R	GAT GCC TGC TTC ACC ACC TTC T	83bp
IL-6 F	GAA CAA CGA TGA TGC ACT TGC AG	60 °C
IL-6 R	CCT TAG CCA CTC CTT CTG TGA C	328bp
IRF-1 F	CAC GGC TGG GAC ATC AAC AAG	68 °C
IRF-1 R	GTC CGG GCT AAC ATC TCC ACA C	299bp
β-MHC F	GCC GCG CCA GTA CTT CAT AGG T	69 °C
β-MHC R	ACT TGC CCA GGT GGT TGT CGT A	326bp
β2-micro F	TGC TGT CTC CAT GTT TGA TGT ATC T	60 °C
β2-micro R	TCT CTG CTC CCC ACC TCT AAG T	187bp
Sgk F	GGC CTG CCC CCG TTT TAT	61 °C
Sgk R	GTC ACT GGG CCC ACT CAC ATT T	267bp

Table 2.5 Oligonucleotide primers for real time PCR

2.2 Animals

This study was performed in accordance with the United Kingdom, Home Office Animals (Scientific Procedures) Act 1986.

2.2.1 Transgenic mice

Mutant *Trp53* (B6.129-*Trp53*^{tmBrd} N12) and *Stat1* (129S6/SvEvTac-*Stat*^{tm1Rds}) gene targeted knockout mice were purchased from Taconic (USA). *αMHC-tTA* (FVB/N-TgN(*αMHC-tTA*)6Smbf) transgenic mice were purchased from the Jackson Laboratory (USA).

2.3 Langendorff perfusion of the isolated adult mouse heart

Langendorff perfusion of mouse hearts was performed using a commercial Langendorff system (#ML870B2, ADInstruments). Male mice (aged 10-12 weeks) were anaesthetised (sodium pentobarbitone, 60 mg/kg intraperitoneal injection) and heparinized (25 IU intraperitoneal injection). Once an adequate level of anaesthesia had been achieved, the chest was opened and the heart of the mouse was rapidly removed, placed in ice-cold (4 °C) Krebs-Henseleit buffer and the aorta was canulated. Hearts were then perfused with a modified Krebs-Henseleit buffer (NaCl 118 mM; $NaHCO_3$ 24 mM; KCl 4 mM; NaH_2PO_4 1 mM; $CaCl_2$ 2.5 mM; $MgCl_2$ 1.2 mM; EDTA 0.5 mM; glucose 10 mM; gassed with 95% O_2/5% CO_2 at 37 °C and a constant pressure of 100 mmHg. In this modified Krebs-Henseleit buffer EDTA was added in order to lower the final calcium concentration to the physiological range of 1.5 mM. Temperature was measured by the placement of a fine thermocouple wire in the left ventricle. Monitoring of perfusion pressure, left ventricular developed pressure (LVDP) and heart rate was performed with a water-filled balloon inserted into the left ventricle.

For the normoxic control, isolated mouse hearts were perfused for 95 minutes under normoxic conditions. For the ischaemia/reperfusion treatments, mouse hearts were subjected to 35 minutes of global ischaemia by stopping the flow of buffer and

immersing the heart in buffer at 37 °C followed by 45 minutes of reperfusion initiated by returning the flow of buffer. At the end of each experimental protocol, the infarct size was assessed by 2,3,5-triphenyltetrazolium chloride (TTC) staining. 2 ml of a 1% solution of TTC was perfused through the heart followed by immersing the heart in TTC solution at 37 °C for 1 minute. Hearts were frozen at -20 °C and sectioned into 1.5 mm slices. These slices were laid out and compressed between thin glass plates 0.5 mm apart. The sections were scanned, enlarged, and infarct size assessed using computerised planimetry (Planimetry+, Boreal Software, Norway).

2.4 Langendorff perfusion of the isolated adult rat heart

Hearts were removed from male Sprague-Dawley rats (250-260 g), placed in ice-cold (4 °C) Krebs-Henseleit buffer and the aorta was canulated. The heart was perfused with Krebs-Henseleit buffer (NaCl 118.0 mM; $NaHCO_3$ 25 mM; KCl 4.8 mM; NaH_2PO_4 1.2 mM; $CaCl_2$ 1.2 mM; $MgSO_4$ 1.2 mM; EDTA 0.5mM; glucose 11 mM; gassed with 95% O_2/5% CO_2 at 37 °C) at a constant flow of 12 ml/min. Monitoring of developed pressure (LVDP) was performed with a water-filled balloon inserted into the left ventricle set to give and initial end-diastolic pressure (EDP) of 2.5-5 mmHg. After a 15-minute stabilisation period of perfusion, hearts were perfused for 30 minutes in the presence or absence of 10 nM Ucn in re-circulation mode. Global isothermic ischaemia was induced by halting perfusion and immersing the heart in perfusion buffer at 37 °C. For non-ischaemic controls the perfusion was not interrupted. After 30 minutes of ischaemia, perfusion was restarted (in the presence or absence of Ucn) and continued for 30 minutes. Samples of perfusate were collected prior to ischaemia, every minute for the first five minutes of reperfusion and at every 5 minutes of reperfusion for the spectrophometric determination of lactate dehydrogenase (LDH) activity.

2.5 Measurement of mitochondrial permeability transition pore opening in situ using [^{3}H]-2-deoxyglucose entrapment

Following the 15-minute stabilisation period of perfusion, hearts were perfused in recirculating mode in Krebs-Henseleit buffer containing 0.5 mM [^{3}H]-2-deoxyglucose

([^{3}H]-DOG) (0.1 μCi/ml) for 30 minutes. Perfusion was then returned to non-circulating mode with normal Krebs-Henseleit buffer for 15 minutes to wash out extracellular [^{3}H]-DOG. The buffer was then halted to initiate isothermic (37 °C) ischaemia. After 30 minutes of ischaemia, hearts were reperfused for 30 minutes in presence or absence of 10 nM Ucn prior to mitochondrial preparation and determination of [^{3}H]-DOG and citrate synthase activity.

At the end of reperfusion the ventricles were rapidly cut away, weighed, and homogenized with a Polytron homogenizer at setting 3 for 5s in 5 ml of ice-cold sucrose buffer (300 mM sucrose, 10 mM Tris-HCl, 2 mM EGTA, pH 7.4) and then made up to 40 ml with buffer containing 5 mg/ml BSA. The homogenate was centrifuged at 10 000 x g for 5 minutes. The pellet was resuspended in 6 ml sucrose buffer containing 20% (w/v) Percoll and centrifuged at 12 000 x g for 10 minutes to yield a purified mitochondrial pellet. The pellet was washed once in 40 ml of BSA-free sucrose buffer followed by centrifugation at 12 000 x g and finally resuspended in 0.5 ml of sucrose buffer. A 100 μl sample of the suspension was retained for assay of citrate synthase to correct for mitochondrial recovery. An equal volume of perchloric acid (PCA) was added to release the entrapped [^{3}H]. The homogenate was centrifuged at 12 000 x g for 2 minutes and the supernatant was assayed for radioactivity in 10 ml scintillant (Packard Emulsifier-Safe).

2.6 Cell culture

All protocols were carried out in sterile conditions using a laminar flow cabinet (Heraeus) and cells were maintained at 37 °C and 5% CO_2 in a humidified HeraCELL™ (Heraeus). Mammalian cell lines were cultured in growth medium (Dulbecco's Modified Eagle Medium containing 10% foetal bovine serum, penicillin and streptomycin) in tissue culture plastic ware (Nunc).

2.6.1 Cell Harvesting

Adherent cells were washed once with Hanks Buffered Saline Solution (HBSS) and harvested by incubating in Trypsin for 2-5 minutes. The trypsin was inactivated by

addition of growth medium and cells were gently pipetted to detach clumped cells. Cells were passaged when cultures reached 70-80% confluence.

2.6.2 Cryopreservation of Cells

Stocks of mammalian cells were stored in 1.8 ml cryovials under liquid nitrogen. Cell suspensions were centrifuged at 1000 x g for 5 minutes. The supernatant was discarded and the cell pellet was re-suspended in growth medium supplemented with 20% FBS and 10% DMSO. Cell suspensions were transferred to cryovials and placed in liquid nitrogen storage.

2.6.3 Thawing of Cells

Mammalian cell line stocks stored in cryovials were thawed at 37 °C in a water bath. The cells were washed once by adding the suspension to 10 ml of growth medium and were centrifuged at 1000 x g for 5 minutes. The cell pellet was re-suspended in growth medium and the suspension transferred by pipette to tissue culture flasks.

2.6.4 Determination of cell number

Viable cells were quantified using the Trypan Blue exclusion assay. 200 μl of cell suspension was added to 500 μl of Trypan Blue and 300 μl of HBSS in a bijou and was mixed by inverting. 20 μl was pipetted onto a haemocytometer overlaid with a coverslip and the number of non-Trypan blue containing cells were counted under light microscopy.

2.6.5 Determination of cell growth

Cellular growth rates were measured using the CellTiter 96® Aqueous One Solution Cell Proliferation Assay kit (G3582, Promega). Cells were seeded at a density of $1x10^3$ cells per well (100 μl volume) in 96-well plates. The day of plating was termed day 0 (zero). The quantity of cells was determined on subsequent days according to

manufacturer's instructions. Absorbance was measured at 492 nm by a Genios microplate reader (Tecan, UK).

2.7 Primary culture of adult rat cardiac myocytes

Adult rat ventricular cells (ARVC) were isolated by perfusion of the heart with collagenase. Hearts from 250-300 g male Sprague-Dawley rats, that were freshly culled, were excised and placed in ice-cold Krebs-Henseleit buffer (130 mM NaCl, 5.4 mM KCl, 3.5 mM MgCl, 750 μM $CaCl_2$, 0.4 mM NaH_2PO_4, 5 mM HEPES and 10mM glucose) containing 10.5U/ml heparin. The aorta was canulated and the heart was perfused with Krebs-Henseleit buffer for 1 minute followed by Ca^{2+}-free Krebs-Henseleit buffer containing 100 μM EGTA for 3 minutes. Hearts were then perfused with Krebs-Henseleit buffer containing 350U/ml collagenase and 180 μM $CaCl_2$ for 15 min. During collagenase perfusion the waste pipe was closed to allow the heart to become immersed in the perfusate inside a water jacket and the collagenase buffer was re-circulated. All buffers were oxygenated prior and during perfusion, maintained at 37 °C and hearts were perfused at 2 ml/min.

The heart was then cut into fine pieces with a scalpel and was incubated in shake solution (13.5 ml re-circulated collagenase buffer and 1.5 ml of 10% BSA) for 5 minutes with gentle shaking. The dissociated cells were filtered through muslin into a fresh tube. The cells were spun at 1000 rpm for 1 minute and the supernatant was discarded. The cell pellet was washed with 10 ml of restore buffer (10 parts Krebs-Henseleit buffer to 1 part 10% BSA and 180 μM $CaCl_2$) and spun at 1000 rpm for 1 minute. The supernatant was discarded and the cells were re-suspended in medium 199 containing 5 mM creatine, 2 mM carnitine, 5 mM taurine, 0.8 mM EGTA. Cells were then plated on laminin (L-2020, Sigma) coated culture dishes. After 1 hour the media was replaced and non-adhered cells were discarded.

2.8 Primary culture of neonatal rat or mouse cardiac myocytes

Hearts were excised from 2-day old Sprague Dawley rats or mice and incubated in Krebs-Henseleit bicarbonate buffer. Once all hearts were excised the isolation of myocytes was continued in sterile conditions in a laminar flow cabinet. Hearts were

trisected and transferred to a 25 cm^2 culture flask. The Krebs-Henseleit buffer was removed by pipette and discarded and hearts were washed once with 7 ml of Krebs-Henseleit buffer. Cells were enzymatically dissociated by incubating in 7 ml of oxygenated digestion buffer (0.1% ($^w/_v$) Collagenase in Krebs-Henseleit) at 37 °C in a humidified incubator maintained at 5% CO_2 for 15 minutes. The cell suspension was transferred to 15 ml tube, 2 ml of foetal bovine serum (FBS) was added to terminate the reaction and cells were centrifuged at 1000 x g for 5 minutes. The supernatant was discarded and the cell pellet was re-suspended in 4 ml of FBS. Hearts were incubated in fresh digestion buffer and the enzymatic dissociation of cardiac cells was repeated 8 times. The cell suspensions were pooled in a 50 ml tube and centrifuged at 1000 x g for 5 minutes. The supernatant was discarded and the cell pellet was re-suspended in plating medium (DMEM, 15% FBS, penicillin and streptomycin) and transferred to a culture flask. The cell suspension was pre-plated for 1 hour in a humidified incubator (37 °C /5% CO_2) to remove non-myocytes from the suspension. The enriched myocyte suspension was counted and plated onto tissue culture plates pre-coated with 1% gelatin in PBS. On the following morning the plating medium was removed from myocyte-attached cultures and replaced with maintenance medium (DMEM, 1% FBS, penicillin and streptomycin) in order to minimize fibroblast growth.

2.9 Primary culture of mouse embryonic fibroblasts

Mouse embryonic fibroblast (MEF) cells were isolated from embryos aged day 13.5 days post coitum (dpc). Embryos were isolated, washed in PBS, and the head and visceral organs were removed. The carcasses were washed in PBS and then minced into fine pieces in 2 ml Trypsin-EDTA followed by incubation at 37 °C for 30 minutes. The carcasses were then vigorously mixed by pipette to dissociate the cells. A 10 ml volume of DMEM containing 10% FBS was added. The large debris was allowed to settle and the supernatant was then plated to culture dishes. After 1 hour non-adhered cells were washed off and the cells were cultured in growth medium.

2.10 Simulated ischaemia/reperfusion in cultured cells

Simulated ischaemia was performed in cells using an ischaemic chamber supplied with carbon dioxide/argon (95%/5%) and maintained at 37 °C. Cells were washed with HBSS and incubated in 137 mM NaCl, 12 mM KCl, 0.49 mM $MgCl_2$, 0.9 mM $CaCl_2$, 4 mM HEPES, 10 mM deoxyglucose and 20 mM Na lactate (pH 6.2) during simulated ischaemia. Cells were removed from the chamber and reperfusion was simulated by replacing the ischaemic buffer with maintenance media and incubating the cells in normal conditions. Non-ischaemic control cells were incubated in 137 mM NaCl, 3.8 mM KCl, 0.49 mM $MgCl_2$, 0.9 mM $CaCl_2$, 4 mM HEPES, 10 mM glucose and 20 mM Na lactate (pH 7.4) for an equal length of time to the ischaemic treated cells. The cultures were incubated in an incubator with normal conditions (37 °C and 5% CO_2) and the ischaemic control buffer was replaced with maintenance media in synchronisation with ischaemic cells.

2.11 Measurement of MPTP opening in adult rat cardiac myocytes using Tetramethyl rhodamine methyl ester (TMRM) fluorescent dyes

MPTP opening in isolated adult rat cardiac myocytes was assessed using TMRM, a cell permeable, voltage-sensitive dye that accumulates in energized but not depolarised mitochondria. Cytofluorimetric analysis was performed using an Epics XL flow cytometer (Beckman Coulter, UK) equipped with a 488 nm argon ion-laser. The TMRM signal was analysed in the FL2 channel, which was equipped with a bandpass filter 575 ± 20 nm. Data were acquired on a logarithmic scale. Arithmetic mean values of the median fluorescent intensities were determined for TMRM.

2.12 Immunocytochemistry

Cells were cultured on round 13 mm coverslips. Cells were washed with PBS and then fixed in 4% PFA or ice-cold methanol for 10 minutes. Cells were washed in PBS and PFA fixed cells were permeabilised in 0.1% NP-40 in PBS for 10 minutes. Cells were then blocked in 3% BSA in PBS for 1 hour. The blocking solution was discarded and the cells were incubated in primary antibody at concentrations of 1:5 to 1:500 in 1% BSA for 1 hour or overnight at 4 °C. The primary antibody was washed off five times with PBS. The cells were then incubated with the fluorescent tagged secondary antibody in 1% BSA at a concentration of 1:1000. The secondary antibody was washed off by rinsing the cells five times with PBS. The coverslips were then mounted onto glass slides with fluorescent mounting medium (#302380, Dako).

2.13 Histology

Mouse hearts were perfused with Krebs-Henseleit buffer for 5 minutes to wash out the blood. Hearts were fixed in 4% formalin overnight at room temperature. Hearts were then dehydrated in the following graded series of ethanol (2 hours for each); 50%, 70%, 80, 90%, 96% and 100%. Hearts were then incubated in butanol at room temperature overnight. Hearts were then transferred to glass scintillation vials and incubated in a 1:1 ratio of butanol:molten pastillated wax at 60 °C for 20 minutes. The butanol/wax mix was discarded and replaced with 100% molten wax for four hours followed by replacement with fresh wax and incubation overnight. Hearts were then embedded in fresh wax in disposable plastic sectioning blocks with mount and allowed to set at room temperature.

Wax embedded hearts were sliced into 8 μm sections with a rotary microtome (Leica-microsystems). Sections were placed in a water bath heated to 42 °C and then mounted onto TESPA coated glass slides. Slides were stood upright to remove excess water and then dried at 42 °C for 1 hour. Sections were de-waxed by five minute incubations in the following order; 2 x Histoclear (HS-200, National Diagnostics), 2 x 100% ethanol, 95% ethanol, 80% ethanol and 70% ethanol.

Sections were stained in Haematoxylin for 10 minutes. The slides were removed and dipped twice in dH_2O. Sections were then stained in Eosin (#ASO25, Raymond-A-Lamb) for 5 minutes followed by dipping twice in dH_2O. Slides were left to dry overnight at room temperature. Coverslips were then mounted using DPX mount for microscopy (#36029, BDH).

2.14 Quantification of nucleic acid concentration

The concentration of double stranded DNA (dsDNA) was quantified in two ways; either by running the linearized DNA samples alongside molecular weight markers of known DNA concentration on an agarose gel and comparing the intensity of the bands or by using ultraviolet (UV) absorbance spectrophotometry. The amount of UV light absorbed by a solution of nucleic acid is directly proportional to the amount of nucleic acid in the sample. Absorbance was measured at 260 nm, at which wavelength an absorbance (A_{260}) of 1.0 corresponds to 50 μg of dsDNA per ml or 40 μg of RNA per ml.

UV absorbance was also measured at the wavelength 280 nm in order to check the purity of the nucleic acid preparation. The ratio of the absorbance at 260 nm and 280 nm (A_{260}/A_{280}) of a pure sample of nucleic acid would be 1.9-2.1. A ratio of less than 1.8 indicated that the preparation was contaminated with protein. The integrity RNA was checked by separating 1 μg of RNA and observing 28S and 18S ribosomal RNA.

2.15 DNA cloning in bacterial cells

2.15.1 Production of Heat Shock Competent DH5α Strain E.coli Cells

A culture of DH5α-strain *E.coli* was then grown overnight in a shaking incubator (250 rpm) at 37 °C. 100 μl of this overnight culture were added to 100 ml LB medium in a 2.5 L sterile (autoclaved) conical flask and then returned to the shaking incubator (250 rpm) for approximately three hours.

After 2 hours and then every 30 minutes after that, the growth of the cell culture was checked by measuring absorbance at 600 nm. The 100 ml culture was removed from the incubator when the culture was in the exponential log phase of the growth curve (i.e. clouds of bacteria swirling in the medium were just visible when held up to the light and when the absorbance reading of the culture when measured on the spectrometer at 600 nm was between 0.3 and 0.8).

The culture was then divided between two 50 ml sterile tubes, placed on ice for five minutes and centrifuged at 3000 rpm for 10 minutes in a Sorvall RT-7 Plus at 4 °C. The supernatant was discarded and the pellet in each tube was resuspended in 20 ml ice-cold transformation buffer 1 and incubated on ice for 5 minutes. Each tube was again centrifuged at 3000 rpm for 10 minutes at 4 °C and the supernatant discarded. Each pellet was then resuspended in 1 ml of transformation buffer 2 and incubated on ice for 15 minutes. 100 μl of this suspension were then aliquoted into pre-chilled 1.5 ml microcentrifuge tubes and stored at -80°C or used directly for transformations.

2.15.2 Transformation of heat shock competent E.coli cells

In a 1.5 ml microfuge tube, 100 μl of heat shock competent *DH5α* strain *E.coli* cells were thawed on ice and 50-100 ng of plasmid DNA was added, mixed by gently stirring with a pipette tip and incubated on ice for 30 minutes. Cells were heat shocked by incubating at 42 °C for 1 minute in a water bath and further incubated on ice for 2 minutes. 900 μl of LB medium was added to the cells and were incubated at 37 °C for 1 hour. Cells were centrifuged at 3000 x g for 10 minutes, the supernatant was poured off and the cells were re-suspended in the residual supernatant. The re-suspended cells were then pipetted onto selective LB agar plates containing appropriate antibiotic. A glass Pasteur pipette was sterilised by passing through a flame and used to the spread the cells over the surface and the plates were incubated at 37 °C overnight. The following day antibiotic resistant clones were picked, grown LB with appropriate antibiotic.

2.15.3 Purification of plasmid DNA

Large-scale extraction to produce 100-500 μg of DNA per preparation was carried out using the Qiagen Plasmid Maxi purification buffers and protocol. A single colony of plasmid transformed clones was picked from a freshly prepared LB/Ampicillin plate to inoculate a starter culture of 5 ml LB/Ampicillin medium. This culture was incubated for approximately eight hours at 37 °C with vigorous shaking at 300 rpm. 1 ml of the starter culture was then diluted into 500 ml of LB/Ampicillin medium and incubated at 37 °C for 16 hours overnight with vigorous shaking at 300 rpm. On the following day, bacterial cells were harvested by centrifugation at 9000 rpm in a Sorvall RC26 Plus (SLA 3000 rotor) for 15 minutes at 4 °C. Supernatant was discarded and the bacterial pellet resuspended in 10 ml of ice cold buffer P1 and 10 ml of buffer P2 was added. After mixing and incubation at RT for 5 minutes 10 ml of chilled buffer P3 was added. The mixture was kept on ice for 20 minutes then centrifuged at 12000 rpm in a Sorvall RC26 Plus (SS-34 rotor) for 30 minutes at 4 °C. Supernatant containing plasmid DNA was promptly removed and re-centrifuged for 15 minutes at 4 °C. A Qiagen tip 500, containing DNA binding resin, was equilibrated by the addition and free gravity flow of 10 ml Buffer QBT. Supernatant was then applied to the Qiagen tip and allowed to enter and bind DNA to the resin by free gravity flow while all other components pass through. The DNA was then washed by passing 30 ml of buffer QC through the tip twice and eluted with 15 ml of buffer QF. To precipitate the DNA 10.5 ml (0.7 volumes) of RT isopropanol was added to the eluted DNA, mixed and then centrifuged at 3000 rpm (in a Sorvall RT7 Plus) for 45 minutes at 4 °C. Following which supernatant was carefully decanted and the DNA pellet washed with 5 ml of RT 70% ethanol and centrifuged at 3000 rpm (in a Sorvall RT7 Plus) for 15 minutes at 4 °C. The supernatant was discarded, the pellet dried under a vacuum for 2-5 minutes and then redissolved in 1 ml of autoclaved water.

2.15.4 Separation of DNA fragments by agarose gel electrophoresis

DNA were separated by agarose gel electrophoresis. Agarose was mixed in TAE buffer and boiled in a microwave oven until dissolved and was left to cool at 55 °C. 3 μl of 10 mg/ml ethidium bromide was added to 100 ml of boiled agarose and then poured and left to solidify in a casting gel tray with the open ends closed off by tape.

20-well or 14-well gel combs were inserted. Once the gel solidified the tape and combs were removed. The tray with the gel was then placed in an electrophoresis tank and TAE buffer was poured into the tank until the gel was covered. Bromophenol Blue loading buffer was added to the DNA sample and the sample was pipetted into the well. 0.5 μg 2-Log DNA ladder was loaded adjacent to samples so that the molecular weight of DNA fragments could be determined. Electrophoresis of DNA was carried out at 100mA until resolution of DNA fragments was sufficient. DNA fragments were visualized on a long wave UV transilluminator and photographed using the Syngene doc system.

2.15.5 Purification of DNA from agarose gels

DNA was purified from agarose gel using the QIAquick gel extraction (Qiagen, Crawley, West Sussex, UK) kit. An excised band of DNA of up to 0.4 g was placed in a 1.5 ml microfuge tube and 1 ml of buffer QG added. The mixture was then incubated at 55 °C for 10 minutes until all agarose had dissolved. 700 μl of this solution was then added to a spin column placed in a collection tube and centrifuged at 13000 rpm for 10 seconds. The flow through was discarded from the collection tube and the procedure repeated until all of the initial mixture had been passed through the spin column. A further 500 μl of buffer QG was added to each spin column and centrifuged at 13000rpm for 10 seconds. After discarding the flow through, the column was washed twice with 500 μl of buffer PE and centrifuged as above. Each column was then placed into a fresh 1.5 ml microfuge tube and dried under a lamp for 5 minutes. Elution of DNA from each column was performed by addition of 50 μl of solution EB (10mM Tris-HCl pH 8.5), allowing the column to stand for 1 minute followed by centrifugation as above. The product was then stored at -20°C.

2.16 Transgenesis by pronuclear injection

The expression constructs pBIG-C9s, pBIG-FLIP and pCAGGS-Hsp56 were linearized and dialyzed against injection buffer (7.5mM Tris pH7.4 and 0.02mM EDTA) prior to pronuclear injection by the Institute of Child Health (ICH) transgenic facility. Expression constructs were injected in the male pronucleus of fertilized eggs from

FVB/N strain mice and were re-implanted into the FVB/N foster mothers after 1-2 days culture. For injections by the Karolinska Institute, expression constructs were sent in non-linearized form and restriction digestions were performed as part of the service.

2.17 Genotyping by polymerase chain reaction (PCR)

2.17.1 Purification of genomic DNA from tail biopsies

Tail biopsies were digested in 700 µl of tail digestion buffer overnight at 55 °C. An equal volume of Tris equilibrated phenol was added to the digested tail, mixed by inverting the tube vigorously and centrifuged at 13000 rpm in a micro centrifuge for 5 minutes. The upper aqueous phase was removed by pipetting to a clean 1.5 ml microfuge tube. An equal volume of chloroform: isoamylalchohol (24:1) was added, mixed and centrifuged as before. The upper aqueous phase was removed to a clean tube and DNA was precipitated by adding an equal volume of isopropanol and mixed gently until a DNA precipitate was visible. The precipitated DNA was pelleted by centrifugation at 13000 rpm for 10 minutes at 4 °C and the supernatant was discarded. The DNA pellet was washed with 700 µl of 70% (v/v) ethanol and centrifuged at 13000 rpm for 5 minutes. The ethanol was discarded and the DNA pellet was left to air dry. Once dry, the DNA was re-suspended in 300 µl of TE buffer.

2.17.2 Mouse genotyping by Polymerase Chain Reaction (PCR)

The genotypes of mice for αMHC-tTA, pBIG-C9s, pBIG-FLIP, pCAGGs-hsp56 transgenes and *Trp53* and *Stat1* alleles were determined by PCR. Primer pair sequences, annealing temperatures and amplicon sizes are shown in Table 2.4. A region of the αMHC-tTA transgene was amplified with primers oIMR0015 and oIMR0016 in duplex with primers oIMR0856 and oIMR0857 for an internal DNA control. Regions of $STAT1^{+/+}$ and $STAT1^{-/-}$ alleles were amplified in separate reactions using specific wild type (STAT1F and STAT1R) and knockout (STAT1565F and STAT1852R) primer pairs. Regions of $Trp53^{+/+}$ and $Trp53^{-/-}$ alleles were amplified

in a single reaction using a common forward oligonucleotide primer (p5314F) with specific wild-type (p53E5R) and knockout (OPT-21) reverse primers.

1 μl of mouse genomic DNA was assayed per reaction in a total volume of 25 μl containing 1x PCR buffer, 2 mM $MgCl_2$, 0.2 mM dNTPs, and 1 unit Taq polymerase. Primer pairs were used at a final concentration of 1 μM each with the following exceptions. *Trp53* primers were used at the following concentrations: 0.5 μM p5314F, 1 μM p53E5R and 0.5 μM OPT-21. Primers oIMR0015 and oIMR0016 were used at 1.05 μM and primers oIMR0856 and oIMR0857 were used at 1.66 μM. A master mix of PCR buffer, $MgCl_2$, dNTPs, primers and Taq polymerase in ddH_2O was prepared in a 1.5 ml microfuge tube. 24 μl aliquots of the master mix were transferred to 0.2 ml PCR tubes and 1 μl of DNA was added. The tubes were then placed into a PCR machine and the cycling parameters were used as follows:

Initial denaturation at 95 °C for 3 minutes

Then 35 cycles as follows:
Denaturation - 95 °C for 1 minute
Annealing - 60 °C for 1 minute
Extension - 72 °C for 1 minute

Final extension at 72 °C for 5 minute
The reaction was then held at 4 °C until samples were removed.

2.18 Southern Blotting

2.18.1 Restriction endonuclease digestion, electrophoresis and denaturing of DNA

10 μg of mouse genomic DNA was restriction digested overnight at 37 °C in an incubator. Each sample was digested in a volume made up to 80 μl with ddH_2O containing 1x restriction enzyme buffer, 1 mg/ml BSA, and 1 μl of restriction enzyme.

40 µl of restriction digested DNA was separated by electrophoresis in a 20 x 20 cm 1% agarose gel overnight at 35 V. DNA was depurinated by incubating the gel in 500 ml of 0.25 M HCl for 10 minutes and gently agitated on a shaker. The gel was washed once with ddH_2O and the gel was denatured in 500 ml of denaturing buffer (0.5 M NaOH, 1.5 M NaCl) for 20 minutes while shaking. The reaction was then neutralised by incubating the gel in neutralising buffer (0.5 M Tris, 1.5M NaCl) for 20 minutes.

2.18.2 Transfer of DNA to nylon membrane

DNA was transferred from the gel to a nylon membrane, Hybond N^+ (Amersham), by capillary action. A flat and solid support for the gel was placed in the centre of a tray that acted as a reservoir and was filled with 500 ml of 20x SSC so that the support was not submerged. A piece of Whatmann 3MM filter paper was cut to a length so that it covered the support and hung over at two ends reaching the bottom of the reservoir so that it would function as a wick. The filter paper was saturated with 20x SSC and the gel was placed on top. The gel and reservoir was covered with a piece of cling film. The cling film covering the gel was cut away with a scalpel so that the cling film covered only a few millimetres of the edges of the gel and the reservoir. Hybond-N nitrocellulose membrane was cut to the dimensions of the gel, soaked in 2x SSC and positioned on the gel. Two pieces of 3MM filter paper were pre-wet in 2x SSC and placed on top of the blot and covered by four more pieces of dry 3MM filer paper. Absorbent paper towels were then placed on top of the 3MM filter paper and a solid weight of approximately 500 g was placed on top so that the towels were compressed. Blotting was carried out overnight. On the following the day the DNA was cross-linked to the membrane by exposing it to 1.2 Joules of UV light. The membrane was then pre-hybridised in 20 ml of hybridisation buffer in a glass hybridisation bottle beaker whilst rotating in an oven at 65 °C for 1 hour.

2.18.3 ^{32}P-labelling of DNA probes

DNA probes were radiolabelled by random primer extension with ^{32}P-labelled dCTP (Amersham, PB10205) using DNA labelling beads (Amersham, 27-9240-01). The DNA labelling bead was dissolved in its tube with 10 µl of ddH_2O. The DNA probe was

denatured by boiling at 100 °C on a hot plate for 5 minutes, pulse centrifuged and incubated on ice for 2 minutes. 50 ng of denatured DNA was added to the dissolved bead and 5 μl (1.85MBq) of ^{32}P-labelled dCTP was then added. The reaction was made up to 50 μl with ddH_2O and mixed. The primer extension was carried out at 37 °C for 1 hour in a water bath. The probe was then purified from unincorporated ^{32}P-labelled dCTP, random primers and dNTPs by affinity column chromatography. 150 μl of ddH_2O was added to the probe and then added to the column and centrifuged at 1000 x g for 2 minutes. The eluate was collected in a 1.5 ml microfuge tube and 2 μl was transferred to another microfuge tube and the radioactivity was measured in a scintillation counter. Probes measuring less than 15000 counts per second were not used.

2.18.4 Hybridisation of DNA probes to membrane and detection

Boiling for 5 minutes denatured the radiolabelled probe and 50 μl was added to 20 ml hybridising buffer. The pre-hybridising buffer was discarded and replaced by 20 ml of hybridising buffer containing the radiolabelled probe. The membrane was incubated with the probe overnight at 65 °C. The probe was discarded and the membrane was washed by incubating the membrane in 0.5 M phosphate buffer containing 0.5% SDS for 10 minutes at 42 °C. The wash solution was discarded and the membrane was then washed in 0.25 M phosphate buffer containing 0.5% SDS for 10 minutes at 42 °C. Membranes with hybridised radiolabelled DNA fragments were visualised by exposing the membrane to Kodak auto-radiographic film or phosphor imager plates for quantitation.

2.19 Quantification of mRNA expression

2.19.1 RNA extraction

RNA was extracted from cells or tissue using Trizol (#15596-026, Invitrogen). Cell monolayers were washed once with PBS. For cells cultured in 6-well plates (3 mm), 750 μl of Trizol was added to the cells and the plates were rotated on an orbital shaker at 60 rpm for 10 minutes at room temperature. The homogenate was then

collected by pipette and transferred to 1.5 ml microfuge tube. For tissue, 100-200 mg was frozen in liquid nitrogen and was crushed with a pestle and mortar. The crushed tissue was transferred to a dounce glass homogeniser and was homogenised in 1 ml of Trizol at room temperature. The homogenate was then collected by pipette and transferred to a 1.5 ml microfuge tube. The RNA extraction procedure for cells or tissue continued as follows. 200 µl of chloroform was added to the Trizol homogenate and the tubes were shaken vigorously for 15 seconds. The samples were incubated at room temperature for 15 minutes and were then spun at 12 000 rpm for 5 minutes at room temperature. The aqueous phase was transferred to a clean 1.5 ml microfuge tube by pipette and 500 µl of isopropanol was added. The samples were incubated at room temperature for 10 minutes and were then spun at 12 000 rpm for 15 minutes at 4 °C. The supernatant was removed, leaving the RNA pellet in the tube. The RNA was washed with 1 ml of absolute alcohol and was spun at 4000 rpm for 5 minutes. The alcohol was removed and the RNA was left to air dry at room temperature with the lids open. The RNA was then re-suspended in 20 µl of ddH_2O.

2.19.2 First strand cDNA synthesis

First-strand cDNA was reverse transcribed from messenger RNA (mRNA) by Super Script II (SSII) reverse transcriptase (RT) using a first-strand cDNA synthesis kit from Invitrogen (18064-022) and random hexamer primers. 1 µg of total RNA was primed with 250 ng of random hexamer primer in a reaction made up to 11 µl with ddH_2O. The RNA was denatured by incubation at 72 °C for 10 minutes followed by immediately placing on ice. The contents were collected by brief centrifugation and then 8 µl of the following premix was added: 4 µl of 5x buffer, 2 µl 0.1 M DTT, 1 µl 10 mM dNTPs and 1 µl RNaseOut (40U/µl) (Invitrogen, 10777-019).

The contents of the tube were mixed gently by pipette and were incubated at room temperature for 2 minutes. 1 µl (200 units) of SSII RT was then added and the reaction was mixed gently by pipette followed by incubation at room temperature for 10 minutes. First-strand cDNA was then synthesised by incubating the reaction at 42 °C for 60 minutes. Incubating at 72 °C for 10 minutes inactivated the reaction. The cDNA sample was diluted with ddH_2O to 100 µl prior to use in real-time PCR.

2.19.3 Quantitative real-time PCR

Gene expression was measured quantitatively by real-time PCR. Real-time PCR was performed using SYBR I green technology on the DNA engine Opticon system (MJ research). The following premix was prepared (for PCR primer pairs see Table 2.5): 10 μl 2x SYBR green mix, 0.75 μl each primer (20 μM) and 3.5 μl ddH_2O. 5 μl of cDNA was added and the tubes were briefly vortexed and pulse centrifuged. Real-time PCR was then performed using the following parameters: SYBR green activation step, 94 °C for 3 min; 50 cycles of; denaturing, 94 °C for 30 seconds; annealing (see table for annealing temperature) for 30 seconds; extension, 72 °C for 30 seconds.

Real-time PCR quantification of two or three of the following reference genes was performed to normalize for differences in template concentration: β-Actin, Gapdh and β2-microglobulin. Relative expression was quantified using the 2(-Delta Delta C(T)) (ΔΔCT) method described by Livak and Schmittgen (Livak and Schmittgen, 2001). Primer pair efficiencies were assessed by performing PCR on serial dilutions of cDNA template.

2.20 Protein extraction and quantification

2.20.1 Protein extraction from heart for one-dimensional electrophoresis

Whole mouse heart was frozen in liquid nitrogen and crushed to a fine powder using a pre-chilled pestle and mortar. The crushed tissue was then transferred using a scalpel blade to a pre-chilled 1.5 ml microcentrifuge tube. The tissue was then lysed in 1 ml of radioimmunoprecipitation (RIPA) buffer (0.75 M NaCl, 5% ($^{v}/_{v}$) NP40, 2.5% ($^{w}/_{v}$) deoxycholate, 0.5% ($^{w}/_{v}$) SDS, 0.25 M Tris-HCl pH 8.0, 10 mM Dithio-L-threitol (DTT) containing protease inhibitors) and incubated on ice for 20 minutes. The lysate was then centrifuged at 13000 x g for 5 minutes at 4 °C. The supernatant was transferred to a clean 1.5 ml microfuge tube and was stored at –80 °C until use.

2.20.2 Protein assay of lysates prepared for one-dimensional electrophoresis

Protein concentration was determined by the bicinchoninic acid (BCA) protein assay (#23255, Pierce). A standard curve between 0-50 μg of bovine serum albumin (BSA) was prepared and 2 μl of protein lysates were assayed. BCA solution was prepared by mixing 50 parts of reagent A with 1 part reagent B. 200 μl of BCA solution was mixed with the protein standards and lysates and were incubated at 37 °C for 30 minutes. Absorbance was measured at 560 nm by a Genios microplate reader (Tecan, UK). Protein concentration was determined by extrapolating the O.D of the protein lysate with the BSA standard curve.

2.20.3 Protein extraction from heart for two-dimensional electrophoresis

Whole mouse heart was frozen in liquid nitrogen and crushed to a fine powder using a pestle and mortar. The crushed tissue was then transferred using a scalpel blade to a 1.7 ml siliconised microcentrifuge tube. The tissue was then lysed in 1 ml of lysis buffer (8M Urea, 0.2 % DTT, 0.5% CHAPS containing protease inhibitors) and passed through a 21-gauge needle five times. Lysis was continued at room temperature for 20 minutes and the lysate was then centrifuged at 13000 x g for 5

minutes at room temperature. The supernatant was transferred to a clean 1.7 ml siliconised microfuge tube and was stored at –80 °C until use.

2.20.4 Protein assay of lysates prepared for two-dimensional electrophoresis

The 2-D Quant Kit (Amersham) was used to determine protein concentration of lysates prepared for 2-DE. 2 µl of protein lysates that were to be assayed were pipetted to 1.5 ml microfuge tubes. 500 µl of precipitant was added to each tube and mixed using a vortex. 500 µl of co-precipitant was then added, mixed and centrifuged at 13 000 x g for 5 minutes. The supernatant was discarded, the tubes were centrifuged briefly and the remaining supernatant was removed using a Gilson pipette. 100 µl of copper solution and 400 µl of ddH_2O was added to each tube, mixed using a vortex and incubated at room temperature for 20 minutes. The absorbance was measured at 480 nm and protein concentration was determined by comparing the O.D of the protein lysate with a BSA standard curve.

2.21 One-dimensional SDS-PAGE and Western blotting

2.21.1 SDS-PAGE

Protein extracts were separated according to their molecular weight by SDS-Polyacrylamide Gel Electrophoresis (SDS-PAGE). SDS-PAGE gels were cast in 8 x 7 cm plates with 1.5 mM thick spacers. The resolving gel was prepared containing 12% acrylamide, 0.375 M Tris pH 8.8, 0.1% SDS, 0.1% ammonium persulfate (APS) and 4 µl TEMED (per 10 ml of gel mix). The mix was poured into the plates until it reached 1.5 cm below the small plate. Gels were overlaid with butan-2-ol and left to polymerise for at least 1 hour. The butan-2-ol was poured off and the gel surface was washed 4-5 times with ddH_2O. The stacking gel was then prepared containing 5% acrylamide, 125 mM Tris pH 6.8, 0.1% SDS, 0.1% APS and 10 µl of TEMED (per 10 ml of gel mix) and poured on top of the resolving gel and a comb was inserted and left to polymerize for at least 45 minutes

Following polymerization the comb was removed and the plates were attached to the Mini-Protean electrophoresis system (Bio-Rad). The cathodic chamber was filled to the top with running buffer and the tank comprising the anodic end was filled with 300 ml of running buffer. The wells were flushed out with running buffer using a 20 ml syringe and 21-guage needle to remove any non-polymerised acrylamide. Protein samples were then loaded into the wells using a Gilson pipette. 10 μl of pre-stained molecular weight protein standard (New England Biolabs, #P7708) was also run. Electrophoresis was carried out at 150 V until sufficient separation of the pre-stained standard was achieved.

2.21.2 Western Blotting

Proteins separated by SDS-PAGE were transferred to Hybond-C nitrocellulose membrane (Amersham) using the Mini-Protean transfer system (Bio-Rad). Firstly, the stacking gel was detached from the resolving gel and discarded. The resolving gel was removed from the glass plates and incubated in transfer buffer. Hybond-C and 2 pieces of 3MM filter paper were cut to the size of the resolving gel and were wetted in transfer buffer. The Hybond-C membrane was placed on top of the gel and sandwiched by 3MM filter paper and on the outside by sponges. Firstly, the 3MM filter paper was laid on top of a sponge followed by the gel. Then, 3MM filter paper was placed on the gel and bubbles between the gel and membrane were smoothed out using a glass Pasteur pipette. A piece of 3MM filter paper was then placed on the membrane followed by sponge and the 'sandwich' was enclosed in a transfer cassette. The cassette was fitted into the transfer tank and electrophoresis was carried out at 100 V for 1 hour.

The membrane was removed and incubated in 5% ($^{w}/_{v}$) non-fat milk in Tris-buffered saline (TBS) for 1 hour. The membrane was then incubated with primary antibody (1:500-1:2500) dissolved in 5% ($^{w}/_{v}$) non-fat milk/TBS overnight at 4 °C. The membrane was then washed in 0.1% Tween-20 in TBS for 5 minutes 3 times. The membrane was then incubated with a horseradish peroxidase (HRP) conjugated secondary antibody (1:2000) in 5% ($^{w}/_{v}$) non-fat milk/TBS for 30 minutes and then washed in 0.1% Tween-20 in TBS for 5 minutes 3 times.

HRP conjugated antibodies bound to protein were visualized using enhanced chemiluminescence (ECL) (Amersham). Excess TBS/Tween-20 was removed from the membrane and was placed on cling film. The ECL reagent was pipetted onto the membrane incubated for 2 minutes. Excess ECL reagent was removed and the membrane was wrapped in cling film. The membrane was exposed to x-omat x-ray film and developed.

2.22 Two-dimensional electrophoresis

2.22.1 First Dimension - Isoelectric Focusing (IEF)

Proteins were separated on the basis of their isoelectric point using Immobiline DryStrip gel strips (Amersham), which contain an immobilised pH gradient (IPG), and an Ettan IPGphor II (Amersham) isoelectric focusing system. Proteins were applied to the IPG strips by passive rehydration in an Immobiline DryStrip reswelling tray (Amersham). Passive rehydration buffer was added to 100-400 μg of protein to a total of 340 μl in a siliconised microfuge tube and was pipetted into the slot of the tray. IPG strips were then loaded into the wells, covered with mineral oil and left to rehydrate for 20 hours. IPG strips were then placed on the Ettan IPGphor II manifold ceramic tray. Paper wicks (Amersham) were saturated with 150 μl of ddH_2O water and were placed in contact with the acrylamide at each end of the IPG strips. The electrodes were connected and the tray was covered with 108 ml of mineral oil. Proteins were then focused using the following programme.

Step 1 Gradient	0-300 V	30 minutes
Step 2 Step and Hold	300 V	4hours
Step 3 Gradient	300-1000 V	6 hours
Step 4 Gradient	1000-8000 V	4 hours
Step 5 Step and Hold	8000 V	To a total of 81 kV hours

IPG strips were stored in 10 ml pipettes wrapped in cling film at –80 °C until use.

2.22.2 Resolubilisation of proteins following IEF

Focused proteins were resolubilised and carboamidomethylated prior to SDS-PAGE. Proteins were denatured by incubating the strip for 15 minutes at room temperature in 6 M Urea, 50 mM Tris-HCl pH 8.8, 30% ($^{v}/_{v}$) glycerol, 2% ($^{w}/_{v}$) SDS and 1% ($^{w}/_{v}$) DTT. The solution was discarded and replaced with 50 mM Tris-HCl pH 8.8, 30% ($^{v}/_{v}$) glycerol, 2% ($^{w}/_{v}$) SDS and 2.5% ($^{w}/_{v}$) iodoacetamide with a trace of bromophenol blue and incubated at room temperature for 15 minutes.

2.22.3 Second Dimension – SDS-PAGE

Following IEF and protein resolubilisation, proteins were then separated on the basis of their molecular weight by SDS-PAGE using the Ettan Dalt*six* electrophoresis system (Amersham). Using the Ettan gel-casting chamber, 12% acrylamide/bis-acrylamide gels were cast in 25.5 x 20.5 cm gel plates with 1 mM thick spacers. 500 ml of gel mix was prepared containing 12% acrylamide, 0.375 M Tris pH 8.8, 25 μM sodium thiosulphate, 500 μl of 10% ($^{w}/_{v}$) APS and 50 μl of TEMED. The gel was poured into the chamber until it reached 1 cm below the top of the smaller plate and the gels were immediately overlaid with butan-2-ol and left to polymerise for two hours. The butan-2-ol was poured off and tops of the gels were thoroughly washed with ddH_2O to remove any traces of butan-2-ol. Gels were either used immediately or were overlaid with 0.375 M Tris pH 8.8, wrapped in cling film, stored overnight at 4 °C and used the following day.

Following resolubilisation of proteins each IPG strip placed at the surface of a gel. The Ettan electrophoresis tank was filled with 1x running buffer and the gels were loaded into the tank and the upper chamber that creates the cathodic chamber was attached and filled with 1x running buffer. Electrophoresis was carried out at 80 V for 1 hour followed by 250 V until the line of bromophenol blue exited the gels. Gels were removed from the plates and placed into fixative solution (50% methanol and 10% acetic acid).

2.22.4 Silver Staining

Proteins were visualized by staining with silver nitrate. Gels were transferred from fixative solution and incubated in sensitising solution (30% ethanol, 6.8% ($^{w}/_{v}$) sodium acetate and 0.1% ($^{w}/_{v}$) sodium thiosulphate) and gently rotated on a bench top shaker for 30 minutes. Sensitising solution was discarded and gels were washed three times with ddH_2O for 5 minutes while shaking. Gels were then incubated in staining solution (2.5% ($^{w}/_{v}$) silver nitrate and 0.1 ml of 37% formaldehyde in 250 ml ddH_2O) for 30 minutes while shaking. Gels were then washed twice with ddH_2O for 1 minute followed by incubation in developing solution (2.5% sodium carbonate and 0.05 ml formaldehyde in 250 ml ddH_2O). Gels were developed until protein spots were seen and incubating the gels in 5% acetic acid terminated the process. Gels were bag sealed and scanned using a GS-800 Densitometer (Bio-Rad).

Silver stained 2D gels were scanned and the expression profiles of cardiac proteomes were compared using ImageMaster™ 2D Platinum software (Amersham). ImageMasterTM detected silver stained protein spots with the minimum for parameters of spot detection being set as follows: minimum area of 2, smoothness of 5 and saliency of 150. Proteins were selected by ImageMaster™ and were matched between gels by choosing proteins as landmarks. Expression analysis using ImageMaster™ identified differences in expression of proteins by comparing the ratio of percentage volume density of gel of proteins between the cardiac proteomes of wild-type, *Trp53*$^{-/-}$, *STAT1*$^{-/-}$ and *Trp53*$^{-/-}$/*STAT1*$^{-/-}$ mice. ImageMaster™ selected proteins that had an average ratio of more than 2 and did not have overlapping class intervals as significant changes. ImageMaster™ regarded proteins with the largest gap between class intervals as the most significant. Manual analysis of 2D gels verified proteins that were identified by ImageMaster™ as authentic protein spots.

2.23 Identification of proteins by peptide mass fingerprinting (PMF)

2.23.1 In-gel cysteine residue derivatisation

Protein spots were excised from gels using a scalpel and were transferred to a 1.5 ml siliconised microfuge tube. The gel piece was then washed 3 times with 100 mM

ammonium bicarbonate pH 7.8. The gel piece was then partially dehydrated in 500 µl of acetonitrile whilst rotating on a wheel for 20 minutes. The acetonitrile was discarded and the gel piece was dehydrated completely by centrifugal evaporation at 37 °C. The gel piece was then washed 5 times with 100 mM ammonium bicarbonate pH 7.8 to remove excess iodoacetamide. Gel pieces were either used immediately or stored at –80 °C until use.

2.23.2 In-gel trypsin digestion

60 µl of 12.5 ng ml^{-1} Trypsin in 50 mM ammonium bicarbonate pH 7.8 was added to the dehydrated gel piece and incubated overnight at 37 °C.

2.23.3 Extraction of peptides

Peptides were released from the gel matrix following in-gel trypsin digestion with 500 µl of 50% ($^{v}/_{v}$) acetonitrile containing 0.1% TFA for 60 minutes whilst mixing on a wheel. The acetonitrile/TFA containing peptides was transferred to a fresh siliconised microfuge tube and the acetonitrile was removed by centrifugal evaporation at 37 °C. Hydrophobic peptides were then released from the gel piece by incubating in 300 µl of 4 M Urea whilst mixing on a wheel for 30 minutes. The 4 M urea solution, containing peptides, was transferred to the tube containing the dried peptides extracted with acetonitrile in the previous step and were resolubilised by vortexing for 60 seconds.

2.23.4 De-salting peptide samples

Peptide samples were de-salted using Zip-Tip C-18 micro columns (Millipore, ZTC185024). Zip-Tip micro columns were conditioned by aspirating 20 ml of 50% ($^{v}/_{v}$) acetonitrile containing 0.1% ($^{v}/_{v}$) TFA 5 times followed by 0.1% TFA 5 times. 20 ml of peptide sample was then aspirated 10 times and peptides bound to the tip were washed 5 times by aspirating 20 ml of 0.1% ($^{v}/_{v}$) TFA. Peptides were eluted with 20 ml of 50% acetonitrile containing 0.1% TFA and transferred to a fresh

siliconised microfuge tube Peptides were dried by centrifugal evaporation and were resolubilised in 20 ml of 0.1% ($^{v}/_{v}$) TFA.

2.23.5 Preparation of MALDI-TOF matrix

20 mg of a-cyano-4-hydroxycinnamic acid (#70990, Fluka) was dissolved in 1 ml of a 1:1 solution of acetonitrile: ethanol. 300 ml of this solution was added to 300 ml of 50 mM Fucose (Biochemika). 4.5 ml of this solution was added to a mix of 1.5 ml of peptide sample and 1.5 ml each of the standards ACTH and Angiotensin II. 1.5 ml of this peptide and matrix/Fucose mix was spotted onto the reservoir of the MALDI-TOF plate.

2.23.6 MALDI-TOF mass spectrometry

Mass spectrometry was carried out on a MALDI TOF MS instrument, fitted with a reflectron and a 337 nm U.V laser (TOF Spec E. MicroMass, Manchester, UK). Peptide analyses were performed in positive ion mode with the following voltages, source 20 kV, extraction 19.95 kV, focus 16.5 kV, reflectron 25kV and a pulse voltage of 2.9 kV. Spectra were acquired by averaging over a period of 5 scans of highest signal. Data were acquired in reflectron mode, operating over a mass range of 6000 m/z with matrix suppression set out at 650 Da and analyzed using Mass Lynx software (MicroMass, UK) (figure 2.3).

2.24 Enzyme-linked immunosorbent assay

Enzyme-linked immunosorbent assay (ELISA) detection of interleukin-6 (IL-6) was performed using the READY-SET-GO! Mouse IL-6 ELISA kit (88-7064-88, Bioscience). Mouse cardiac protein lysates were diluted in PBS and concentrated with Centricon-YM30 centrifugal concentrators (Amicon Bioseparations, Millipore, UK) to remove ELISA inhibiting components present in the protein extraction buffer. The medium of cultured MEF cells was used directly in the ELISA. The ELISA procedure was performed according to manufacturer's instructions. Absorbance was measured at 450 nm using a Genios microplate reader (Tecan, UK).

2.25 X-Gal Staining

The substrate 5-bromo-4-chloro-3-indolyl-ß-D-galactoside (X-gal) was used to detect expression of the β-galactosidase protein in cell cultures and hearts. Cells were fixed on the plate in 4% paraformaldehyde (PFA) in PBS for 20 minutes. Hearts were fixed in 2% PFA in PBS containing 2 mM $MgCl_2$ for 20 minutes. Cells were washed in PBS and hearts were washed in PBS containing 2 mM $MgCl_2$. The staining solution (1x PBS, 20 mM $K_3Fe(CN)_6$, 20 mM $K_4Fe(CN)_6$, 2mM $MgCl_2$, 0.01% DOC, 0.4 mg/ml X-gal (0.02% NP-40 for hearts)) was then added to cells or hearts were incubated at 37 °C until the stain developed.

2.26 Statistical analysis

Statistical tests were performed using Graphpad Prism 4.0 software.

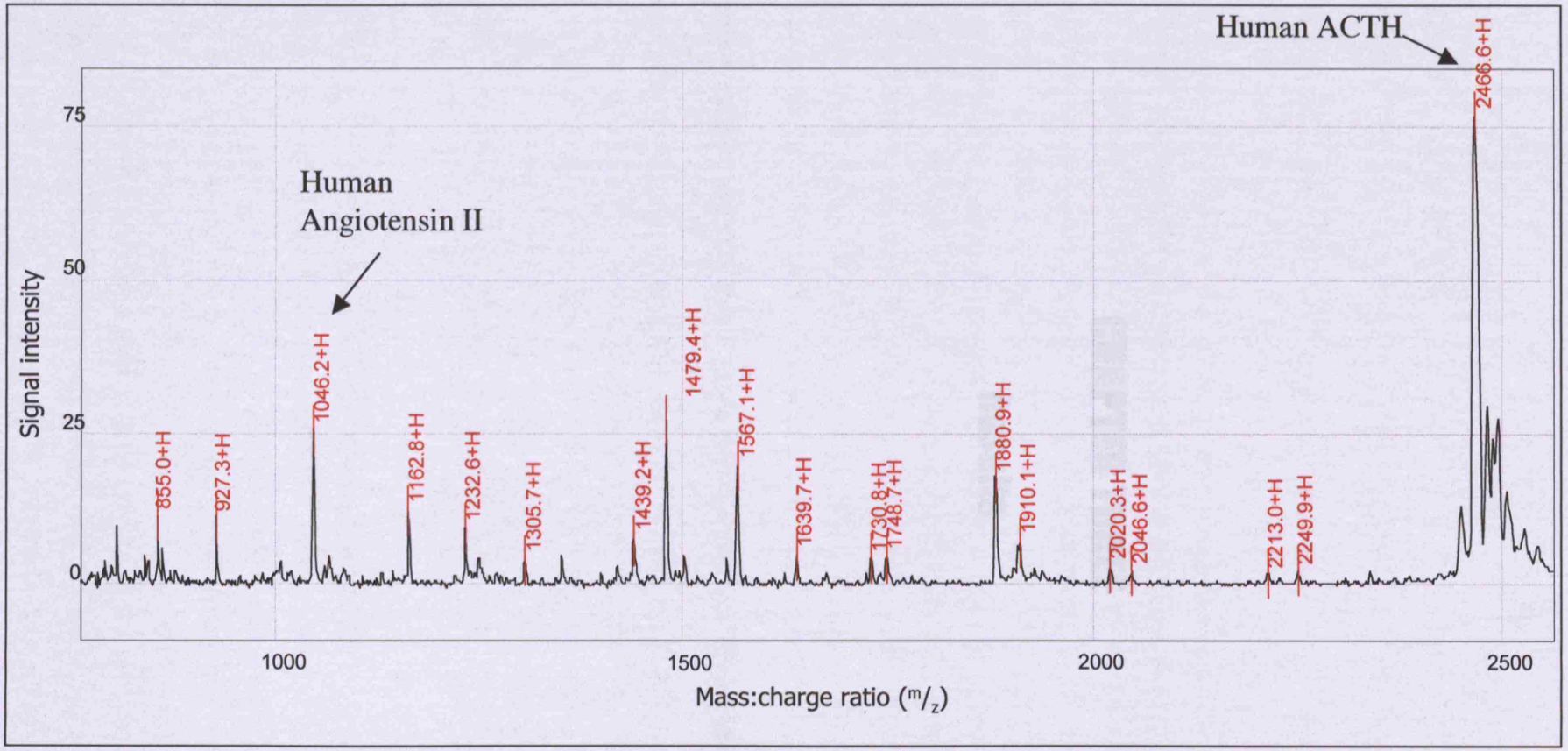

Figure 2.3. Peptide mass fingerprinting by MALDI-TOF. Shown is a peptide mass fingerprint of trypsin digested bovine serum albumin (BSA). BSA was trypsin digested and the masses of the digested peptides were measured by MALDI-TOF. Peptides of known mass from human angiotensin II ($^m/_z$ = 1046.2) and adrenocorticotrophic hormone (ACTH) ($^m/_z$ = 2466.6) were included in the BSA peptide mix and used as standards to measure BSA peptides.

CHAPTER THREE

Results

CHAPTER THREE

Generation of transgenic mice with inactivated caspase-8 or caspase-9 signalling

3.1 Introduction and aims of this chapter

Apoptosis contributes to cell death in ischaemia/reperfusion (I/R) in the heart (reviewed by MacLellan and Schneider, 1997). Apoptotic death proceeds by two distinct signalling pathways, the death receptor and mitochondrial pathways, which are mediated by initiator caspases -8 and -9 respectively. These two pathways are regulated by other proteins that promote or inhibit the apoptotic process. The transcription factor, signal transducer and activator of transcription 1 (STAT1), is a pro-apoptotic member of the STAT family and the primary mediator of interferon gamma (IFNγ) response. STAT1 has also been shown to be a mediator of apoptotic cell death induced by I/R (Stephanou et al., 2000). However, it is not known what contribution the caspase-8 and caspase-9 pathways have in STAT1 mediated I/R-injury.

Transgenic mice that are deficient in caspase-8 or caspase-9 activation would enable the relative contribution of the death receptor and mitochondrial pathways in STAT1 mediated I/R-injury to be determined. Specific inhibition of caspase-8 and caspase-9 has been achieved in isolated cells by over-expression of flice-like inhibitory protein (FLIP) or caspase-9 short (C9s) respectively (Stephanou et al., 2001, Stephanou et al., 2002).

The major aim of the work presented here was is generate transgenic mice, that over-express FLIP or C9s using the pronuclear injection method. Transgenic mouse production by pronuclear injection of DNA is a routine technique in many transgenic facilities (reviewed by Bianco et al., 2003). Constructs are injected into the pronucleus of a one-cell fertilized mouse embryo where the DNA randomly integrates into the mouse genome in the form of head-to-tail concatemers, resulting in multiple copies of the transgene inserting into a single site (Bianco et al., 2003). Caspase-8 knockout mice have an embryonic lethal phenotype with impaired heart muscle development and caspase-9 knockout mice have a perinatal lethal phenotype (Kuida

et al., 1998, Varfolomeev et al., 1998). Transgenic mice that over-express FLIP or C9s may have the same lethal phenotype as caspase-8 and caspase-9 knockout mice. Therefore, the tetracycline transactivator (tTA) system was used so that transgene expression could be temporally regulated.

3.2 Generation of Tet responder transgenic mice for C9s or FLIP over-expression

The Tet-inducible system is a binary system that involves two distinct transgenic mice; a Tet mouse and a Tet-responder mouse. The Tet mouse is a transgenic mouse expressing the tTA protein and the Tet-responder mouse is a transgenic mouse with a transgene that is transcriptionally regulated by the tTA protein (see figure 1.3). Progeny from these mice that have inherited both transgenes (compound transgenics) will express the Tet-responsive gene in tissues that the tTA protein is expressed. Expression is inducible with the addition or removal of tetracyclines, depending on whether the Tet mouse is Tet-on or Tet-off, respectively. The pBIG plasmid is an expression vector in which expression of an inserted transgene is induced by tTA. The pBIG plasmid also contains a bi-directional promoter, which is linked to the inserted transgene and the β-galactosidase reporter gene, *lacZ*. The *lacZ* reporter gene is used in the pBIG vector for easy identification of transgene expression. Thus, tTA induces the expression of both β-galactosidase and the inserted transgene.

Therefore, pBIG expression vectors containing C9s (pBIG-C9s) (Figure 3.1) or FLIP (pBIG-FLIP) (Figure 3.2) transgenes, which have been previously generated, linearized and prepared for pronuclear injection in our laboratory, were used in the generation of tTA responder transgenic mice.

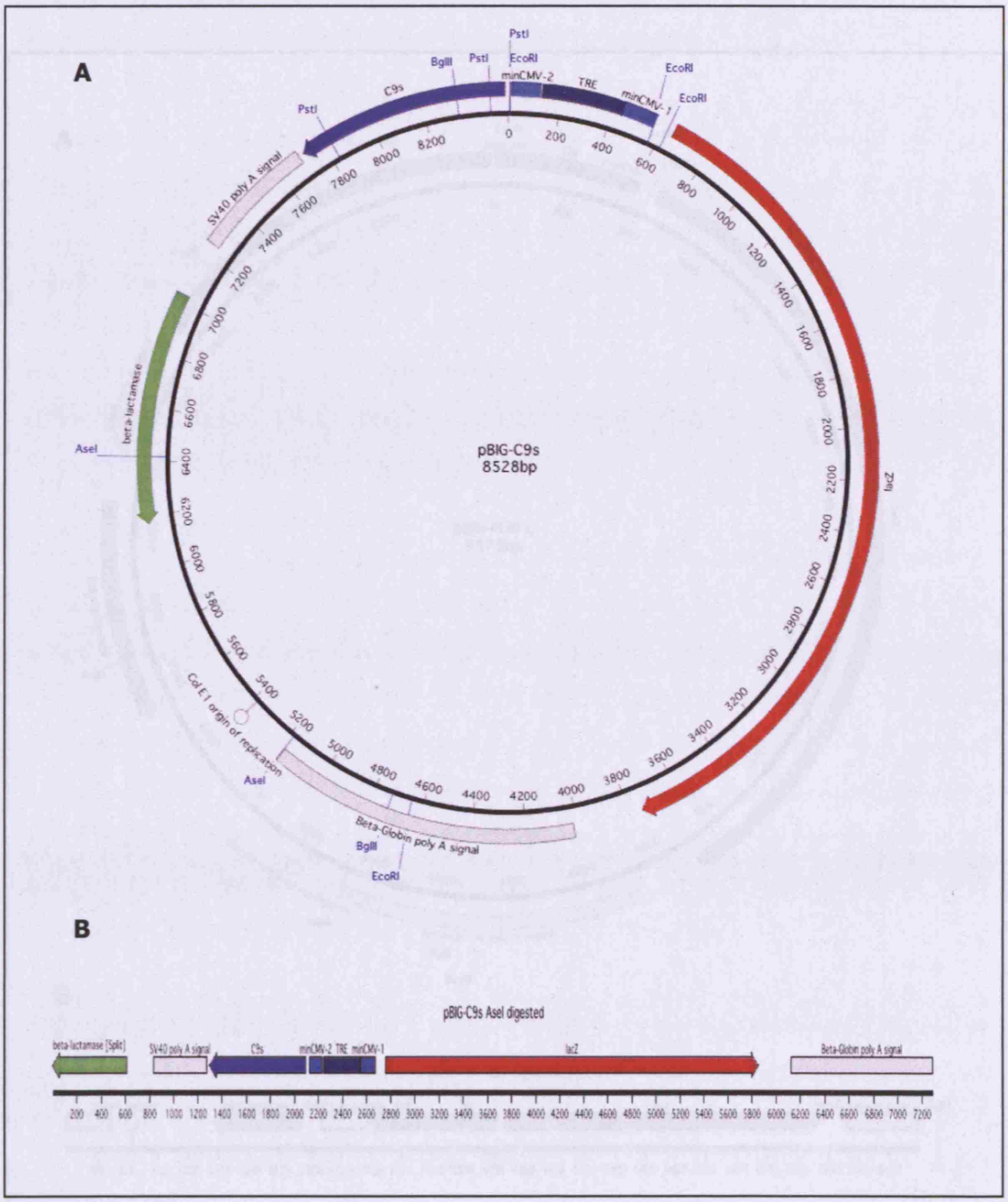

Figure 3.1 Linearization of the pBIG-C9s expression vector. A) Restriction map of the circular pBIG-C9s expression vector. B) The pBIG-C9s vector, linearized by *AseI* digestion, was used in transgenesis.

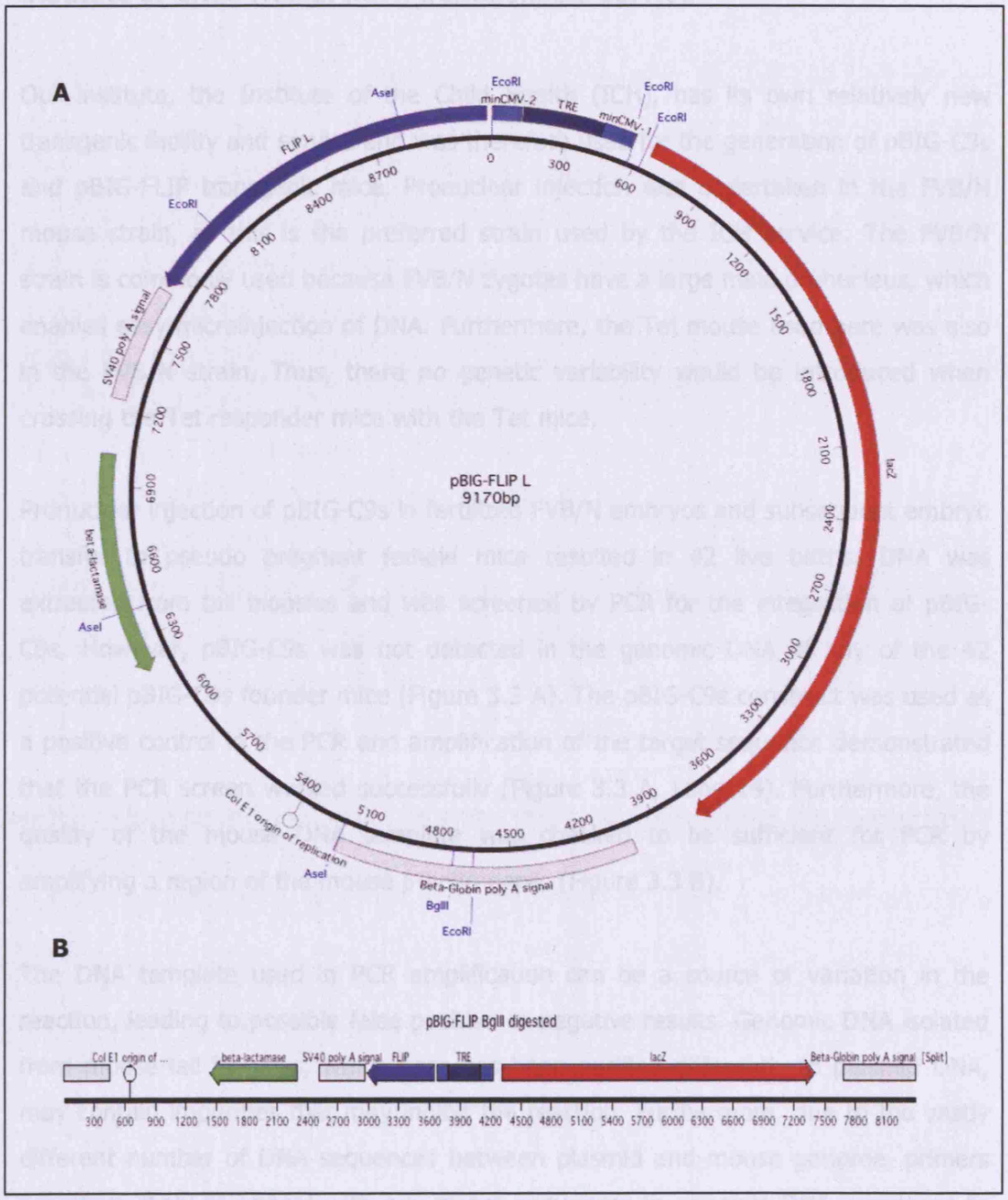

Figure 3.2 Linearization of the pBIG-FLIP expression vector. A) Restriction map of the circular pBIG-FLIP expression vector. B) The pBIG-FLIP vector, linearized by *BglII* digestion, was used in transgenesis.

3.2.1 Mouse pronuclear injection with pBIG-C9s and pBIG-FLIP using the Institute of Child Health (ICH) transgenesis service

Our institute, the Institute of the Child Health (ICH), has its own relatively new transgenic facility and service and was therefore used for the generation of pBIG-C9s and pBIG-FLIP transgenic mice. Pronuclear injection was undertaken in the FVB/N mouse strain, as this is the preferred strain used by the ICH service. The FVB/N strain is commonly used because FVB/N zygotes have a large male pronucleus, which enables easy microinjection of DNA. Furthermore, the Tet mouse used here was also in the FVB/N strain. Thus, there no genetic variability would be introduced when crossing the Tet responder mice with the Tet mice.

Pronuclear injection of pBIG-C9s in fertilized FVB/N embryos and subsequent embryo transfer to pseudo pregnant female mice resulted in 42 live births. DNA was extracted from tail biopsies and was screened by PCR for the integration of pBIG-C9s. However, pBIG-C9s was not detected in the genomic DNA of any of the 42 potential pBIG-C9s founder mice (Figure 3.3 A). The pBIG-C9s construct was used as a positive control in the PCR and amplification of the target sequence demonstrated that the PCR screen worked successfully (Figure 3.3 A, Lane 14). Furthermore, the quality of the mouse DNA template was checked to be sufficient for PCR by amplifying a region of the mouse β-actin gene. (Figure 3.3 B).

The DNA template used in PCR amplification can be a source of variation in the reaction, leading to possible false positive or negative results. Genomic DNA isolated from mouse-tail biopsies, which here has been purified differently to plasmid DNA, may contain impurities that may inhibit the reaction. Furthermore, due to the vastly different number of DNA sequences between plasmid and mouse genome, primers are more likely to anneal with non-target sequences in genomic DNA compared to plasmid DNA. Therefore, using purified plasmid DNA alone may not necessarily be considered as a sufficient control for the comparison of amplification of sequences from genomic DNA. Therefore, further validation of the PCR screen was required. To this end, the target sequence was amplified using pBIG-C9s diluted in mouse genomic DNA. The plasmid was serially diluted in mouse genomic DNA to concentrations of lower than 1 plasmid copy per cell of genomic DNA. The target sequence and was amplified by PCR at the all the concentrations tested, including the lowest of 1×10^{-8} (Figure 3.4). Therefore, the mouse genomic DNA samples were

not inhibiting the PCR amplification of pBIG-C9s, suggesting that the potential pBIG-C9s founder mice were indeed negative.

Southern blot screening of potential pBIG-C9s founder transgenics also did not detect the transgene. The same validation procedure of detecting pBIG-C9s when diluted in mouse genomic DNA used for PCR was also applied Southern blotting. The pBIG-C9s plasmid was detected in all the dilutions tested (Figure 3.5). Therefore, based on the PCR and Southern blot evidence, the conclusion made was that the pBIG-C9s transgene did not integrate into the DNA of any of the 42 potential founders.

Similarly, the ICH transgenic service failed to produce any mice from pronuclear injection of pBIG-FLIP in FVB/N strain zygotes. Further pBIG-FLIP DNA was prepared, separately to the first, and was provided to the ICH service. However, no potential founder mice were produced. This failure was not limited to pronuclear injections with the pBIG-FLIP construct as other service users also experienced similar problems. Technical difficulties and signs of animal stress, such as mice neglecting their pups, were cited by the ICH transgenic service. Therefore, it was not possible to attribute toxicity of pBIG-FLIP in pronuclear injection as the reason for failure to produce potential founder mice. Therefore, we opted to outsource the generation of pBIG-C9s and pBIG-FLIP transgenic mice to an established provider.

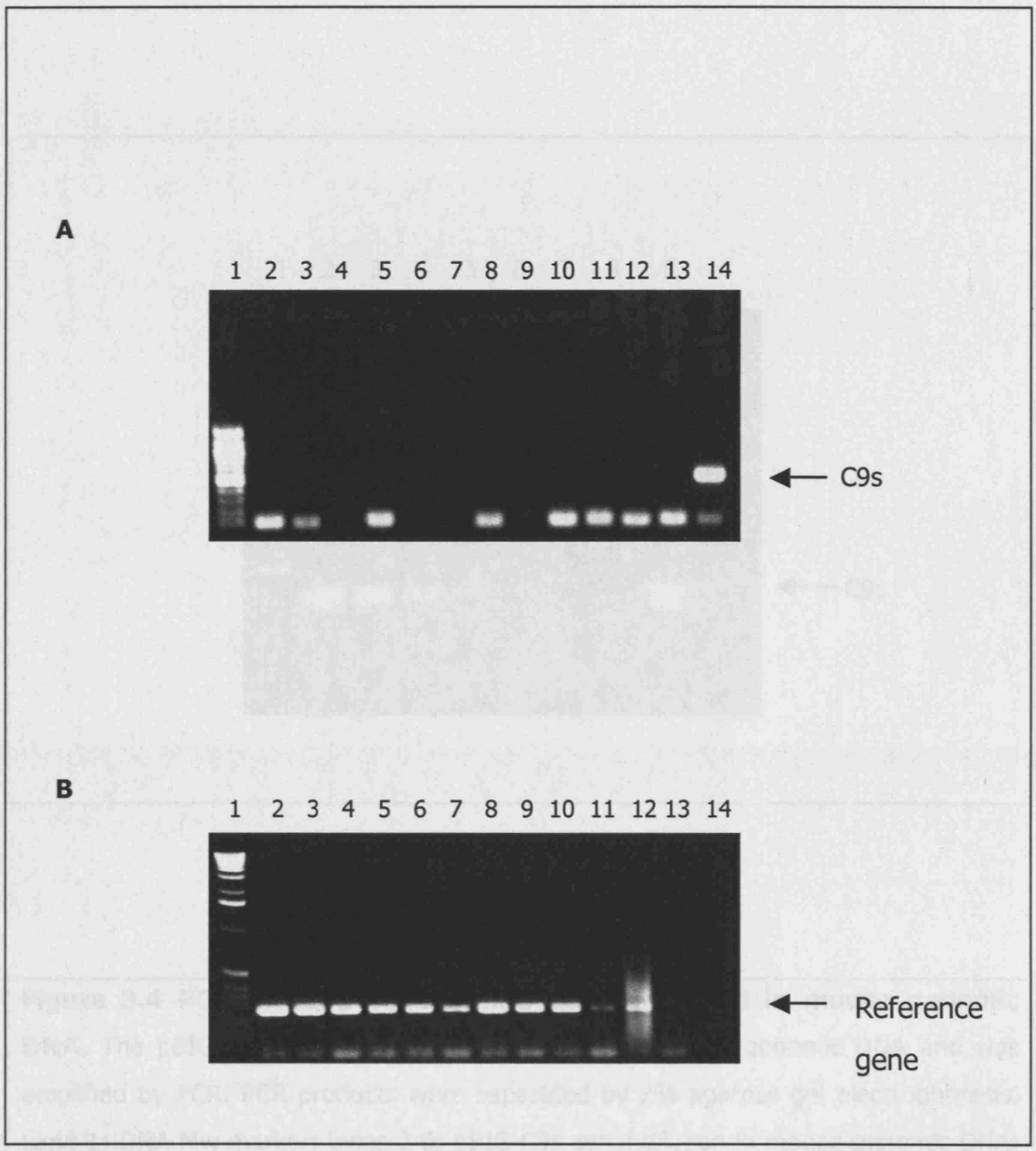

Figure 3.3 PCR genotyping of potential pBIG-C9s founder mice generated by the ICH service. PCR products of (A) pBIG-C9s transgene and (B) genomic DNA control (reference gene) were separated by 2% agarose gel electrophoresis. Lane 1; DNA Mw marker; lanes 2-11; pBIG-C9s founders 1-10; lane 12; non-transgenic mouse; lane 13; water; lane 14; pBIG-C9s plasmid.

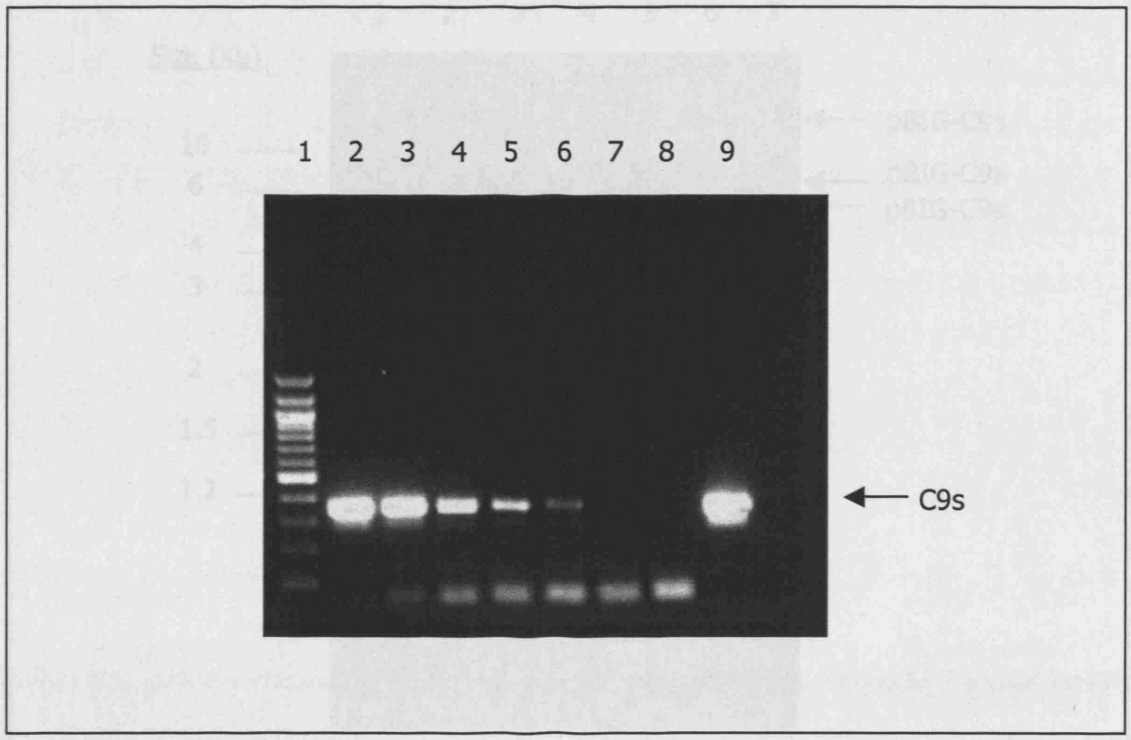

Figure 3.4 PCR of pBIG-C9s plasmid serially diluted in mouse genomic DNA. The pBIG-C9s plasmid was serially diluted in mouse genomic DNA and was amplified by PCR. PCR products were separated by 2% agarose gel electrophoresis. Lane 1; DNA Mw marker; lanes 2-6; pBIG-C9s serial dilution in mouse genomic DNA; lane 2; 1×10^{-3}; lane 3; 1×10^{-4}; lane 4; 1×10^{-5}; lane 5; 1×10^{-6}; lane 6; 1×10^{-7}; lane 7; mouse genomic DNA only; lane 8; water; lane 9; undiluted plasmid.

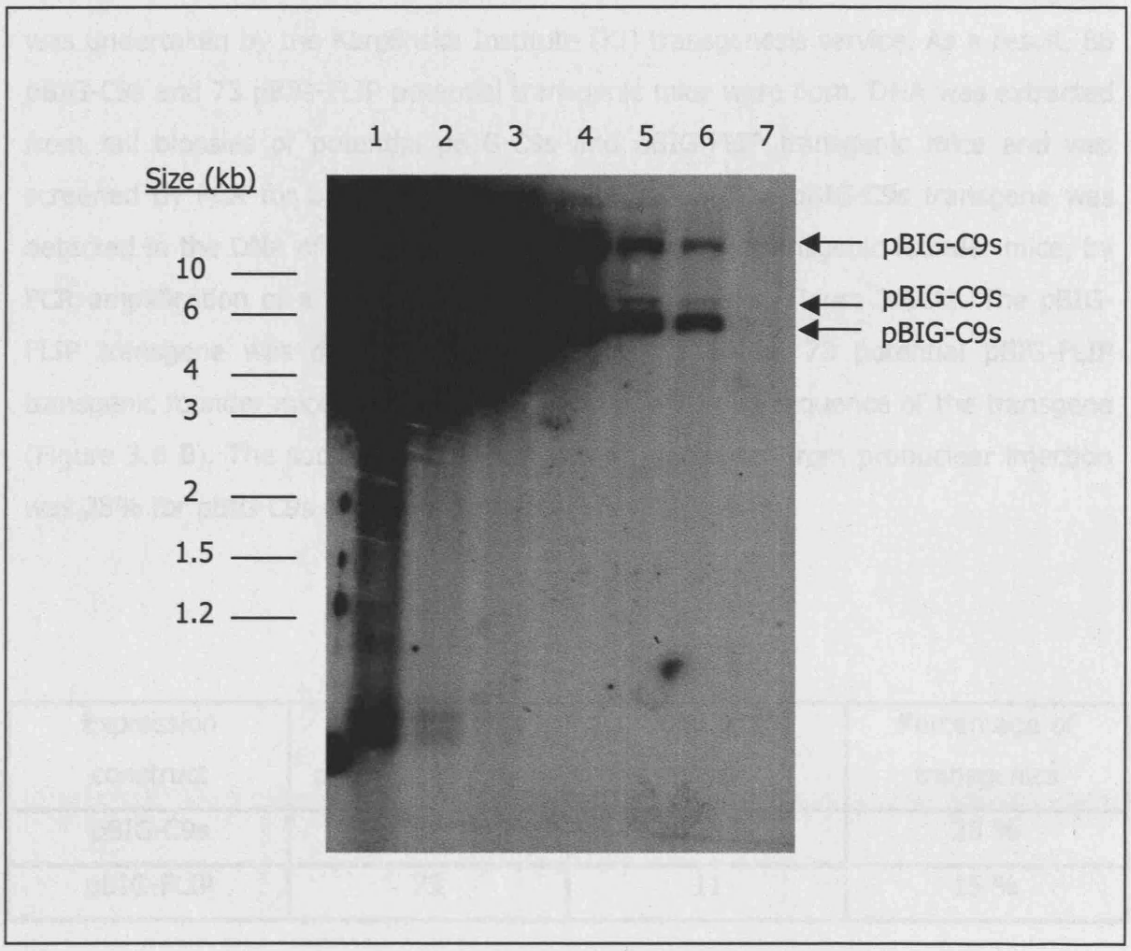

Figure 3.5 Southern blot of pBIG-C9s plasmid serially diluted in mouse genomic DNA. The pBIG-C9s plasmid was serially diluted in *EcoR1* restriction digested mouse genomic DNA and separated by 1% TAE agarose gel electrophoresis. Separated DNA was transferred to Hybond-N^+ nitrocellulose membrane and a [^{32}P]-dCTP radiolabelled fragment of pBIG-C9s was hybridised to the membrane. Three distinct bands were observed, representing different supercoiled forms of the pBIG-C9s plasmid. Lanes 1-6; pBIG-C9s serially diluted in mouse genomic DNA; Lane 1; 1 x 10^{-3}; lane 2; 1 x 10^{-4}; lane 3; 1 x 10^{-5}; lane 4; 1 x 10^{-6}; lane 5; 1 x 10^{-7}; lane 6; 1 x 10^{-8}; lane 7; mouse genomic DNA only.

3.2.2 Mouse pronuclear Injection using the Karolinska Institute transgenesis service

Pronuclear injection of pBIG-C9s and pBIG-FLIP DNA in FVB/N mouse strain zygotes was undertaken by the Karolinska Institute (KI) transgenesis service. As a result, 88 pBIG-C9s and 73 pBIG-FLIP potential transgenic mice were born. DNA was extracted from tail biopsies of potential pBIG-C9s and pBIG-FLIP transgenic mice and was screened by PCR for potential transgene integration. The pBIG-C9s transgene was detected in the DNA of 25 of the 88 potential pBIG-C9s transgenic founder mice, by PCR amplification of a 220bp sequence of the transgene (Figure 3.6 A). The pBIG-FLIP transgene was detected in the DNA of 11 of the 73 potential pBIG-FLIP transgenic founder mice by PCR amplification of a 150 bp sequence of the transgene (Figure 3.6 B). The success rate of transgenics generated from pronuclear injection was 28% for pBIG-C9s and 15% for pBIG-FLIP (Table 3.1).

Expression construct	Number of potential founders	Number of transgenics	Percentage of transgenics
pBIG-C9s	88	25	28 %
pBIG-FLIP	73	11	15 %

Table 3.1. Quantity and percentage of transgenics identified in potential pBIG-C9s and pBIG-FLIP founders generated by the KI transgenic service.

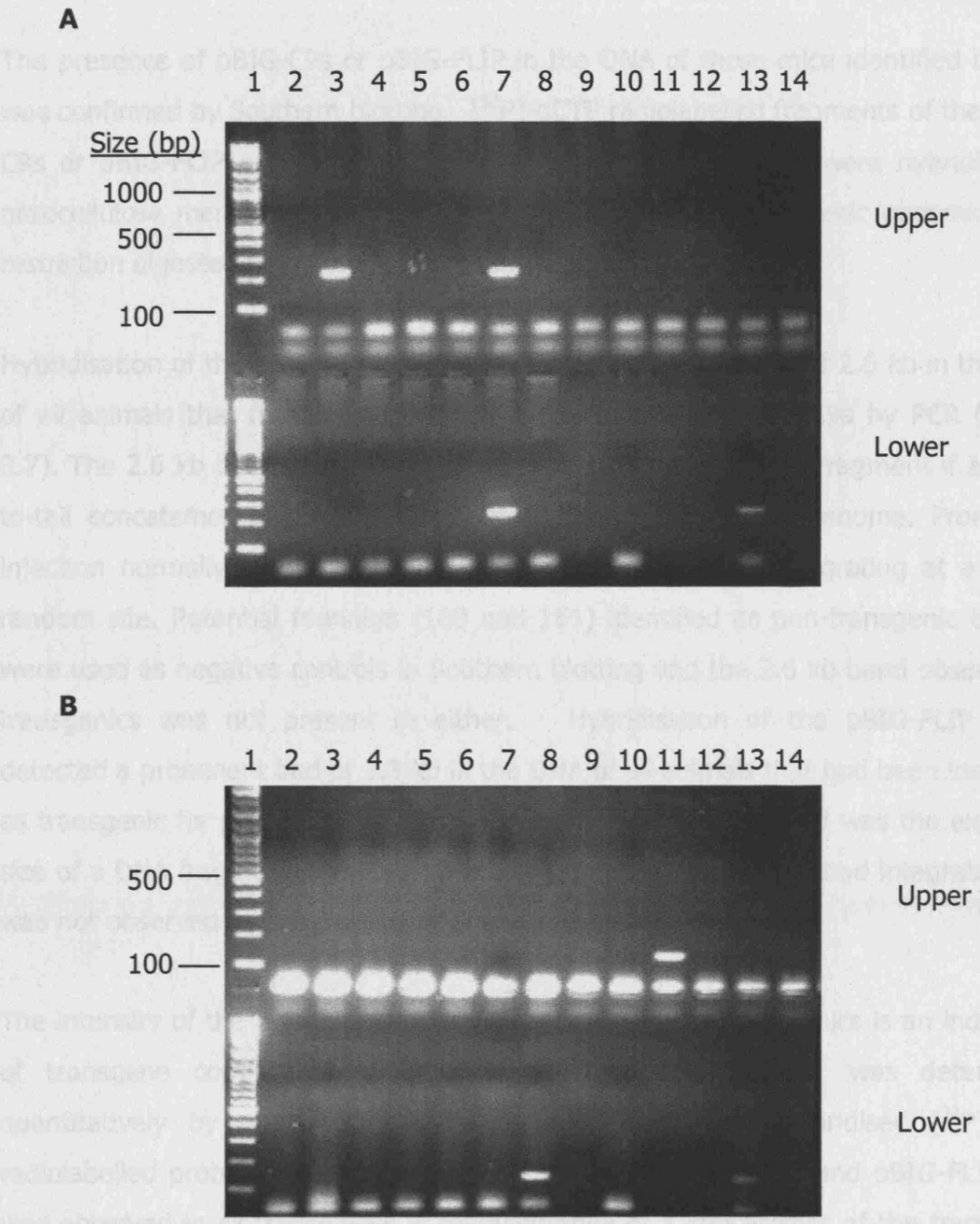

Figure 3.6 PCR genotyping of potential pBIG-C9s and pBIG-FLIP transgenic founders generated by the KI transgenic service. PCR products of (A) potential pBIG-C9s founders and (B) potential pBIG-FLIP founders were separated by 2% TAE agarose gel electrophoresis. (A) Lane 1; Upper and lower; DNA Mw marker; lanes 2-14 top and 2-8 bottom; pBIG-C9s founders 74-93; lane 10 bottom; water; lane 13 bottom; pBIG-C9s plasmid. (B) Lane 1 Top and bottom; DNA Mw marker; lanes 2-14 top and 2-8 bottom; pBIG-FLIP founders 1-20; lane 10 bottom; water; lane 13 bottom; pBIG-FLIP plasmid.

3.2.3 Southern blot detection of pBIG-C9s or pBIG-FLIP transgenic mice

The presence of pBIG-C9s or pBIG-FLIP in the DNA of those mice identified by PCR was confirmed by Southern blotting. [^{32}P]-dCTP radiolabelled fragments of the pBIG-C9s or pBIG-FLIP expression vector were used as probes and were hybridised to nitrocellulose membranes on which the potential founder transgenic genomic DNA, restriction digested with *EcoR1*, had been transferred.

Hybridisation of the pBIG-C9s probe detected a prominent band of 2.6 kb in the DNA of all animals that had been identified as transgenic for pBIG-C9s by PCR (Figure 3.7). The 2.6 kb band observed was the expected size of a DNA fragment if a head-to-tail concatemer of pBIG-C9s has integrated in the mouse genome. Pronuclear injection normally results in concatemers of the transgene integrating at a single random site. Potential founders (160 and 161) identified as non-transgenic by PCR were used as negative controls in Southern blotting and the 2.6 kb band observed in transgenics was not present in either. Hybridisation of the pBIG-FLIP probe detected a prominent bad of 3.3 kb in the DNA of all animals that had been identified as transgenic for pBIG-FLIP by PCR (Figure 3.8). The 3.3 kb band was the expected size of a DNA fragment if a head-to-tail concatemer of pBIG-FLIP had integrated and was not observed in non-transgenic animals (1 and 2).

The intensity of the 2.6 kb or 3.3 kb band present in the transgenics is an indication of transgene copy number. However, relative copy number was determined quantitatively by phosphor imaging of membranes with hybridised [^{32}P]-dCTP radiolabelled probes. The 2.6 kb band for pBIG-C9s or 3.3 kb band pBIG-FLIP that was observed in all transgenics is representative of a concatemer of the transgene. Therefore, a minimum of two copies of the transgene is present in all transgenics. To determine relative copy number, the lowest value recorded for a pBIG-C9s transgenic was designated as having two copies of the transgene, and based on this value the copy number of all other pBIG-C9s transgenics was determined. Quantification of pBIG-GLIP transgenics was determined in an identical manner. The transgene copy number for pBIG-C9s and pBIG-FLIP transgenics are shown in Table 3.2.

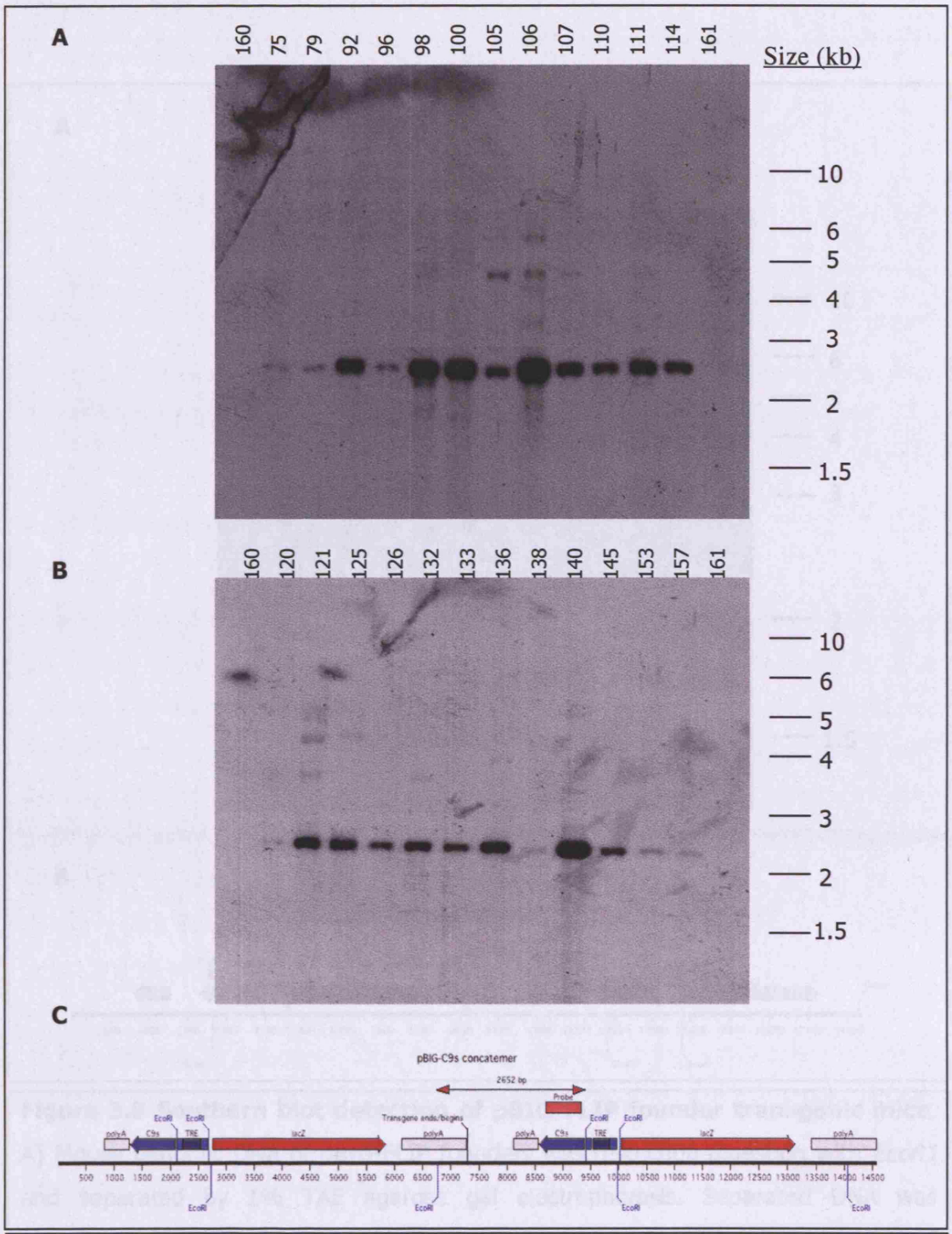

Figure 3.7 Southern blot detection of pBIG-C9s transgenic founder mice. (A and B) Mouse genomic DNA of pBIG-C9s founders were restriction digested with *EcoR1* and separated by 1% TAE agarose gel electrophoresis. Separated DNA was transferred to Hybond-N^+ nitrocellulose membrane and a [^{32}P]-dCTP radiolabelled fragment of pBIG-C9s (*PstI* digested) was hybridised to the membrane. 160 and 161 are non-transgenic DNA controls. A band of 2.6 kb was observed in transgenic mice that represents head-to-tail concatemers of the inserted transgene. C) Schematic detailing how the 2.6 Kb band is derived as a result of integration of concatemers.

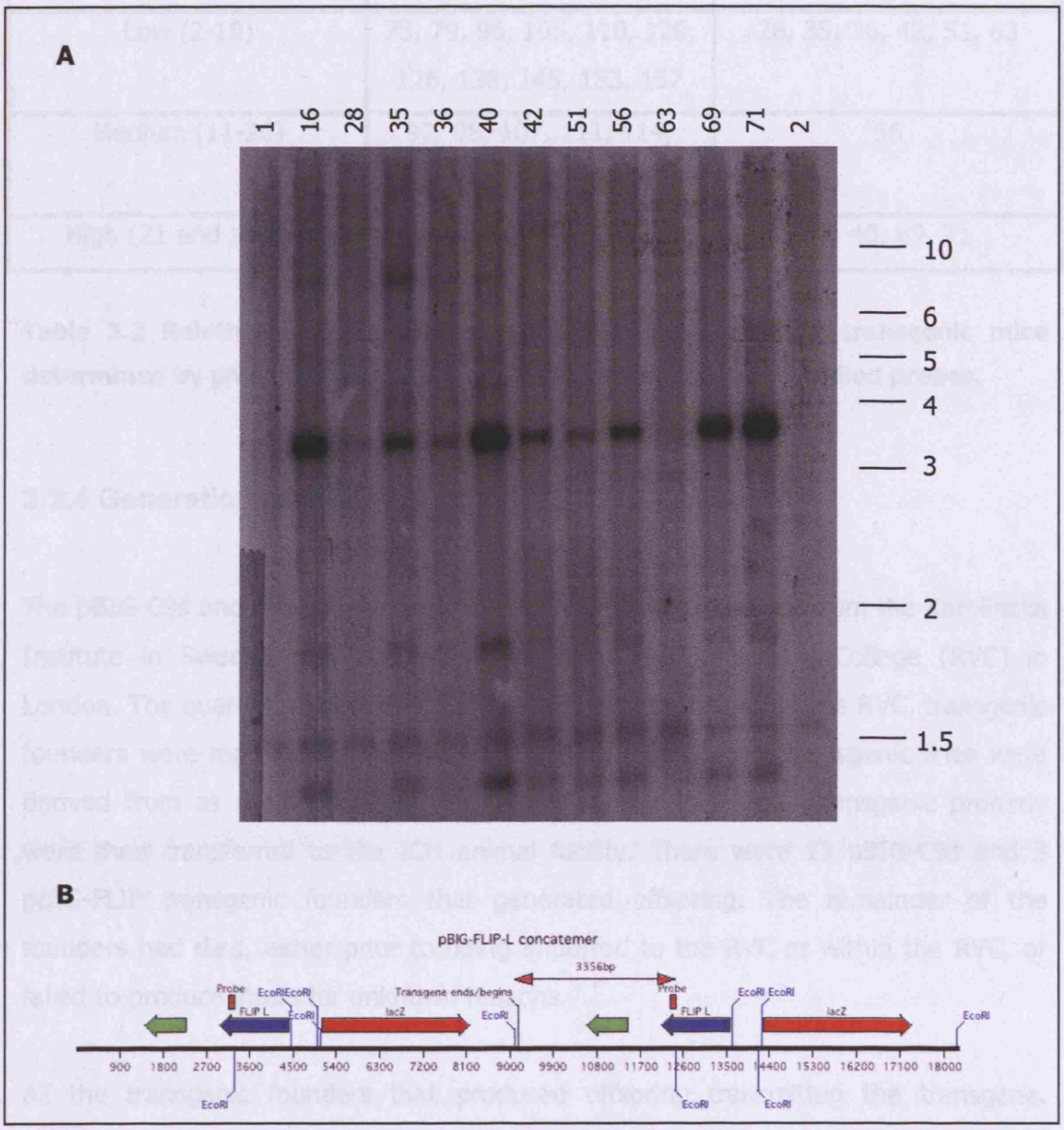

Figure 3.8 Southern blot detection of pBIG-FLIP founder transgenic mice. A) Mouse genomic DNA of pBIG-FLIP founders was restriction digestion with *EcoR1* and separated by 1% TAE agarose gel electrophoresis. Separated DNA was transferred to Hybond-N^+ nitrocellulose membrane and a [^{32}P]-dCTP radiolabelled fragment of pBIG-FLIP (PCR amplified) was hybridised to the membrane. Animals 1 and 2 are non-transgenic controls. A band of approximately 3.3 kb was observed in transgenic mice that represents head-to-tail concatemers of the inserted transgene. B) Schematic detailing how the 3.3 Kb band is derived as a result of integration of concatemers.

Transgene Copy number	pBIG-C9s founders	pBIG-FLIP founders
Low (2-10)	75, 79, 96, 105, 110, 120, 126, 138, 145, 153, 157	28, 35, 36, 42, 51, 63
Medium (11-20)	92, 98, 107, 111, 114, 121, 125, 132, 133, 136	56
High (21 and above)	98, 100, 106, 140,	16, 40, 69, 71

Table 3.2 Relative copy number of pBIG-C9s and pBIG-FLIP transgenic mice determined by phosphor imaging of southern blots with radiolabelled probes.

3.2.4 Generation of pBIG-C9s and pBIG-FLIP F1 progeny

The pBIG-C9s and pBIG-FLIP transgenic founders were imported from the Karolinska Institute in Sweden and quarantined at the Royal Veterinary College (RVC) in London. The quarantine period was for six months. Therefore, at the RVC, transgenic founders were mated with FVB/N strain wild types to ensure transgenic lines were derived from as many founders as possible during this time. Transgenic progeny were then transferred to the ICH animal facility. There were 13 pBIG-C9s and 3 pBIG-FLIP transgenic founders that generated offspring. The remainder of the founders had died, either prior to being imported to the RVC or within the RVC, or failed to produce litters for unknown reasons.

All the transgenic founders that produced offspring transmitted the transgene. However, transmission of the transgene from transgenic founder to progeny varied between 17% and 75%. The expected Mendelian ratio for transgene transmission would be 50%. A ratio higher than this is likely to reflect too small a sample size (the number of progeny screened) thereby giving an artificially high value. This same reason may also explain a low ratio. However, lower ratios may be a sign of mosaicism. Transgenic mice that are described as mosaics do not contain the transgene in all the cells of the body. Mosaic mice are generated if the microinjected DNA has integrated into the zygote after the single cell stage. Thus, if not all the sex cells contain the transgene then transmission will be lower than 50%. However, in all subsequent generations normal Mendelian inheritance of transgenes was observed.

3.2 Tet transgenic mice

The Tet transgenic mice used here, αMHC-tTA, express the tTA protein under control of the alpha myosin heavy chain (αMHC) promoter. The transcriptional activity of the tTA protein in αMHC-tTA is inhibited by tetracyclines and thus these mice are Tet-off mice. Expression of αMHC in the adult mouse is restricted to the heart, specifically cardiac myocytes. Therefore, when αMHC-tTA transgenic mice are crossed with Tet responder mice, the expression of Tet responsive genes in compound transgenics will also be restricted to cardiac myocytes. The αMHC-tTA transgenic mice were obtained from Jackson Laboratories and were crossed with FVB/N strain wild types, which was done to establish a colony of αMHC-tTA transgenics. The αMHC-tTA transgene in these mice is present as a single allele and thus are described as hemizygous. Therefore, it is necessary to screen αMHC-tTA transgenic progeny for the presence of the transgene. Progeny of αMHC-tTA mice were genotyped by PCR and αMHC-tTA transgenic mice were identified (Figure 3.9).

Neonatal mouse cardiac myocyte (NMCM) cells were isolated from αMHC-tTA transgenic mice and transfected with the pBIG expression vector to confirm they produced functional tTA protein. This was assayed by detecting the expression of β-galactosidase, the product of the Tet responsive reporter gene harboured by the pBIG vector, *lacZ*. Expression of β-galactosidase was determined by X-gal staining and Western blotting (Figure 3.10). X-gal (5-bromo-4-chloro-3-indolyl-b-D-galactopyranoside) is a glycoside that is cleaved by β-galactosidase to yield galactose and 5-bromo-4-chloro-3-hydroxyindole, which is then is oxidized into 5,5'-dibromo-4,4'-dichloro-indigo, an insoluble blue product. Blue cardiac myocytes were observed following X-gal staining and β-galactosidase expression was also detected by Western blotting. Only a few myocytes observed in Figure 3.10 are blue, which is a reflection of the low transfection efficiency achieved by calcium phosphate mediated transfection in primary cardiac myocyte cultures that is routinely experienced in our laboratory. Nevertheless, this experiment demonstrates that NMCM cells isolated from αMHC-tTA transgenic mice express functional tTA that can induce expression of genes in the pBIG vector.

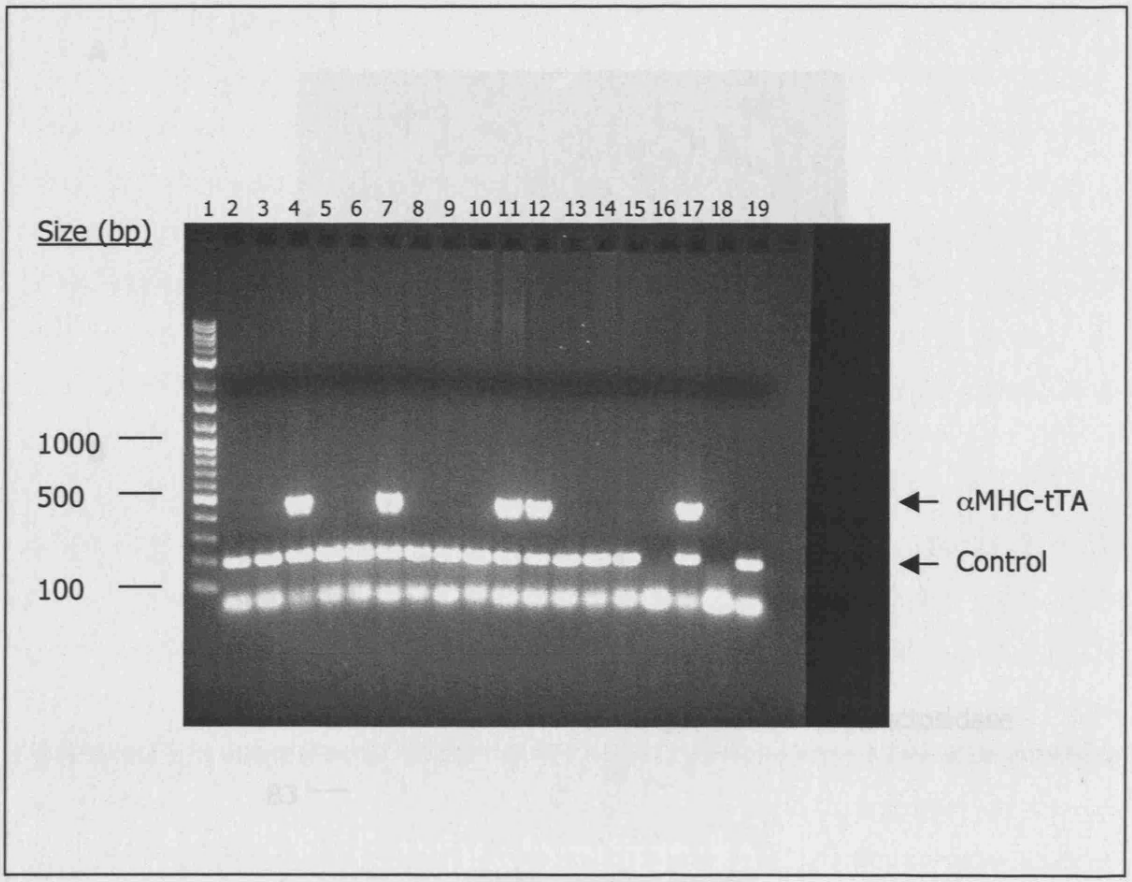

Figure 3.9 PCR genotyping of αMHC-tTA transgenic mice. PCR products from αMHC-tTA screening of litters derived form αMHC-tTA and wild type FVB/N matings were separated by 2% agarose gel electrophoresis. Duplex PCR was performed for amplification of the transgene (450 bp) and a genomic DNA control (200 bp). Lane 1; DNA Mw marker; lanes 2-15; progeny of an αMHC-tTA transgenic and FVB/N wild type parent; lane 16; water; lane 17; αMHC-tTA parent; lane 18; water; lane19; wild type FVN/N parent.

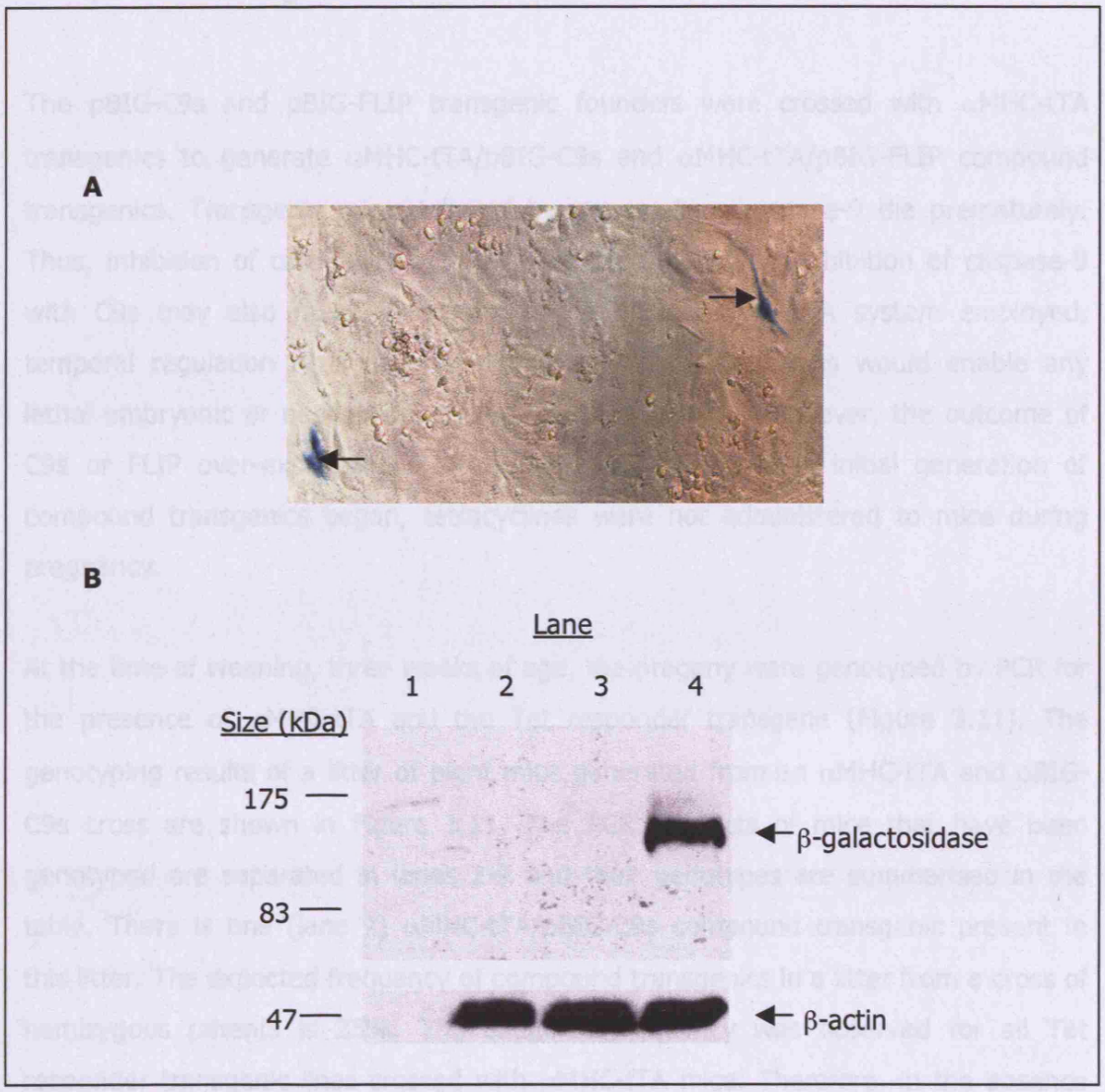

Figure 3.10 Induction of Tet responsive genes in cardiac myocytes isolated from αMHC-tTA transgenic mice. Neonatal mouse cardiac myocyte (NMCM) cells were isolated from αMHC-tTA transgenic mice and transfected with pBIG expression vectors and tTA activity was determined by induction of β-galactosidase. (A) Light microscopic image of X-gal stained culture of αMHC-tTA NMCM cells transfected with the pBIG expression vector (magnification x25). Arrows indicate blue cells that are expressing the pBIG reporter, β-galactosidase. (B) Western blot of cell extracts form αMHC-tTA NMCM cells transfected with pBIG-C9s construct or a C9s expression construct that lacks the *lacZ* gene. Blots were probed with anti-β-galactosidase or anti-β-actin antibodies. Lane 1; Protein Mw marker; lane 2; non-transfected cells; lane 3; CMV-C9s; lane 4; pBIG-C9s.

3.3 Generation of αMHC-tTA/pBIG-C9s and αMHC-tTA/pBIG-FLIP compound transgenic mice

The pBIG-C9s and pBIG-FLIP transgenic founders were crossed with αMHC-tTA transgenics to generate αMHC-tTA/pBIG-C9s and αMHC-tTA/pBIG-FLIP compound transgenics. Transgenic mice deficient in caspase-8 or caspase-9 die prematurely. Thus, inhibition of caspase-8 by over-expression of FLIP or inhibition of caspase-9 with C9s may also result in premature death. With the tTA system employed, temporal regulation of transgene expression with tetracyclines would enable any lethal embryonic or neonatal phenotype to be overcome. However, the outcome of C9s or FLIP over-expression is not known. Therefore, when initial generation of compound transgenics began, tetracyclines were not administered to mice during pregnancy.

At the time of weaning, three weeks of age, the progeny were genotyped by PCR for the presence of αMHC-tTA and the Tet responder transgene (Figure 3.11). The genotyping results of a litter of eight mice generated from an αMHC-tTA and pBIG-C9s cross are shown in Figure 3.11. The PCR products of mice that have been genotyped are separated in lanes 2-9 and their genotypes are summarised in the table. There is one (lane 7) αMHC-tTA/pBIG-C9s compound transgenic present in this litter. The expected frequency of compound transgenics in a litter from a cross of hemizygous parents is 25%. The expected frequency was observed for all Tet responder transgenic lines crossed with αMHC-tTA mice. Therefore, in the absence of tetracyclines, αMHC-tTA/pBIG-C9s and αMHC-tTA/pBIG-FLIP compound transgenics do not result in embryonic or perinatal death.

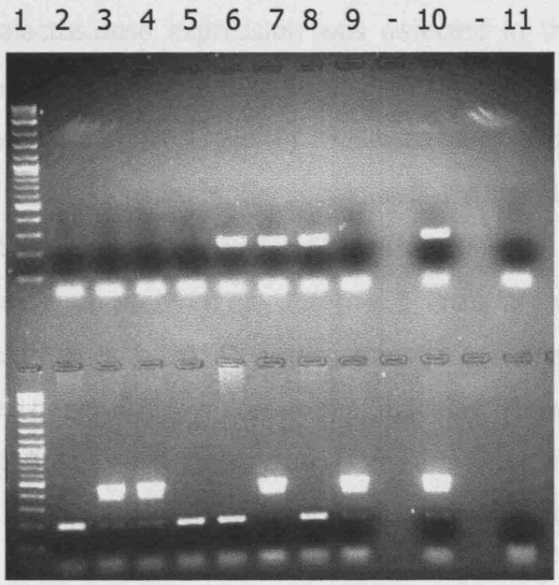

Lane	2	3	4	5	6	7	8	9
pBIG-C9s	-	-	-	-	+	+	+	-
αMHC-tTA	-	+	+	-	-	+	-	+

Figure 3.11. Genotyping of compound transgenic mice. PCR genotyping of αMHC-tTA and pBIG-C9s screening of progeny derived from an αMHC-tTA and pBIG-C9s parent. PCR products from amplification of pBIG-C9s and αMHC-tTA and genomic controls were separated by 2% agarose gel electrophoresis. Lane 1; DNA Mw Marker; lanes 2-9; progeny from αMHC-tTA and pBIG-C9s parents; lane 10; pBIG-C9s or αMHC-tTA parent; lane 11; water. The genotypes of mice are summarized in the table. One αMHC-tTA/pBIG-C9s compound transgenic was identified in this litter (lane 7).

3.3.1 LacZ reporter expression in compound transgenics

Identification of compound transgenic lines that express the transgene construct was determined by the induction of the pBIG reporter gene, *lacZ*. The expression of the *lacZ* reporter product, β-galactosidase, was assayed in the hearts of compound transgenic mice. β-galactosidase expression was detected in the hearts of αMHC-tTA/pBIG-C9s compound transgenics in 2 out of 3 lines tested by X-gal staining and Western blotting (Figure 3.12). The level 0f β-galactosidase expression observed in αMHC-tTA/pBIG-C9s line 145 was higher compared to line 121. β-galactosidase expression was not detected in αMHC-tTA/pBIG-C9s line 75. However, β-galactosidase was not expressed in any of the 3 lines of αMHC-tTA/pBIG-FLIP compound transgenics (Figure 3.13). Failure of transgene expression is expected in some transgenic lines generated by pronuclear injection. However, as only three pBIG-FLIP transgenic lines were generated from the original eleven pBIG-FLIP transgenic founders, the chances of generating an expressing αMHC-tTA/pBIG-FLIP line were reduced.

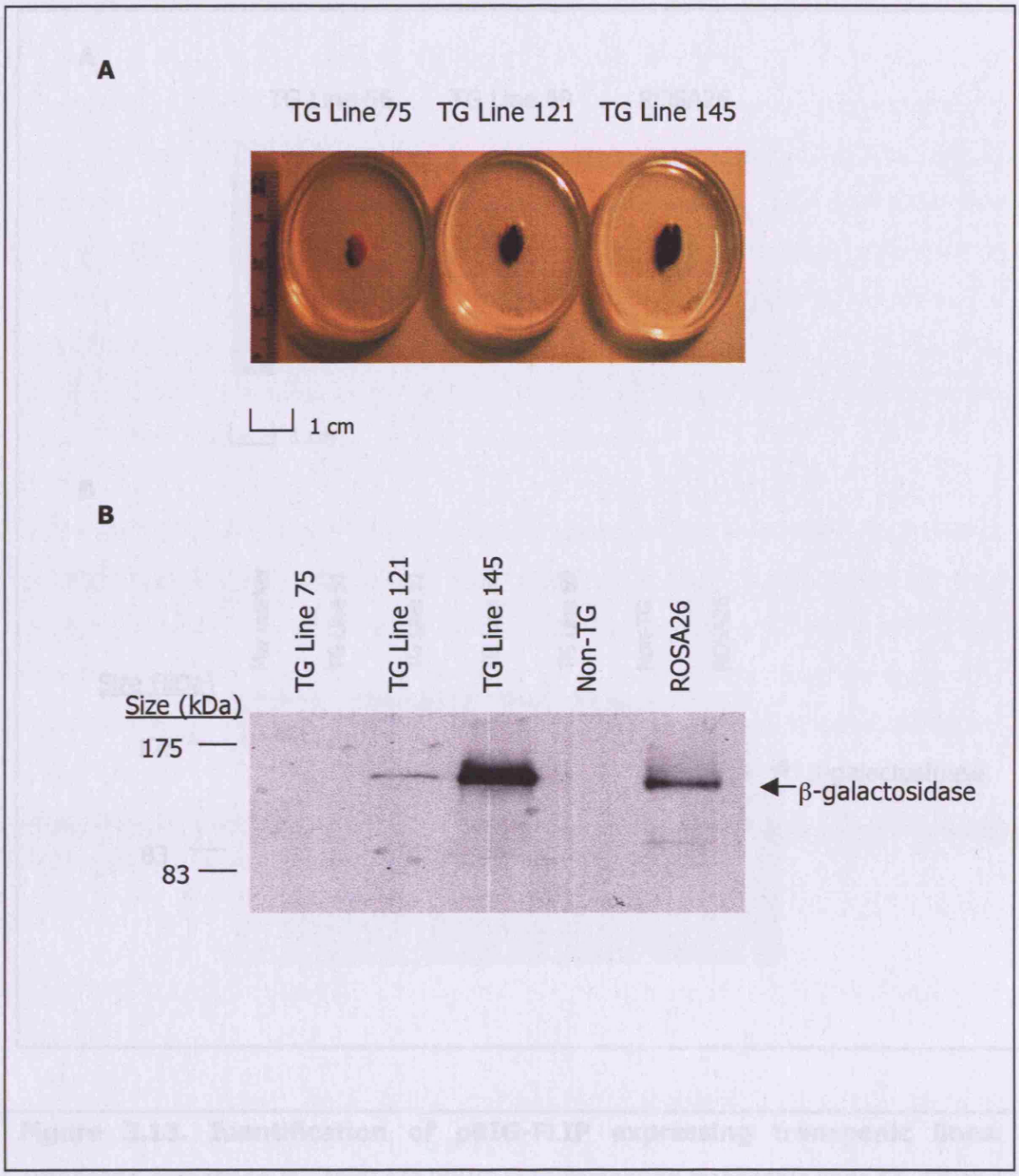

Figure 3.12. Identification of pBIG-C9s expressing transgenic lines. Transgene expression in αMHC-tTA/pBIG-C9s compound transgenic lines 75, 121 and 145 was determined by detection of β-galactosidase expression. (A) Digital image of hearts stained with X-gal. Hearts expressing β-galactosidase appear blue. (B) Western blot of cardiac protein probed with anti-β-galactosidase antibody. Protein extract from ROSA26, a β-galactosidase expressing mouse, was used as a positive control. Expression of β-galactosidase was detected by X-gal staining and Western blotting in hearts from lines 121 and 145 but not 75.

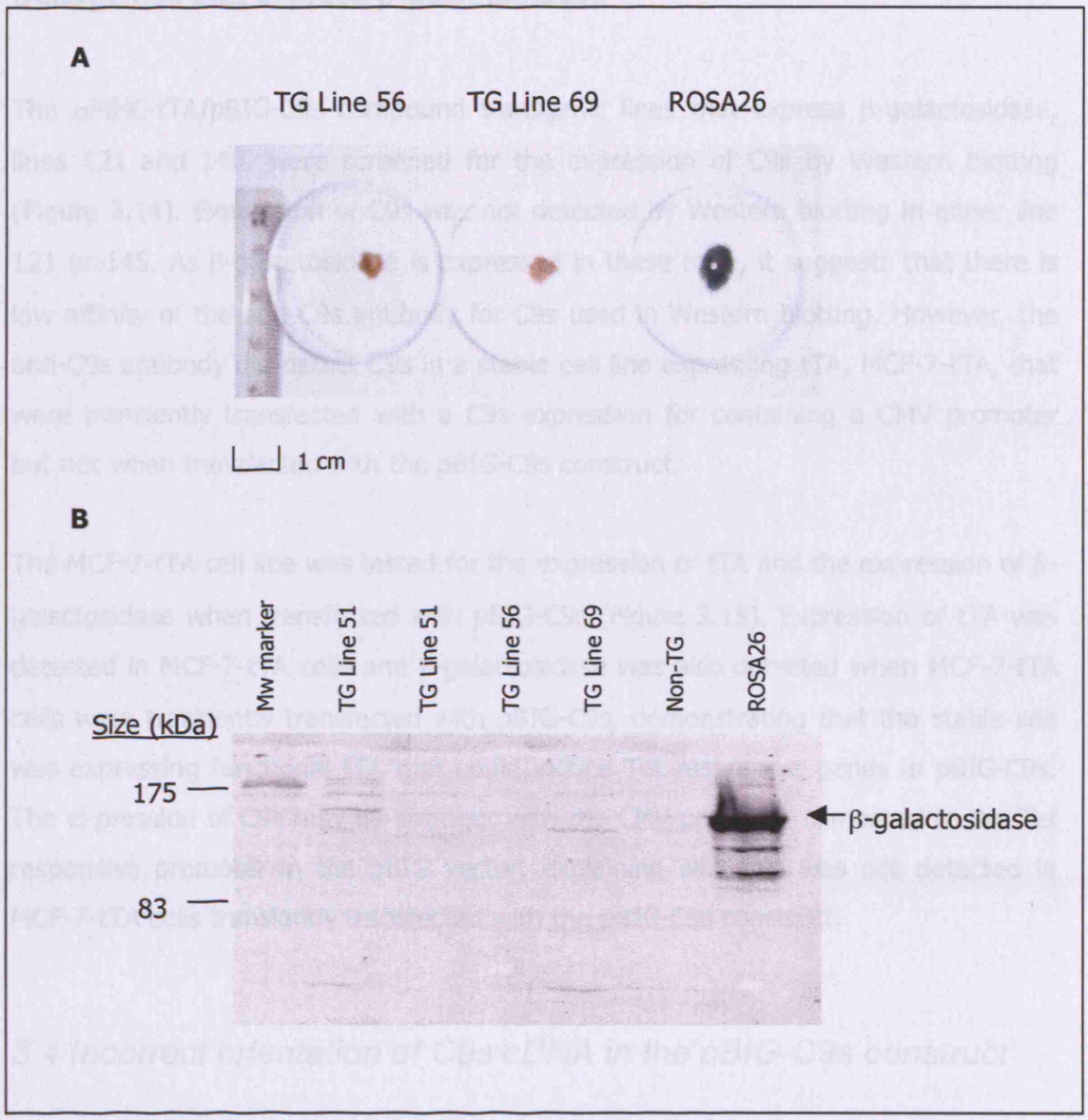

Figure 3.13. Identification of pBIG-FLIP expressing transgenic lines. Transgene expression in αMHC-tTA/pBIG-FLIP compound transgenic lines 51, 56 and 69 was determined by detection of β-galactosidase expression. (A) Digital image of hearts stained with X-gal. A hearts from the β-galactosidase expressing ROSA26 mouse was used a positive control (B) Western blot of cardiac protein probed with anti-β-galactosidase antibody. Expression of β-galactosidase was not detected by X-gal staining or Western blotting in hearts of any αMHC-tTA/pBIG-FLIP transgenic lines.

3.3.2 C9s expression screening in αMHC-tTA/pBIG-9s compound transgenics that express β-galactosidase

The αMHC-tTA/pBIG-C9s compound transgenic lines that express β-galactosidase, lines 121 and 145, were screened for the expression of C9s by Western blotting (Figure 3.14). Expression of C9s was not detected by Western blotting in either line 121 or 145. As β-galactosidase is expressed in these mice, it suggests that there is low affinity of the anti-C9s antibody for C9s used in Western blotting. However, the anti-C9s antibody did detect C9s in a stable cell line expressing tTA, MCF-7-tTA, that were transiently transfected with a C9s expression for containing a CMV promoter but not when transfected with the pBIG-C9s construct.

The MCF-7-tTA cell line was tested for the expression of tTA and the expression of β-galactosidase when transfected with pBIG-C9s (Figure 3.15). Expression of tTA was detected in MCF-7-tTA cells and β-galactosidase was also detected when MCF-7-tTA cells were transiently transfected with pBIG-C9s, demonstrating that the stable line was expressing functional tTA that could induce Tet responsive genes in pBIG-C9s. The expression of C9s may be stronger with the CMV promoter compared to the Tet responsive promoter in the pBIG vector, explaining why C9s was not detected in MCF-7-tTA cells transiently transfected with the pBIG-C9s construct.

3.4 Incorrect orientation of C9s cDNA in the pBIG-C9s construct

The inability to detect C9s in αMHC-tTA/pBIG-C9s compound transgenic lines or in the MCF7-tTA cell line transiently transfected with pBIG-C9s may possibly be due to low antibody affinity for C9s. However, as anti-C9s antibody does detect C9s in cells transiently transfected with a C9s expression construct with a CMV promoter but not the pBIG-C9s construct suggests there may be an error with the pBIG-C9s construct. Therefore, the pBIG-C9s construct used in transgenesis was sequenced. Analysis of the sequence revealed that the C9s sequence is in reverse orientation in the pBIG vector (Figure 3.16). Therefore, C9s could not possibly be expressed with the pBIG-C9s construct that we were given and that was used to generate the pBIG-C9s transgenic mice.

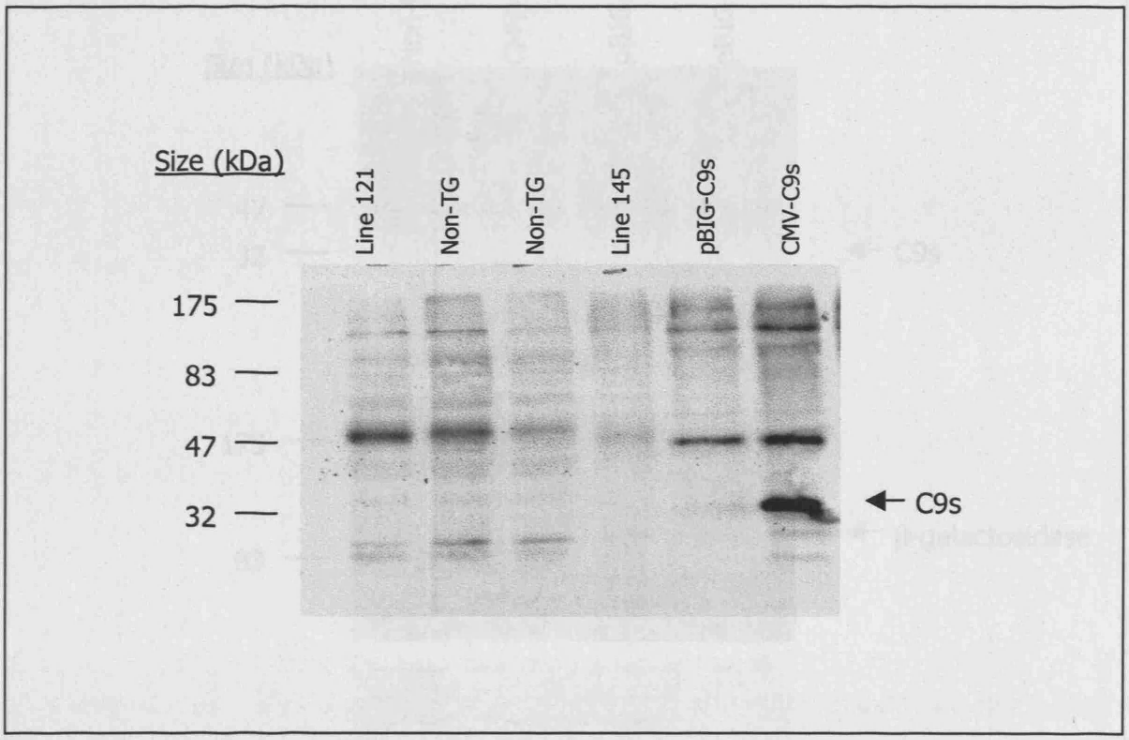

Figure 3.14. Probing C9s expression in β-galactosidase expressing αMHC-tTA/pBIG-C9s transgenic lines. Western blot of cardiac protein from transgenic lines αMHC-tTA/pBIG-C9s 121 and 145 probed with anti-C9s antibody. Protein extract from MCF7-tTA cells transiently transfected with pBIG-C9s or CMV-C9s expression constructs were used as positive controls. A prominent band of 30 kDa representing C9s was observed in MCF7-tTA cells transiently transfected with CMV-C9s. However, a band of 30 kDa was not observed in αMHC-tTA/pBIG-C9s mice.

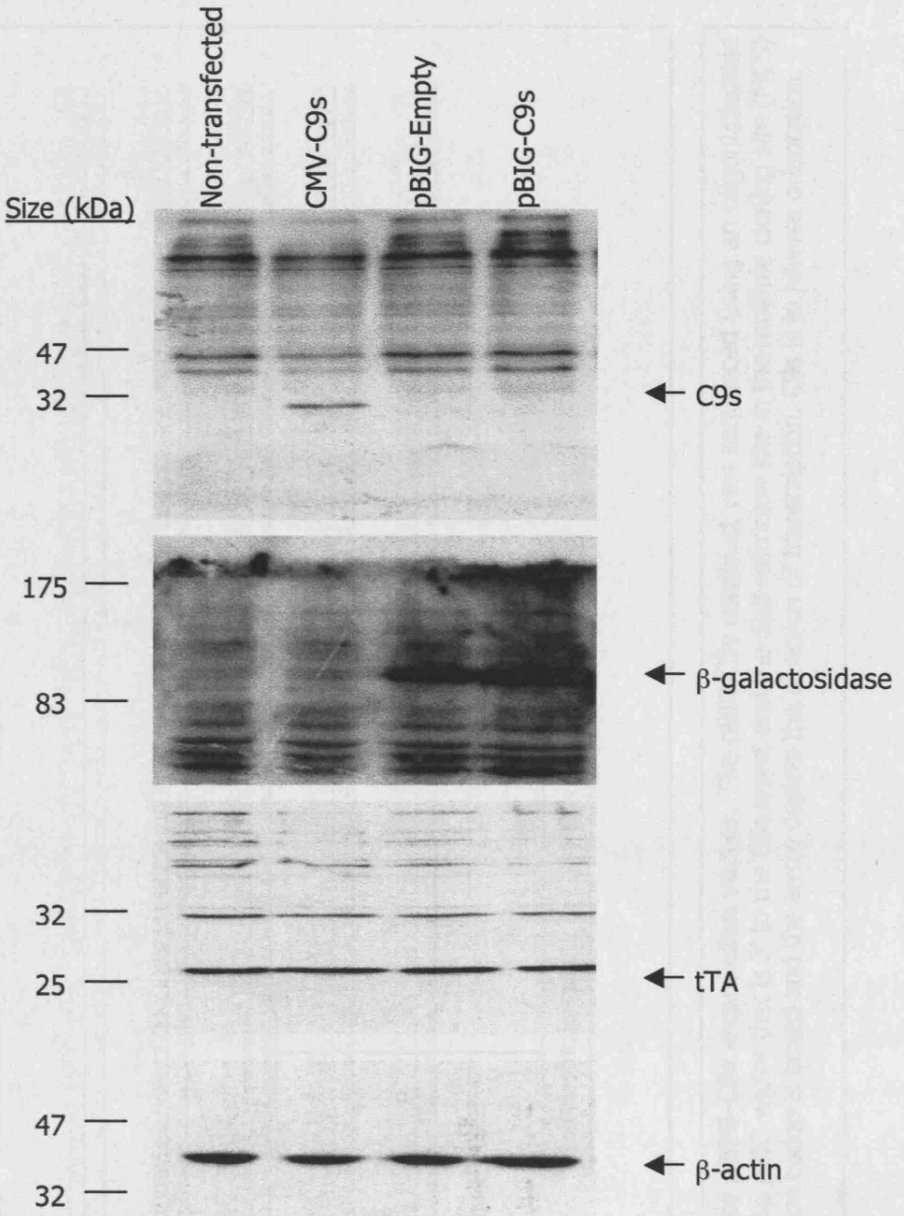

Figure 3.15 Induction of Tet responsive genes in MCF7-tTA stable cell line. Western blot of MCF7-tTA cells transfected with pBIG, pBIG-C9s or CMV-9s constructs. Blots were probed with anti-C9s, anti-β-galactosidase, anti-tTA or anti-β-actin antibodies. The expression of tTA was detected in the MCF7-tTA cells and expression of β-galactosidase was induced when transfected with pBIG or pBIG-C9s. C9s expression was only observed in cells transfected with the CMV-C9s construct.

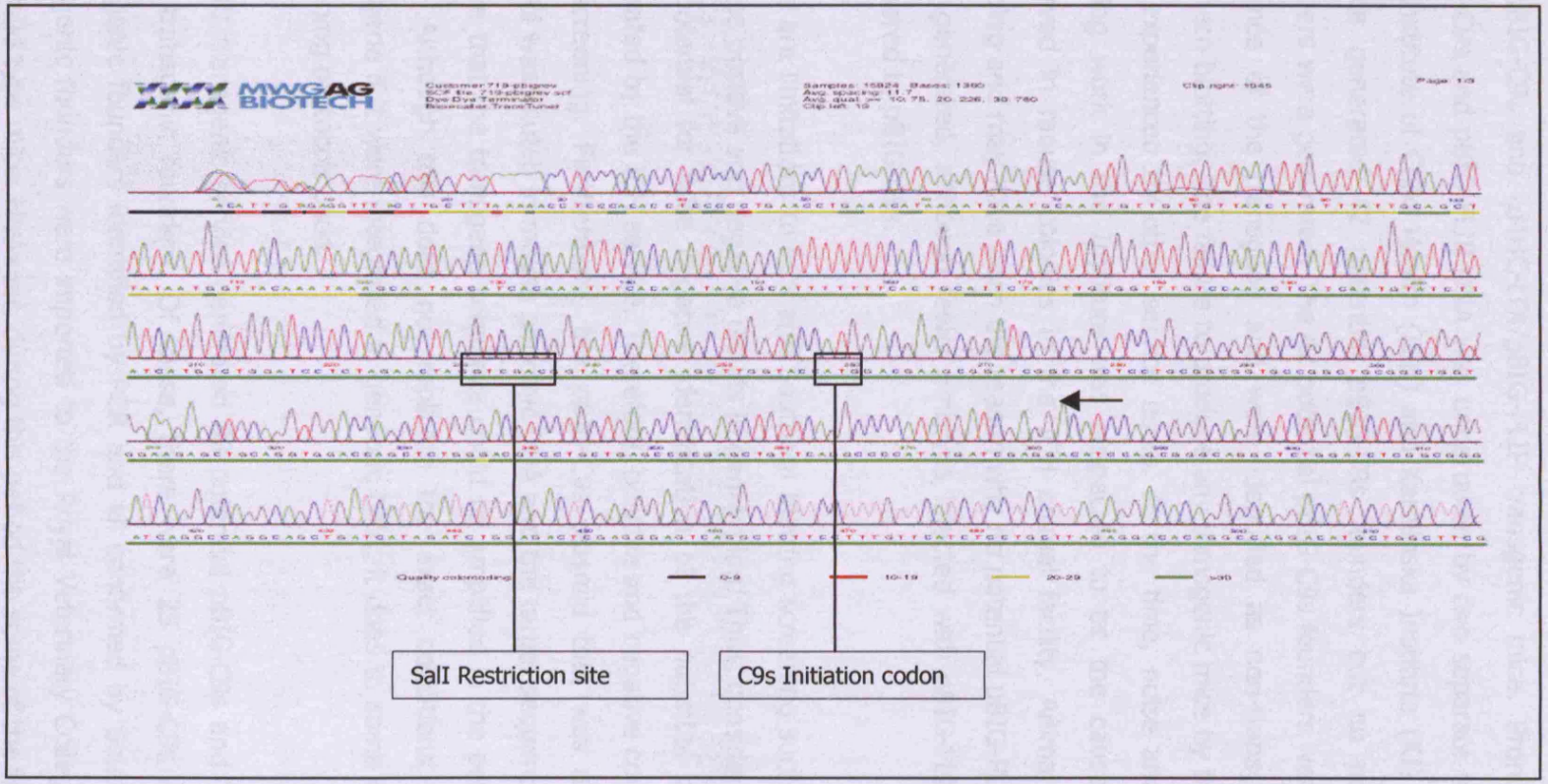

Figure 3.16 Sequencing of pBIG-C9s expression vector. The pBIG-C9s construct was sequenced using an oligonucleotide designed for a sequence in the pBIG vector that is 3' to the C9s insert and the *SalI* restricton site in the multiple cloning site (MCS) of the vector. The C9s initiation codon is boxed and the arrow depicts the direction of transcription. C9s is in reverse orientation.

3.5 Discussion

The data presented here describes the generation and identification of αMHC-tTA/pBIG-C9s and αMHC-tTA/pBIG-FLIP transgenic mice. Pronuclear injection of pBIG-C9s and pBIG-FLIP DNA was undertaken by two separate transgenic services, the Institute of Child Health (ICH) and Karolinska Institute (KI) services. The ICH service generated 42 potential pBIG-C9s founders but no potential pBIG-FLIP founders were generated. The 42 potential pBIG-C9s founders were screened for the presence of the transgene and were identified as non-transgenic by PCR and Southern blotting. The failure to produce any transgenic mice by the ICH service was also experienced by other service users. At the time, noise and vibration due to building work in the Institute was suspected to be the cause of animal stress observed in mouse colonies in the ICH animal facility. Animal stress can affect breeding and may have been the reason why no potential pBIG-FLIP transgenic mice were generated, although fewer embryos injected with pBIG-FLIP were attempted compared to pBIG-C9s.

There are limitations to PCR and Southern blotting screening such as the generation of false positive and negative results in genotyping. Thus, consideration was given to the potential for false negative identification of the potential pBIG-C9s founders generated by the ICH service. Therefore, positive and negative controls were used in the screening. Furthermore, the pBIG-C9s plasmid that was used as a positive control was diluted in mouse genomic DNA and the target sequence was amplified to ensure that the transgene sequence could be amplified in the presence of genomic DNA. Although this does not replicate the exact conditions of amplifying the transgene if it were integrated in genomic DNA, it does to some extent validate the screening protocols used.

The KI transgenic service generated 88 potential pBIG-C9s and 73 potential pBIG-FLIP transgenic founders. Of these, there were 25 pBIG-C9s and 11 pBIG-FLIP transgenic founders identified by PCR and all confirmed by Southern blotting. The transgenic founders were imported to the Royal Veterinary College (RVC) and bred with wild type mice. However, during this period the some of the transgenic founders had died, possibly due to the stresses suffered during transportation. Nevertheless, the progeny derived from transgenic founders were then crossed with αMHC-tTA transgenic mice to generate compound transgenics.

There were two of the three αMHC-tTA/pBIG-C9s transgenic lines that expressed β-galactosidase. However, none of the three αMHC-tTA/pBIG-FLIP transgenic lines that were generated expressed β-galactosidase. The location of DNA integration of transgenes by pronuclear injection is random. The nature of random integration of the transgene can have detrimental effects on expression. Heterochromatin is densely packed DNA and a region of little transcriptional activity (Bianco et al., 2003). Thus, integration of transgenes into this region may result in the transgene not being expressed. Furthermore, integration into close proximity to the regulatory elements of another gene can have subtle or dramatic effects on the expression level or expression profile of the transgene (Bianco et al., 2003). This phenomenon has been termed the "position effect" (reviewed by Sigmund, 1993). The position effect may explain why no αMHC-tTA/pBIG-FLIP transgenic lines expressed the transgene.

The relative transgene copy number in pBIG-C9s and pBIG-FLIP transgenics was determined by phosphor imaging of hybridised [^{32}P]-radiolabelled probes in Southern blotting. The copy number of the two αMHC-tTA/pBIG-C9s expressing lines, 121 and 145, did not correlate with expression of the *lacZ* transgene product, β-galactosidase. The transgene copy number of line 121 was double that of line 145 but β-galactosidase expression was higher in line 145, as determined by X-gal staining and Western blotting. The lack of correlation between transgene copy number and expression is well documented. In 99% of transgene constructs, especially those containing simple promoter-cDNA fusions, copy number is not proportional to transgene expression (Bianco et al., 2003).

The level of transgene expression is of much importance in production of transgenic mouse disease models. For example, in mouse models for dominantly inherited diseases such as Huntington's disease, the desired level of mutant protein expression would be on a par with the normal expression levels of that protein. An alternative transgenic approach may be adopted to avoid some of the problems faced with transgenic over-expression using plasmid based constructs. Transgenic animals can be produced using yeast artificial chromosome (YAC) and bacterial artificial chromosome (BAC) vectors, as alternatives to plasmid based vectors. YAC and BAC vectors are much larger than plasmids and allow large sequences to be inserted. Therefore, the whole sequence of a gene including regulatory elements can be used to generate a transgenic mouse instead of only the cDNA sequence. The whole gene is more likely to express normal levels of the protein with normal temporal and

spatial expression. Thus, YAC and BAC based vectors can be used to overcome the position effect, including copy number dependent expression (Sinn et al., 1999). However, the interests of our study were in assessing the relative contribution of caspase-8 and caspase-9 in STAT1 mediated I/R-injury by specific inhibition by FLIP or C9s over-expression respectively. Therefore, the use of plasmid based vectors for over-expression was an appropriate choice. Furthermore, the tTA transgenic system also allows the expression of the transgene to be regulated temporally, and therefore was an appropriate system to use given that inhibition of caspase-8 or caspase-9 may result in developmental defects.

Producing transgenic mice is an expensive and time consuming procedure and does not always result in expression of transgenes integrated as a result of pronuclear injection. However, transgenic mice are a fundamental tool in the study of cardiovascular diseases and dissection of the signalling pathways involved. Transgenic mice have been used to highlight the importance of particular genes in I/R induced apoptosis. For example, hearts from mice over-expressing caspase-3 are more susceptible to I/R induced apoptosis (Condorelli et al., 2001).

The discovery that the C9s cDNA sequence in the pBIG-C9s construct was in reverse orientation meant that expression of C9s could not be derived from this vector and the pBIG-C9s transgenic mice generated were in effect redundant. Nevertheless, the results described in this chapter demonstrate that Tet responsive transgenic over-expressing mice were successfully generated, as demonstrated by β-galactosidase expression. Therefore, using the tTA system is a viable option for the cardiac over-expression of transgenes.

CHAPTER FOUR

Results

CHAPTER FOUR

Regulation of cardiac I/R injury and the cardiac proteome by STAT1 and p53

4.1 Introduction and aims of this chapter

The transcription factor STAT1 has been demonstrated to contribute to apoptosis of isolated neonatal rat cardiac myocyte (NRCM) cells following simulated I/R injury (Stephanou et al., 2000). It has also been found that different N-terminal truncated STAT1 mutants that retain the transactivation domain in the C-terminus, including those lacking part or all of the DNA-binding domain, were sufficient for stress induced apoptosis (Janjua et al., 2002). Moreover, cardiac myocytes and intact hearts from *Stat1*$^{-/-}$ mice, which express a C-terminal STAT1 fragment, were more sensitive to simulated I/R injury compared to hearts from wild type mice (Stephanou et al., 2002).

The transcriptional effect of STAT1 on most genes is through direct binding of the gene promoter. However, STAT1 is increasingly recognised to activate transcription by acting as a co-activator for other transcription factors. In this regard, STAT1 has been shown to associate with the transcription factor p53 in mouse embryonic fibroblast (MEF) cells and it was demonstrated that this association is required for maximal induction of p53 responsive genes (Townsend et al., 2004). Furthermore, p53 has also been shown to contribute to apoptosis in NRCM cells and in the Langendorff perfused rat heart following simulated I/R-injury (Long et al., 1997, Matsusaka et al., 2006).

The hypothesis being tested in this chapter is that the enhanced sensitivity of cardiac myocytes and hearts from *Stat1*$^{-/-}$ mice to I/R injury occurs through an association of the truncated C-terminal STAT1 protein expressed in these mice and p53, resulting in enhanced p53 induced apoptosis. The main aim of this chapter is to investigate this hypothesis using neonatal mouse cardiac myocyte (NMCM) cells isolated from wild type, *Stat1*$^{-/-}$, *Trp53*$^{-/-}$, and *Trp53*$^{-/-}$/*Stat1*$^{-/-}$ mice.

The second aim of this chapter is to use a proteomic approach to identify differentially expressed proteins in adult hearts from these gene knockout mice. This will further our knowledge of the proteins regulated by STAT1 and/or p53 and identify new candidate proteins that may mediate STAT1 and/or p53 induced apoptosis in cardiac I/R-injury.

4.2 Generation of mice deficient in p53 and STAT1

Stat1$^{-/-}$ and *Trp53*$^{-/-}$ mice were purchased from Taconic and were crossed to produce offspring that were heterozygous knockout for each gene (*Trp53*$^{+/-}$/*Stat1*$^{+/-}$). Compound heterozygous mice were crossed and the offspring generated were genotyped by PCR (Figure 4.1). There are nine possible genotypes for offspring generated from compound heterozygous crosses and one in sixteen were expected be wild-type, *Trp53*$^{-/-}$, *Stat1*$^{-/-}$ or *Trp53*$^{-/-}$/*Stat1*$^{-/-}$. There were no apparent anomalies between the actual and expected ratio of genotypes of mice born.

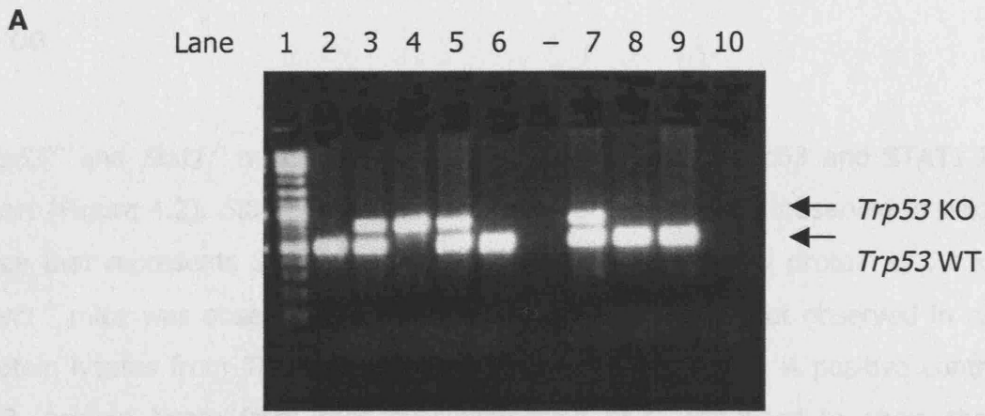

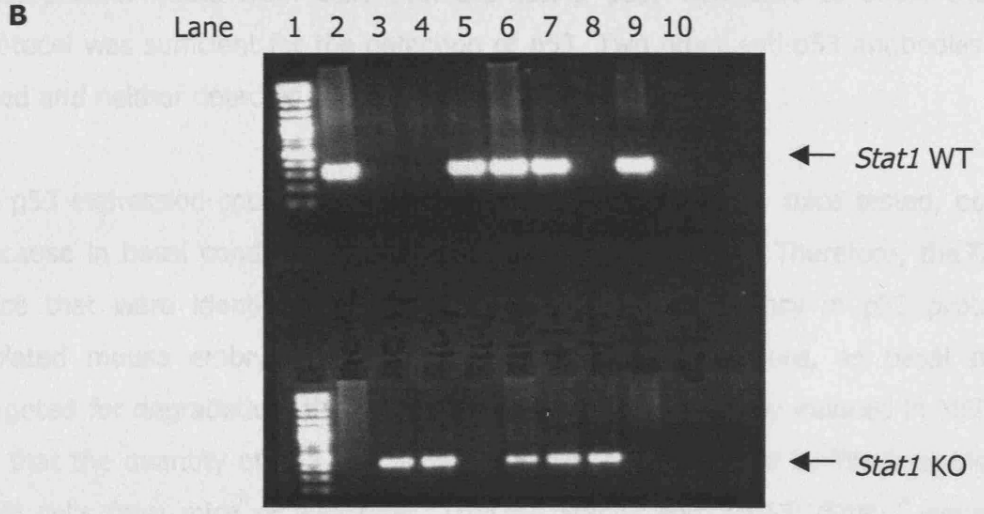

C

Lane	2	3	4	5	6	7	8	9
Trp53	+/+	+/-	-/-	+/-	+/+	+/-	+/+	+/+
Stat1	+/+	-/-	-/-	+/+	+/-	+/-	-/-	+/-

Figure 4.1 PCR genotyping of *Trp53* and *Stat1* knockouts. Mice progeny of compound heterozygous parents (*Trp53*$^{+/-}$/*Stat1*$^{+/-}$) were genotyped by PCR. PCR products from (A) *Trp53* and (B) *Stat1* genotyping were separated by 2% agarose gel electrophoresis and visualized under UV light. (A) The PCR products of *Trp53* wild type (500 bp) and knockout (750 bp) allele screening were amplified in a single reaction by 'duplex' PCR. (B) *Stat1* wild type and knockout alleles were screened for in separate reactions. (C) The genotypes of mice in lanes 2-9 are summarized. Lane 1; DNA Mw marker; lanes 2-9; progeny of *Trp53*$^{+/-}$/*Stat1*$^{+/-}$ parents; lane 10; water.

4.3 Analysis of p53 and STAT1 protein expression in knockout mice

Trp53$^{-/-}$ and *Stat1*$^{-/-}$ mice were tested for the expression of p53 and STAT1 in the heart (Figure 4.2). *Stat1*$^{-/-}$ mice lack a 91 kDa protein product observed in wild type mice that represents STAT1α. The expected STAT1 truncated protein of 72 kDa in *Stat1*$^{-/-}$ mice was observed. A band representing p53 was not observed in cardiac protein lysates from *Trp53*$^{-/-}$ or wild type mice (Figure 4.2 B). A positive control for p53, protein lysate from cells over-expressing p53, was used to show that the protocol was sufficient for the detection of p53. Two other anti-p53 antibodies were used and neither detected p53.

As p53 expression could not be detected in the hearts of any mice tested, possibly because in basal conditions p53 is targeted for degradation. Therefore, the *Trp53*$^{-/-}$ mice that were identified by PCR were verified for deficiency in p53 protein in isolated mouse embryonic fibroblast (MEF) cells. Furthermore, as basal p53 is targeted for degradation, the expression of p53 was chemically induced in MEF cells so that the quantity of p53 was sufficient for it to be detected by Western blotting. MEF cells from mice of wild type, *Trp53*$^{-/-}$, *Stat1*$^{-/-}$ and *Trp53*$^{-/-}$/*Stat1*$^{-/-}$ genotypes were isolated and cultured. MEF cells from wild type and *Stat1*$^{-/-}$ mice ceased to proliferate after approximately 10 days in culture. However, MEF cells from *Trp53*$^{-/-}$ and *Trp53*$^{-/-}$/*Stat1*$^{-/-}$ mice continued to proliferate. Therefore, p53 expression was tested in these cells and immortalized wild types MEF cells used in our laboratory, that express p53, were used as a positive control for p53. Wild type, *Trp53*$^{-/-}$ and *Trp53*$^{-/-}$/*Stat1*$^{-/-}$ MEF cells were treated with etoposide, a chemical that induces DNA-damage and expression of p53.

A band of 53 kDa was present in protein lysates from etoposide treated MEF cells from wild type mice but not in etoposide treated MEF cells from *Trp53*$^{-/-}$ or *Trp53*$^{-/-}$ /*Stat1*$^{-/-}$ mice (Figure 4.3). STAT1 alpha and beta isoforms were observed in *Trp53*$^{-/-}$ mice but not in *Trp53*$^{-/-}$/*Stat1*$^{-/-}$ mice (Figure 4.3). These experiments demonstrate that *Trp53*$^{-/-}$ mice are deficient in p53 expression.

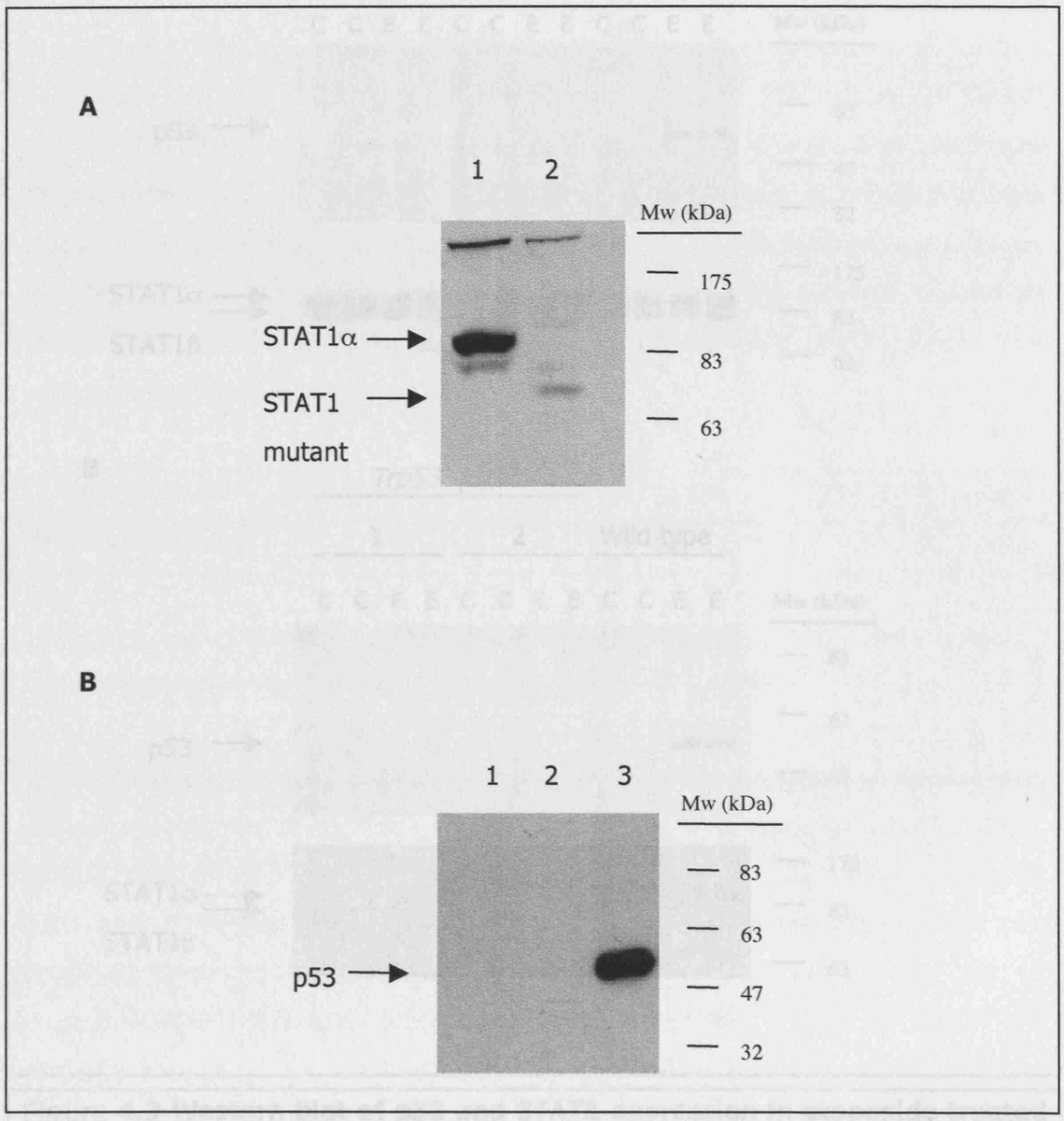

Figure 4.2 Western blot of STAT1 and p53 expression in hearts from (A) *Stat1*$^{-/-}$ and (B) *Trp53*$^{-/-}$ mice. Cardiac protein samples from a wild type (lane1) and a *Stat1*$^{-/-}$ or *p53*$^{-/-}$ (lane 2) mouse were separated by 12% SDS-PAGE. (A) *Stat1*$^{-/-}$ mice lack the 91 kDa STAT1α protein but express the truncated 72 kDa STAT1 protein. (B) No bands for p53 are present in wild type or *Trp53*$^{-/-}$ samples. A protein lysate from cells over-expressing p53 was used as a positive control (lane 3).

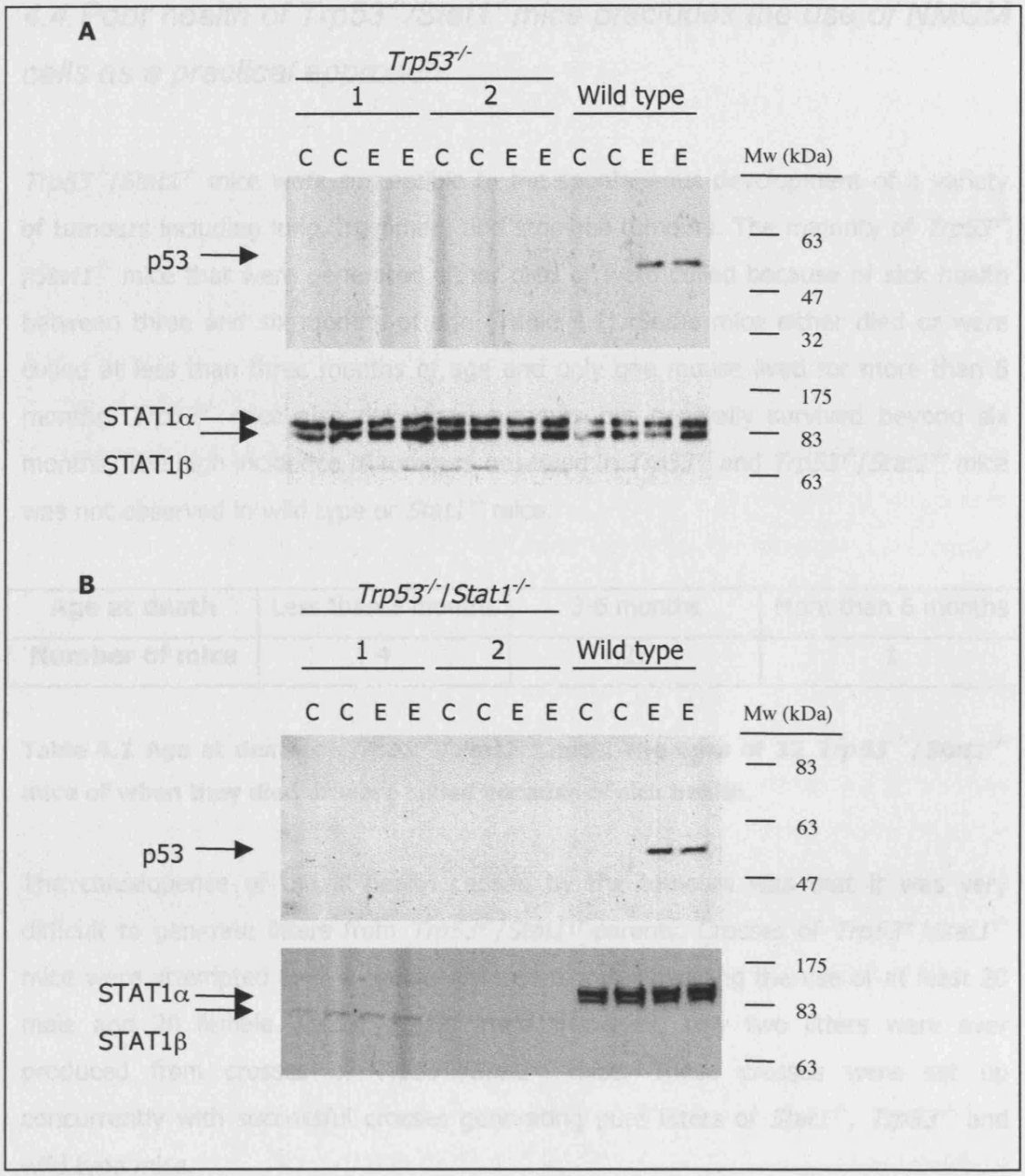

Figure 4.3 Western blot of p53 and STAT1 expression in etoposide treated MEF cells. MEF cells from (A) *Trp53*$^{-/-}$ and (B) *Trp53*$^{-/-}$/*Stat1*$^{-/-}$ mice were treated with a vehicle control or etoposide (labelled C or E, respectively). MEF cells from two animals of each genotype were tested (labelled 1 and 2), in duplicate, and were compared with MEF cells from wild type mice. MEF cells were tested for the expression of p53 and STAT1. No protein bands were observed in *Trp53*$^{-/-}$ or *Trp53*$^{-/-}$/*Stat1*$^{-/-}$ MEF cells following control or etoposide treatments. A band of 53 kDa was observed in wild type MEF cells. Bands of sizes corresponding to STAT1 α and β isoforms were observed in wild type and *Trp53*$^{-/-}$ MEF cells but not in *Trp53*$^{-/-}$/*Stat1*$^{-/-}$ MEF cells.

4.4 Poor health of *Trp53*$^{-/-}$/*Stat1*$^{-/-}$ mice precludes the use of NMCM cells as a practical approach

Trp53$^{-/-}$/*Stat1*$^{-/-}$ mice were susceptible to the spontaneous development of a variety of tumours including lung, mammary and stomach tumours. The majority of *Trp53*$^{-/-}$/*Stat1*$^{-/-}$ mice that were generated either died or were culled because of sick health between three and six months of age (Table 4.1). Some mice either died or were culled at less than three months of age and only one mouse lived for more than 6 months. *Trp53*$^{-/-}$ mice also developed tumours but generally survived beyond six months. The high incidence of tumours observed in *Trp53*$^{-/-}$ and *Trp53*$^{-/-}$/*Stat1*$^{-/-}$ mice was not observed in wild type or *Stat1*$^{-/-}$ mice.

Age at death	Less than 3 months	3-6 months	More than 6 months
Number of mice	4	27	1

Table 4.1 Age at death of *Trp53*$^{-/-}$/*Stat1*$^{-/-}$ mice. The ages of 32 *Trp53*$^{-/-}$/*Stat1*$^{-/-}$ mice of when they died or were culled because of sick health.

The consequence of the ill health caused by the tumours was that it was very difficult to generate litters from *Trp53*$^{-/-}$/*Stat1*$^{-/-}$ parents. Crosses of *Trp53*$^{-/-}$/*Stat1*$^{-/-}$ mice were attempted over a course of three months involving the use of at least 20 male and 20 female *Trp53*$^{-/-}$/*Stat1*$^{-/-}$ mice. However, only two litters were ever produced from crosses of *Trp53*$^{-/-}$/*Stat1*$^{-/-}$ mice. These crosses were set up concurrently with successful crosses generating pure litters of *Stat1*$^{-/-}$, *Trp53*$^{-/-}$ and wild type mice.

The implication, for this study, of the poor success rate for generating litters from *Trp53*$^{-/-}$/*Stat1*$^{-/-}$ crosses was that the isolation and culture of NMCM cells from *Trp53*$^{-/-}$/*Stat1*$^{-/-}$ was impractical as myocytes could only be isolated from individual neonates, which would not provide a sufficient quantity of cells. The first aim of this chapter was to ascertain whether the increased sensitivity of hearts from *Stat1*$^{-/-}$ mice to I/R-injury was dependent on p53. These experiments would have been performed in cardiac myocytes, isolated and cultured by a method routinely used in our laboratory, from pooled neonatal hearts of wild type, *Trp53*$^{-/-}$, *Stat1*$^{-/-}$ or *Trp53*$^{-/-}$/*Stat1*$^{-/-}$ mice. This was dependant on crosses of *Trp53*$^{-/-}$/*Stat1*$^{-/-}$ mice to generate

pure litters of homozygous *Trp53*$^{-/-}$/*Stat1*$^{-/-}$ neonatal mice. Therefore, this approach was not practical for testing the hypothesis in question.

4.5 Proteomic approach to identification of proteins regulated by p53 and/or STAT1 in the mouse heart

Both p53 and STAT1 have been implicated in apoptosis signalling in response to I/R. Although p53 and STAT1 mediated effects occur in response to stress, they have also been shown to be involved in the constitutive expression of some genes. The second aim of this chapter was the identify proteins regulated in a manner dependent on p53 and/or STAT1. This was achieved by means of proteomic screening of cardiac protein samples from wild type, *Trp53*$^{-/-}$, *Stat1*$^{-/-}$ and *Trp53*$^{-/-}$/*Stat1*$^{-/-}$ mice.

Cardiac protein samples were separated by 2D-PAGE using broad range pH 3-10 IPG acrylamide strips and 12% SDS-PAGE gels (Figure 4.4). Good resolution of proteins on the basis of molecular weight was achieved, however, there was horizontal streaking between pH 7-10. Poor resolution of basic proteins in isoelectric focusing had been previously experienced in our laboratory. Therefore, further analyses of cardiac proteomes were continued using IPG acrylamide strips of ranges between pH 4-7.

Cardiac protein samples from 8-10 week old wild type, *Trp53*$^{-/-}$, *Stat1*$^{-/-}$ and *Trp53*$^{-/-}$/*Stat1*$^{-/-}$ male mice were separated using IPG acrylamide strips of narrow-range pH 4-7 (figure 4.5) and micro-range pH 5.5-6.7 (figure 4.6). 2D-PAGE gel comparisons using ImageMaster™ analysis software revealed few differences between the experimental groups. The protein most differentially expressed was the spot labelled 1269 (figure 4.7). The expression of spot 1269 was relatively high in the cardiac proteome of *Trp53*$^{-/-}$ mice compared to all other groups, the lowest expression being in the wild type group. As protein 1269 was the most differentially expressed spot between any of the groups, it was thus a candidate for identification by peptide mass fingerprinting (PMF). Spot 1269 was observed to be a distinct spot with a pI close to 7.0 and was considered to be sufficiently abundant for potential identification by (PMF) (Figure 4.8).

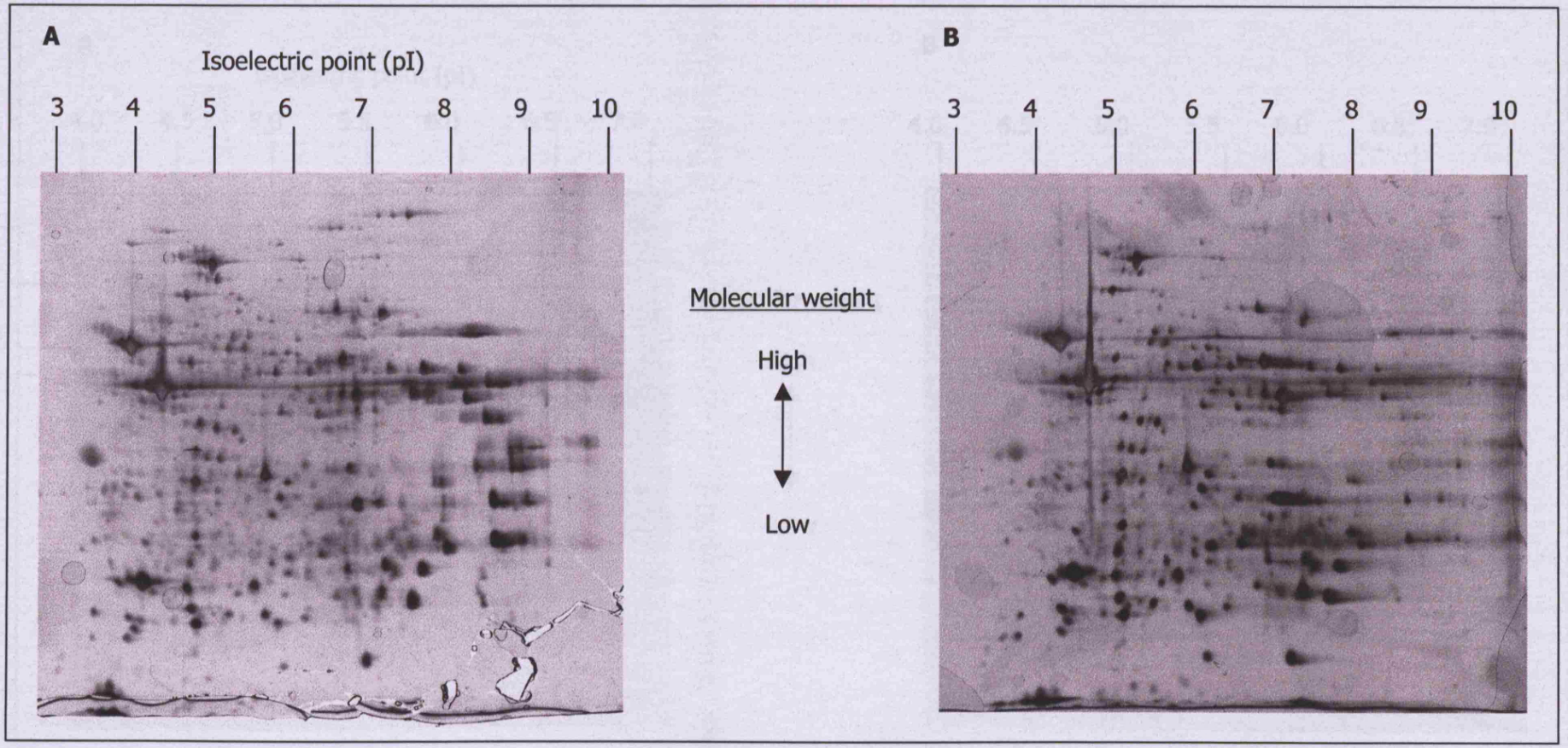

Figure 4.4 Mouse cardiac protein separated by 2D-PAGE using broad range pH 3-10 IPG acrylamide strips. Horizontal streaking of cardiac protein from wild type (A) and *Trp53*$^{-/-}$ null (B) mice was observed when separated using pH 3-10 acrylamide strips. 100 μg of protein was ran on 12 % SDS-PAGE gels and were stained with silver nitrate.

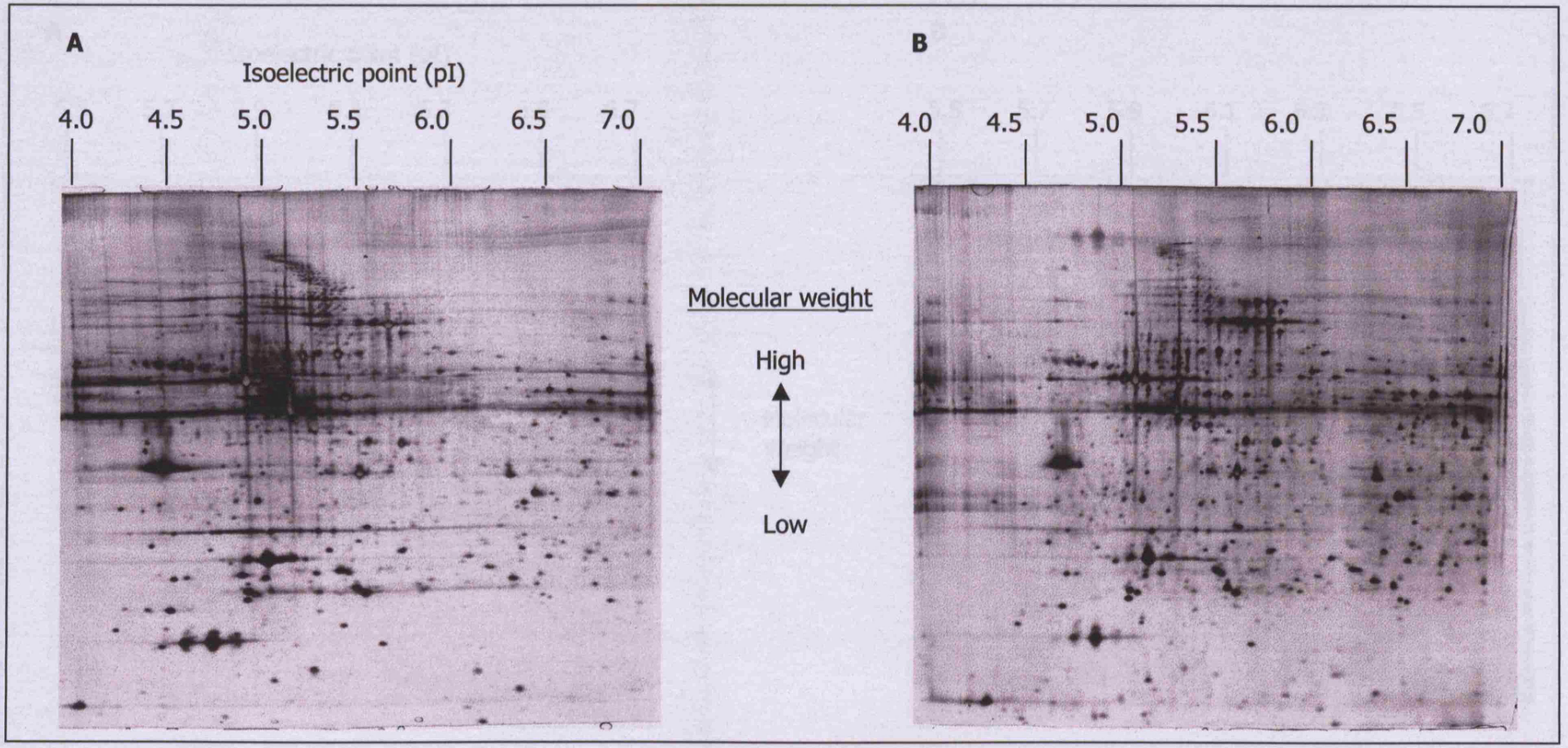

Figure 4.5 Mouse cardiac protein separated by 2D-PAGE using broad range pH 4-7 IPG acrylamide strips. Cardiac protein from wild type (A) and *Trp53*$^{-/-}$ null (B) mice was separated using pH 4-7 acrylamide strips. 100 μg of protein was ran on 12% SDS-PAGE gels and were stained with silver nitrate.

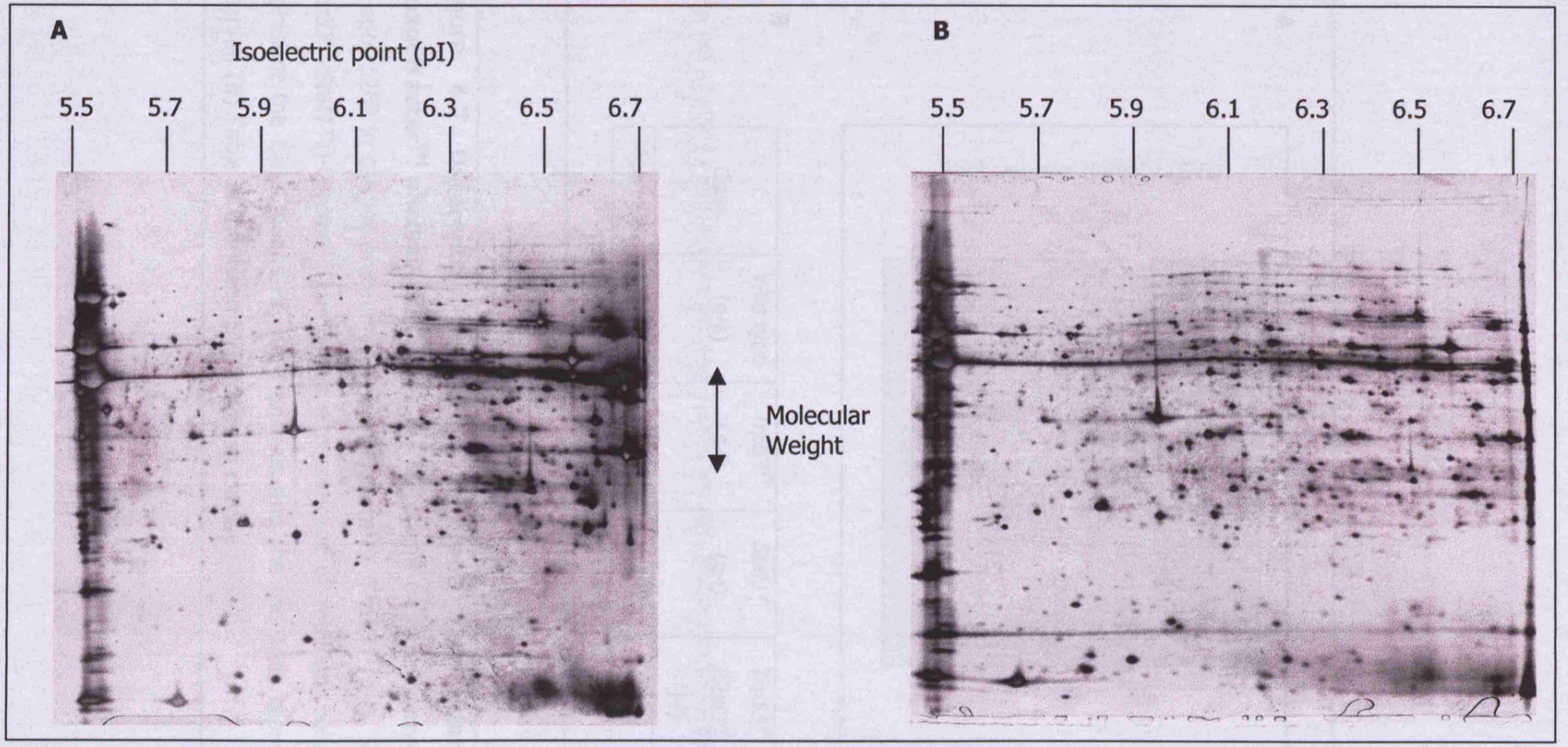

Figure 4.6 Mouse cardiac protein separated by 2D-PAGE using micro range pH 5.5-6.7 IPG acrylamide strips. Cardiac protein from wild type (A) and *Trp53*$^{-/-}$ null (B) mice was separated using pH 5.5-6.7 acrylamide strips. 100 μg of protein was ran on 12% SDS-PAGE gels and were stained with silver nitrate.

A

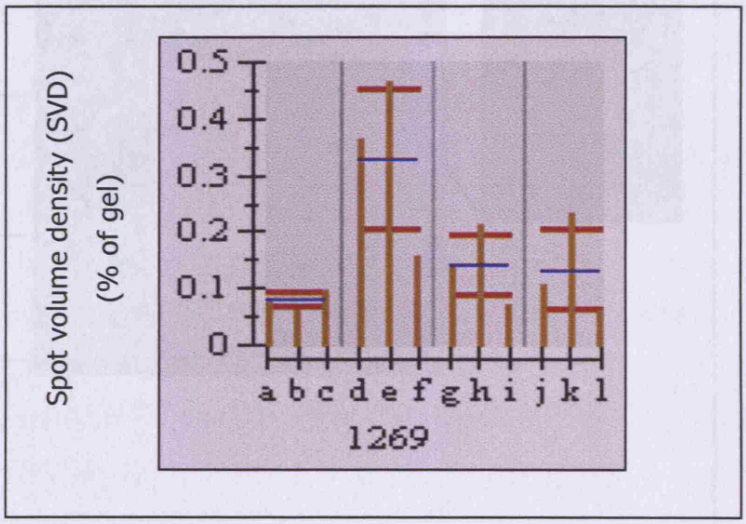

B

Class	Wild type (a-c)	*Trp53*$^{-/-}$ (d-f)	*Stat1*$^{-/-}$ (g-i)	*Trp53*$^{-/-}$ */Stat1*$^{-/-}$ (j-l)
Mean SVD	0.079	0.327	0.142	0.132

Figure 4.7 Differential expression of spot 1269 identified using ImageMaster™ analysis software. (A) Histogram of spot volume density (SVD) of spot 1269 in cardiac proteomes of wild type (a-c), *Trp53*$^{-/-}$ (d-f), *Stat1*$^{-/-}$ (g-i) and *Trp53*$^{-/-}$*/Stat1*$^{-/-}$(j-l) mice. The SVD is a percentage of total gel volume. Blue lines represent the class means of three animals and the red lines represent the class interval. (B) Table of the mean SVD for each class.

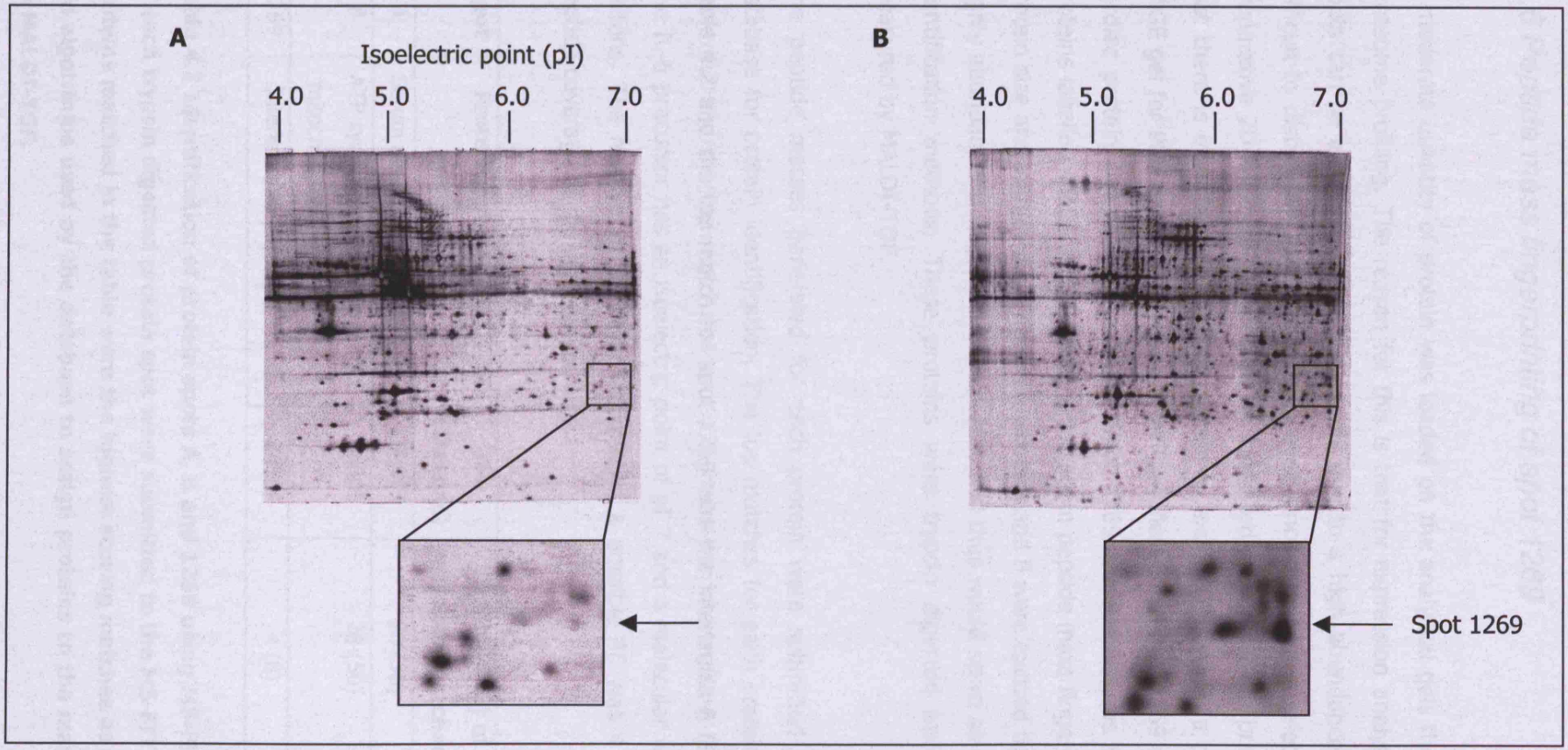

Figure 4.8 Spot 1269 identified as differentially expressed between groups using ImageMaster. Shown are cardiac protein from wild type (A) and *Trp53*$^{-/-}$ (B) mice separated using narrow range pH 4-7 acrylamide strips. 100 μg of protein was ran on 12% SDS-PAGE gels and were stained with silver nitrate.

4.6 Peptide mass fingerprinting of spot 1269

A moderate quantity of protein was loaded on the analytical gels that were run for proteome profiling. The reason for this is that for expression analysis only distinct spots can be analyzed; overlapping spots due to a high abundance of protein are difficult to distinguish and analyze. However, once a protein is selected for PMF, a preparative 2D-PAGE gel is run with an increased amount of the protein sample so that there is more of the selected protein to excise. Therefore, a preparative 2D-PAGE gel for PMF of proteins was run for identification of spot 1269 using a *Trp53*$^{-/-}$ cardiac protein sample (Figure 4.9). Spot 1269 was excised, as were additional proteins labelled spot A and B. Limiting factors in peptide mass fingerprinting include protein size and abundance. Therefore, spots A and B were excised because they are highly abundant and larger than spot 1269, and thus would serve as controls for the identification methods. These proteins were trypsin digested and masses were measured by MALDI-TOF.

The peptide masses generated for each protein were submitted to the MS-FIT database for protein identification. The top matches for each protein are shown in Table 4.2 and the top match for spot 1269 was the interleukin-6 (IL-6) precursor. The IL-6 precursor has an isoelectric point of pI 7 and a molecular weight of 24384 Daltons. The number of peptides matched of a possible 46 was 4 (8%) and the peptide coverage of the protein was 18%.

Spot	Protein matched by MS-FIT	pI	Mw (Daltons)	Number (%) of peptides matched	Peptide Coverage
A	Serum albumin precursor	5.7	68693	20 (38)	41 %
B	ATP synthase beta chain, mitochondrial precursor	5.2	56301	28 (50)	48 %
1269	Interleukin-6 precursor	7	24384	4 (8)	18 %

Table 4.2 Identification of protein spots A, B and 1269 using MS-FIT. The masses of each trypsin digested protein spot were submitted to the MS-FIT database. The proteins matched in the table were the highest scoring matches as determined by the algorithms used by the database to assign proteins to the masses measured by MALDI-TOF.

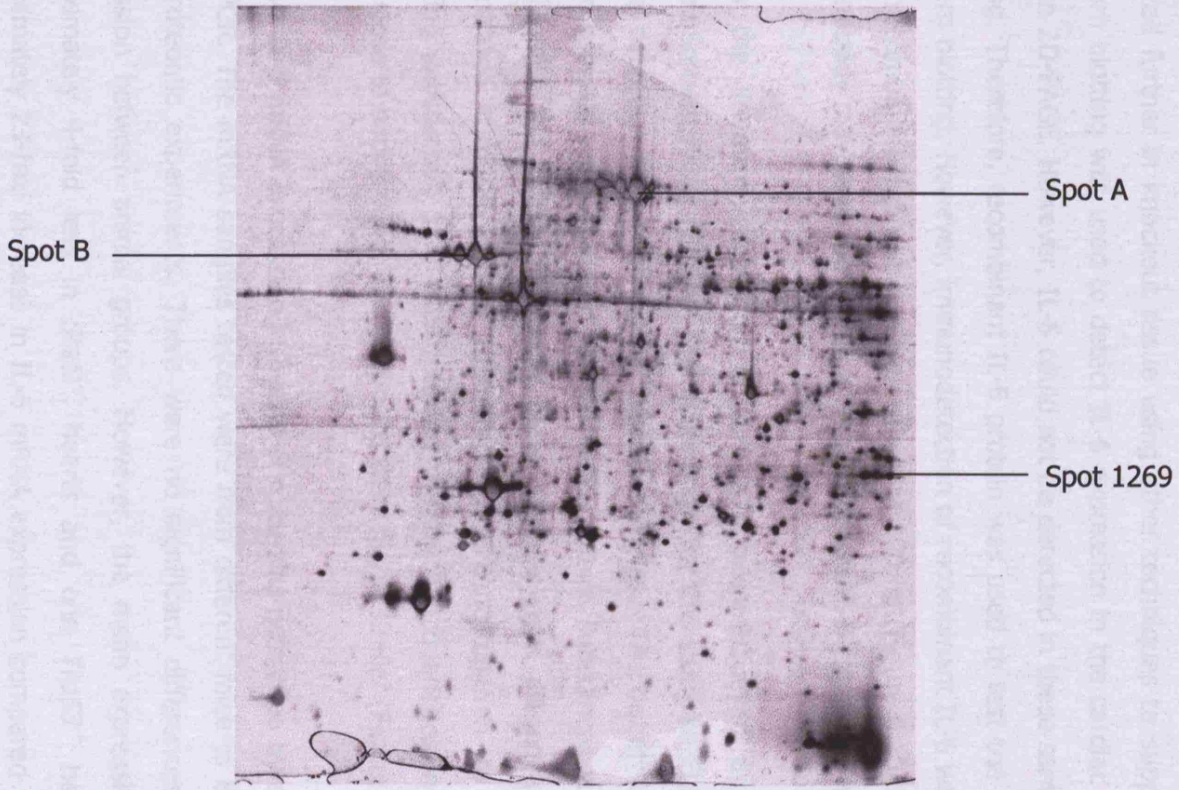

Figure 4.9 Preparative 2D-PAGE separating cardiac protein from a *Trp53*$^{-/-}$ mouse. For spot extraction and identification by mass spectrometry, 400 μg of cardiac protein was separated by 2D-PAGE. The protein spot of interest that was observed as having increased in expression in hearts from *Trp53*$^{-/-}$ mice by ImageMaster analysis was excised from the gel for identification. Two other proteins (Spots A and B) were also excised from the gel for identification.

4.7 Analysis of IL-6 expression in knockout mice

4.7.1 IL-6 expression in the heart

The most differentially expressed protein, spot 1269, was identified as the IL-6 precursor protein by PMF. Therefore, IL-6 mRNA and protein expression was analyzed further in knockout tissue using other techniques to support this finding. Western blotting was used to detect IL-6 expression in the cardiac protein samples used in 2D-PAGE. However, IL-6 could not be detected in these samples by Western blotting. Therefore, recombinant IL-6 protein was used to test the IL-6 antibody in Western blotting. However, immunodetection of recombinant IL-6 was only observed when recombinant IL-6 was in a high quantity, 100 ng (Figure 4.10A). Therefore, the IL-6 antibody may have too low an affinity to detect IL-6 expressed in the tissue.

Within the literature, detection of IL-6 has been achieved by Enzyme-Linked ImmunoSorbent Assay (ELISA), and accordingly for this study an ELISA kit was used for the detection of IL-6 in cardiac protein samples. The buffer for which cardiac protein samples were prepared for 2D-PAGE contains substances such as Urea that would inhibit the ELISA. Therefore these samples were diluted in PBS and then concentrated through porous membranes by centrifugation to remove ELISA inhibiting substances. IL-6 was detected in very low quantities in all samples, at levels close to background, and all groups were highly similar (Figure 4.10B).

Relative IL-6 mRNA expression in hearts of mice was quantified by quantitative, real time PCR. The mRNA samples tested were from different mice to the ones used in the proteomic experiments. There were no significant differences in IL-6 mRNA expression between animal groups. However, the mean expression of IL-6 was approximately 4-fold less in *Stat1*$^{-/-}$ hearts and one *Trp53*$^{-/-}$ heart showed an approximately 23-fold increase in IL-6 mRNA expression compared to the wild type group.

4.7.2 IL-6 expression in MEF cells

There was insufficient sensitivity in the Western blotting and ELISA techniques to detect IL-6 in the cardiac protein samples. Furthermore, although there were

differences in IL-6 mRNA between the groups they were not statistically significant. Therefore, IL-6 expression was measured in MEF cells to find any supporting evidence for the regulation of IL-6 by STAT1.

MEF cells from wild type and *Stat1*$^{-/-}$ mice were not used as they had become senescent. Therefore, the regulation of IL-6 by STAT1 was investigated in *Trp53*$^{-/-}$ and *Trp53*$^{-/-}$/*Stat1*$^{-/-}$ MEF cells. *Trp53*$^{-/-}$ and *Trp53*$^{-/-}$/*Stat1*$^{-/-}$ MEF cells were pooled from 5 animals. Relative IL-6 mRNA expression was 4.26 ± 2.11 fold higher in *Trp53*$^{-/-}$/*Stat1*$^{-/-}$ MEF cells compared to *Trp53*$^{-/-}$ MEF cells (Figure 4.11). However, this was not a statistically significant difference. The IL-6 secreted from MEF cells was measured by ELISA. Secreted IL-6 was 1.73 ± 0.45 fold higher in *Trp53*$^{-/-}$/*Stat1*$^{-/-}$ MEF cells compared to *Trp53*$^{-/-}$ cells, however, was not significant.

The enhanced IL-6 mRNA and protein expression observed in *Trp53*$^{-/-}$/*Stat1*$^{-/-}$ MEF cells compared to *Trp53*$^{-/-}$ MEF cells was not a statistically significant one. However, enhanced IL-6 expression is associated with different types of cancers and is involved in the growth of renal cell carcinomas (Paule et al., 2000). Thus, the lack of any statistically significant difference may be due to a small sample size. Furthermore, *Trp53*$^{-/-}$/*Stat1*$^{-/-}$ mice are more susceptible to the spontaneous development of tumours compared to *Trp53*$^{-/-}$ mice. This posed the question: is the growth rate of *Trp53*$^{-/-}$/*Stat1*$^{-/-}$ MEF cells faster compared to *Trp53*$^{-/-}$ MEF cells and if so, is it dependent on enhanced IL-6 expression? Therefore, the growth rates of MEF cells from knockout mice were determined by the MTS assay.

MEF cells were passaged seven days after isolation and were cultured in low (1%) or high (10%) serum. MEF cells from wild type and *Stat1*$^{-/-}$ mice ceased to proliferate after the first passage whereas *Trp53*$^{-/-}$ and *Trp53*$^{-/-}$/*Stat1*$^{-/-}$ MEF cells continued to proliferate (Figure 4.12). The abnormal growth of MEF cells was correlative with the observation that *Trp53*$^{-/-}$ and *Trp53*$^{-/-}$/*Stat1*$^{-/-}$ mice, but not wild type or *Stat1*$^{-/-}$ mice, spontaneously developed tumours. The growth rates of *Trp53*$^{-/-}$ and *Trp53*$^{-/-}$/*Stat1*$^{-/-}$ MEF cells were highly similar when grown in either low or high serum (Figure 4.12). Therefore, the increased susceptibility of *Trp53*$^{-/-}$/*Stat1*$^{-/-}$ mice to generate tumours, compared to *Trp53*$^{-/-}$ mice, was not reflected in the growth rates of MEF cells from these mice.

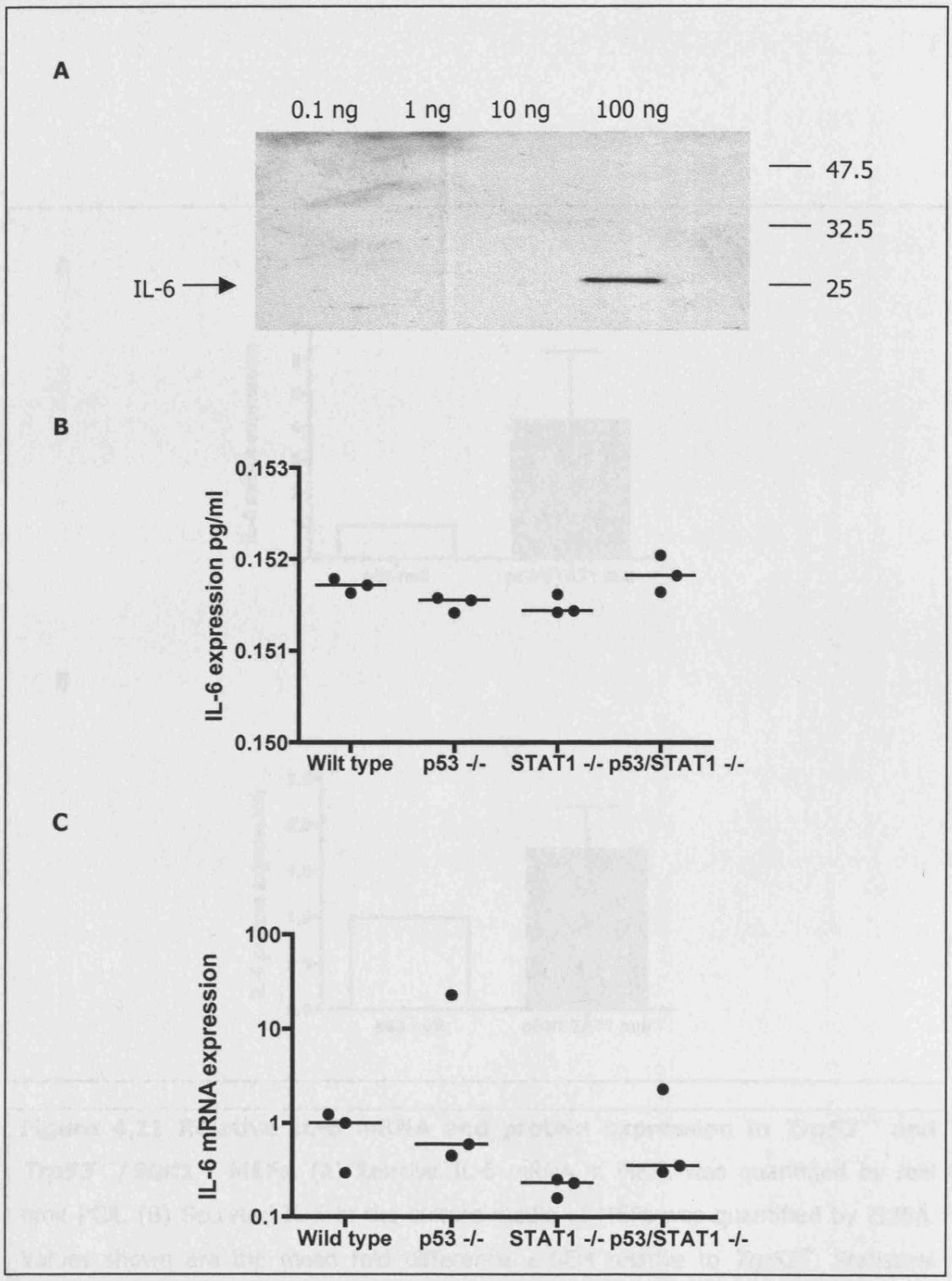

Figure 4.10 IL-6 protein and mRNA expression. (A) Western blot of purified IL-6 detection using anti-IL-6 antibody showing only 100 ng of IL-6 was detectable. (B) Measurement of IL-6 protein by ELISA of samples following dilution and concentration to remove ELISA inhibiting substances. (C) IL-6 mRNA expression in hearts. Values shown are normalised medians relative to wild type group. Statistical analysis of mRNA expression was performed by a Kruskal-Wallis test with Dunn's post test. There were no significant differences between any animal groups.

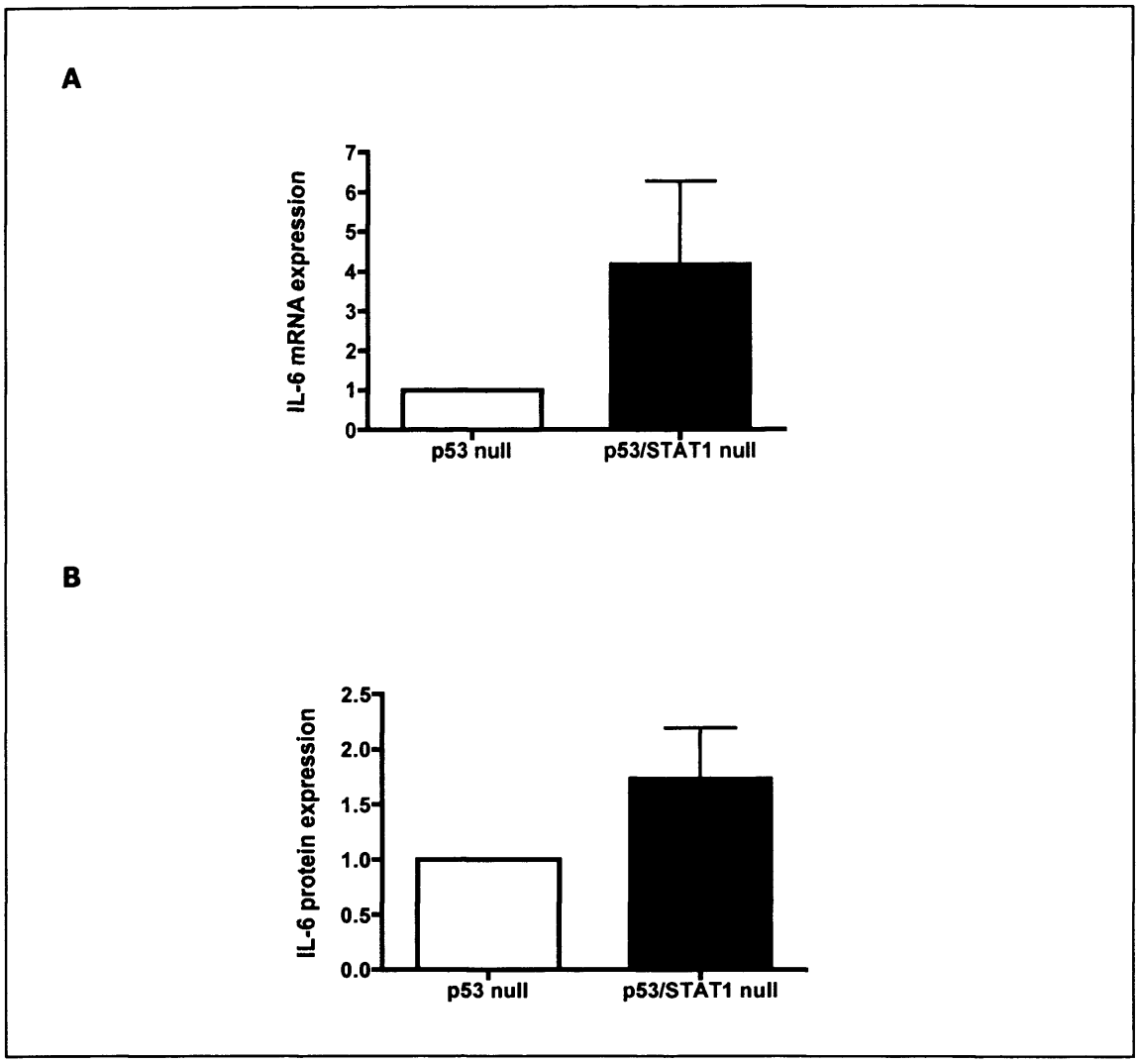

Figure 4.11 Relative IL-6 mRNA and protein expression in *Trp53*$^{-/-}$ and *Trp53*$^{-/-}$/*Stat1*$^{-/-}$ MEFs. (A) Relative IL-6 mRNA in MEFs was quantified by real time PCR. (B) Secreted IL-6 in the culture media of MEFs was quantified by ELISA. Values shown are the mean fold difference ± SEM relative to *Trp53*$^{-/-}$. Statistical analysis of mRNA and protein expression was performed by a two-tailed Student's *t* test and there were no significant differences between *Trp53*$^{-/-}$ and *Trp53*$^{-/-}$/*Stat1*$^{-/-}$ MEF cells.

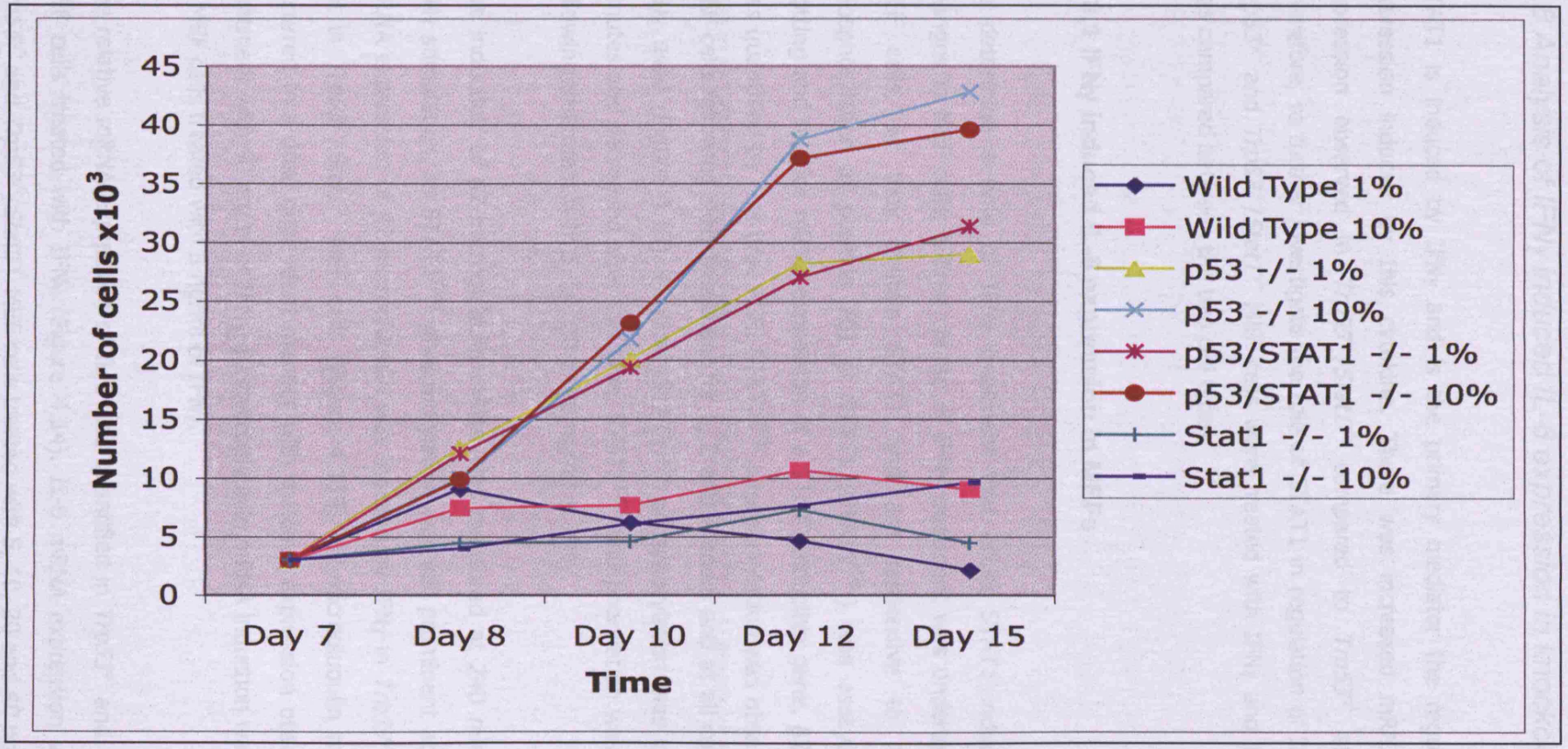

Figure 4.12 Growth assay of cultured MEFs from gene knockout mice. MEFs were passaged after seven days following isolation and were seeded at a density of 1 x 10^3 cells in 96 well plates and were grown in low (1%) or high (10%) serum. Growth was measured by the MTS assay on days 8, 10, 12 and 15.

4.8 Analysis of IFNγ induced IL-6 expression in knockout mice

STAT1 is induced by IFNγ and is the primary mediator the regulation of gene expression induced by this cytokine. There was increased mRNA and protein expression observed in *Trp53*$^{-/-}$/*Stat1*$^{-/-}$ compared to *Trp53*$^{-/-}$ and MEF cells. Therefore, to further investigate the role of STAT1 in regulation of IL-6 expression, *Trp53*$^{-/-}$ and *Trp53*$^{-/-}$/*Stat1*$^{-/-}$ MEF cells were treated with IFNγ and IL-6 expression was compared between the two cell types.

4.8.1 IFNγ induced IL-6 expression in MEFs

To determine a time of IFNγ treatment that elicits STAT1 induced expression changes in MEF cells, a time course of IFNγ treatment was undertaken in *Trp53*$^{-/-}$ MEF cells, as they contain STAT1 and are responsive to IFNγ. Tyrosine phosphorylation at position 701 of STAT1 (STAT1^{Y701}) was assayed by Western blotting and relative mRNA expression of a STAT1 inducible gene, β2-microglubulin, was quantified by real time PCR. STAT1^{Y701} phosphorylation was observed in *Trp53*$^{-/-}$ MEF cells following IFNγ treatment for 1, 2 and 4 hours and at all concentrations of IFNγ used (Figure 4.13). Maximal STAT1^{Y701} phosphorylation was observed at 60 minutes and decreased after this time. STAT1^{Y701} phosphorylation was similar in cells following treatment with 5, 10, 20 or 40 ng/ml of IFNγ.

The induction of β2-microglubulin mRNA was measured at 240 minutes following IFNγ stimulation, as STAT1^{Y701} phosphorylation was still prominent at this time. The mRNA expression of β2-microglubulin was induced by IFNγ in *Trp53*$^{-/-}$ MEF cells but not in *Trp53*$^{-/-}$/*Stat1*$^{-/-}$ MEF cells (Figure 4.13B). β2-microglubulin mRNA induction occurred in a dose dependent manner with maximal expression observed following treatment with 40 ng/ml or IFNγ. β2-microglubulin mRNA induction was not observed in MEF cells treated with 5 ng/ml of IFNγ.

The relative mRNA expression of IL-6 was quantified in *Trp53*$^{-/-}$ and *Trp53*$^{-/-}$/*Stat1*$^{-/-}$ MEF cells treated with IFNγ (Figure 4.14). IL-6 mRNA expression was induced in *Trp53*$^{-/-}$ and *Trp53*$^{-/-}$/*Stat1*$^{-/-}$ MEF cells treated with 5, 10, 20 and 40 ng/ml of IFNγ for 240 minutes. Maximal induction was observed in both *Trp53*$^{-/-}$ and *Trp53*$^{-/-}$/*Stat1*$^{-/-}$

MEF cells following treatment with 40 ng/ml IFNγ. Total IL-6 mRNA expression was higher in *Trp53*$^{-/-}$/*Stat1*$^{-/-}$ MEF cells compared to *Trp53*$^{-/-}$ MEF cells following treatment with IFNγ at all concentrations. However, this was not statistically significant.

The secreted IL-6 in the culture media of *Trp53*$^{-/-}$ and *Trp53*$^{-/-}$/*Stat1*$^{-/-}$ MEF cells following treatment with 5 ng/ml of IFNγ for 24 hours was assayed by ELISA (Figure 4.15). Secreted IL-6 in the culture medium of *Trp53*$^{-/-}$/*Stat1*$^{-/-}$ MEF cells treated with IFNγ increased 1.55 ± 0.22 fold higher compared to *Trp53*$^{-/-}$/*Stat1*$^{-/-}$ MEF cells without IFNγ treatment. Secreted IL-6 in the culture medium of *Trp53*$^{-/-}$ MEF cells was not increased following IFNγ treatment (0.97 ± 0.23 relative to control). The induction of IL-6 protein expression by IFNγ in *Trp53*$^{-/-}$/*Stat1*$^{-/-}$ MEF cells was statistically significant. Therefore, IFNγ induces expression of IL-6 in *Trp53*$^{-/-}$/*Stat1*$^{-/-}$ MEF cells but not *Trp53*$^{-/-}$ MEF cells.

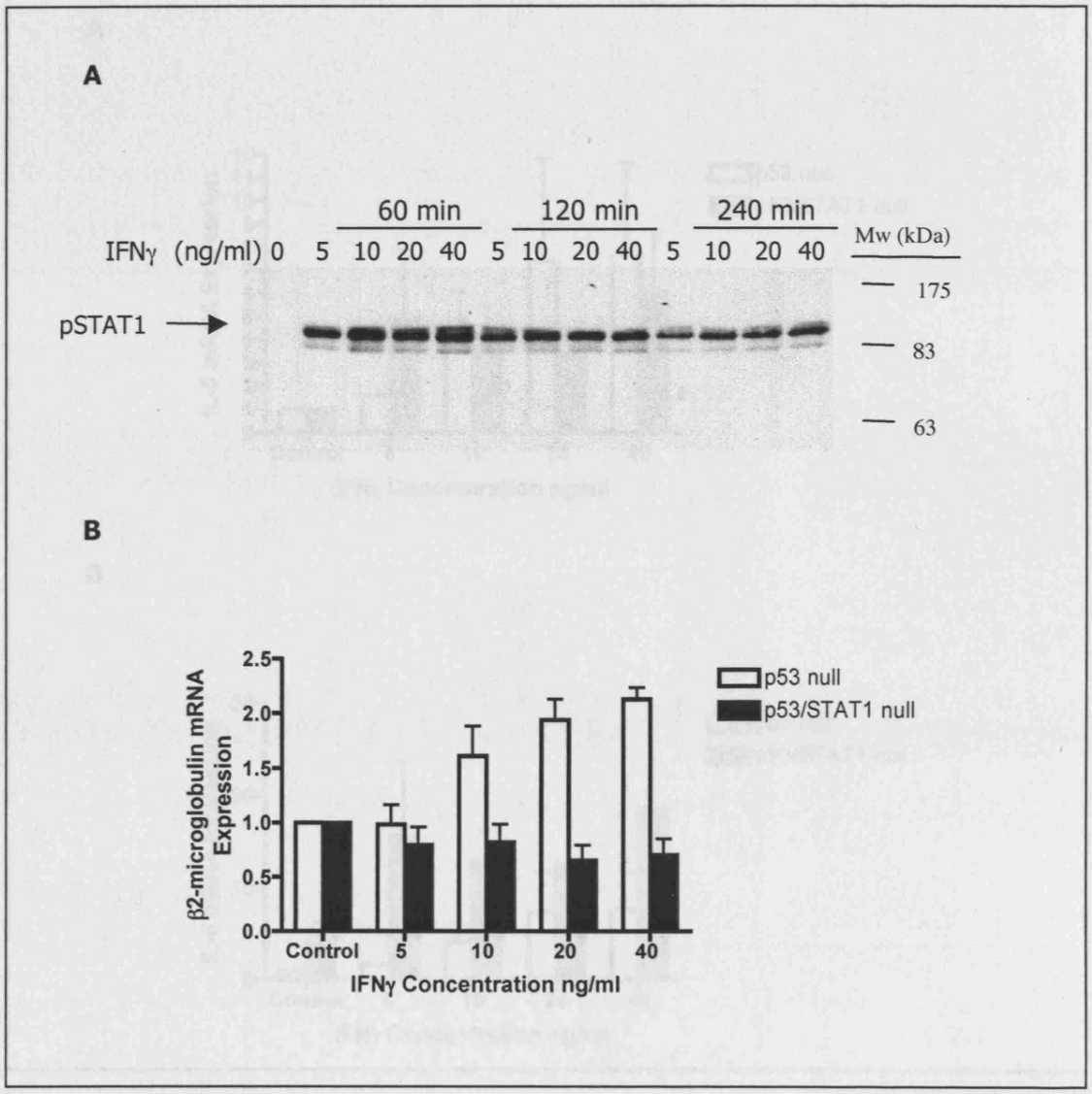

Figure 4.13 STAT1 phosphorylation and β2-microglobulin gene expression in IFNγ treated MEFs. (A) Western blot of IFNγ treated *Trp53*$^{-/-}$ MEFs immunoblotted for phosphorylated tyrosine residue 701 of STAT1. (B) Relative IL-6 mRNA in *Trp53*$^{-/-}$ and *Trp53*$^{-/-}$/*Stat1*$^{-/-}$ MEF cells treated with IFNγ was quantified by real time PCR. Values shown are mean fold difference ± SEM relative to relevant control (untreated MEF cells of the same genotype).

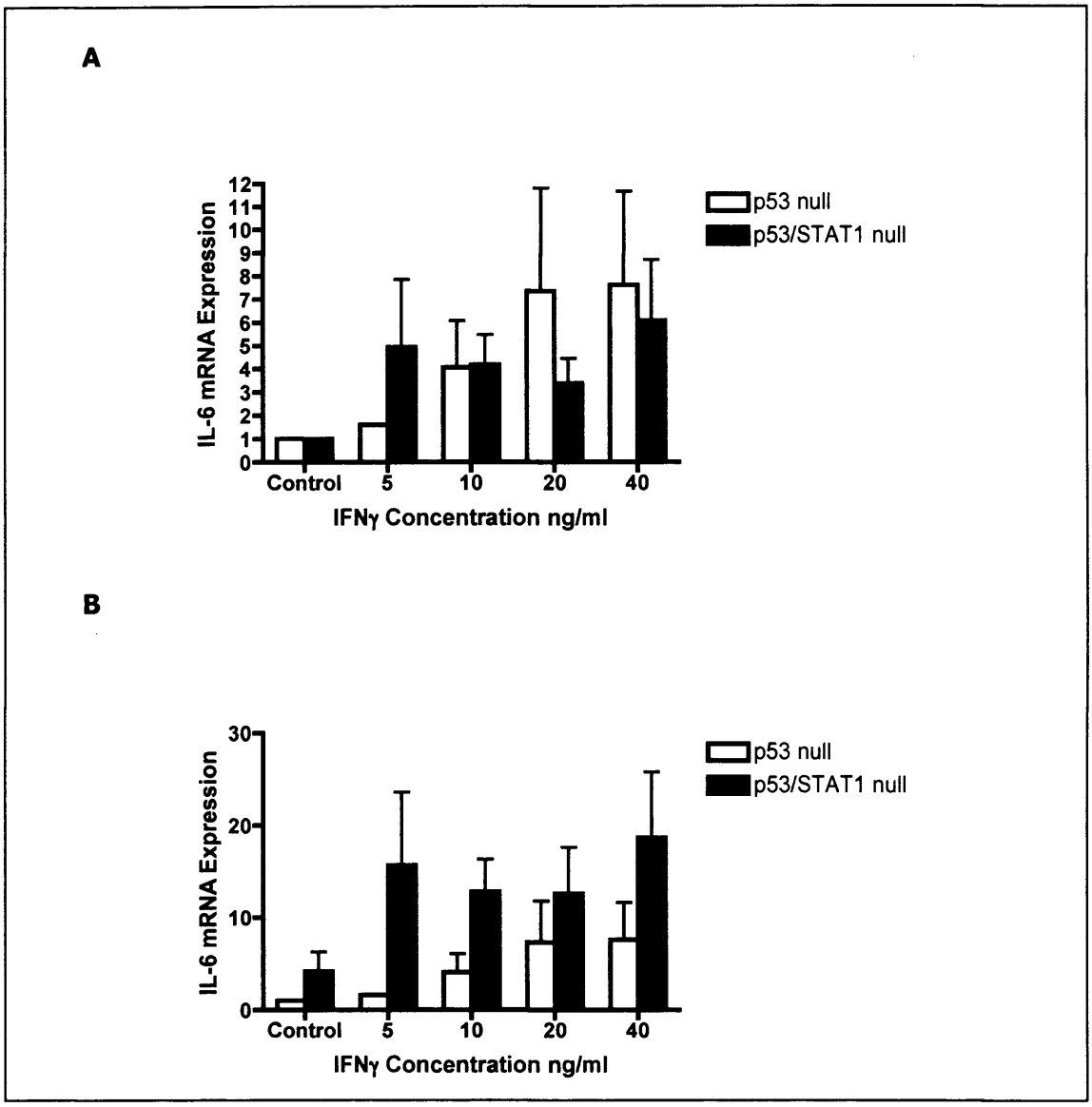

Figure 4.14 IL-6 mRNA expression in IFNγ treated MEFs. IL-6 mRNA expression was quantified by real time PCR and is presented in two ways; (A) IL-6 mRNA expression in *Trp53*$^{-/-}$ and *Trp53*$^{-/-}$/*Stat1*$^{-/-}$ relative to respective control (untreated cells of the same genotype); (B) IL-6 mRNA expression relative to *Trp53*$^{-/-}$ control (untreated *Trp53*$^{-/-}$ cells). Values shown are mean fold difference ± SEM of three experiments. For each experiment, IFNγ treatments and PCR reactions of each treatment were performed in triplicate. Statistical analysis was performed by a two-way ANOVA with Bonferroni post-tests and there were no significant differences between *Trp53*$^{-/-}$ and *Trp53*$^{-/-}$/*Stat1*$^{-/-}$ cells.

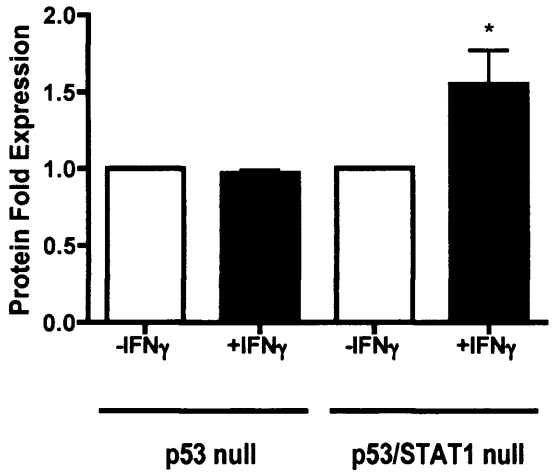

Figure 4.15 Secreted IL-6 from IFNγ treated MEFs quantified by ELISA. MEFs were treated with 5 ng/ml of IFNγ and media was collected after 24 h. Values shown are mean fold differences ± SEM of 5 experiments. For each experiment IFNγ treatments performed in triplicate. . Statistical analysis was performed by a two-way ANOVA with Bonferroni post-tests. *P <0.05 compared to p53/STAT1 null -IFNγ treated cells.

4.8.1 IFNγ induced IL-6 expression in the heart

There was increased expression of IL-6 in *Trp53*$^{-/-}$/*Stat1*$^{-/-}$ MEF cells compared to *Trp53*$^{-/-}$ MEF cells in response to IFNγ treatment and when untreated. This suggests STAT1 may have a repressive effect on IL-6 expression. However, the highest level of IL-6 expression in the hearts of untreated mice was observed in *Trp53*$^{-/-}$ hearts, as determined by 2D-PAGE expression analysis and PMF identification of IL-6. This suggests that STAT1 may have positive effect on IL-6 expression in the absence of p53 repression. To further investigate the role of STAT1 in IL-6 regulation in the heart, knockout mice were treated with IFNγ and cardiac IL-6 mRNA expression was quantified.

The optimal dose and time of IFNγ treatment required for studying the expression of STAT1 regulated genes in the hearts of gene knockout mice was determined by undertaking a dose response and time course of IFNγ treatment in wild type mice. Cardiac STAT1^{Y701} phoshorylation was assayed by Western blotting and the relative mRNA expression of several STAT1 regulated genes was quantified by real time PCR.

Wild type mice aged 8 weeks were injected intraperitoneally with IFNγ in doses of 1, 10, 50, 100 or 200 ng, or a vehicle control for 2 hours. STAT1^{Y701} phoshorylation increased in a dose dependent manner and maximal phosphorylation was observed in mice injected with 200 ng of IFNγ, the maximum dose used (Figure 4.16).

Interferon regulatory factor-1 (*IRF-1*), major histocompatibility complex class II transactivator (*C2ta*) and β2-microglobulin (*B2m*) are three genes that have been demonstrated to be positively regulated by STAT1. The mRNA expression of IRF-1 and C2ta increased in hearts following IFNγ in a dose dependent manner (Figure 4.17). B2m mRNA expression was increased following IFNγ treatment and maximal induction was observed with 10 ng/ml of IFNγ.

FBJ osteosarcoma oncogene (*Fos*) mRNA expression has been shown to be repressed by STAT1. Repression of Fos mRNA expression in hearts following IFNγ treatment was observed although not for all doses of IFNγ. Similar results were observed when mRNA expression levels were normalized to the mRNA expression of β-Actin and Gapdh.

The optimal time of IFNγ treatment was determined using a dose of 200 ng of IFNγ. Mice were injected intraperitoneally with 200 ng of IFNγ for 1, 2, 4 or 24 hours. $STAT1^{Y701}$ phoshorylation in hearts was observed following 1 and 2 hours following IFNγ treatment (Figure 4.18). $STAT1^{Y701}$ phoshorylation was not observed following 4 or 24 hours of IFNγ treatment. Maximal induction of IRF-1 and B2m mRNA was observed at 2 hours and C2ta was highest at 4 hours (Figure 4.19). The mRNA expression of these genes had returned to near normal levels after 24 hours of IFNγ treatment. Fos mRNA expression was lowest at 24 hours following IFNγ treatment.

These experiments demonstrated that IFNγ responsive genes were responding in the classical manner according to the literature. Therefore, IL-6 mRNA expression was quantified to determine the optimal time and dose for investigating IL-6 expression in knockout mice in response to IFNγ. IL-6 mRNA expression was highest in response to the maximal dose of IFNγ used, 200 ng. The peak of IL-6 mRNA expression was at 2 hours following IFNγ treatment (Figure 4.20). Therefore, cardiac IL-6 mRNA expression was measured in knockout mice at 2 hours post 200 ng of IFNγ.

The induction of cardiac IL-6 mRNA expression by IFNγ was determined in wild type and *Stat1*$^{-/-}$ mice. Thus, for this experiment, the direct effect of STAT1 on IL-6 was tested. Cardiac IL-6 mRNA expression was induced by IFNγ in both wild type and *Stat1*$^{-/-}$ mice (Figure 4.21). The level of cardiac IL-6 mRNA expression following IFNγ treatment was less in *Stat1*$^{-/-}$ mice compared to wild type mice, although the basal level of cardiac IL-6 expression was also less in *Stat1*$^{-/-}$ mice. Moreover, there were no statistically significant differences between the groups.

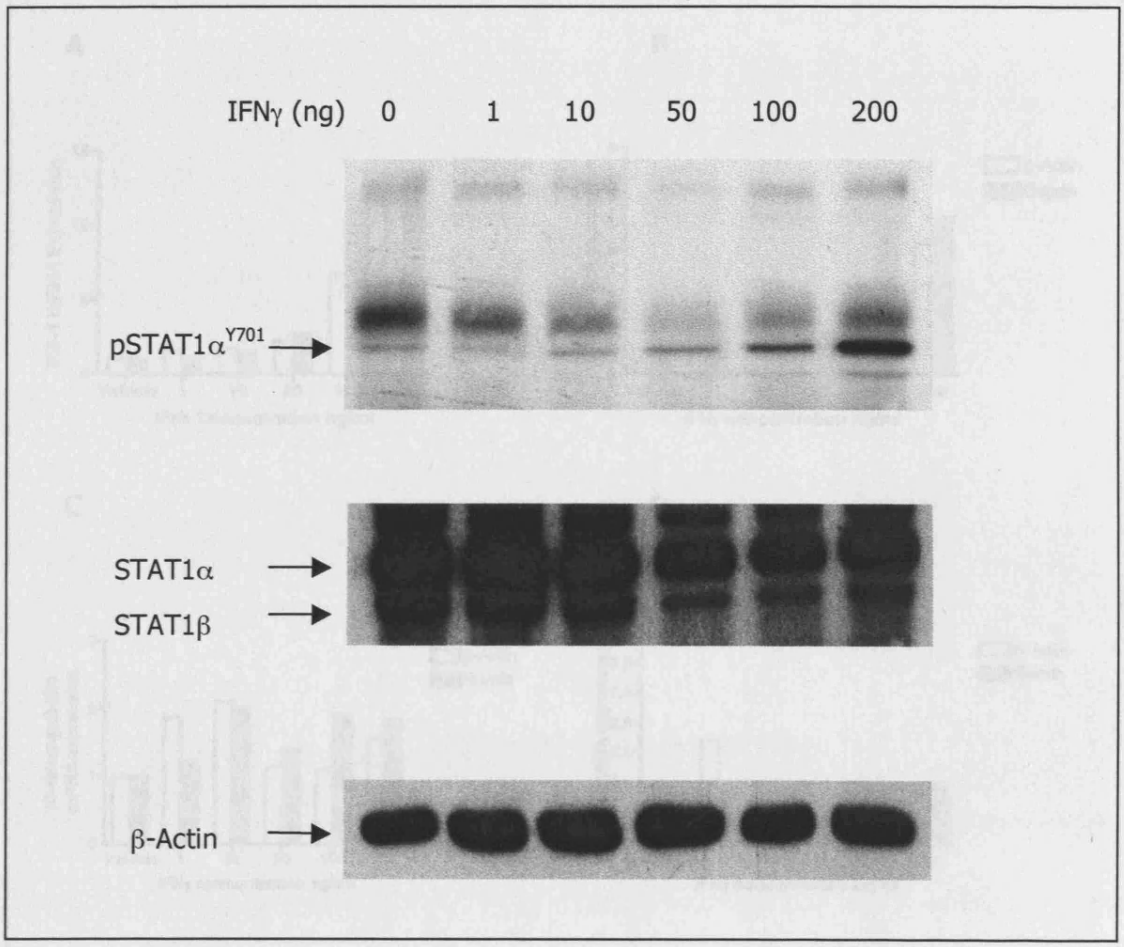

Figure 4.16 Western blot showing dose dependent induction by IFNγ of STAT1^{Y701} phosphorylation in hearts of mice. Wild type mice were treated with IFNγ by intraperitoneal injection for 2 h. 25 μg of protein was separated by 12% SDS-PAGE and immunoblotted for STAT1^{Y701}, total STAT1 and β-Actin.

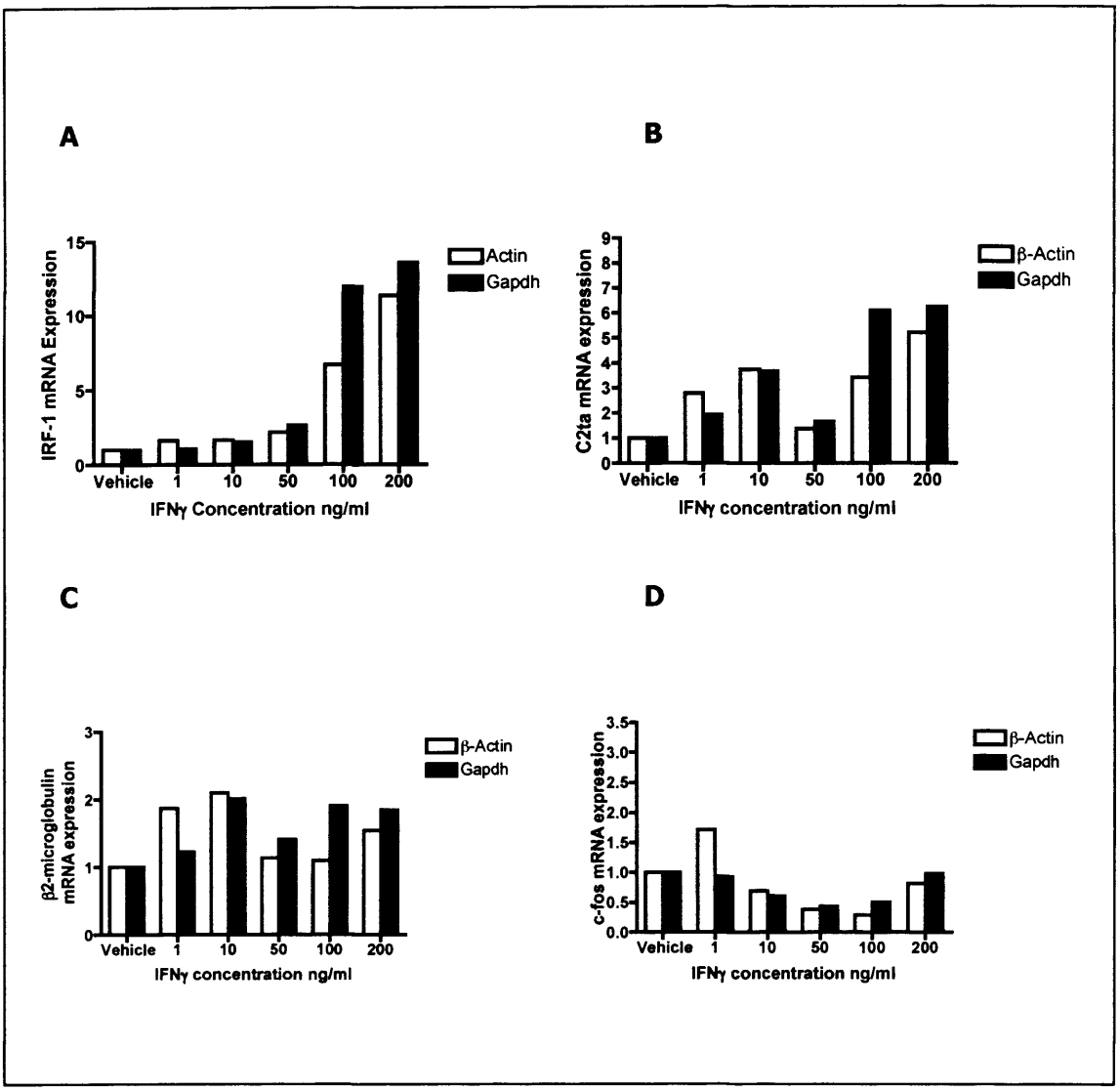

Figure 4.17 Dose dependent mRNA induction by IFNγ of STAT1 regulated genes in hearts of mice. Wild type mice were treated with IFNγ by intraperitoneal injection for 2 h. The mRNA expression of IRF-1 (A), C2ta (B), β2m (C) and Fos (D) was quantified by real time PCR and normalised to the expression of β–Actin or Gapdh. Values shown are mean fold difference of 2 animals for each treatment group relative to vehicle group. For the 200 ng treatment group only 1 animal was used.

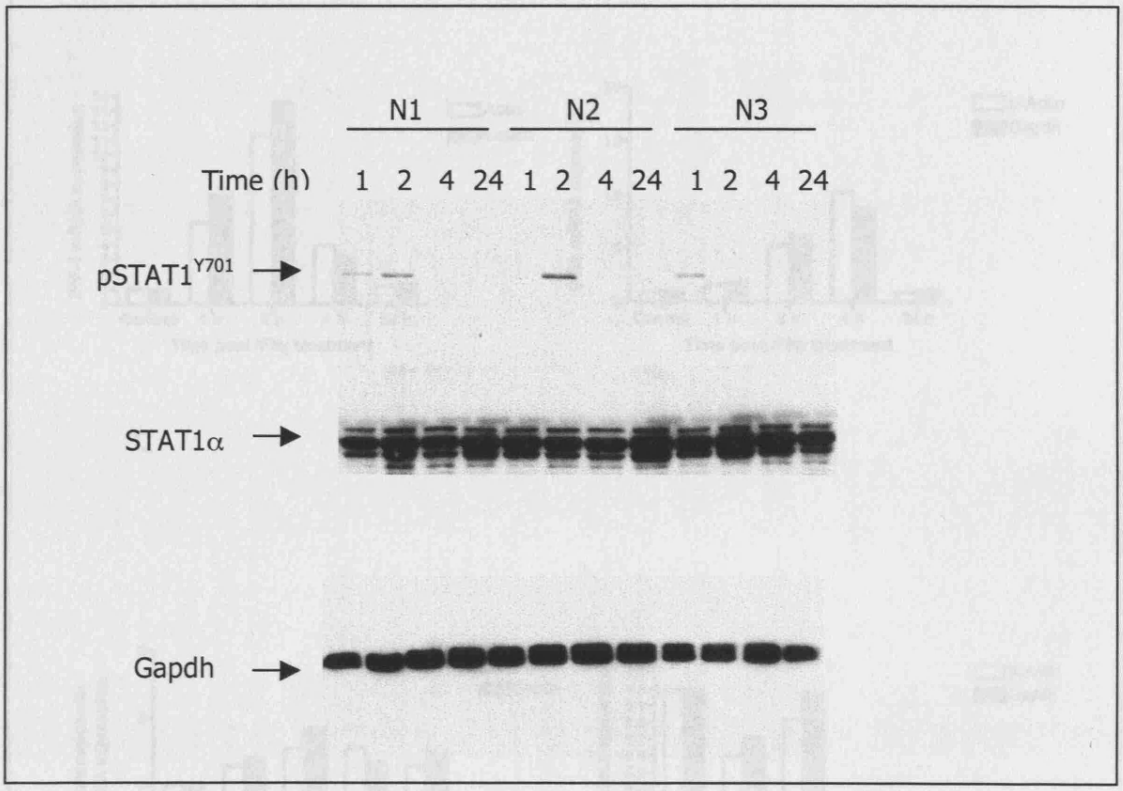

Figure 4.18 Western blot showing time course of induction by IFNγ of STAT1^{Y701} phosphorylation in hearts of mice. Wild type mice were treated with 200 ng of IFNγ by intraperitoneal injection for 1, 2, 4 or 24 h. Each time-point was performed in three animals (N1-3); 12 animals used in total. 25 μg of protein was separated by 12% SDS-PAGE and immunoblotted for STAT1^{Y701}, total STAT1 and Gapdh.

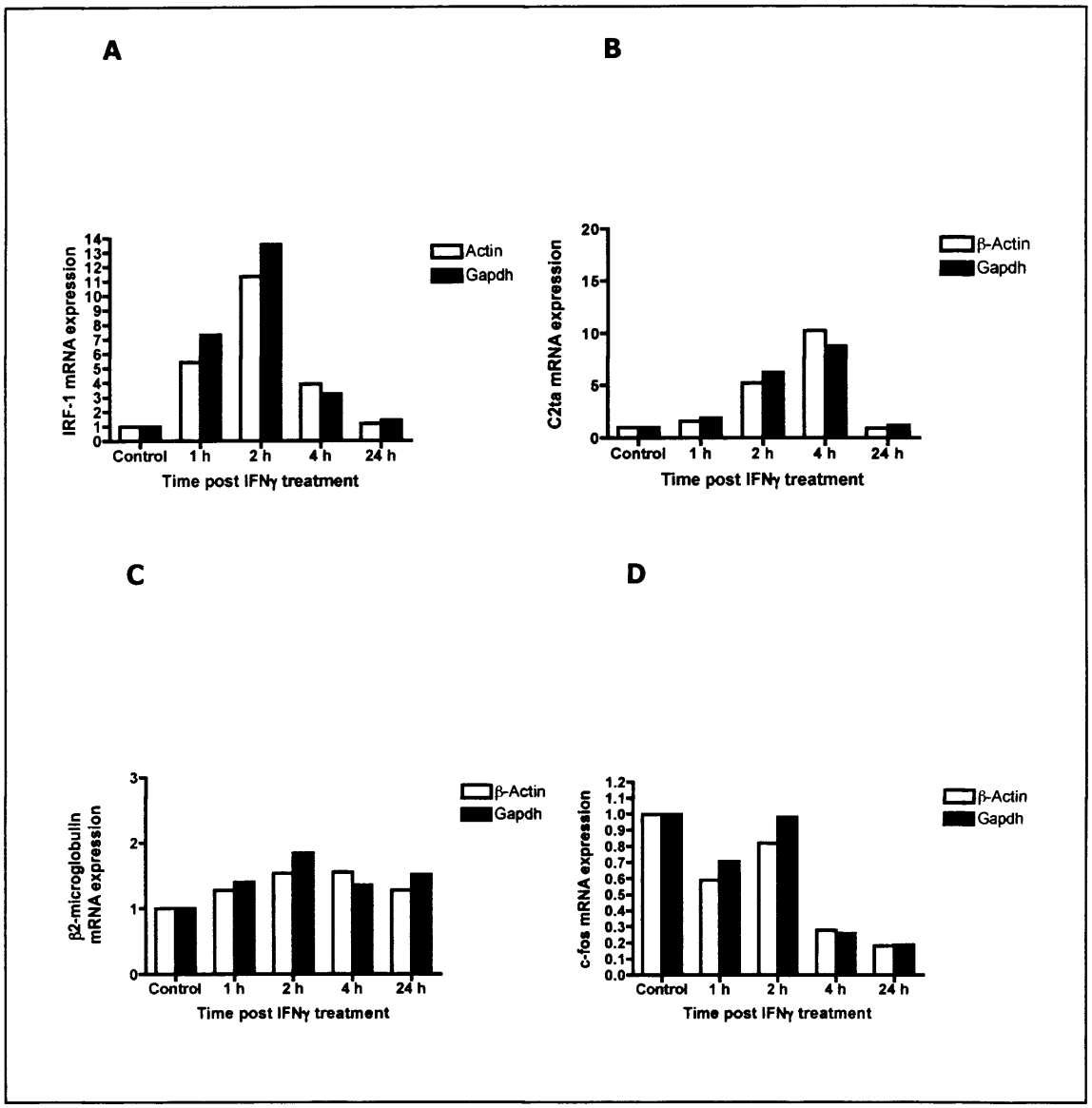

Figure 4.19 Time dependent mRNA induction by IFNγ of STAT1 regulated genes in hearts of mice. Wild type mice were treated with 200 ng of IFNγ by intraperitoneal injection for 1, 2, 4 or 24 h. The mRNA expression of IRF-1 (A), C2ta (B), B2m (C) and Fos (D) was quantified by real time PCR and normalised to the expression of β–Actin or Gapdh. Values shown are mean fold difference of 2 animals for each treatment group relative to vehicle group. For the 2 h treatment group only 1 animal was used.

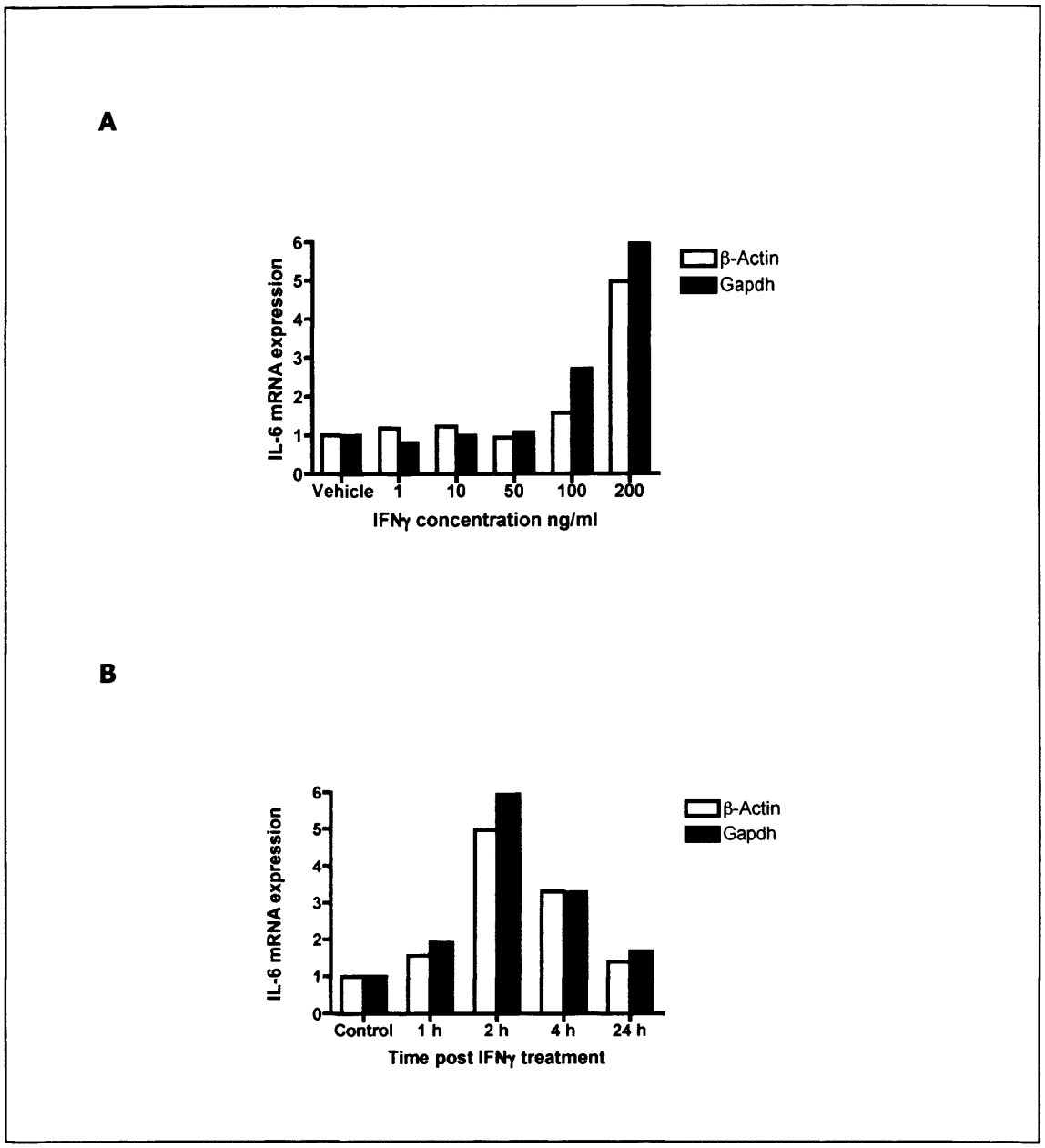

Figure 4.20 Dose and time dependent induction of IL-6 mRNA by IFNγ in hearts of mice. Wild type mice were treated with IFNγ by intraperitoneal injection for 2 h for the dose response (A) and with 200 ng for the time course (B). IL-6 mRNA expression was quantified by real time PCR and normalised to β-Actin or Gapdh. Values shown are mean fold difference of 2 animals for each treatment group relative to vehicle group. For the 200 ng and 2 h treatment groups only 1 animal was used.

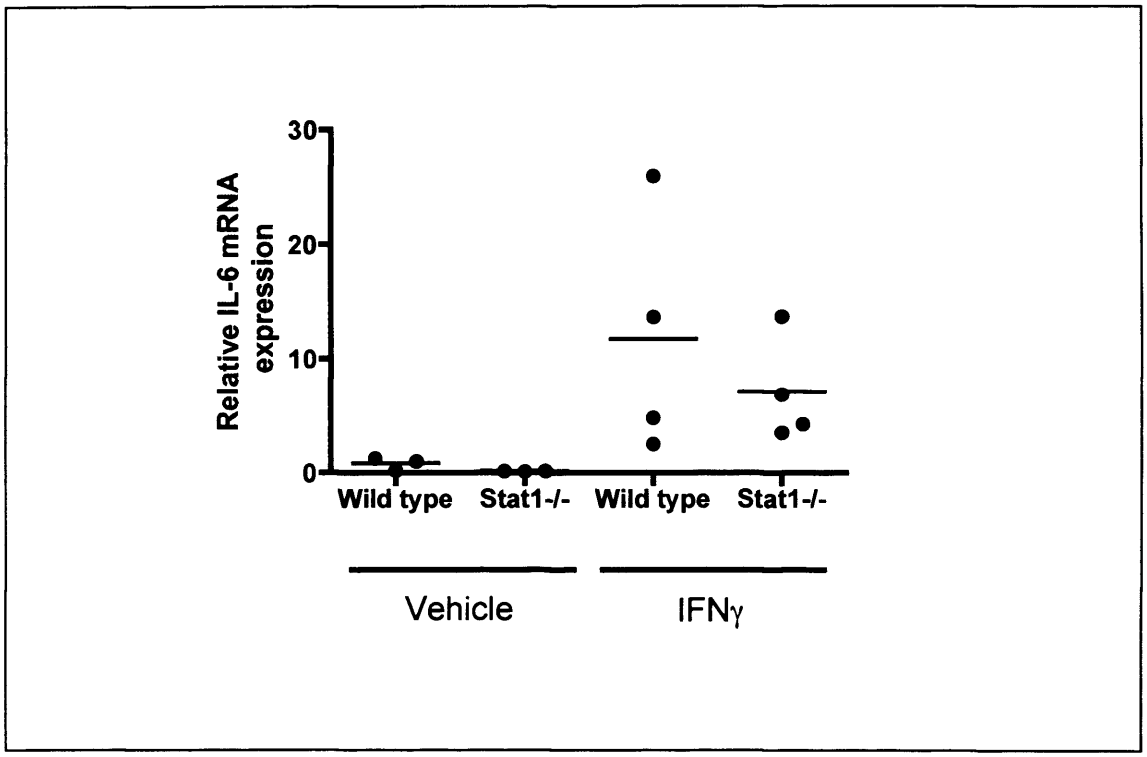

Figure 4.21 Cardiac IL-6 mRNA expression in IFNγ wild type and *Stat1*$^{-/-}$ treated mice. Values shown are normalised medians relative to wild type vehicle group. Statistical analysis of mRNA expression was performed by a Mann-Whitney U test. There were no significant differences between wild type and *STAT1*$^{-/-}$ mice following vehicle or IFNγ treatments.

4.11 Discussion

The results described in this chapter show that mice doubly deficient in p53 and STAT1, derived from commercially available B6.129-*Trp53*^{tm1Brd}N12 and 129S6/SvEv-*Stat*^{tm1Rds} strains, are viable. It has previously been demonstrated that mice deficient in p53 and STAT1 are viable when derived from 129/Sv/J-*Trp53*$^{-/-}$ and 129/Sv/Ev-*Stat1*$^{-/-}$ strains (Kaplan et al., 1998).

These transgenic mice, with the disrupted *Stat1* gene, express a truncated STAT1 protein of 72 kDa in the heart, a finding that has been previously described (Meraz et al., 1996, Stephanou et al., 2002). Expression of p53 was not detected in the hearts of wild type or p53 deficient mice. In normal physiological conditions, the expression of p53 is negatively regulated by the E3 ubiquitin ligase Mdm2, which results in its degradation by the proteosomal pathway (Lukashchuk and Vousden, 2007). Therefore, the expression of p53 was tested in MEF cells treated the etoposide, a DNA-damaging agent that induces p53. Etoposide treated *Trp53*$^{-/-}$ and *Trp53*$^{-/-}$/*Stat1*$^{-/-}$ MEF cells were shown to be deficient in the p53 protein compared to immortalized wild type MEF cells cultured in our laboratory.

MEF cells isolated from wild type and *Stat1*$^{-/-}$ mice became senescent after approximately eight days in culture whereas *Trp53*$^{-/-}$ and *Trp53*$^{-/-}$/*Stat1*$^{-/-}$ MEFs continued to proliferate. Studies have shown that senescence of cultured wild type MEF cells occurs within weeks of isolation and it has been demonstrated that MEF cells deficient in p53 grown for over 50 passages never entered a non-growing senescent phase (Harvey et al., 1993).

One of the principal aims of this work was to investigate the role that p53 plays in the increased sensitivity to I/R-injury of *Stat1* knockout mice that express a C-terminal fragment of STAT1. The experimental system for this was the use of a hypoxic chamber to simulate I/R-injury in isolated NMCM cells. *Trp53*$^{-/-}$/*Stat1*$^{-/-}$ mice were susceptible to the spontaneous development of a variety of tumours at an early age. A previous study also demonstrated that *Trp53*$^{-/-}$/*Stat1*$^{-/-}$ mice developed a wider variety of tumours, with increased frequency at an earlier age compared to *Trp53*$^{-/-}$ mice (Kaplan et al., 1998). In this study, the majority of *Trp53*$^{-/-}$/*Stat1*$^{-/-}$ mice that were generated either died or were culled because of ill health between three

and six months of age. Male and female *Trp53*$^{-/-}$/*Stat1*$^{-/-}$ mice were required to generate pure *Trp53*$^{-/-}$/*Stat1*$^{-/-}$ litters of mice in synchronisation with the generation of pure wild type, *Trp53*$^{-/-}$ and *Stat1*$^{-/-}$ mouse litters. This methodology was thought necessary for the following reasons. Firstly, pure litters were required to generate a sufficient number of cells for experimentation and to eliminate the majority, and surplus, production of mice that would be heterozygous knockout for either *Trp53* or *Stat1* if homozygous crosses were not the approach used to generate the mice of required genotype. Secondly, the synchronisation of matings and generation of litters of all genotypes was required so that I/R-injury in cardiac myocytes would have been simulated in the ischaemic chamber at the same time, therefore eliminating a cause for potential variability. However, *Trp53*$^{-/-}$/*Stat1*$^{-/-}$ mice were of a poor physical condition at an early age and consequently were poor breeders. Thus, pure *Trp53*$^{-/-}$/*Stat1*$^{-/-}$ litters could not be produced without an exhaustive breeding programme that would generate a huge surplus of wild type, *Trp53*$^{-/-}$ and *Stat1*$^{-/-}$ mice that would be generated concurrently for comparison to *Trp53*$^{-/-}$/*Stat1*$^{-/-}$ mice. The use of NMCM cells as an experimental system for testing the hypothesis in question was impractical and was not used. Therefore, the role that p53 plays in the increased sensitivity of *Stat1*$^{-/-}$ mice, compared to wild type mice, to cardiac I/Rinjury remains to be determined. This is currently being investigated in the adult mouse heart using Langendorff perfusion to simulate I/R-injury in our laboratory.

Expression profiling by 2D-PAGE revealed few differences in the cardiac proteomes of wild type, *Trp53*$^{-/-}$, *Stat1*$^{-/-}$ and *Trp53*$^{-/-}$/*Stat1*$^{-/-}$ mice. However, one protein that was highly abundant in hearts from *Trp53*$^{-/-}$ mice when compared to wild type, *Stat1*$^{-/-}$ and *Trp53*$^{-/-}$/*Stat1*$^{-/-}$ mice was identified by peptide mass fingerprinting as the IL-6 precursor protein.

IL-6 is a pleiotropic cytokine that is involved in antibody production, inflammation and growth (reviewed by Kishimoto, 2006). Studies have demonstrated that p53 is a transcriptional repressor of the IL-6 promoter in cancer cell lines (Santhanam et al., 1991, Angelo et al., 2002) and using *Trp53*$^{-/-}$ mice it has also been shown that p53 represses IL-6 expression in the thymus following treatment with LPS (Komarova et al., 2005). In this study, the finding that IL-6 is highly abundant in *Trp53*$^{-/-}$ cardiac samples supports those previous studies showing that p53 is a repressor of IL-6. However, IL-6 was not found to be highly abundant in the cardiac proteome of *Trp53*$^{-/-}$/*Stat1*$^{-/-}$ mice, suggesting that STAT1 is a potential activator of IL-6 in the

heart. The relative differences observed in the level of IL-6 protein expression were not observed in the level of mRNA expression. Therefore, the differences may be due to post-translational regulation, for example, altered degradation of the protein.

IL-6 is expressed in cardiac myocytes and IL-6 mRNA expression is induced in an awake canine model of I/R-injury (Kukielka et al., 1995). IL-6 protein expression has been shown to increase in NRCM cells following hypoxic stress and this is augmented by reperfusion (Yamauchi-Takihara et al., 1995). IL-6/soluble IL-6 receptor complex reduces infarct size in rats following I/R injury (Matsushita et al., 2005). Induction of IL-6 by hypoxia in NRCM cells has been demonstrated to be mediated by the transcription factor, nuclear factor (NF)-κB (NF-κB) (Matsui et al., 1999). In human monocytic cells, induction of the IL-6 gene by IFNγ and TNFα involves cooperation between IRF-1 and NF-κB (Sanceau et al., 1995). Although STAT1 was not directly implicated, it is a primary mediator of the IFNγ signalling pathway and IRF-1 is positively regulated by STAT1. Therefore, STAT1 may be inducing cardiac IL-6 expression in the absence of p53 and would explain why this induction was not observed in *Trp53*$^{-/-}$/*Stat1*$^{-/-}$ mice.

The ELISA and Western blotting techniques used in this chapter were not sensitive enough for the detection of IL-6 in cardiac protein samples. Thus, there was no additional evidence to support the enhanced IL-6 protein expression in hearts of *Trp53*$^{-/-}$ mice identified by proteomic screening. The protein samples required diluting and concentrating prior to ELISA, possibly resulting in too dilute a concentration or degradation of the protein. Furthermore, the antibody used in Western blotting was shown to have a low affinity for IL-6.

The increased IL-6 expression observed in cardiac tissue of *Trp53*$^{-/-}$ compared to *Trp53*$^{-/-}$/*Stat1*$^{-/-}$ mice was not equalled in MEF cells. Conversely, IL-6 mRNA expression was higher in *Trp53*$^{-/-}$/*Stat1*$^{-/-}$ compared to *Trp53*$^{-/-}$ MEFs. Moreover, the induction of IL-6 protein expression by IFNγ treatment in *Trp53*$^{-/-}$/*Stat1*$^{-/-}$ MEFs was not observed in *Trp53*$^{-/-}$ MEF cells. It has been demonstrated that STAT1 is not required for IL-6 production in MEF cells treated with IFNγ (Samardzic et al., 2001). IL-6 has been implicated in inflammation-induced causes of cancer (Rose-John and Schooltink, 2007) and the increased IL-6 expression in *Trp53*$^{-/-}$/*Stat1*$^{-/-}$ mice may contribute to why spontaneous development of tumours occur at a higher frequency and at an earlier age in these mice compared to *Trp53*$^{-/-}$ mice. However, the reason

why IL-6 mRNA expression and IFNγ induced protein expression is higher in *Trp53*$^{-/-}$/*Stat1*$^{-/-}$ MEF cells compared to *Trp53*$^{-/-}$ MEFs remains to be determined.

Cell type specific regulation may explain why such dissimilar observations were made for IL-6 expression between hearts and MEF cells. A limitation of this work was the few number of animals used in the proteome study, only three for each group. The mixed genetic background of the mice, coupled with them possibly in different stages of tumour development, may have been causes of variable IL-6 expression between mice. However, little variability in the proteome was observed between groups, therefore suggesting the IL-6 finding was specific to the genotype of the mice.

In summary, mice deficient in p53 and STAT1 are viable when derived from 129/Sv/J-*Trp53*$^{-/-}$ and 129/Sv/Ev-*Stat1*$^{-/-}$ strains. However, due to poor health and consequent poor breeding isolated neonatal cardiac myocytes from pure *Trp53*$^{-/-}$/*Stat1*$^{-/-}$ litters were not produced. A proteomic approach was used to identify that the IL-6 precursor protein was highly abundant in hearts from *Trp53*$^{-/-}$ mice when compared to wild type, *Stat1*$^{-/-}$ and *Trp53*$^{-/-}$/*Stat1*$^{-/-}$ mice. The normal level of IL-6 observed in *Trp53*$^{-/-}$/*Stat1*$^{-/-}$ mice suggests that STAT1 may be a potential activator of IL-6. Conversely, IL-6 mRNA expression was higher *Trp53*$^{-/-}$/*Stat1*$^{-/-}$ MEF cells compared to *Trp53*$^{-/-}$ MEF cells. Furthermore, induction of IL-6 protein expression by IFNγ in *Trp53*$^{-/-}$/*Stat1*$^{-/-}$ MEF cells was not observed in *Trp53*$^{-/-}$ MEF cells. Therefore, STAT1 may be involved in inducing the level of IL-6 in the heart but not in all tissue types.

CHAPTER FIVE

Results

CHAPTER FIVE

The role of hsp56 in ischaemia/reperfusion injury and hypertrophy in the mouse heart

5.1 Introduction and aims of this chapter

Circulating levels of the cytokine cardiotrophin-1 (CT-1) are increased in humans with chronic heart failure (Talwar et al., 1999) and expression of CT-1 is increased in the ventricles of humans with cardiomyopathies (Zolk et al., 2002) and in a variety of animal models of heart failure (Jougasaki et al., 2000, Aoyama et al., 2000). CT-1 has been shown to be a potent hypertrophic molecule in isolated rodent cardiac myocytes (Pennica et al., 1995) and to a lesser extent *in vivo* following chronic administration of the peptide in mice (Jin et al., 1996). In addition to inducing hypertrophy, CT-1 has been shown to confer protection from simulated I/R-induced injury in the isolated Langendorff perfused rat heart (Liao et al., 2002) and isolated NRCM cells (Brar et al., 2001).

Progress has been made in experiments using isolated rat cardiac myocytes to uncover the signalling pathways that connect CT-1 and the physiological responses it elicits. The expression of the heat shock protein hsp56 increases in isolated myocytes following CT-1 treatment and when expression of hsp56 was inhibited the hypertrophic effect of CT-1 was abrogated (Railson et al., 2001). However, the protection conferred by CT-1 from I/R-injury was not dependent on hsp56 (Brar et al., 2001). An earlier study demonstrated that hsp56 over-expression did not protect isolated NRCM cells from I/R-injury (Brar et al., 1999). However, identification of hsp56 as a mediator of CT-1 induced hypertrophy led to experiments that showed that over-expression of hsp56 in isolated myocytes was sufficient for the induction of hypertrophy (Railson et al., 2001). The hypertrophy induced by hsp56 was demonstrated to be dependent on several well-characterized signal transduction pathways (Jamshidi et al., 2004).

The expression profile of hsp56 in human heart failure or animal models of heart failure is not known, other than in the context of CT-1 induced hypertrophy in rodent

hearts and isolated cardiac myocytes. However, as CT-1 expression has been shown to increase in heart failure and that CT-1 induced hypertrophy *in vitro* is dependent on hsp56. Considering this relationship between CT-1 and hsp56, coupled with the observation that over-expression of hsp56 alone induces hypertrophy of cardiac myocytes *in vitro*, the following question remains to be answered: is hsp56 a mediator of hypertrophy *in vivo*? To answer this question this chapter describes how transgenic mice that over-express hsp56 were generated and assayed for myocardial hypertrophy by measuring heart-to-body weight ratios, myocyte cell size and the use of real-time PCR for quantifying the expression of genes that are commonly reactivated as part of the foetal growth program in hypertrophy.

Studies using isolated cardiac myocytes found that over-expression of hsp56 did not confer any protection from I/R-injury. However is not known if hsp56 over-expression is cardio-protective in the intact heart. To test this, hearts from hsp56 over-expressing mice were subjected to I/R-induced injury *ex vivo* by the Langendorff perfusion method.

5.2 Generation of hsp56 over-expressing transgenic mice

5.2.1 Mouse pronuclear injection of pCAGGS-hsp56 expression vector

Pronuclear injection of pCAGGS-hsp56 in FVB/N strain zygotes was undertaken at the ICH transgenic facility and resulted in the birth of 22 potential founder transgenic mice. At 3 weeks of age the genomic DNA from tail biopsies of the mice was screened for the integration of pCAGGS-hsp56 by PCR (figure 5.1a, upper row). pCAGGS-hsp56 was not detected in the genomic DNA of mice generated by pronuclear injection at the Institute of Child Health transgenic facility. The quality of the genomic template was shown to be sufficient for PCR by the amplification of an endogenous DNA control (figure 5.1a, lower row).

Subsequent to the initial attempt of pronuclear injections, the ICH transgenic facility was being relocated, therefore further pronuclear injections were undertaken by the KI facility. Pronuclear injection of pCAGGS-hsp56 in B6CBAF1 strain zygotes resulted in the birth of 45 potential transgenic founder mice. pCAGGS-hsp56 was detected in the DNA of 5 mice (numbers 5, 6, 21, 36 and 46) by PCR amplification of a 451 bp sequence of the transgene (figure 5.2). The percentage of mice born from pronuclear injection of pCAGGS-hsp56 that were transgenic was 11%.

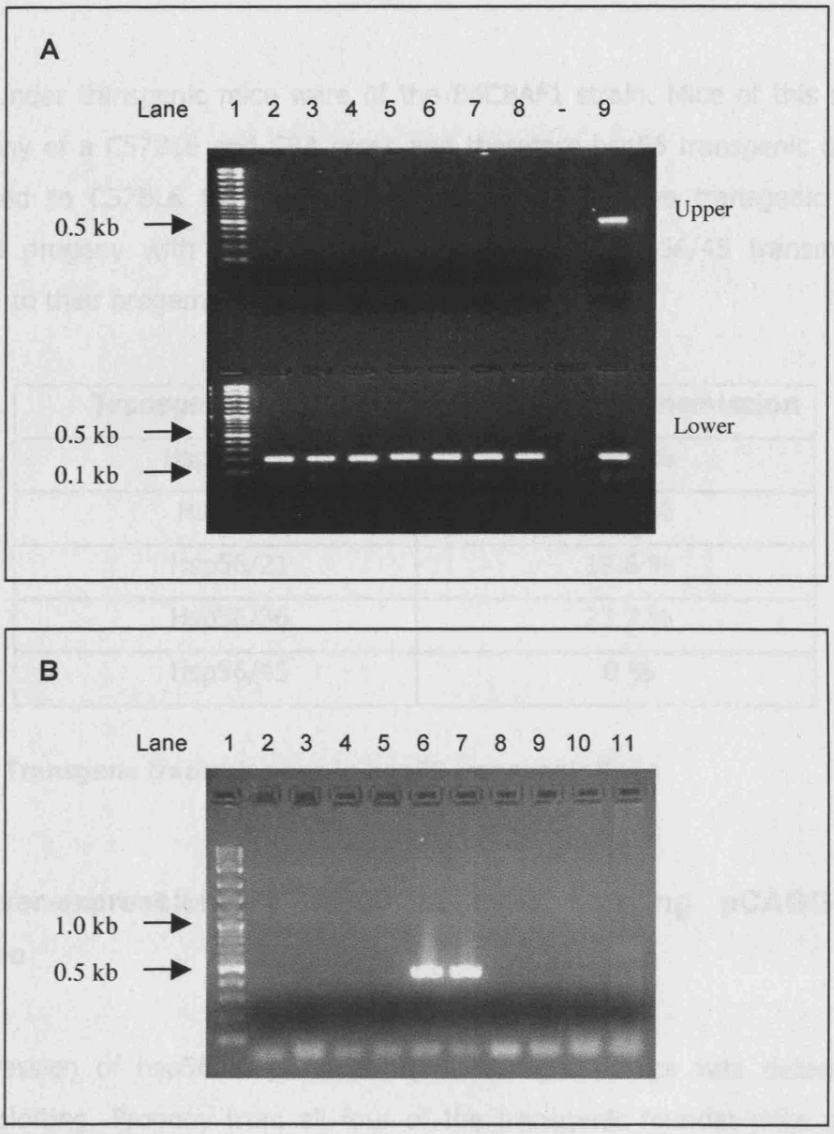

Figure 5.1 PCR screening of hsp56 transgenic mice generated by pronuclear injection using the ICH (A) and KI (B) transgenic services. PCR products were separated by agarose gel (2%) electrophoresis. A) PCR products from screening of the hsp56 transgene (upper) and an endogenous DNA control (lower). Lane 1; DNA molecular weight marker. Lanes 2-8; potential founders. Lane 9; PCR positive control. B) hsp56 transgene products. Lane 1; DNA molecular weight marker. Lanes 2-11; potential founders.

5.2.3 Transmission of hsp56 transgene

Hsp56 founder transgenic mice were of the B6CBAF1 strain. Mice of this strain are the progeny of a C57BL6 and CBA cross and therefore hsp56 transgenic mice were backcrossed to C57BL6 to reduce genetic variation. All five transgenic founders generated progeny with C57BL6 mice and all except hsp56/45 transmitted the transgene to their progeny (Table 5.1).

Transgenic founder	Transgene transmission
Hsp56/5	53.1 %
Hsp56/6	18.2 %
Hsp56/21	18.6 %
Hsp56/36	23.7 %
Hsp56/45	0 %

Table 5.1 Transgene transmissions in hsp56 transgenic lines

5.2.3 Over-expression of hsp56 in mice carrying pCAGGS-hsp56 transgene

Over-expression of hsp56 in pCAGGS-hsp56 transgenic mice was determined by Western blotting. Progeny from all four of the transgenic founder mice generated over-expressed hsp56 in the heart compared to wild-type littermates (figure 5.2). Protein expression of transgenic hsp56 varied between the lines with the highest observed in line 36 and the lowest in line 21.

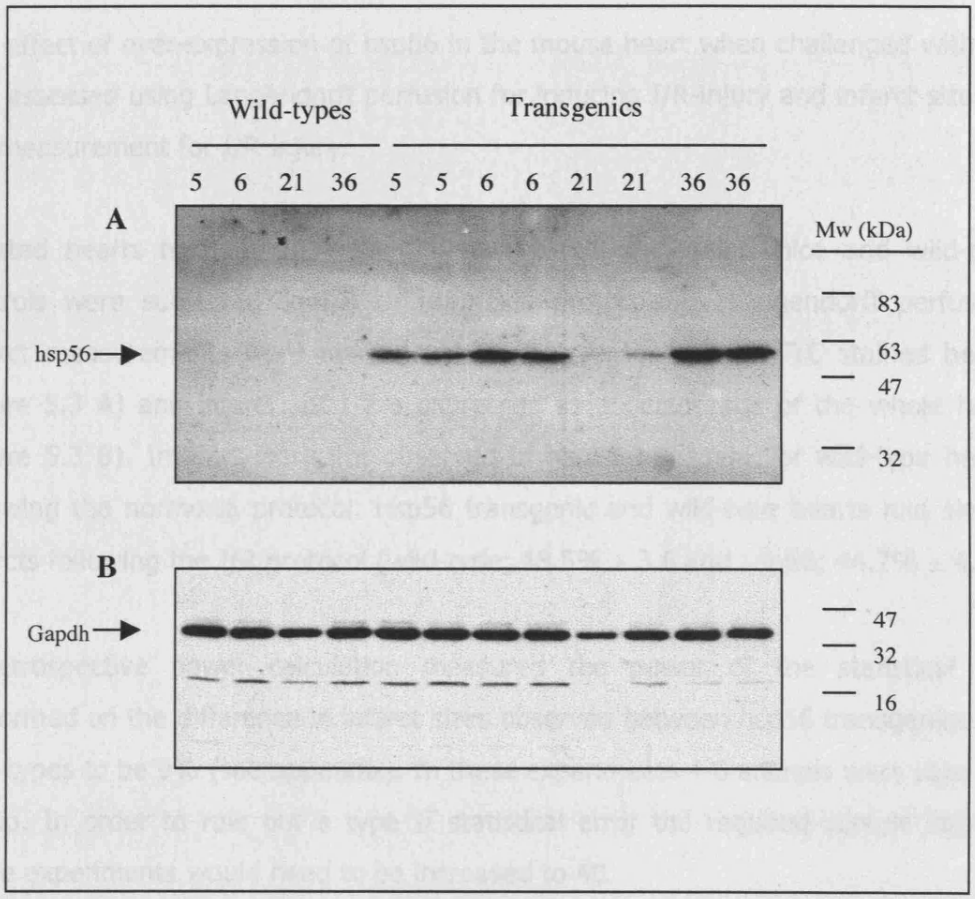

Figure 5.2 Western blot analysis of transgenic hsp56 over-expression. Heart protein lysates from hsp56 transgenic mice from lines 5, 6, 21, 36 and wild-type littermates were separated on 12% SDS-PAGE gels and immunoblotted for hsp56 (A) or Gapdh (B). Two animals from each line are shown.

5.3 Hearts from hsp56 over-expressing mice failed to be protected from ischaemia/reperfusion induced injury

The effect of over-expression of hsp56 in the mouse heart when challenged with I/R was assessed using Langendorff perfusion for inducing I/R-injury and infarct sizes as the measurement for I/R-injury.

Isolated hearts from 10-12 week-old male hsp56 transgenic mice and wild-type controls were subjected to I/R or normoxia protocols by Langendorff perfusion. Infarct measurements were made from transverse sections of TTC stained hearts (figure 5.3 A) and infarct sizes are expressed as a percentage of the whole heart (figure 5.3 B). Infarcts were not observed in hsp56 transgenic or wild-type hearts following the normoxia protocol. Hsp56 transgenic and wild-type hearts had similar infarcts following the I/R protocol (wild-type; 48.5% ± 3.6 and hsp56; 44.7% ± 4.2).

A retrospective power calculation measured the power of the statistical test performed on the difference in infarct sizes observed between hsp56 transgenics and wild-types to be 9% (see appendix). In these experiments 4-6 animals were used per group. In order to rule out a type II statistical error the required sample size for these experiments would need to be increased to 40.

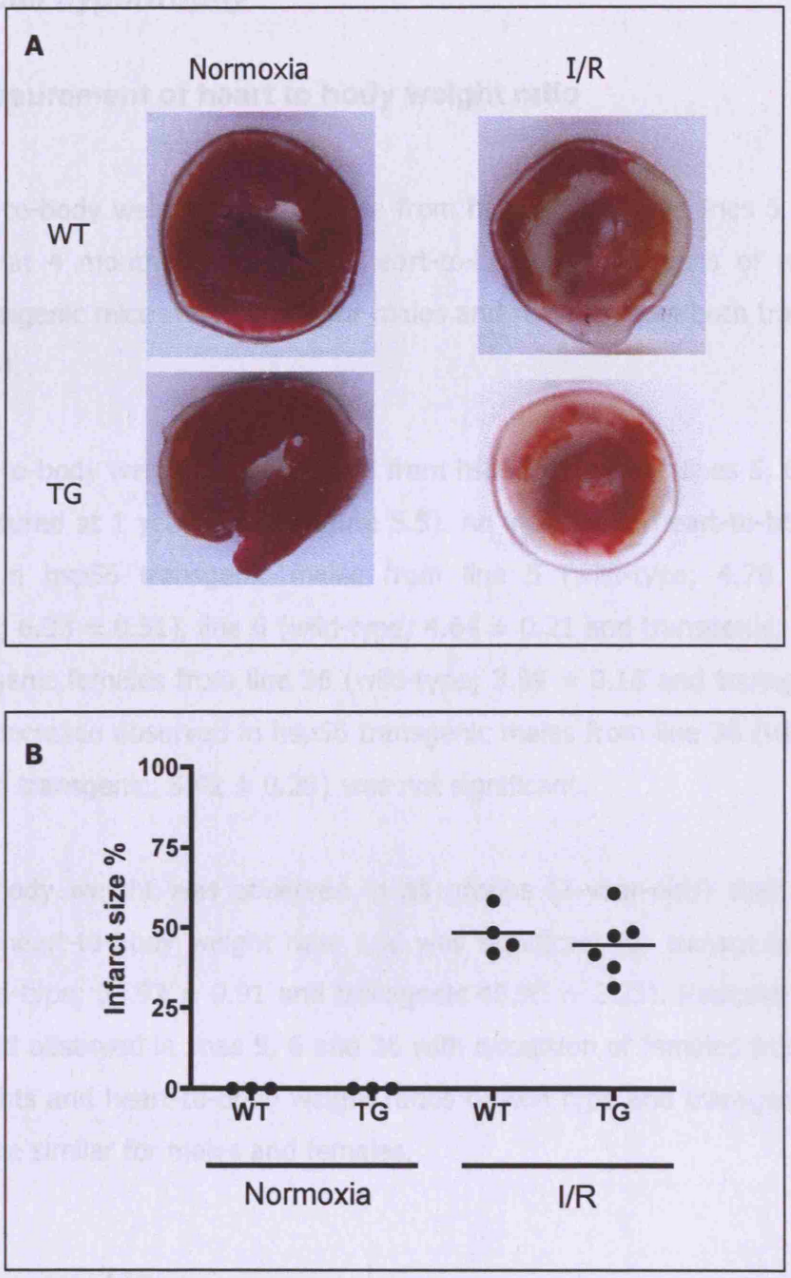

Figure 5.3 Infarct size analysis of Langendorff perfused hearts from hsp56 transgenic mice and wild-type controls. (A) Transverse sections of TTC stained hearts following I/R or normoxia control protocols. Infarct appears white and viable tissue appears red. (B) Infarct sizes were measured using a planimetry board and are expressed as a percentage of total heart. Means are shown as horizontal lines. See appendix for power calculation.

5.4 Over-expression of hsp56 alone in mice did not induce myocardial hypertrophy

5.4.1 Measurement of heart to body weight ratio

The heart-to-body weight ratios of mice from hsp56 transgenic lines 5 and 36 were measured at 4 months of age. The heart-to-body weight ratios of wild-type and hsp56 transgenic mice were similar for males and females from both transgenic lines (figure 5.4).

The heart-to-body weight ratios of mice from hsp56 transgenic lines 5, 6, 21, and 36 were measured at 1 year of age (figure 5.5). An increase in heart-to-body ratio was observed in hsp56 transgenic males from line 5 (wild-type; 4.78 ± 0.34 and transgenic; 6.33 ± 0.51), line 6 (wild-type; 4.64 ± 0.21 and transgenic; 5.88 ± 0.07) and transgenic females from line 36 (wild-type; 3.89 ± 0.18 and transgenic; 4.52 ± 0.02). An increase observed in hsp56 transgenic males from line 36 (wild-type; 4.98 ± 0.26 and transgenic; 5.42 ± 0.29) was not significant.

Reduced body weight was observed in all groups (1-year-olds) that exhibited an increased heart-to-body weight ratio and was significant for transgenic males from line 6 (wild-type; 53.92 ± 0.91 and transgenic 45.85 ± 2.25). Reduced body weight was a trend observed in lines 5, 6 and 36 with exception of females from line 6. The body weights and heart-to-body weight ratios of wild-type and transgenic mice from line 21 were similar for males and females.

5.4.2 Myocyte width measurements

Crude cardiac myocyte width measurements were made from haematoxylin and eosin stained sections from transgenic line 36 mice (figure 5.7). This is a crude method because for each section the myocytes are sectioned at different planes and thus the width measured is not consistent for each cell in the same way measuring the maximum width of isolated myocytes would be. Nevertheless, there were no differences observed between transgenics and their wild-type littermates with this method.

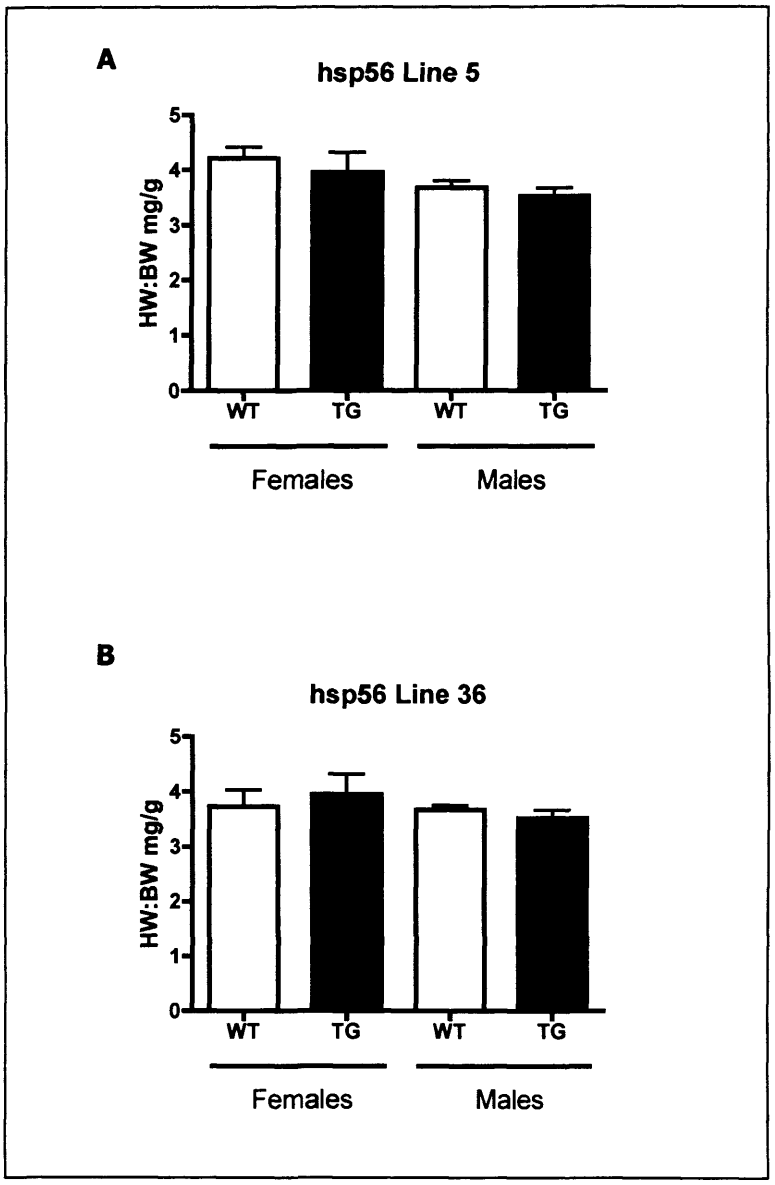

Figure 5.4 Heart-to-body weight ratios of 4-month-old *hsp56* transgenic mice and their wild-type littermates from line 5 (A) and line 36 (B). Values represent the mean ± SEM of 3 animals. There is no significant difference between male or female transgenics and their wild-type littermates in either line 5 or 36, as determined by two-way ANOVA with Bonferroni post-tests.

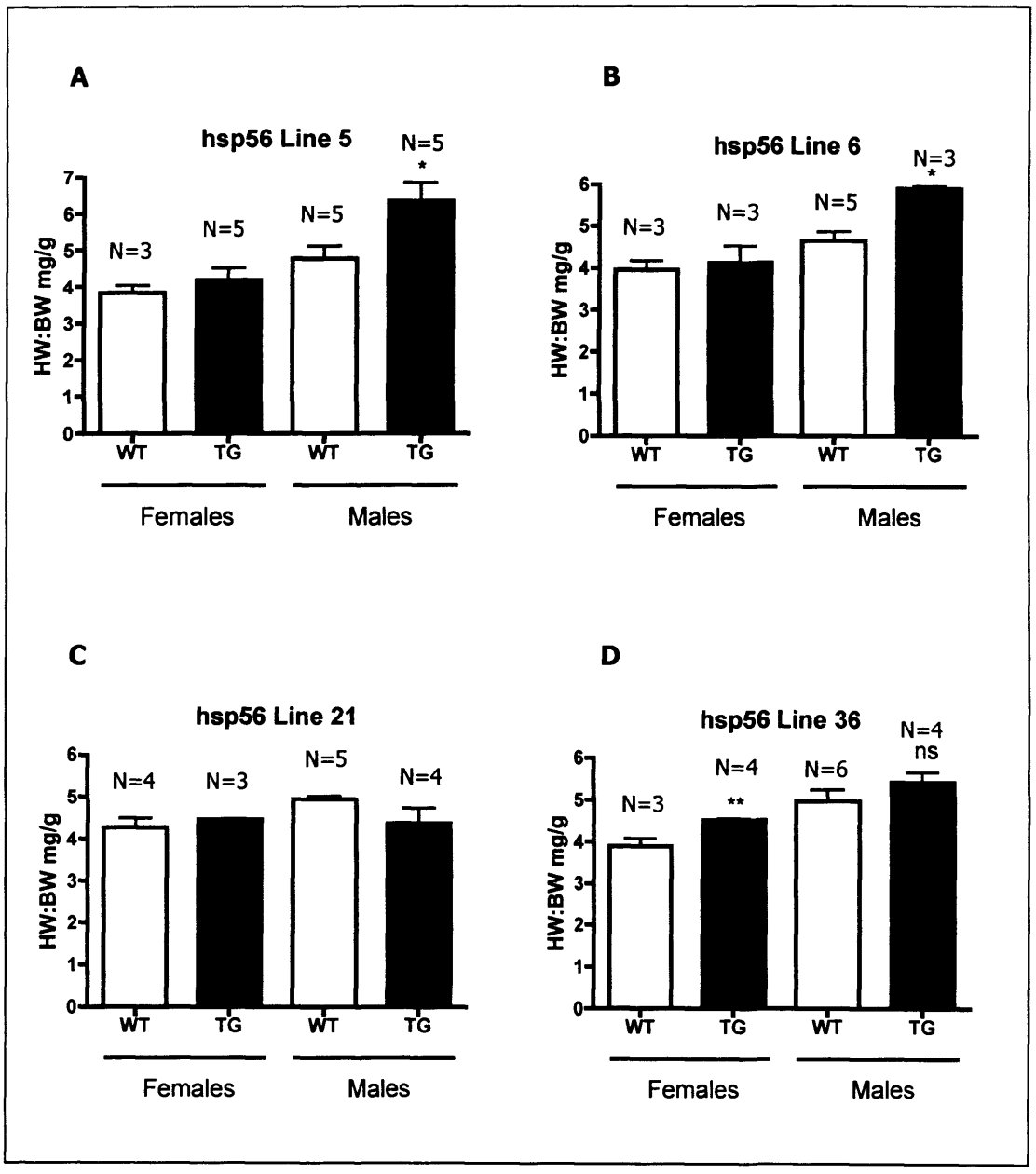

Figure 5.5 Heart-to-body weight ratios of 1-year-old *hsp56* transgenic mice and their wild-type littermates from line 5 (A), line 6 (B), line 21 (C) and line 36 (D). At least three mice from each group were analyzed and values represent the mean ± SEM. Statistical analysis was performed by a two-way ANOVA with Bonferroni post-tests.

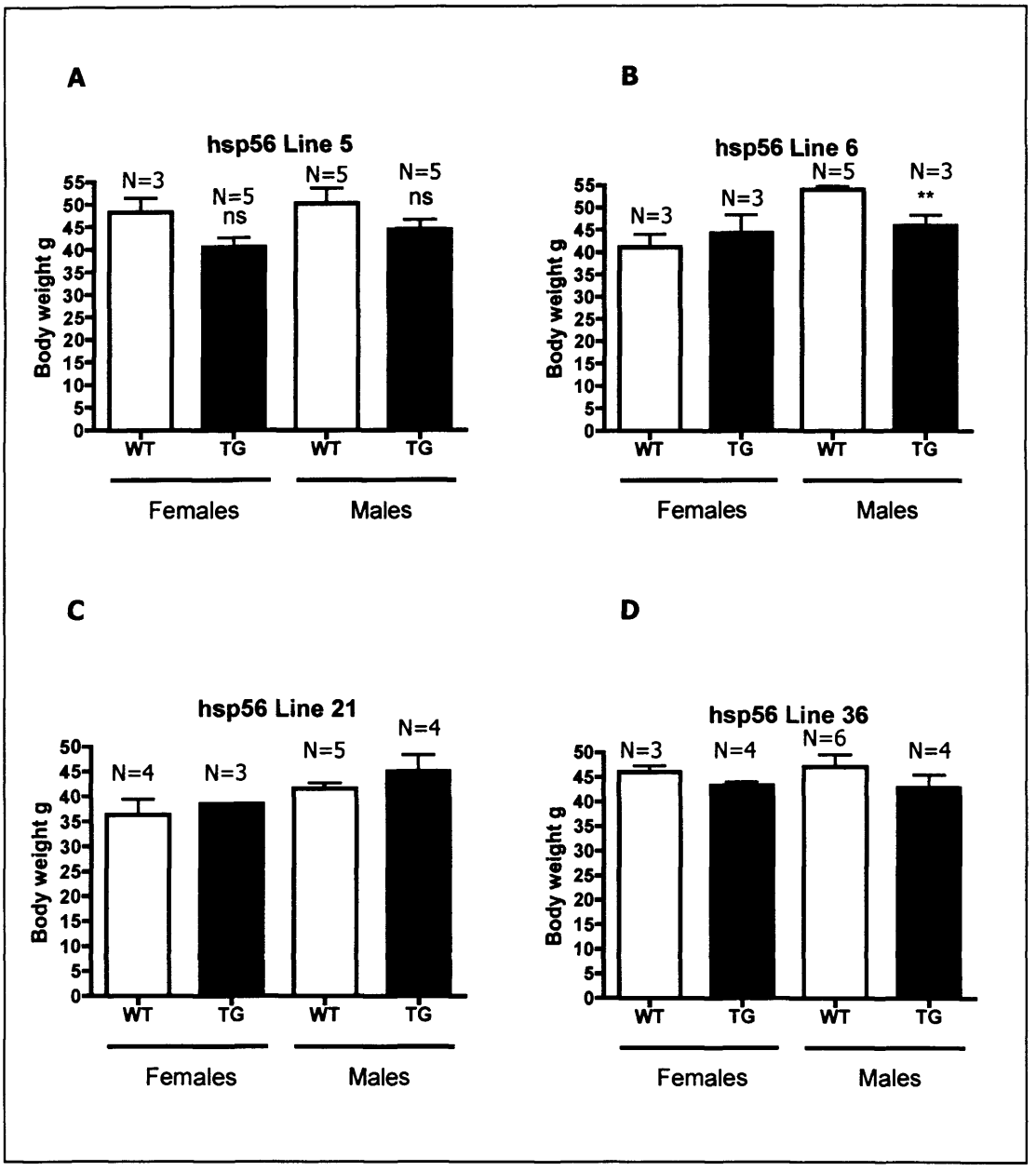

Figure 5.6 Body weights of 1-year-old *hsp56* transgenic mice and their wild-type littermates from line 5 (A), line 6 (B), line 21 (C) and line 36 (D). At least three mice were analyzed from each group and were those used in heart-to-body weight ratio measurements. Values represent the mean ± SEM. Statistical analysis was performed by a two-way ANOVA with Bonferroni post tests.

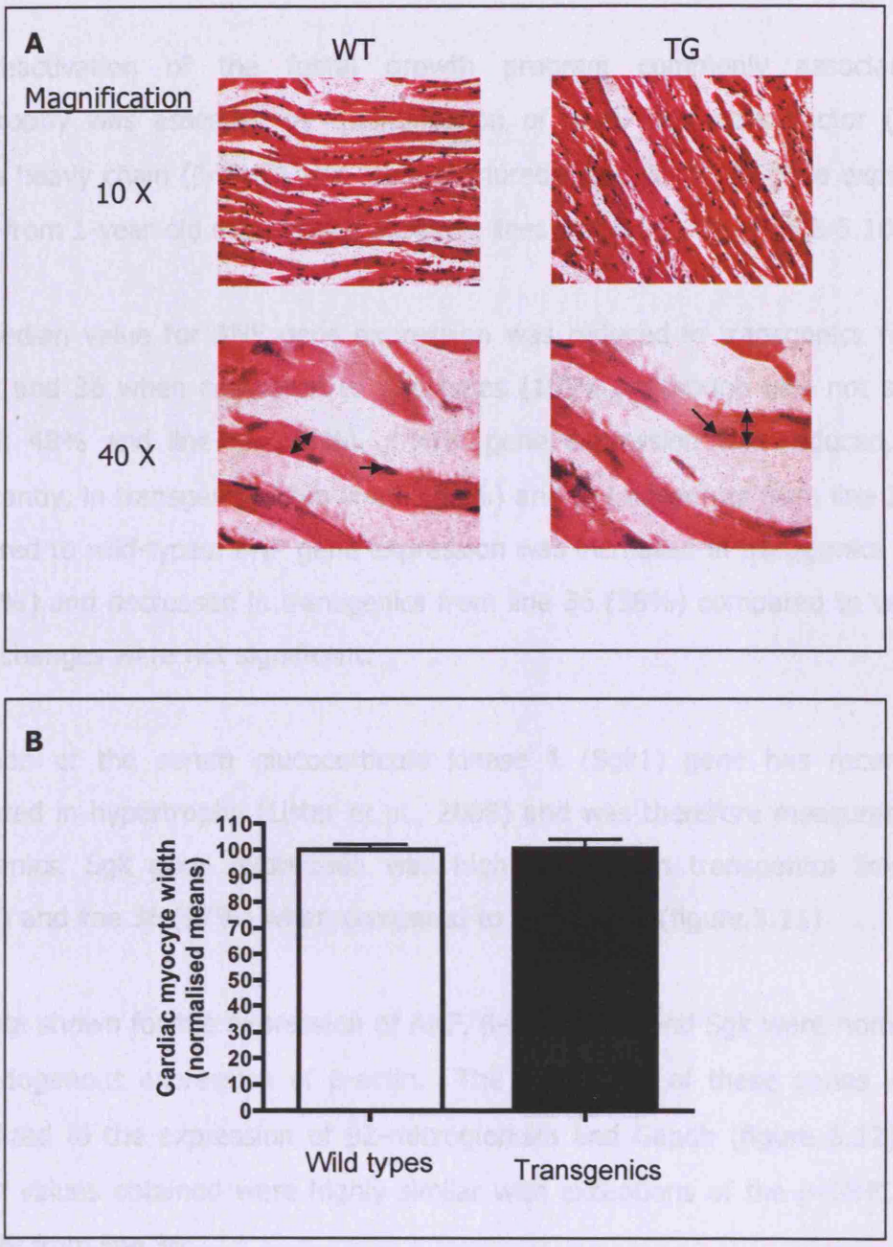

Figure 5.7 Cardiac myocyte width measurements in hsp56 transgenic mice and wild-type controls. (A) Cross sections of haematoxylin and eosin stained 8 μm heart slices. Single black arrows show myocyte nuclei. Double black arrows show myocyte width. (B) Relative cell width measurements were made using Axiovision analysis software. Values represent means of 100 cells measured from 3 animals per group

5.4.3 Gene expression analysis of hypertrophic markers

The reactivation of the foetal growth program commonly associated with hypertrophy was assessed by quantification of atrial natriuretic factor (ANF), β-myosin heavy chain (β-MHC) and brain natriuretic peptide (BNP) gene expression in hearts from 1-year-old mice from transgenic lines 5 and 36 (figures 5.8-5.10).

The median value for ANF gene expression was reduced in transgenics from both lines 5 and 36 when compared to wild-types (100%), although was not significant (line 5; 48% and line 36; 44%). β-MHC gene expression was reduced, but not significantly, in transgenics from line 5 (46%) and in transgenics from line 36 (79%) compared to wild-types. BNP gene expression was increased in transgenics from line 5 (126%) and decreased in transgenics from line 36 (38%) compared to wild-types. These changes were not significant.

Induction of the serum glucocorticoid kinase 1 (Sgk1) gene has recently been implicated in hypertrophy (Lister et al., 2006) and was therefore measured inhsp56 transgenics. Sgk gene expression was highly similar in transgenics from line 5 (103%) and line 36 (97%) when compared to wild-types (figure 5.11)

The data shown for the expression of ANF, β-MHC, BNP and Sgk were normalized to the endogenous expression of β-actin. The expression of these genes were also normalized to the expression of β2-microglobulin and Gapdh (figure 5.12) and the median values obtained were highly similar with exceptions of the β–MHC in line 5 and BNP from line 36.

When normalized to β-Actin the expression β-MHC in line 5 decreases (46%), however expression of β-MHC increases when normalized to β2-microglobulin (161%) and Gapdh (129%). The expression of BNP in line 36 is reduced when normalized to β-Actin (38%) and Gapdh (65%), however, is increased when normalized to β2-microglobulin (172%). These results suggest there may be some variation in the reference genes.

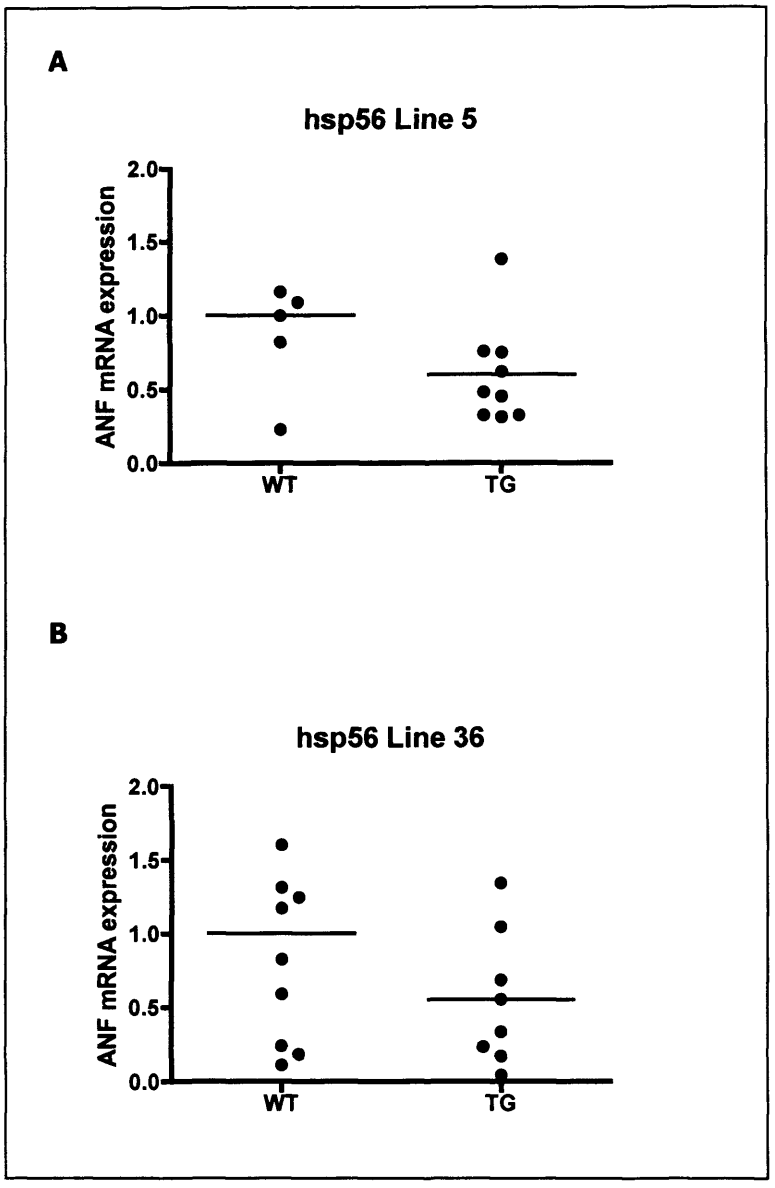

Figure 5.8 ANF mRNA expression in hearts from *hsp56* transgenic mice and their wild-type littermates from line 5 (A) and line 36 (B). Values represent ANF mRNA expression normalized to β-actin. Results with β–actin, Gapdh and β2-microglobulin normalizations are highly similar. Medians are shown as horizontal lines.

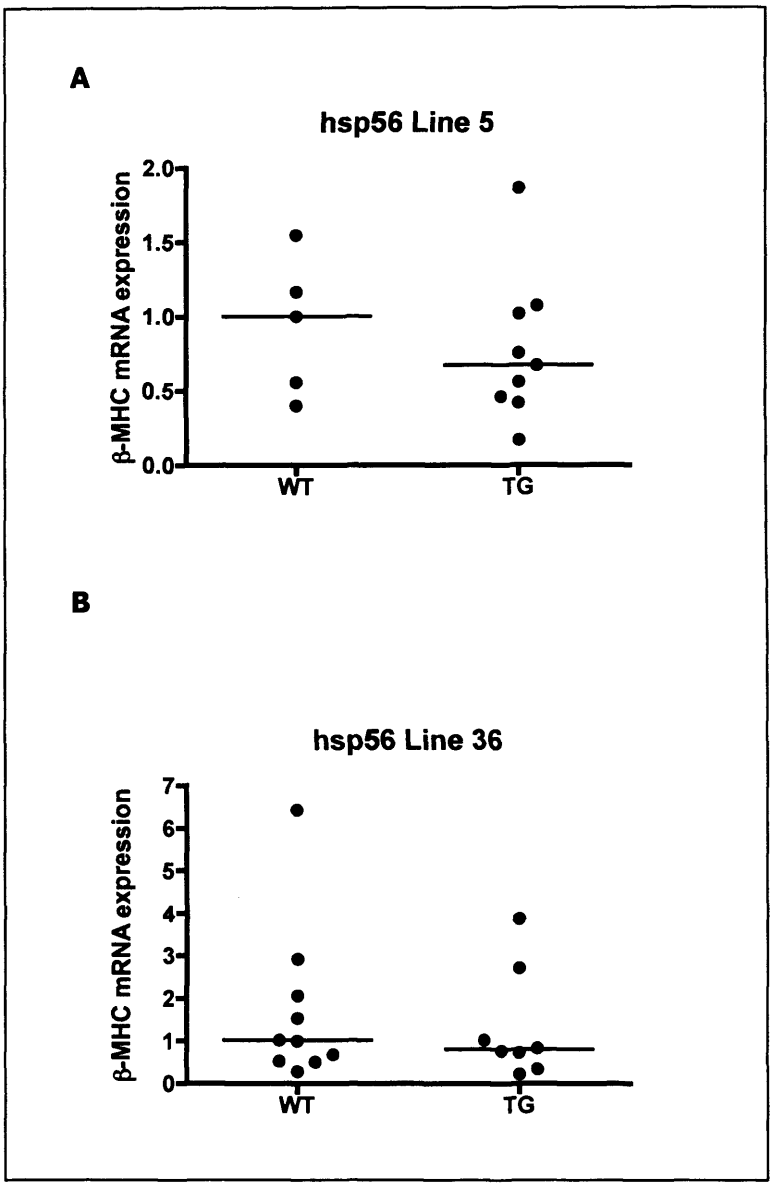

Figure 5.9 β-MHC mRNA expression in hearts from *hsp56* transgenic mice and their wild-type littermates from line 5 (A) and line 36 (B). Values represent β-MHC mRNA expression normalized to β-actin. Results with β–actin, Gapdh and β2-microglobulin normalizations are highly similar. Medians are shown as horizontal lines.

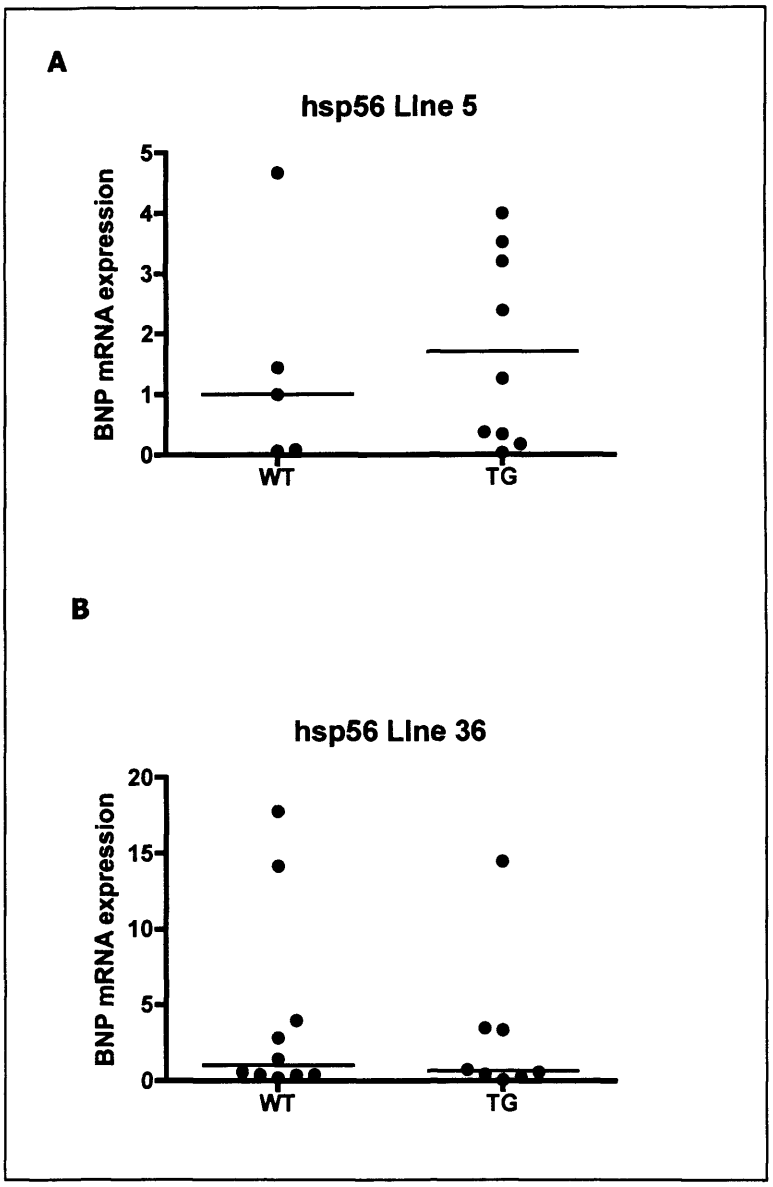

Figure 5.10 BNP mRNA expression in hearts from *hsp56* transgenic mice and their wild-type littermates from line 5 (A) and line 36 (B). Values represent BNP mRNA expression normalized to β-actin. Results with β–actin, Gapdh and β2-microglobulin normalizations are highly similar. Medians are shown as horizontal lines.

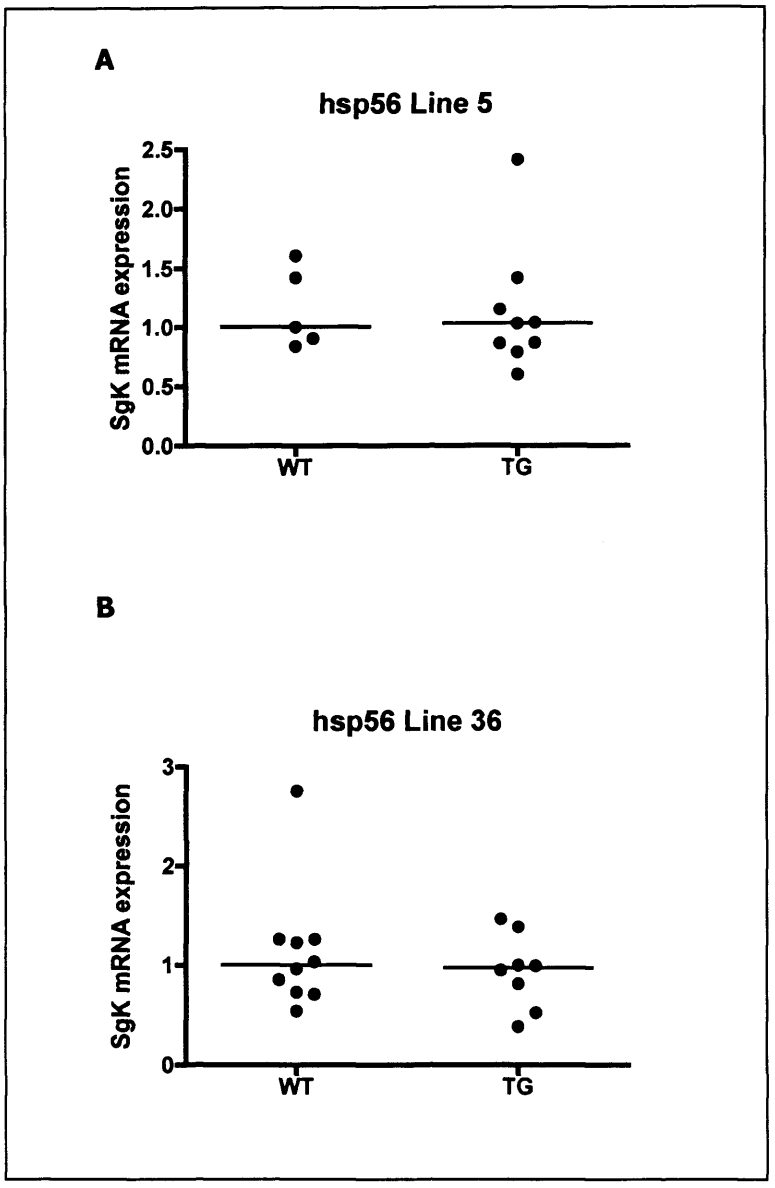

Figure 5.11 Sgk mRNA expression in hearts from *hsp56* transgenic mice and their wild-type littermates from line 5 (A) and line 36 (B). Values represent Sgk mRNA expression normalized to β-actin. Results with β–actin, Gapdh and β2-microglobulin normalizations are highly similar. Medians are shown as horizontal lines.

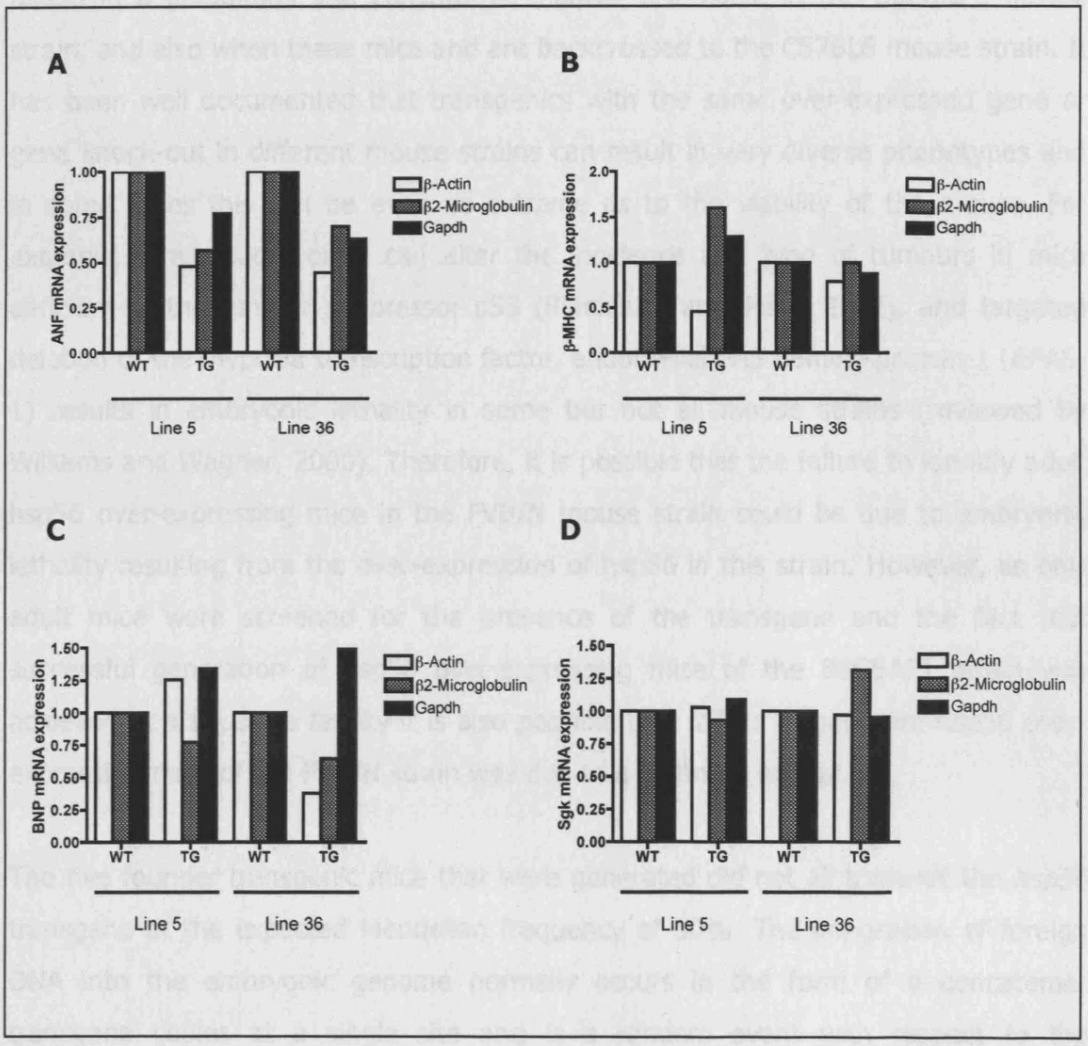

Figure 5.12 Comparison of normalizing expression of ANF (A), β-MHC (B), BNP (C) and Sgk (D) to 3 reference genes. Normalizing to β–Actin, β2-microglobulin and Gapdh gave highly similar results with the exceptions of β-MHC in line 5 and BNP in line 36. Values shown are normalised medians.

5.5 Discussion

The results described in this chapter show that transgenic mice over-expressing hsp56 in a ubiquitous and constitutive manner are viable in the B6CBAF1 mouse strain, and also when these mice and are backcrossed to the C57BL6 mouse strain. It has been well documented that transgenics with the same over-expressed gene or gene knock-out in different mouse strains can result in very diverse phenotypes and in some cases this can be even as extreme as to the viability of the mouse. For example, strain background can alter the incidence and type of tumours in mice deficient of the tumour suppressor p53 (Blackburn and Jerry, 2002), and targeted deletion of the hypoxia transcription factor, endothelial PAS domain protein-1 (EPAS-1) results in embryonic lethality in some but not all mouse strains (reviewed by Williams and Wagner, 2000). Therefore, it is possible that the failure to identify adult hsp56 over-expressing mice in the FVB/N mouse strain could be due to embryonic lethality resulting from the over-expression of hsp56 in this strain. However, as only adult mice were screened for the presence of the transgene and the fact that successful generation of hsp56 over-expressing mice of the B6CBAF1 strain was achieved at a separate facility it is also possible that failure to generate hsp56 over-expressing mice of the FVB/N strain was due to a technical matter.

The five founder transgenic mice that were generated did not all transmit the *hsp56* transgene at the expected Mendelian frequency of 50%. The integration of foreign DNA into the embryonic genome normally occurs in the form of a concatemer transgene copies at a single site and is a random event with respect to the chromosomal locus (Brinster et al., 1985). If integration doesn't occur until the two-cell stage or later-stage embryo then a mosaic mouse will be generated. Therefore those founders transmitting the transgene at a frequency of less than 50% may be mosaic. The transgenic founder *hsp56*/45 did not transmit the transgene to any progeny and it is possible that integration of the transgene occurred so that is was then only present in the somatic cells of this mouse.

As integration is random, the transgenic founders generated are unique and transgenic mice derived from the four transmitting founders represent four distinct *hsp56* transgenic lineages. Furthermore, the large majority of the genome consists of non-coding sequences and although the likelihood of disrupting a host gene and

inadvertently affecting the phenotype is small, the possibility does exist. Therefore it is favourable to have generated several transgenic lines, as findings that are reproduced in different lines give a greater confidence that they are a direct result of the over-expressed protein and not the consequence of disrupting a host gene.

One phenotypical characteristic that illustrates how transgenics generated from different founders are distinctly different is in the range of hsp56 protein expression exhibited between the lines. Having differential expression between transgenic lines is also a favourable feature as this may allow determination of relationships between quantity of protein expression and any physiological responses.

Hearts from mice over-expressing hsp56 were not protected from I/R-injury simulated by Langendorff perfusion. The lack of cardioprotection exhibited by hsp56 over-expression is consistent with a previous study that demonstrated there was no cardioprotective effect of hsp56 over-expression in cardiac cells subjected to a lethal dose of hypoxia (Brar et al., 1999). However, that particular study also demonstrated that unlike hsp56, over-expression of heat shock proteins hsp27 and hsp70 did protect cardiac cells from hypoxia. Moreover, hearts from transgenic mice that over-express hsp27 (Efthymiou et al., 2004) or hsp70 (Marber et al., 1995, Plumier et al., 1995) are protected from I/R-injury. This study further highlights how different heat shock proteins are distinctly different in conferring cardioprotection from I/R-injury.

Myocardial hypertrophy was not observed in hsp56 over-expressing mice aged 4-months, as measured by heart-to-body weight ratio. This observation was made in two transgenic lines. This finding is contradictory to the effects of hsp56 over-expression in isolated NRCM cells (Railson et al., 2001, Jamshidi et al., 2004). However, myocardial hypertrophy is progressive and studies of transgenic mice over-expressing the hypertrophy inducing protein Myotrophin (Sarkar et al., 2004) and knock-out mice deficient in the hypertrophy suppressing protein HDAC9 (Zhang et al., 2002) have demonstrated that differences in heart-to-body weight ratios increase with age and may only become apparent in older mice.

Myocardial hypertrophy was therefore measured in 1-year-old mice from four transgenic lines. Heart-to-body weight ratios increased for both transgenic male and female groups from line 5, line 6 and line 36. Of these, increases in the male

transgenic groups from line 5 and line 6, and in the female transgenic group from line 36 were statistically significant. Interestingly, although there were increases in heart-to-body weight ratios for male and female transgenics from line 5, line 6 and line 36, the body weights for all these groups were reduced when compared to their wild-type littermates, with the exception of the female transgenic group from line 6. Therefore, the observed increase in heart-to-body weight ratios was a function of the reduced body weight in hsp56 over-expressing mice and not increased heart weight. This observation also contradicts the finding that hsp56 causes hypertrophy.

Myocardial hypertrophy occurs as cardiac myocyte volume increases as a result of increasing length and/or width. The hypertrophic effect of hsp56 over-expression in isolated cardiac myocytes in some instances manifested as a 20% increase in cell size (Jamshidi et al., 2004). Such subtle increases *in vivo* could go undetected in the heart-to-body weight ratio assay as the heart consists of a large proportion of cell types other than cardiac myocytes that do not undergo hypertrophy. However, the width of cardiac myocytes were measured in haematoxylin and eosin stained cross sections of heart tissue and no increase was observed in transgenics when compared to wild-type controls.

A characteristic feature of myocardial hypertrophy is the reactivation of the foetal growth program that commonly includes the high expression of ANF, BNP and β-MHC mRNAs. mRNA expression for each of these genes was quantified and were not elevated in transgenics of either of the two lines assayed. It has been previously shown that over-expression of hsp56 in isolated NRCM cells induces a luciferase reporter containing the ANF promoter (Jamshidi et al., 2004). However in this study ANF mRNA expression in hsp56 over-expressing mice was reduced in two transgenic lines although not statistically significant.

Glucocorticoids have been have shown to induce myocardial hypertrophy (Whitehurst et al., 1999) and it was recently demonstrated that such hypertrophy involves the increased expression and requirement of serum and glucocorticoid induced kinase 1 (SGK1) (Lister et al., 2006). Hsp56 is part of the glucocorticoid receptor complex (Peattie et al., 1992) and thus may have in role glucocorticoid induced hypertrophy. As hsp56 over-expression induces hypertrophy in isolated cardiac myocytes, SGK1 mRNA expression was quantified in order to determine if hsp56 over-expression

could induce the expression of SGK1, however, no increase was observed in transgenics from the two lines analyzed.

In summary, hearts from transgenic mice that over-express hsp56 in a constitutive and conditional manner are not protected from I/R-injury and are not hypertrophic. The lack of cardioprotection is consistent with hsp56 over-expression in isolated NRCM cells (Brar et al., 1999) but the absence of hypertrophy does not reproduce the findings *in vitro*. (Railson et al., 2001, Jamshidi et al., 2004).

An unexpected observation was that mice from three transgenic lines over-expressing hsp56 had reduced body weight compared to wild-type controls. The effects of glucocorticoid signalling include the stimulation of fat breakdown in adipose tissue and the ability of hsp56 to bind the glucocorticoid receptor may be modulating this effect. A reduction in body weight was not exhibited by transgenics from line 21. Line 21 was the lowest hps56 expressing transgenic line and this may be why a reduction in body weight was not observed. Although defects in reproductive tissues of mice deficient in hsp56 have been demonstrated (Cheung-Flynn et al., 2005, Tranguch et al., 2005), no changes in body weight were reported. It may be expected that the opposite effect would occur in a knock-out mouse compared to on over-expressing transgenic for the same gene however abnormally high levels of a protein has the potential to produce artificial results. Nevertheless, these findings suggest that hsp56 may have a physiological role in glucocorticoid signalling that could be studied in either mice deficient or over-expressing hsp56.

The findings in this study do not necessarily preclude hsp56 from having a role in hypertrophy. Although hsp56 over-expression in mice was not sufficient to induce hypertrophy it may still be required for hypertrophy induced by other stimuli. For example, hsp56 is required for hypertrophy induced by CT-1 in isolated NRMC cells. The hsp56 over-expressing mice generated in this study could therefore be used to further examine this role by testing their sensitivity to CT-1 treatment.

Over-expression of hsp56 in the mouse could potentially induce hypertrophy if an alternative approach to the one taken in this study was used. In this study transgenic mice were transformed with an expression construct for hsp56 that was under control of a chicken β-actin promoter that gave ubiquitous and constitutive expression. The null hypertrophic phenotype observed in these mice could be a

result of physiological compensation. Expression of hsp56 in the developing embryo may have at some stage induced compensatory factors to overcome and hide the hypertrophic effect of hsp56. This may explain why ANF mRNA expression was lower in transgenics from the two lines assayed. If this were the case, an alternative approach to consider would be to generate a transgenic in which the temporal expression of hsp56 could be controlled. One such example would be to use a tetracycline transactivator system.

CHAPTER SIX

Results

CHAPTER SIX

Urocortin mediated protection from simulated I/R injury in the adult rat heart and ARVC cells is associated with inhibition of mitochondrial permeability transition pore opening ($\Delta_m\Psi$)

6.1 Introduction and aims of this chapter

The expression of the endogenous cardioprotective peptide CT-1 has been shown to be induced by a further, possibly upstream, endogenous cardioprotective peptide, Urocortin (Ucn) (Janjua et al., 2003). Cardiac myocyte survival in heart biopsies exposed to I/R injury is associated with induced Ucn expression (Scarabelli et al., 2004). Exogenous application of Ucn has been shown to protect NRCM cells and the Langendorff perfused rat heart from simulated I/R injury, when given prior to ischaemia or at reperfusion (Brar et al., 2000, Scarabelli et al., 2002). Therefore, clearly Ucn may have some therapeutic benefit, for example by minimizing ischaemic damage in patients undergoing cardiac surgery or as adjunct in patients with undergoing thrombolytic intervention.

The mechanism by which Ucn protects from I/R-injury has been under investigation although it is not fully understood. Activation of p42/p44 MAPK and PI-3K/Akt pathways have been demonstrated to be necessary for Ucn mediated protection (Brar et al., 2000, Brar et al., 2002b). Mediators of the protective effect of ischaemic preconditioning (IPC), PKCε (Scarabelli et al., 2004) and the K_{ATP} channel subunit Kir6.1, have also been implicated (Lawrence et al., 2002, Lawrence et al., 2005). Furthermore, Ucn mediated protection in NRCM cells has also been shown to involve prevention of mitochondrial damage and associated inhibition of opening of the mitochondrial permeability transition pore (MPTP) (Lawrence et al., 2004). However, the relationship between Ucn mediated protection in the adult heart and mitochondrial permeability, designated by $\Delta_m\Psi$, remains to be assessed.

Cardiac I/R-injury is predominantly an adult disease and many differences exist between the neonatal and adult heart, therefore, the aim of this study is to ascertain

whether the protection conferred by Ucn in the adult rat heart and adult cardiac myocytes involves inhibition of MPTP opening. One major aim of the work presented in this chapter was the setting up and establishment of adult rat ventricular myocyte (ARVC) cultures. In this chapter, the relationship between Ucn and the MPTP in protection from simulated I/R-injury will be presented. The data uses both ARVC cells and in the intact isolated rat heart by Langendorff perfusion.

6.2 Isolation and culture of adult rat ventricular cells

The isolation and culture of adult rat ventricular cells (ARVC) was not an established technique in our laboratory. Therefore, the enzymatic dissociation by retrograde perfusion and rapid attachment technique was observed in Professor Chris Proud's laboratory (Dundee University) and was then successfully reproduced in our laboratory.

Isolations of ARVC cells varied between approximately 50-90% in the proportion of viable cells, as measured by the distinctive rod-shaped morphology of viable ARVC cells, compared to round necrotic cells. Cultured ARVC cells have distinctive rod shaped morphology and are bi-nucleated (Figure 6.1). Spontaneous contraction was observed in only a few of the cultured ARVC cells. Unlike cultures of neonatal cardiac myocytes, spontaneous contraction of cultured ARVC cells is associated with stress and a progression towards apoptosis (Maruyama et al., 2001). Expression of the cardiac myocyte specific marker desmin was observed in all rod shaped cells and the ventricular specific marker MLC2v was observed in the majority of rod shaped cells by immunocytochemistry (Figure 6.1).

6.3 Simulating I/R and assessment of survival in ARVC cultures

Simulation of I/R resulted in death of ARVC cells, as observed by the increased number of rounded up cells following I/R (Figure 6.2). Membrane blebbing, a characteristic feature of apoptosis, was initially observed in ARVC cells in early reperfusion. However, our standard biochemical techniques for detection of apoptosis were not successful in ARVC cells. It was observed that the buffer used for annexin V staining induced rapid death of ARVC cells. Shortly after incubation with annexin V buffer all cells began to contract, followed by shortening of cells and absolute death of cultures within 5 minutes as observed by rounding up of all cells. Neither ARVC cells subjected to simulated I/R or normoxic conditions showed positive Terminal-dUTP nucleotide end labelling (TUNEL). Thus, the use of standard biochemical techniques could not be used in subsequent experiments to measure apoptotic cell death. Therefore, only total cell death was determined, which was based on cell morphology; rod-shaped viable cells compared to round dead cells.

Simulated I/R resulted in death of ARVC cells in an ischaemic time dependent manner (figure 6.3). ARVC cells were subjected to 2, 4 or 6 h of ischaemia followed by 2 h of reperfusion (figure 6.3A). Increased cell death, measured as the percentage of rounded up cells, was observed following increased lengths of ischaemia. ARVC cells were subjected to 2 h of ischaemia followed by 2, 4 or 24 h of reperfusion (Figure 6.3B). Maximum cell death was observed at 4 h of reperfusion. After 24 h of reperfusion the percentage of dead cells was less compared to 4 h of reperfusion, however, the total number of adhered cells was less. This suggests there were more dead cells following 24 h reperfusion except they were not accounted for as a result of them detaching from the culture dish.

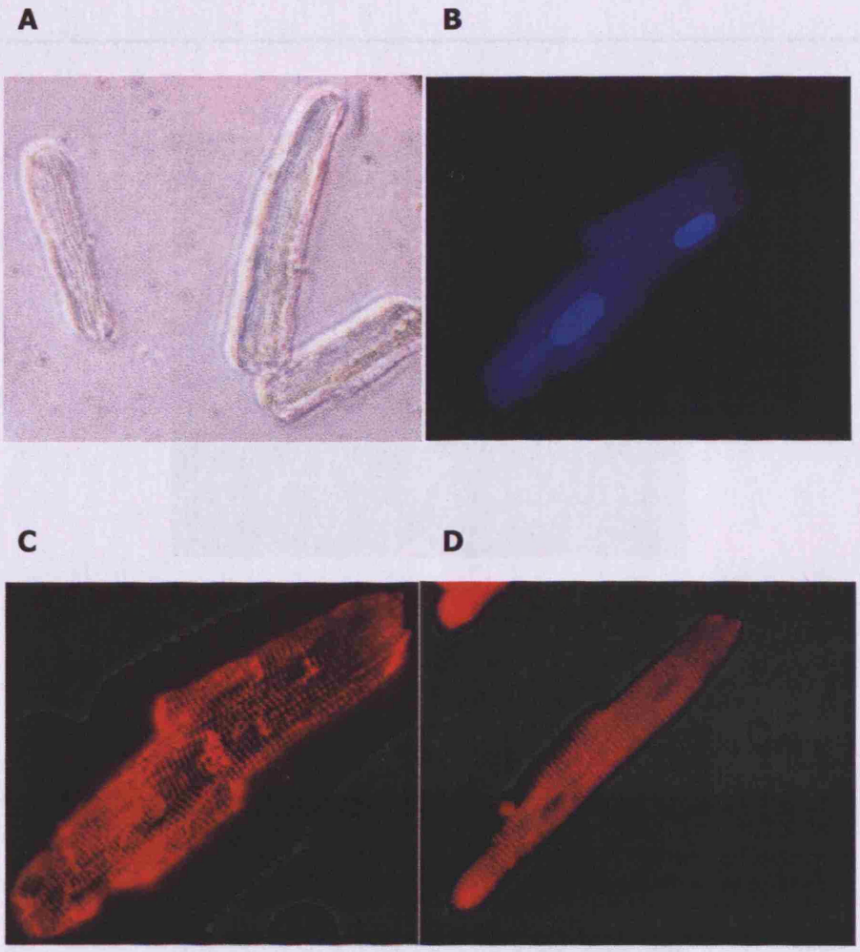

Figure 6.1 Cultured adult rat ventricular myocytes. (A) Myocytes visualized under light microscopy (magnification x25). (B) Fluorescence microscopy of cardiac myocyte showing nuclei stained with Hoechst 33258 (magnification x100). (C and D) Immunoflourescence of cardiac myocytes showing staining of (C) the cardiac myocyte specific protein, desmin (magnification x100), or (D) the ventricular myocyte specific protein, MLC2v (magnification x100).

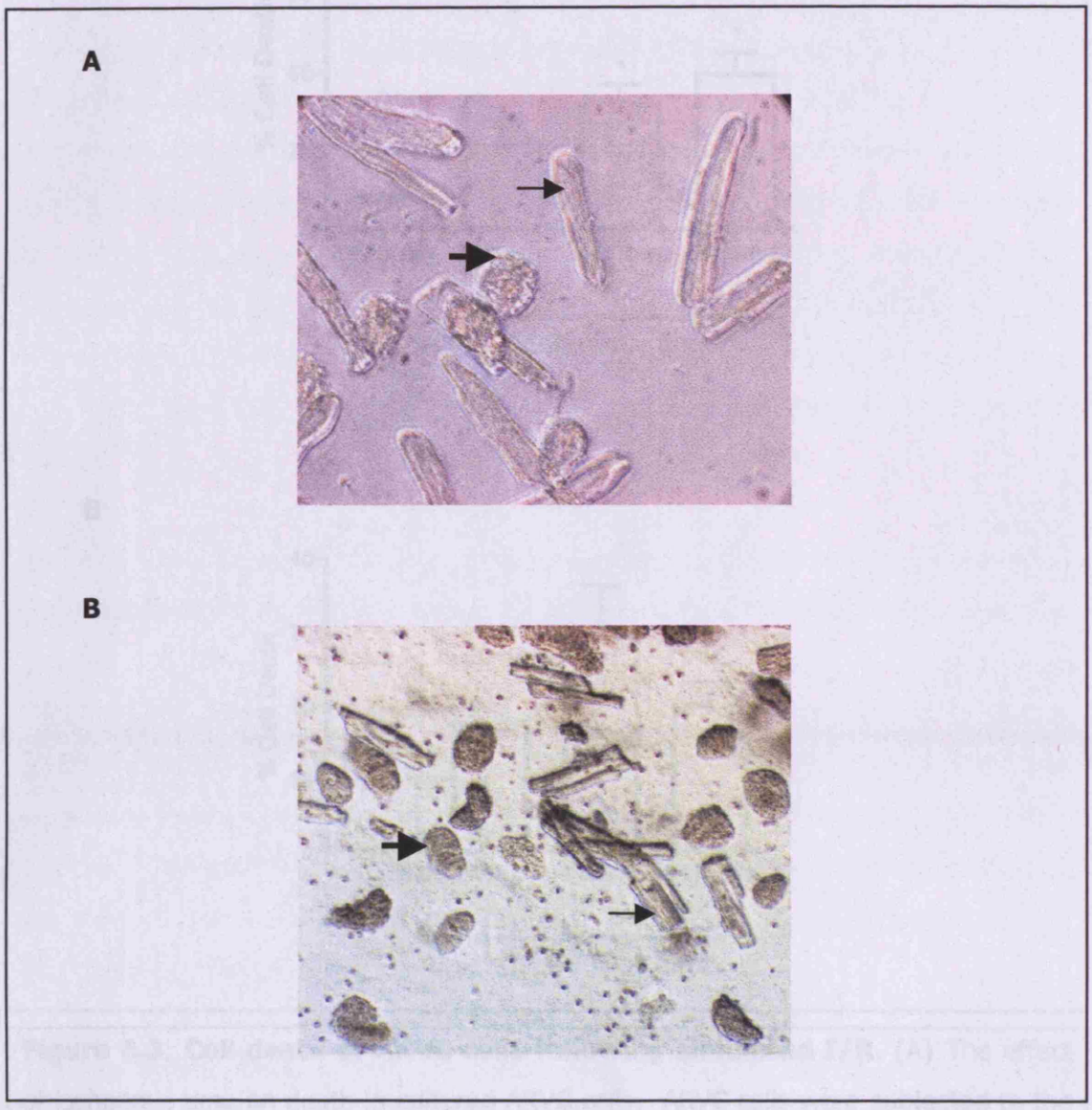

Figure 6.2 Morphological changes of ARVC cells following I/R. Images show ARVC cells viewed under light microscopy (magnification x25). (A) ARVC cells subjected to normoxic conditions. (B) ARVCs subjected to I/R (2h/4h). Thin arrows point towards rod shaped viable cells and thick arrows point towards round dead cells. Cultures of ARVC cells subjected to I/R show a higher number of rounded up cells compared to cultures of cells not subjected to I/R.

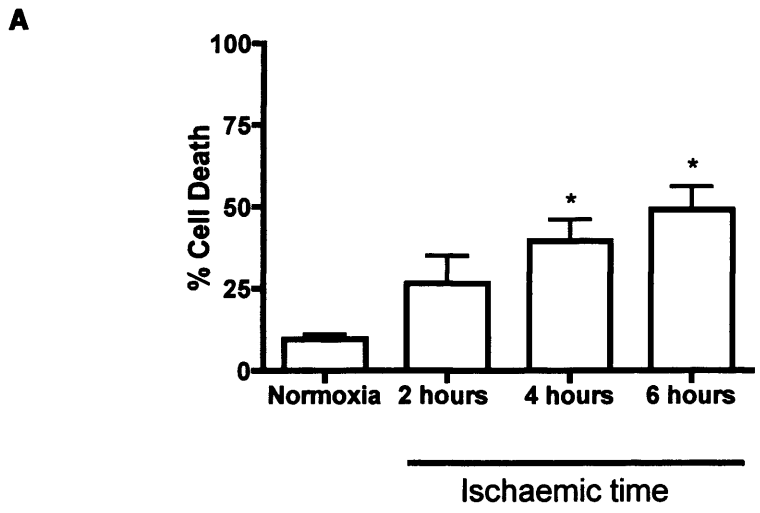

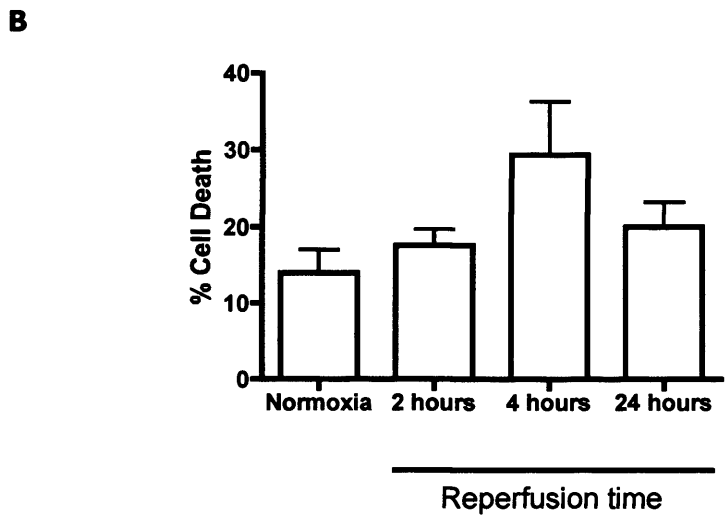

Figure 6.3. Cell death of ARVC ceils following simulated I/R. (A) The effect of ischaemic time on death in cultured ARVC cells. ARVC cells were subjected to the indicated time of ischaemia followed by two hours of reperfusion. (B) The effect of reperfusion time on death of cultured ARVC cells. ARVC cells were subjected to two hours of ischaemia followed by the indicated reperfusion time. Cells were fixed in 4% PFA. Cell morphology was used to determine cell viability. A total of 300 cells were counted per well and each time-point was performed in duplicate. Values represent the mean ± SEM of three experiments. Statistical analysis was performed by a student's *t* test. **P* <0.05 compared to normoxia.

6.4 Urocortin protects ARVC cells from simulated I/R-induced death and is associated with inhibition of the MPTP from opening

Pre-treating ARVC cells with Ucn for 1 h protected them from simulated I/R-induced death (Figure 6.4A). The percentage of dead cells following simulated I/R in cultures pre-treated with Ucn was 36.33% ± 6.06%, compared to 50.67% ± 4.91% in cultures treated with a vehicle control. In cultures subjected to normoxic conditions, the percentage of dead cells in Ucn treated cultures was 14.33% ± 5.24% compared to 19.67% ± 3.18% in cultures treated with a vehicle control. Thus, fewer dead cells were observed in the Ucn treated cultures that were subjected to simulated I/R and a small reduction in cell death in normoxic conditions was observed when treated with Ucn. Therefore, Ucn may confer some resistance to death of ARVC cells in culture.

The protective effect of Ucn was compared when ischaemia was simulated either immediately (1 h) or when delayed (16 h) after Ucn treatment. ARVC cells pre-treated with Ucn for 1 or 16 h were protected from simulated I/R-induced death (Figure 6.4B). The percentage of dead cells following simulated I/R in cultures pre-treated with Ucn for 16 h (46.23% ± 11.75%) or 1 hr (38.00% ± 6.17%) was significantly lower than in cultures pre-treated with a vehicle control (65.17% ± 11.06%). Statistical analysis was performed by a student's *t* test, demonstrating that I/R induced cell death in both 1 h and 16 h pre-treatments was significantly less compared to cultures not treated with Ucn ($P < 0.05$).

The protective effect of Ucn was more potent when ischaemia was simulated immediately (1 h) after Ucn treatment compared to when it was delayed (16h). The reduced cell death observed in ARVC cells pre-treated with Ucn for 1 h prior to simulated I/R was associated with reduced MPTP opening (Figure 6.5). The mitochondria of ARVC cells were preloaded with Tetramethyl rhodamine methyl ester (TMRM). Simulated I/R caused a decrease in the amount of TMRM retained by mitochondria, as determined by the mean fluorescent intensity (MFI). The reduction of MFI was attenuated in cells pre-treated with Ucn for 1 h. Statistical analysis was performed by a student's *t* test, demonstrating that the MFI was significantly higher, following simulated I/R, in Ucn pre-treated cells compared to cultures not treated with Ucn ($P < 0.05$). This suggests that Ucn treatment may inhibit MPTP opening.

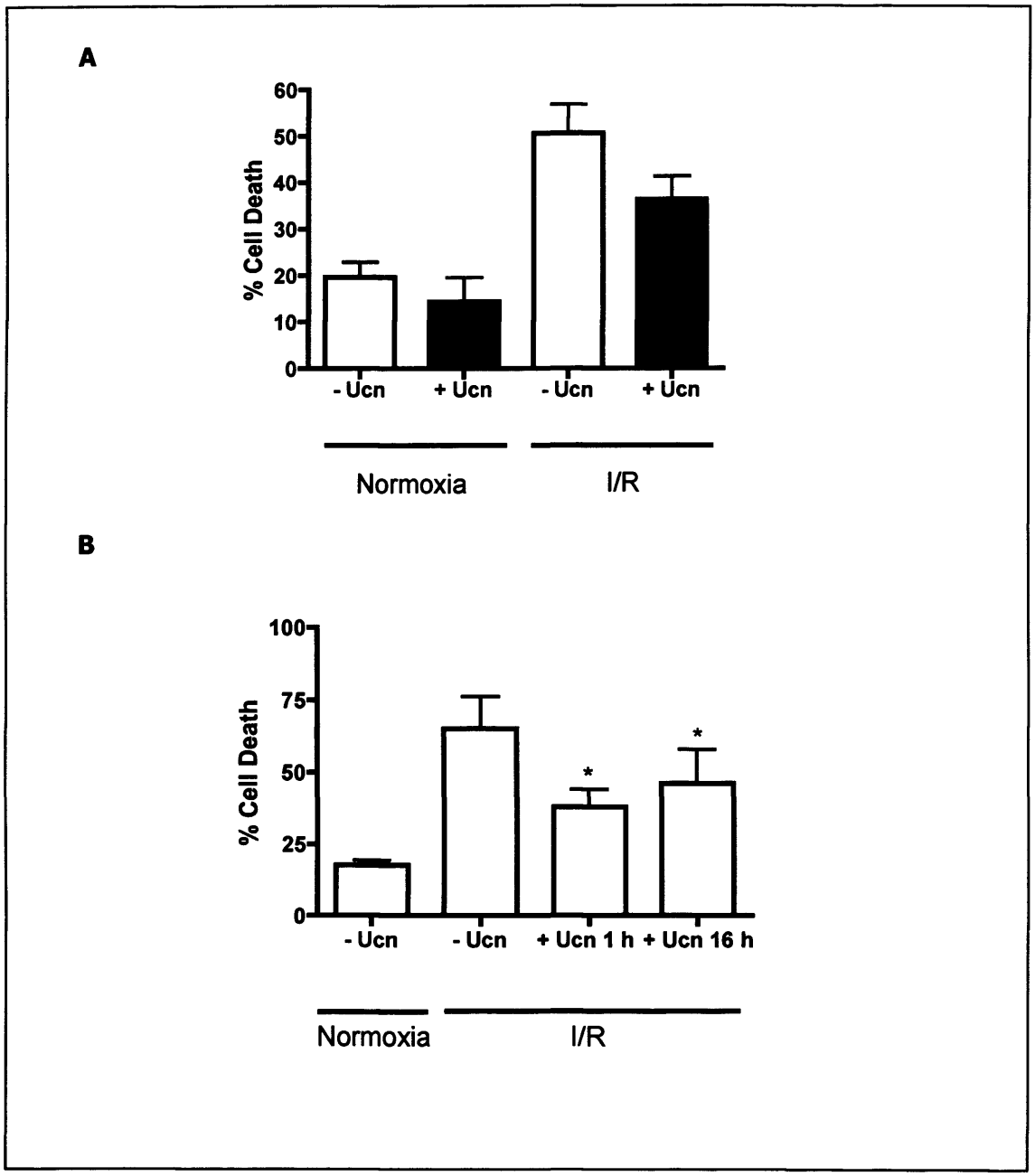

Figure 6.4 Urocortin protects ARVCs from simulated I/R. (A) Effect of Ucn pre-treatment for 1 h on survival of ARVCs subjected to simulated I/R (2h/4h). (B) Comparison of immediate and delayed ischaemia on the protective of 10 nM Ucn in ARVC cells. Cell viability was determined based on cell morphology, 300 cells per well were counted for each treatment group and each treatment group was performed in triplicate. The values for (A) represent the means ± SEM of three separate wells. The values for (B) represent the means ± SEM of three separate experiments. Statistical analysis was performed by a student's t-test. *P <0.05 compared to -Ucn (I/R).

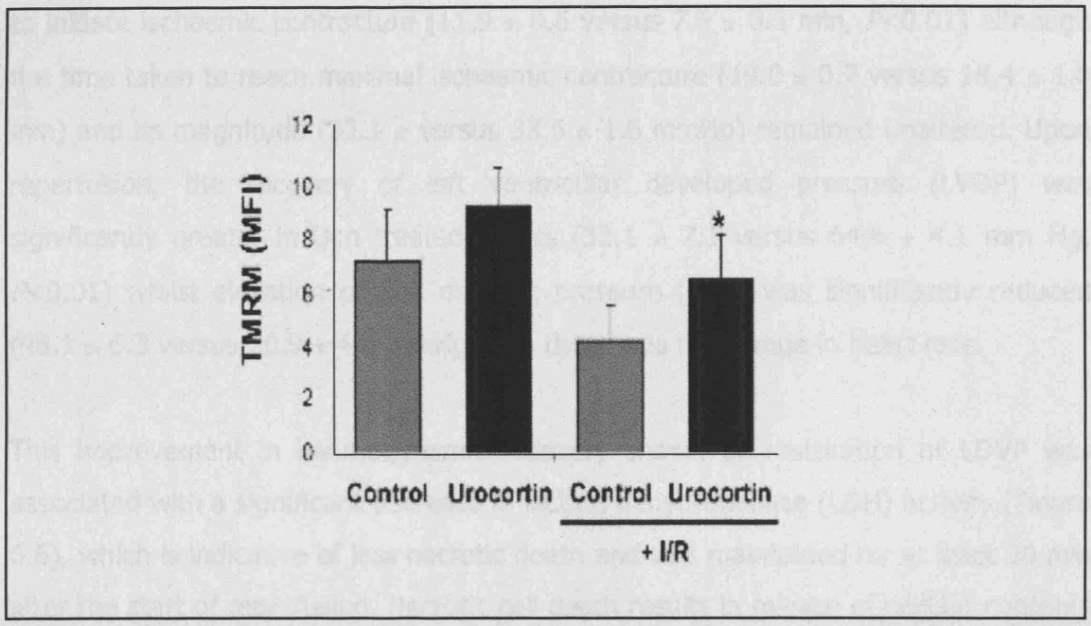

Figure 6.5 Urocortin treatment of ARVCS protects the MPTP from opening in response to simulated I/R. ARVC cells were pre-treated with 10 nM Ucn or a vehicle control for 1 h prior to simulated I/R. Cells were also stained with TMRM prior to simulated I/R. The mean fluorescent intensity is shown from 5000 separate events assayed by flow cytometry. Statistical analysis was performed by a student's *t* test. $*P < 0.05$ compared to relevant control.

6.5 Urocortin improves recovery and survival of adult rat hearts following I/R and decreases MPTP opening

Simulated I/R in adult rat hearts was performed by Langendorff perfusion and haemodynamic data are shown in Table 6.1. Ucn significantly reduced the time taken to initiate ischaemic contracture (11.9 ± 0.6 versus 7.6 ± 0.5 min, $P<0.01$) although the time taken to reach maximal ischaemic contracture (19.0 ± 0.7 versus 18.4 ± 1.0 min) and its magnitude (32.1 ± versus 33.6 ± 1.6 mmHg) remained unaltered. Upon reperfusion, the recovery of left ventricular developed pressure (LVDP) was significantly greater in Ucn treated hearts (32.1 ± 7.1 versus 64.6 ± 4.1 mm Hg, $P<0.01$) whilst elevation of end diastolic pressure (EDP) was significantly reduced (48.1 ± 6.3 versus 20.9 ± 4.0 mmHg) and there was no change in heart rate.

This improvement in haemodynamic recovery shown by restoration of LDVP was associated with a significant decrease in lactate dehydrogenase (LDH) activity (Figure 6.6), which is indicative of less necrotic death and was maintained for at least 30 min after the start of reperfusion. Necrotic cell death results in release of cellular contents and the quantity of LDH in the perfusate is an index of necrotic death. Thus, Ucn prevented necrotic cell death in the Langendorff perfused rat heart from simulated I/R.

In these experiments, in order to examine whether Ucn mediated haemodynamic recovery (Figure 6.7A) protects the heart by reducing the extent of opening of the MPTP, the mitochondrial entrapment of a radioactive marker, [^{3}H]2-deoxyglucose ([^{3}H]-DOG) was used. During perfusion, [^{3}H]-DOG is present in the buffer and mitochondrial uptake of [^{3}H]-DOG is an indication of MPTP opening. Ucn treatment significantly reduced the extent of [^{3}H]-DOG uptake in Langendorff perfused rat hearts subjected to I/R compared to hearts not treated with Ucn (Figure 6.7B). The yield of mitochondria in these experiments, determined as the total citrate synthase activity of the mitochondrial pellet, was not altered by Ucn treatment (Table 6.1). Therefore, Ucn mediated protection from I/R injury is associated with inhibition of MPTP opening in the intact adult rat heart.

	Pre-ischaemic		End-ischaemic		Reperfused	
	Control	Urocortin	Control	Urocortin	Control	Urocortin
LVDP (mmHg)	90.0 ± 1.8	91.6 ± 3.1	-	-	32.1 ± 7.1	64.6 ± 4.1**
EDP (mmHg)	3.4 ± 0.4	3.6 ± 0.5	-	-	48.1 ± 6.3	20.9 ± 4.0 **
Heart rate (bpm)	307.5 ± 7.6	296.3 ± 10.6	-	-	315.0 ± 9.9	315.0 ± 16.2
Aortic pressure (mmHg)	86.6 ± 3.8	78.8 ± 2.3	-	-	107.5 ± 6.6	86.4 ± 2.2*
Time to IC (min)	-	-	11.9 ± 0.6	7.6 ± 0.5**	-	-
Time to max IC (min)	-	-	19.0 ± 0.7	18.4 ± 1.0	-	-
Max IC (mmHg)	-	-	32.1 ± 1.6	33.6 ± 1.6	-	-
Citrate synthase recovery (Units/g wet weight heart)	-	-	-	-	1.87 ± 0.2	1.77 ± 0.2

Table 6.1 The effects of Urocortin on heart function. Langendorff perfused hearts were stabilized and subjected to 30 minutes of ischaemia followed by 30 minutes of reperfusion. Urocortin was present in perfusion buffer throughout experiment except for control hearts. Values shown are means ± SEM for 8 control and 8 Urocortin treated hearts. Statistical analysis was performed by Student's *t* test. $^{**}P < 0.05$; $^{*}P < 0.05$ compared to control.

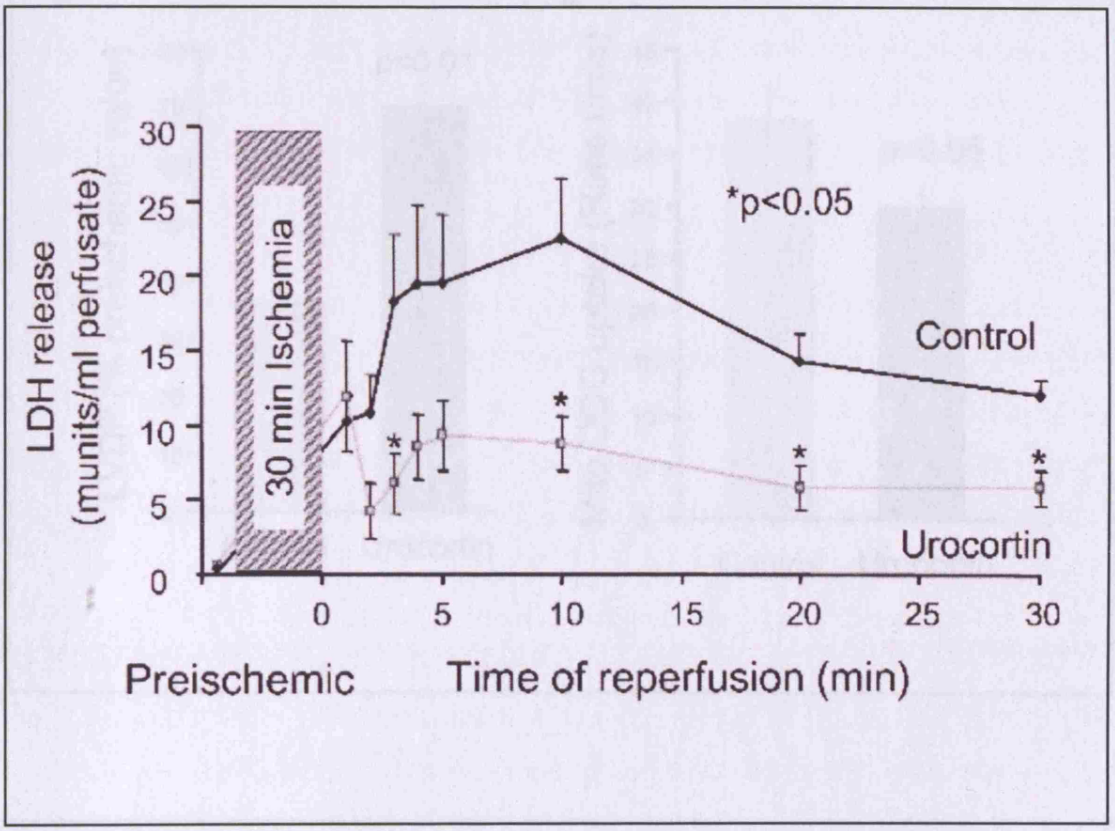

Figure 6.6 Ucn reduces lactate dehydrogenase (LDH) release following ischaemia. LDH measurements were made in samples of the coronary perfusate that were collected every minute for the first 5 minutes of reperfusion and every 5 minutes thereafter. The thick black line shows measurements for control hearts and the Ucn treated hearts the thin black line. LDH release is lower in Ucn treated hearts. Values shown are means ± SEM of 8 control and 8 Ucn-treated hearts. Statistical analysis was performed by a student's *t* test. **P* <0.05 compared to matched time point for control.

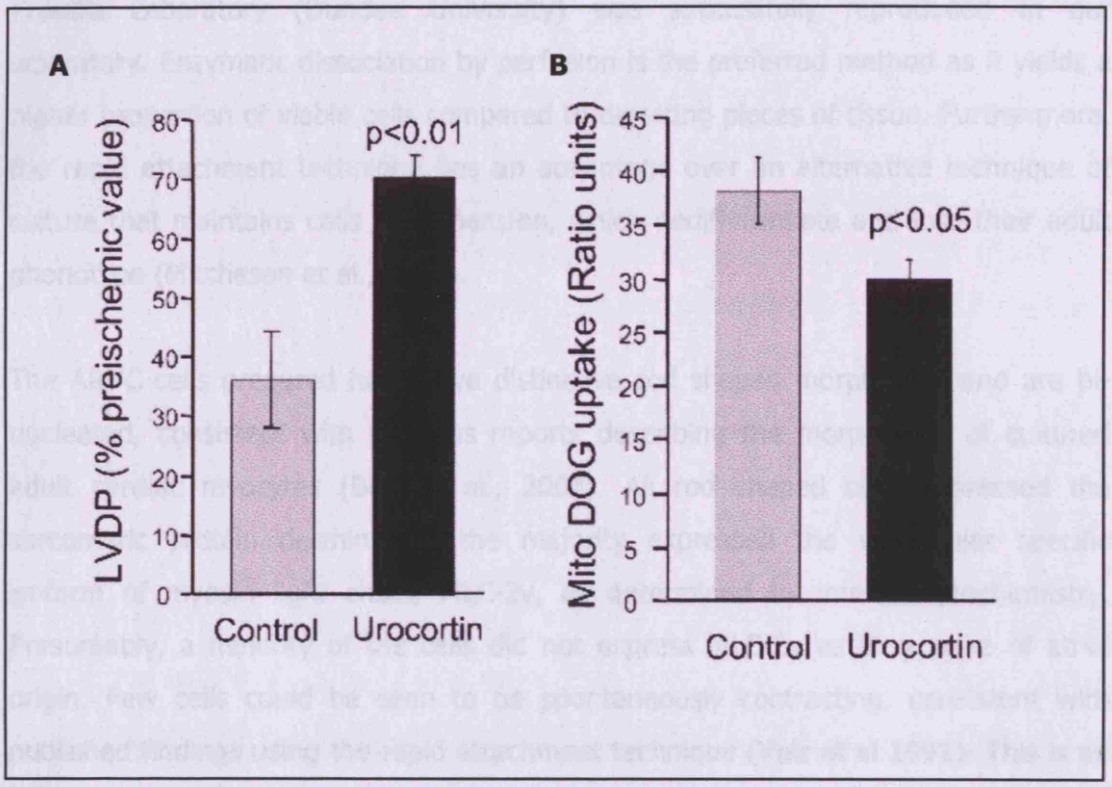

Figure 6.7 Urocortin mediated improvement of haemodynamic recovery of hearts following I/R is associated with decreased MPTP opening. Langendorff perfused rat hearts were preloaded with [^{3}H]-DOG during stabilisation of hearts and were subjected to 30 minutes of ischaemia followed by 30 minutes of reperfusion. (A) Recovery of LVDP at the end of reperfusion is shown as a percentage of the pre-ischaemic value. (B) Mitochondria were isolated from hearts and [^{3}H]-DOG entrapment was measured. Values shown are means ± SEM of 8 control and 8 Ucn-treated hearts.

6.6 Discussion

The data presented here show that a technique of enzymatic digestion and rapid attachment for the isolation and culture of ARVC cells observed in Professor Chris Proud's Laboratory (Dundee University) was successfully reproduced in our laboratory. Enzymatic dissociation by perfusion is the preferred method as it yields a higher proportion of viable cells compared to digesting pieces of tissue. Furthermore, the rapid attachment technique has an advantage over an alternative technique of culture that maintains cells in suspension, which dedifferentiate and lose their adult phenotype (Mitcheson et al., 1998).

The ARVC cells prepared here have distinctive rod shaped morphology and are bi-nucleated, consistent with previous reports describing the morphology of cultured adult cardiac myocytes (Bird et al., 2003). All rod shaped cells expressed the sarcomeric protein desmin and the majority expressed the ventricular specific isoform of myosin light chain, MLC-2v, as determined by immunocytochemistry. Presumably, a minority of the cells did not express MLC-2v as they were of atrial origin. Few cells could be seen to be spontaneously contracting, consistent with published findings using the rapid attachment technique (Volz et al 1991). This is an indication that the cultures were not only viable but also not stressed as spontaneous contraction of cultured ARVC cells is associated with apoptosis (Maruyama et al., 2001).

A proportion of ARVC cells were necrotic following the isolation procedure and this proportion varied between cultures. The quality of ARVC isolations depend in part on the source of collagenase used in the enzymatic dissociation of cardiac myocytes. Therefore, the quality of several batches of collagenase were tested, assayed by measuring the ratio of rod-shaped to rounded-up cells isolated, and the batch giving the highest proportion of rod shaped cells was used for the experiments in our study. Although there was variation in the amount of necrotic cells between preparations, the isolations reproducibly yielded high quantities of viable cells.

NRCM cells are commonly used as a model system for investigating I/R-injury. However, I/R-injury is predominantly an adult disease and there are phenotypical differences that exist between neonatal and adult cardiac myocytes, which include

the expression of different ion channel and sarcomeric protein isoforms (Mitcheson et al., 1998). Therefore, it is desirable to use adult cardiac myocytes as a model system for investigating I/R injury as opposed to using neonate derived cardiac myocytes. The common use NRCM cells to investigate I/R-injury is presumably because they are technically easier to prepare than adult cardiac myocytes cells.

Cell death of ARVC cells was induced by simulated I/R, as assayed by the percentages of viable rod shaped versus rounder up dead cells. The buffer used in annexin V staining induced spontaneous contraction and rapid death of ARVC cells. Annexin V is a calcium-dependent phospholipid-binding protein with high affinity for phosphatidylserine (Vermes et al., 1995). The annexin V buffer contains a relatively high concentration of calcium compared to the medium ARVC cells are cultured in. Thus, ARVC cells, which are intolerant of high concentrations of calcium, possibly were induced by the high calcium buffer to contract rapidly and die. Furthermore, no ARVC cells could be identified as positive for TUNEL staining following simulated I/R or control treatments. Although there are some publications describing the use of TUNEL staining in ARVC cells it is not common, which suggests that the current TUNEL protocols are not optimal in ARVC cells. Membrane blebbing, a characteristic feature of apoptosis, was observed in cardiac myocytes following I/R, however this was only observed in the first few minutes immediately after ischaemia Therefore, cell morphology was the single determinant used for measuring cell death of ARVC cells in subsequent experiments. Thus, the effects of Ucn on survival could not be attributed to inhibition of apoptosis but on cell death as a whole.

A time-course of simulated I/R was undertaken to test the model and select an optimal time for use in subsequent experiments. Simulated I/R induced cell death of ARVC cells in an ischaemic time dependent manner. This is consistent with a study by Kang and colleagues, although they found that reperfusion induced death was maximal after 24 hours whereas in our study cell death was near basal levels by this time point (Kang et al., 2000). Maximal cell death was observed after four hours of reperfusion, the reduced cell death observed after 24 hours could be explained by the fact that by this time many dead cells had detached from the culture dish.

Ucn protected ARVC cells from simulated I/R-injury, as has been demonstrated for NRCM cells and the isolated adult rat heart (Okosi et al., 1998, Brar et al., 2000, Schulman et al., 2002, Scarabelli et al., 2002). Ucn was able to protect cardiac

myocytes from simulated I/R-injury when given 1 or 16 hours prior to ischaemia, an effect also seen in NRCM cells (Brar et al., 2002a). Gordon and colleagues have also demonstrated that Ucn protects ARVC cells from simulated I/R when given 1 or 16 prior to ischaemia, as measured by LDH and creatine kinase release (Gordon et al., 2003). However, they used glucose deprivation and acidosis as their model of ischaemia whereas in this study the cells were hypoxic during simulated ischaemia.

The protection conferred by Ucn from simulated I/R may have dependent on p42/p44 MAPK and PI-3K/Akt signalling pathways, as has been shown in neonatal cardiac myocytes and the isolated heart (Brar et al., 2000, Brar et al., 2002b, Schulman et al., 2002). The mechanism by which Ucn protects may also have been through the pathways by which ischaemic preconditioning (IPC) protects. There are two phases of protection conferred by IPC, an immediate and a delayed phase (Murry et al., 1986, reviewed by Yellon and Baxter, 1995). It is possible that the protection conferred by Ucn when given 1 hour prior to simulated ischaemia may be through activation of PKCε, an event that ischaemic preconditioning and Ucn mediated protection are dependent upon (Liu et al., 1999, Lawrence et al., 2005). It has been demonstrated that the PKCε inhibitor chelerythrine inhibits Ucn mediated protection from simulated I/R injury in a model of ischaemia without hypoxia (Gordon et al., 2003).

Opening of the MPTP under stressful conditions such as reperfusion injury can lead to apoptotic and necrotic cell death (reviewed by Halestrap et al., 2004). In our study, the protection conferred on ARVC cells by Ucn treatment for 1 hour prior to simulated I/R was associated with inhibition of MPTP opening, a finding also observed in NRCM cells (Lawrence et al., 2004). Although there are advantages of using adult cardiac myocytes, they are not a substitute for *in vivo* or *ex vivo* investigation. A number of changes occur in myocytes when in culture, including reorganisation of cytoskeletal components and contractile proteins as they adapt from a three-dimensional to a two-dimensional environment (Decker et al., 1991). Therefore the effect of Ucn on MPTP opening in the isolated rat heart subjected to simulated I/R injury was also investigated.

Ucn protected rat hearts from simulated I/R-injury, determined by improved functional recovery and reduced LDH release following ischaemia when compared to untreated hearts, as has been previously demonstrated (Scarabelli et al., 2002). Ucn

mediated protection was associated with inhibition of MPTP opening, as determined by the [^{3}H]-DOG entrapment technique. This relationship between Ucn mediated cardioprotection and the MPTP is consistent to what was found here in ARVC cells and previously in NRCM cells (Lawrence et al., 2004).

It has recently been demonstrated in our laboratory that the inhibition of the MPTP from opening that is associated with Ucn mediated protection is not additive with that of Cyclosporin A (CsA), a compound known to prevent MPTP opening, which therefore suggests that Ucn treatment prevented MPTP opening (Townsend et al., 2007). The mechanism by which Ucn inhibits the MPTP from opening was found to be independent of PKCε translocation to the mitochondria, however inhibition of MPTP opening may occur indirectly through the ability of Ucn to reduce oxidative stress, as determined by reduced carbonylation levels in the mitochondria (Townsend et al., 2007).

The cardioprotective effect of Ucn from simulated I/R injury is well documented (reviewed by Lawrence and Latchman, 2006). Ucn has been shown to be protective when given at reperfusion, suggesting it could be of therapeutic benefit in a clinical setting (Brar et al., 2000, Scarabelli et al., 2002). In our study, the role of the MPTP in the cardioprotective effect of Ucn has been investigated when Ucn is given prior to an ischaemic insult followed by reperfusion. Cardioprotective agents given prior to an ischaemic insult may be useful to minimize the effects of ischaemic damage during cardiac surgery or, in the case of transplantation, during transportation of the heart. The potential use of Ucn as a therapeutic agent will be dependent on any undesirable effects that it may have, for example, it has been shown to induce hypertrophy (Railson et al., 2002). Nevertheless, understanding the mechanism of how endogenous molecules provide protection provides valuable knowledge, for example analogues of Ucn that provide protection without any harmful side effects could be developed.

In summary, the data presented here show that Ucn mediated protection from I/R-injury in the isolated perfused rat heart and death of primary ARVC cells is associated with inhibition of the MPTP from opening. In the perfused heart, the enhanced recovery of haemodynamic function mediated by Ucn treatment and the decreased necrotic damage determined by the release of LDH was accompanied by less MPTP opening, as determined by the [^{3}H]-DOG entrapment technique. Similarly, in cultured

ARVM cells, measurement of mitochondrial membrane potential showed Ucn pre-treatment reduced MPTP opening following simulated I/R in association with reduced cell death.

CHAPTER SEVEN

Overview and Ideas for Future Work

CHAPTER SEVEN

Overview and ideas for future work

Components of the IFNγ and CT-1 signalling pathways are endogenous regulators of cardiac I/R injury and pathological hypertrophy. Therefore, the investigation of these pathways improves our understanding of how the disease processes are regulated and how these pathways may be targeted therapeutically to improve the clinical outcome in patients with I/R-injury or hypertrophy. The work described in this thesis increases our understanding of the mechanisms involved in the regulation of cardiac I/R injury or hypertrophy by components of the IFNγ and CT-1 pathways.

The experimental approaches that have been used to test the hypotheses in this thesis have included the use of *in vitro*, *ex vivo* and *in vivo* systems. Furthermore, these different approaches have been used to test the same hypothesis. For example, the involvement of the MPTP in Ucn mediated protection from I/R injury was demonstrated in ARVC cells. The finding that inhibition of MPTP opening is associated with Ucn mediated protection in ARVC cells was corroborated in the Langendorff perfused rat heart. Having demonstrated similar results in two different systems there is more confidence in the data. An *in vivo* approach has been used to test a finding previously demonstrated *in vitro*. Over-expression of hsp56 has been shown to induce hypertrophy of NRCM cells and the hypertrophic effect of hsp56 over-expression in the mouse was tested here. However, over-expression of hsp56 in the mouse did not induce hypertrophy. Once again, this underlines the importance of testing hypotheses in more than one system, especially when using neonatal cells as a model system to investigate disease.

The transcription factor STAT1 is the key mediator of the IFNγ response and has been shown to be involved in I/R-injury. The role of the mitochondrial and death receptor apoptotic pathways in STAT1 mediated I/R-injury was investigated with the generation of transgenic mice that have impaired mitochondrial or death receptor signalling. The generation of transgene expressing mice using the Tet-inducible system was achieved in this thesis. However, due to the incorrect orientation of the C9s insert in the pBIG-C9s transgenic mice and the failure of any pBIG-FLIP lines to express the transgene, these mice could not be used to ask the question; what are the relative contributions of the mitochondrial and death receptor apoptotic pathways

in STAT1-mediated I/R-induced injury? The expression of β-galactosidase in αMHC-tTA/pBIG-C9s expressing lines was proof of principle that the binary Tet system did indeed work. Therefore, the generation of pBIG-C9s and pBIG-FLIP transgenic mice could once again be attempted in the knowledge that the Tet-inducible system used here was functional. Furthermore, although the αMHC-tTA/pBIG-C9s and αMHC-tTA/pBIG-FLIP transgenic lines produced here did not express the transgene of interest, a transgenic approach was successfully applied in the generation mice over-expressing hsp56.

There are some limitations with the Tet-inducible system that may warrant consideration of using an alternative conditional system. One limitation of the Tet-inducible system is the squelching caused by the viral VP16 activating domain of the tTA protein. Squelching is a phenomenon caused by protein over-expression and affects the equilibrium of other cellular proteins, resulting in pleiotropic effects (Lewandoski, 2001). A second limitation is the leakiness associated with the Tet-inducible systems. This refers to the residual expression observed in Tet-on systems in the absence of tetracyclines, or the lack of complete inhibition of expression in Tet-off systems in the presence of tetracyclines. The effect of tetracyclines on tTA-induced expression was not tested in the β-galactosidase expressing αMHC-tTA/pBIG-C9s transgenic mice generated here. Should pBIG-C9s and pBIG-FLIP be generated again, the potential of leakiness in the system could be tested on β-galactosidase expressing αMHC-pBIG-C9s transgenic mice beforehand. Improved Tet-based systems that have reduced leaky expression have been developed (Yan, 2007). Thus, the use of these improved systems could be considered if the αMHC-pBIG-C9s transgenic mice exhibit any leaky expression.

STAT1 is a transcriptional transactivator of many genes. However, it is now also recognised that STAT1 induces transcription as a transcriptional co-activator for other transcription factors such as p53. Both STAT1 and p53 are induced by forms of stress, including I/R, but are also involved in the constitutive expression of some genes. Here, a proteomic screen of cardiac protein samples revealed that IL-6 was highly abundant in samples from mice deficient in p53 but not in wild type mice, mice deficient in STAT1 or mice deficient in both STAT1 and p53. This suggests that STAT1 is involved in the regulation of IL-6, although here it was only identified in the context of p53 deficiency. The relative expression of IL-6 in MEF cells from p53 and p53/STAT1 knockout mice was different to that in heart samples. This demonstrates

that STAT1 mediated regulation of IL-6 occurs in a tissue specific manner. However, the heart is composed of several cell types including myocytes, endothelial cells and fibroblasts, and the abundant IL-6 observed might have been derived from any one or more cell type. Therefore, further investigation is required to understand how STAT1 regulates IL-6 in specific cell types.

Binding of p53 to the IL-6 promoter has previously been demonstrated to repress its expression (Santhanam et al., 1991, Angelo et al., 2002).Thus, highly abundant IL-6 in hearts from p53 deficient mice is a finding that agrees with these previous studies. IL-6 confers protection from I/R-injury and may be responsible for the observed attenuation of I/R injury in p53 deficient mice compared to wild type mice (Matsushita et al., 2005, Matsusaka et al., 2006) . The positive role of STAT1 in IL-6 regulation was apparent only in mice deficient in p53. This questions the physiological relevance of this finding, as p53 would not normally be absent in the heart. However, it does offer a possible explanation as to the mechanism involved when the p53 gene is disrupted or when the p53 protein expression or function is inhibited.

In the context of cardioprotection conferred by p53 inhibition, IL-6 may be a mediator of this effect. In this regard, it might be considered that p53 inhibition is a viable treatment option for limiting the damage caused by I/R-injury, as compounds that inhibit p53 have been reported. For example, Komorava and colleagues discovered a small molecule inhibitor, named Pifithrin-alpha, which inhibits p53 and found that it protected mice from genotoxic stress induced by anticancer treatment (Komarov et al., 1999). Interestingly, they also demonstrated that treatment of mice with Pifithrin-alpha did not promote the formation of tumours, a complication associated p53 inhibition. Moreover, inhibition of p53 by Pifithrin-alpha has been shown to reduce p53-mediated apoptosis and improve cardiac function following I/R-injury in rats (Liu et al., 2006).

The cytokine, CT-1, is produced by cardiac myocytes and has both cardioprotective and hypertrophic effects. The hypertrophic effect, but not the cardioprotective effect, of CT-1 has been shown to be dependent on hsp56, and over-expression of hsp56 in NRCM cells is sufficient for inducing hypertrophy (Jamshidi et al., 2004). To test this, transgenic mice over-expressing hsp56 were generated. Over-expression of hsp56 did not protect from I/R injury, which was consistent with findings in NRCM cells

(Brar et al., 1999). However, myocardial hypertrophy was not detected in any of the transgenic lines generated. Therefore, the hypertrophic effect of hsp56 is unclear. The hypertrophy observed in NRCM cells may be an artefact of protein over-expression rather than a specific effect of hsp56. Furthermore, the expression profile of hsp56 has not been determined in adult cells, either treated with CT-1 or any other hypertrophic stimuli. Studies on the relationship between CT-1 induced hypertrophy and hsp56 should be conducted in cultured adult cells. Thus, hsp56 over-expressing mice may also be used to help determine this relationship by testing if hsp56 over-expression increases sensitivity to CT-1 induced hypertrophy. Furthermore, the expression profile of hsp56 in cardiac myocytes following treatment with other hypertrophic stimuli and in biopsies from hypertrophied hearts should be examined.

The expression of CT-1 is induced by Ucn in cardiac myocytes (Janjua et al., 2002). Ucn is also produced by cardiac myocytes and has cardioprotective and hypertrophic effects. The cardioprotective effect of Ucn was previously shown to be associated with inhibition of the MPTP in NRCM cells. Here, this association was demonstrated in ARVC cells and in the Langendorff perfused heart. Thus, the significance of the MPTP in the mechanism of Ucn mediated protection is supported by this work. Pharmacological inhibition of the MPTP is considered to be an effective and promising strategy for reducing the damage caused by I/R-injury (Javadov and Karmazyn, 2007). Therefore, Ucn has the potential to be used therapeutically in the treatment of reperfusion injury. However, inhibiting the hypertrophic effect of Ucn needs to be addressed. The identification or synthesizing of molecules that have the cardioprotective effect of Ucn, but not its hypertrophic effect, may provide the necessary adjunct to reperfusion of the myocardium.

Although it has been shown here that the cardioprotection conferred by Ucn from I/R-injury is associated with the inhibition of the MPTP, the mechanism by which this occurs is unclear. Additional work since the completion of this thesis suggests that inhibition of MPTP opening may occur indirectly through the ability of Ucn to reduce oxidative stress, as determined by reduced carbonylation levels in the mitochondria (Townsend et al., 2007). It is interesting that Ucn is able to confer protection from I/R-injury when given to cells either 1 or 16 h before I/R. Thus, it should be considered that there might be distinct differences that exist in the mechanism of Ucn mediated protection when given just prior to I/R and when I/R is delayed. As

mitochondrial protection seems to be key to the function of Ucn, it would be interesting to investigate what effects Ucn is having on other aspects of mitochondrial function.

Mitochondria are involved in many processes including the generation of usable energy in the form of ATP in the process of oxidative phosphorylation, Fe-S and haem synthesis. Mitochondria also contain to their own genome, consisting of circular double stranded DNA of approximately 16.5 kb (Anderson et al., 1981). Mitochondrial DNA (mtDNA) is closely linked to oxidative phoshorylation, as it encodes 13 essential polypeptides of the respiratory chain. Each mitochondrion is host to several copies of mtDNA and the maintenance of their genome is necessary for proper respiratory chain function. Hence, respiratory chain dysfunction is a direct consequence of mutated mtDNA. Furthermore, ischaemic disease is also associated with reduced mtDNA copy number and respiratory chain enzyme activities. Several nuclear encoded proteins are responsible for mtDNA maintenance and mutations in genes encoding for those proteins result in respiratory chain dysfunction. Transcription factor A (TFAM) is a nuclear encoded protein involved in mtDNA transcription and replication. Reduced TFAM expression has also been observed in association with reduced mtDNA copy number in cardiac failure. Overexpression of TFAM in mice has been shown to ameliorate the reduced mtDNA copy number and respiratory chain enzyme activities in post-MI hearts (Ikeuchi et al., 2005). The ability to induce the expression of mtDNA maintenance proteins seems an attractive therapeutic approach. Therefore, it would be interesting to test if the protective effect of Ucn is dependent on modulating the expression of mtDNA maintenance proteins, as this would lend further support the idea that inducing expression of these proteins would be beneficial in cardiac disease.

It is also interesting that p53, in addition to functioning as a transcription factor in the nucleus and interacting with STAT1, has also been found to locate to the mitochondria (Achanta et al., 2005). Furthermore, Chen and colleagues demonstrated that p53 is involved in mitochondrial DNA maintenance by a base excision repair mechanism (Chen et al., 2006). This highlights the potential problem of targeted inhibition of proteins that have beneficial effects in addition to the undesirable functions that we would like to prevent.

This thesis describes the IFNγ and CT-1 signalling pathways as being distinct from one another. However, they both regulate I/R and hypertrophic signalling pathways. Furthermore, previous work has shown that there is crosstalk between the two pathways. For example, hsp56 induced hypertrophy in NRCM cells has been shown to be dependent on STAT1 (Jamshidi et al., 2004). The role of p53 in the mitochondria also raises the possibility that p53 may be involved in Ucn mediated protection from I/R-injury. Furthermore, CT-1 induced hypertrophy is mediated by STAT3, which also modulates IFNγ signalling. Therefore, it is of interest that the data in this thesis suggest STAT1 may be involved in IL-6 regulation; CT-1 is an IL-6 family cytokine and therefore is a candidate for STAT1 regulation. Thus, STAT1 may also regulate cardioprotective and hypertrophic effect pathways in addition to death-inducing ones. Jin and colleagues have shown that IFNγ has inhibitory effects on myocardial hypertrophy (Jin et al., 2005). However, enhancing STAT1 expression to inhibit hypertrophy might have complications given its role in promoting apoptosis of cardiac myocytes. Therefore, more work is required to investigate the role of STAT1 in hypertrophy.

The work presented in this thesis describes a novel regulation of IL-6 expression in the heart. This occurs in a manner dependent on p53 and STAT1 to repress or activate IL-6 expression respectively. As IL-6 has the ability to confer protection from I/R, this may explain the mechanism of protection in the absence of p53 and therefore, this pathway may be an attractive target for therapy. Furthermore, this work has shown that mitochondrial dysfunction is a contributing factor in I/R-injury and that the protection conferred by Ucn in the adult heart is associated with inhibition of MPTP opening. These findings therefore further demonstrate that preventing the MPTP from opening is an attractive treatment option for reducing the damage of I/R-injury.

It is therefore necessary to continue the work described here since it would help to further unravel the complexities of the IFNγ and CT-1 signalling pathways in cardiac I/R injury and hypertrophy. The long-term goal of this future research would be to design more effective therapies in the treatment of cardiac reperfusion injury and pathological hypertrophy.

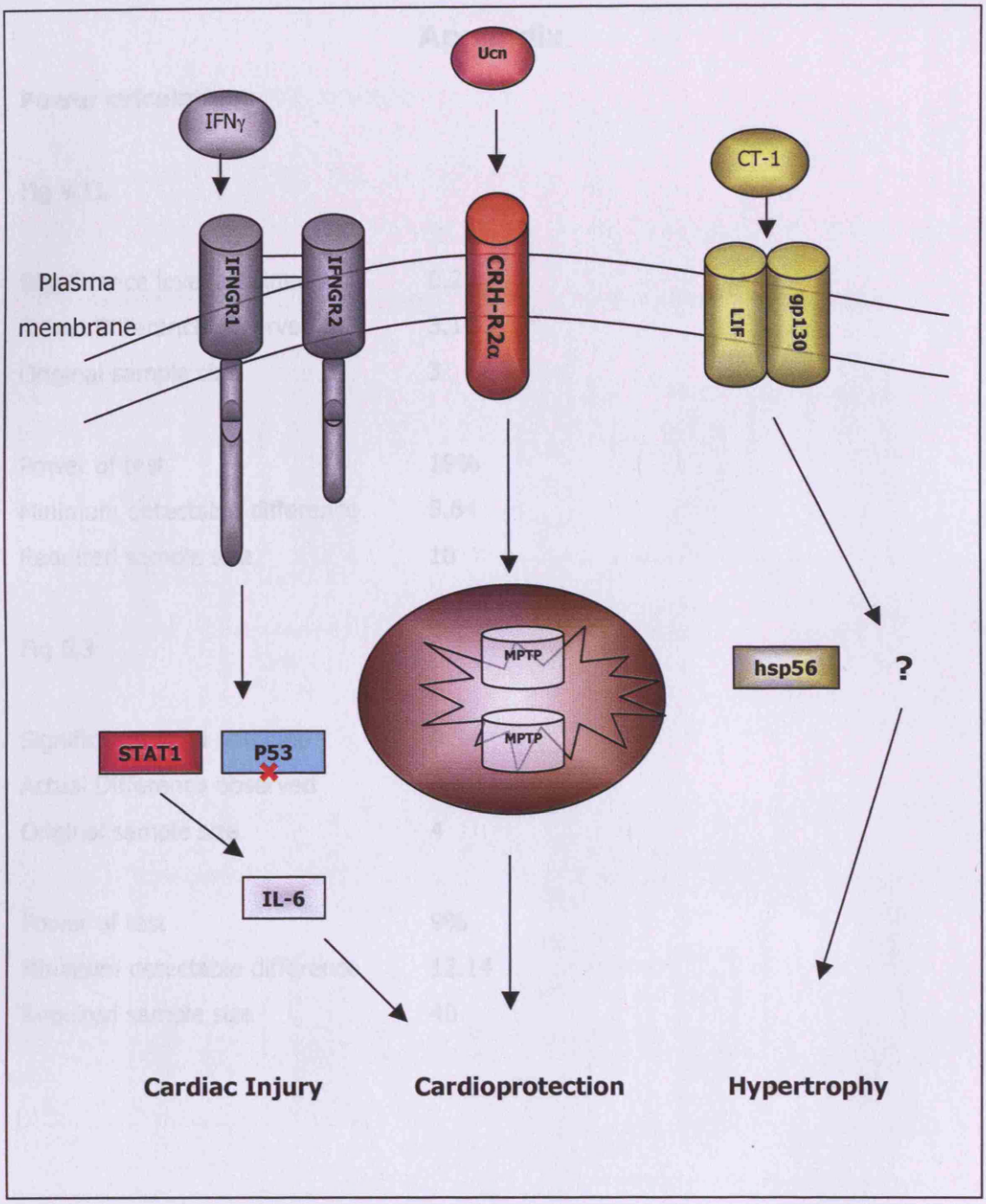

Figure 7.1 The regulation of cardiac injury, cardioprotection and hypertrophy by IFNγ, Ucn and CT-1 signalling pathways: the roles of STAT1/p53, MPTP and hsp56. Inhibition of p53 enables STAT1 mediated induction of IL-6, possibly conferring cardioprotection. Ucn mediated cardioprotection is associated with inhibited opening of the MPTP. The role of hsp56 in hypertrophy is unclear but over-expression of hsp56 is not sufficient to induce hypertrophy.

Appendix

Power calculations

Fig 4.11

Significance level obtained	0.27
Actual Difference observed	3.16
Original sample size	3
Power of test	19%
Minimum detectable difference	5.64
Required sample size	10

Fig 5.3

Significance level obtained	0.54
Actual Difference observed	3.82
Original sample size	4
Power of test	9%
Minimum detectable difference	12.14
Required sample size	40

Hsp56 transgenic heart weights

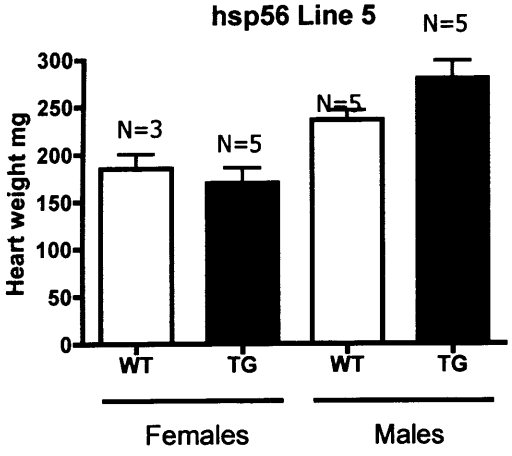

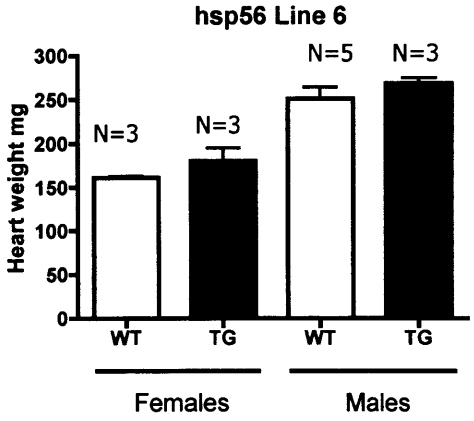

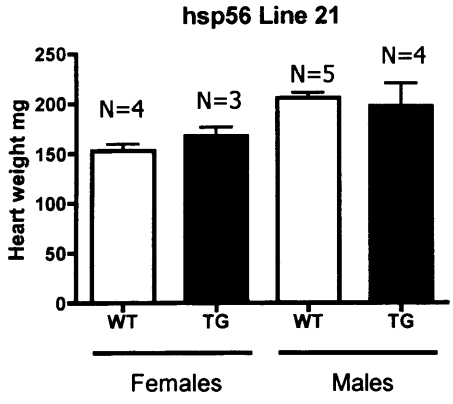

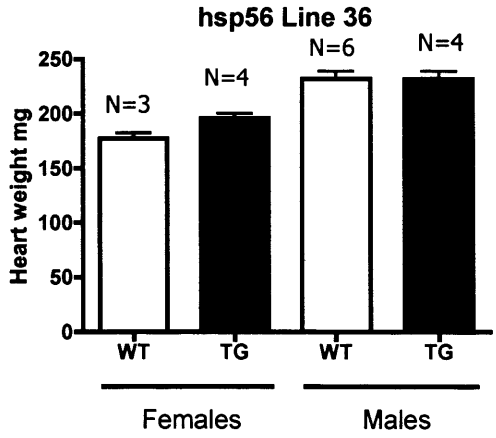

References

AARONSON, D. S. & HORVATH, C. M. (2002) A road map for those who don't know JAK-STAT. *Science,* 296, 1653-5.

ACHANTA, G., SASAKI, R., FENG, L., CAREW, J. S., LU, W., PELICANO, H., KEATING, M. J. & HUANG, P. (2005) Novel role of p53 in maintaining mitochondrial genetic stability through interaction with DNA Pol gamma. *Embo J,* 24, 3482-92.

ALLAN, L. A., MORRICE, N., BRADY, S., MAGEE, G., PATHAK, S. & CLARKE, P. R. (2003) Inhibition of caspase-9 through phosphorylation at Thr 125 by ERK MAPK. *Nat Cell Biol,* 5, 647-54.

ALNEMRI, E. S., LIVINGSTON, D. J., NICHOLSON, D. W., SALVESEN, G., THORNBERRY, N. A., WONG, W. W. & YUAN, J. (1996) Human ICE/CED-3 protease nomenclature. *Cell,* 87, 171.

AMEDEO MODESTI, P., ZECCHI-ORLANDINI, S., VANNI, S., POLIDORI, G., BERTOLOZZI, I., PERNA, A. M., FORMIGLI, L., CECIONI, I., COPPO, M., BODDI, M. & SERNERI, G. G. (2002) Release of preformed Ang II from myocytes mediates angiotensinogen and ET-1 gene overexpression in vivo via AT1 receptor. *J Mol Cell Cardiol,* 34, 1491-500.

ANK, N., WEST, H., BARTHOLDY, C., ERIKSSON, K., THOMSEN, A. R. & PALUDAN, S. R. (2006) Lambda interferon (IFN-lambda), a type III IFN, is induced by viruses and IFNs and displays potent antiviral activity against select virus infections in vivo. *J Virol,* 80, 4501-9.

ANDERSON, S., BANKIER, A. T., BARRELL, B. G., DE BRUIJN, M. H., COULSON, A. R., DROUIN, J., EPERON, I. C., NIERLICH, D. P., ROE, B. A., SANGER, F., SCHREIER, P. H., SMITH, A. J., STADEN, R. & YOUNG, I. G. (1981) Sequence and organization of the human mitochondrial genome. *Nature,* 290, 457-65.

ANGELO, L. S., TALPAZ, M. & KURZROCK, R. (2002) Autocrine interleukin-6 production in renal cell carcinoma: evidence for the involvement of p53. *Cancer Res,* 62, 932-40.

AOYAMA, T., TAKIMOTO, Y., PENNICA, D., INOUE, R., SHINODA, E., HATTORI, R., YUI, Y. & SASAYAMA, S. (2000) Augmented expression of cardiotrophin-1 and its receptor component, gp130, in both left and right ventricles after myocardial infarction in the rat. *J Mol Cell Cardiol,* 32, 1821-30.

BACH, E. A., AGUET, M. & SCHREIBER, R. D. (1997) The IFN gamma receptor: a paradigm for cytokine receptor signaling. *Annu Rev Immunol,* 15, 563-91.

BAINES, C. P., SONG, C. X., ZHENG, Y. T., WANG, G. W., ZHANG, J., WANG, O. L., GUO, Y., BOLLI, R., CARDWELL, E. M. & PING, P. (2003) Protein kinase Cepsilon interacts with and inhibits the permeability transition pore in cardiac mitochondria. *Circ Res,* 92, 873-80.

BAMBERGER, C. M., WALD, M., BAMBERGER, A. M., ERGUN, S., BEIL, F. U. & SCHULTE, H. M. (1998) Human lymphocytes produce urocortin, but not corticotropin-releasing hormone. *J Clin Endocrinol Metab,* 83, 708-11.

BARAN-MARSZAK, F., FEUILLARD, J., NAJJAR, I., LE CLORENNEC, C., BECHET, J. M., DUSANTER-FOURT, I., BORNKAMM, G. W., RAPHAEL, M. & FAGARD, R. (2004) Differential roles of STAT1alpha and STAT1beta in fludarabine-induced cell cycle arrest and apoptosis in human B cells. *Blood,* 104, 2475-83.

BARRY, S. P., TOWNSEND, P. A., LATCHMAN, D. S. & STEPHANOU, A. (2007) Role of the JAK-STAT pathway in myocardial injury. *Trends Mol Med,* 13, 82-9.

BEATO, M., CHAVEZ, S. & TRUSS, M. (1996) Transcriptional regulation by steroid hormones. *Steroids,* 61, 240-51.

BECKER, L. B. (2004) New concepts in reactive oxygen species and cardiovascular reperfusion physiology. *Cardiovasc Res,* 61, 461-70.

BERGERON, L., PEREZ, G. I., MACDONALD, G., SHI, L., SUN, Y., JURISICOVA, A., VARMUZA, S., LATHAM, K. E., FLAWS, J. A., SALTER, J. C., HARA, H., MOSKOWITZ, M. A., LI, E., GREENBERG, A., TILLY, J. L. & YUAN, J. (1998) Defects in regulation of apoptosis in caspase-2-deficient mice. *Genes Dev,* 12, 1304-14.

BERN, H. A. & LEDERIS, K. (1969) A reference preparation for the study of active substances in the caudal neurosecretory system of teleosts. *J Endocrinol,* 45, Suppl:xi-xii.

BIALIK, S., GEENEN, D. L., SASSON, I. E., CHENG, R., HORNER, J. W., EVANS, S. M., LORD, E. M., KOCH, C. J. & KITSIS, R. N. (1997) Myocyte apoptosis during acute myocardial infarction in the mouse localizes to hypoxic regions but occurs independently of p53. *J Clin Invest,* 100, 1363-72.

BIANCO, R. A., KEEN, H. L., LAVOIE, J. L. & SIGMUND, C. D. (2003) Untraditional methods for targeting the kidney in transgenic mice. *Am J Physiol Renal Physiol,* 285, F1027-33.

BIRD, S. D., DOEVENDANS, P. A., VAN ROOIJEN, M. A., BRUTEL DE LA RIVIERE, A., HASSINK, R. J., PASSIER, R. & MUMMERY, C. L. (2003) The human adult cardiomyocyte phenotype. *Cardiovasc Res,* 58, 423-34.

BOEHM, U., KLAMP, T., GROOT, M. & HOWARD, J. C. (1997) Cellular responses to interferon-gamma. *Annu Rev Immunol,* 15, 749-95.

BOLDIN, M. P., GONCHAROV, T. M., GOLTSEV, Y. V. & WALLACH, D. (1996) Involvement of MACH, a novel MORT1/FADD-interacting protease, in Fas/APO-1- and TNF receptor-induced cell death. *Cell,* 85, 803-15.

BOLLI, R., JEROUDI, M. O., PATEL, B. S., ARUOMA, O. I., HALLIWELL, B., LAI, E. K. & MCCAY, P. B. (1989a) Marked reduction of free radical generation and contractile dysfunction by antioxidant therapy begun at the time of reperfusion. Evidence that myocardial "stunning" is a manifestation of reperfusion injury. *Circ Res,* 65, 607-22.

BOLLI, R., JEROUDI, M. O., PATEL, B. S., DUBOSE, C. M., LAI, E. K., ROBERTS, R. & MCCAY, P. B. (1989b) Direct evidence that oxygen-derived free radicals contribute to postischemic myocardial dysfunction in the intact dog. *Proc Natl Acad Sci U S A,* 86, 4695-9.

BOWMAN, J. C., STEINBERG, S. F., JIANG, T., GEENEN, D. L., FISHMAN, G. I. & BUTTRICK, P. M. (1997) Expression of protein kinase C beta in the heart causes hypertrophy in adult mice and sudden death in neonates. *J Clin Invest,* 100, 2189-95.

BRADBURY, D. A., SIMMONS, T. D., SLATER, K. J. & CROUCH, S. P. (2000) Measurement of the ADP:ATP ratio in human leukaemic cell lines can be used as an indicator of cell viability, necrosis and apoptosis. *J Immunol Methods,* 240, 79-92.

BRAR, B. K., JONASSEN, A. K., EGORINA, E. M., CHEN, A., NEGRO, A., PERRIN, M. H., MJOS, O. D., LATCHMAN, D. S., LEE, K. F. & VALE, W. (2004) Urocortin-II and urocortin-III are cardioprotective against ischemia reperfusion injury: an essential endogenous cardioprotective role for corticotropin releasing factor receptor type 2 in the murine heart. *Endocrinology,* 145, 24-35; discussion 21-3.

BRAR, B. K., JONASSEN, A. K., STEPHANOU, A., SANTILLI, G., RAILSON, J., KNIGHT, R. A., YELLON, D. M. & LATCHMAN, D. S. (2000) Urocortin protects against ischemic and reperfusion injury via a MAPK-dependent pathway. *J Biol Chem,* 275, 8508-14.

BRAR, B. K., RAILSON, J., STEPHANOU, A., KNIGHT, R. A. & LATCHMAN, D. S. (2002a) Urocortin increases the expression of heat shock protein 90 in rat cardiac myocytes in a MEK1/2-dependent manner. *J Endocrinol,* 172, 283-93.

BRAR, B. K., STEPHANOU, A., KNIGHT, R. & LATCHMAN, D. S. (2002b) Activation of protein kinase B/Akt by urocortin is essential for its ability to protect cardiac cells against hypoxia/reoxygenation-induced cell death. *J Mol Cell Cardiol,* 34, 483-92.

BRAR, B. K., STEPHANOU, A., LIAO, Z., O'LEARY, R. M., PENNICA, D., YELLON, D. M. & LATCHMAN, D. S. (2001a) Cardiotrophin-1 can protect cardiac myocytes from injury when added both prior to simulated ischaemia and at reoxygenation. *Cardiovasc Res,* 51, 265-74.

BRAR, B. K., STEPHANOU, A., OKOSI, A., LAWRENCE, K. M., KNIGHT, R. A., MARBER, M. S. & LATCHMAN, D. S. (1999) CRH-like peptides protect cardiac myocytes from lethal ischaemic injury. *Mol Cell Endocrinol,* 158, 55-63.

BRAR, B. K., STEPHANOU, A., PENNICA, D. & LATCHMAN, D. S. (2001b) CT-1 mediated cardioprotection against ischaemic re-oxygenation injury is mediated by PI3 kinase, Akt and MEK1/2 pathways. *Cytokine,* 16, 93-6.

BRAR, B. K., STEPHANOU, A., WAGSTAFF, M. J., COFFIN, R. S., MARBER, M. S., ENGELMANN, G. & LATCHMAN, D. S. (1999) Heat shock proteins delivered with a virus vector can protect cardiac cells against apoptosis as well as against thermal or hypoxic stress. *J Mol Cell Cardiol,* 31, 135-46.

BRILLA, C. G., JANICKI, J. S. & WEBER, K. T. (1991) Impaired diastolic function and coronary reserve in genetic hypertension. Role of interstitial fibrosis and medial thickening of intramyocardial coronary arteries. *Circ Res,* 69, 107-15.

BRINSTER, R. L., CHEN, H. Y., TRUMBAUER, M. E., YAGLE, M. K. & PALMITER, R. D. (1985) Factors affecting the efficiency of introducing foreign DNA into mice by microinjecting eggs. *Proc Natl Acad Sci U S A,* 82, 4438-42.

BUENO, O. F., DE WINDT, L. J., LIM, H. W., TYMITZ, K. M., WITT, S. A., KIMBALL, T. R. & MOLKENTIN, J. D. (2001) The dual-specificity phosphatase MKP-1 limits the cardiac hypertrophic response in vitro and in vivo. *Circ Res,* 88, 88-96.

BUJA, L. M. & ENTMAN, M. L. (1998) Modes of myocardial cell injury and cell death in ischemic heart disease. *Circulation,* 98, 1355-7.

CANDE, C., COHEN, I., DAUGAS, E., RAVAGNAN, L., LAROCHETTE, N., ZAMZAMI, N. & KROEMER, G. (2002) Apoptosis-inducing factor (AIF): a novel caspase-independent death effector released from mitochondria. *Biochimie,* 84, 215-22.

CHALMERS, D. T., LOVENBERG, T. W. & DE SOUZA, E. B. (1995) Localization of novel corticotropin-releasing factor receptor (CRF2) mRNA expression to specific subcortical nuclei in rat brain: comparison with CRF1 receptor mRNA expression. *J Neurosci,* 15, 6340-50.

CHAMBRAUD, B., ROUVIERE-FOURMY, N., RADANYI, C., HSIAO, K., PEATTIE, D. A., LIVINGSTON, D. J. & BAULIEU, E. E. (1993) Overexpression of p59-HBI (FKBP59), full length and domains, and characterization of PPIase activity. *Biochem Biophys Res Commun,* 196, 160-6.

CHANALARIS, A., LAWRENCE, K. M., STEPHANOU, A., KNIGHT, R. D., HSU, S. Y., HSUEH, A. J. & LATCHMAN, D. S. (2003) Protective effects of the urocortin homologues stresscopin (SCP) and stresscopin-related peptide (SRP) against hypoxia/reoxygenation injury in rat neonatal cardiomyocytes. *J Mol Cell Cardiol,* 35, 1295-305.

CHATTERJEE-KISHORE, M., WRIGHT, K. L., TING, J. P. & STARK, G. R. (2000) How Stat1 mediates constitutive gene expression: a complex of unphosphorylated Stat1 and IRF1 supports transcription of the LMP2 gene. *Embo J,* 19, 4111-22.

CHEN, R., LEWIS, K. A., PERRIN, M. H. & VALE, W. W. (1993) Expression cloning of a human corticotropin-releasing-factor receptor. *Proc Natl Acad Sci U S A,* 90, 8967-71.

CHEN, Z., CHUA, C. C., HO, Y. S., HAMDY, R. C. & CHUA, B. H. (2001) Overexpression of Bcl-2 attenuates apoptosis and protects against myocardial I/R injury in transgenic mice. *Am J Physiol Heart Circ Physiol,* 280, H2313-20.

CHEUNG-FLYNN, J., PRAPAPANICH, V., COX, M. B., RIGGS, D. L., SUAREZ-QUIAN, C. & SMITH, D. F. (2005) Physiological role for the cochaperone FKBP52 in androgen receptor signaling. *Mol Endocrinol,* 19, 1654-66.

CHIN, Y. E., KITAGAWA, M., KUIDA, K., FLAVELL, R. A. & FU, X. Y. (1997) Activation of the STAT signaling pathway can cause expression of caspase 1 and apoptosis. *Mol Cell Biol,* 17, 5328-37.

CLARKE, S. J., MCSTAY, G. P. & HALESTRAP, A. P. (2002) Sanglifehrin A acts as a potent inhibitor of the mitochondrial permeability transition and reperfusion injury of the heart by binding to cyclophilin-D at a different site from cyclosporin A. *J Biol Chem,* 277, 34793-9.

CONDORELLI, G., RONCARATI, R., ROSS, J., JR., PISANI, A., STASSI, G., TODARO, M., TROCHA, S., DRUSCO, A., GU, Y., RUSSO, M. A., FRATI, G., JONES, S. P., LEFER, D. J., NAPOLI, C. & CROCE, C. M. (2001) Heart-targeted overexpression of caspase3 in mice increases infarct size and depresses cardiac function. *Proc Natl Acad Sci U S A,* 98, 9977-82.

COSTE, S. C., KESTERSON, R. A., HELDWEIN, K. A., STEVENS, S. L., HEARD, A. D., HOLLIS, J. H., MURRAY, S. E., HILL, J. K., PANTELY, G. A., HOHIMER, A. R., HATTON, D. C., PHILLIPS, T. J., FINN, D. A., LOW, M. J., RITTENBERG, M. B., STENZEL, P. & STENZEL-POORE, M. P. (2000) Abnormal adaptations to stress and impaired cardiovascular function in mice lacking corticotropin-releasing hormone receptor-2. *Nat Genet,* 24, 403-9.

COSTE, S. C., QUINTOS, R. F. & STENZEL-POORE, M. P. (2002) Corticotropin-releasing hormone-related peptides and receptors: emergent regulators of cardiovascular adaptations to stress. *Trends Cardiovasc Med,* 12, 176-82.

CREGAN, S. P., FORTIN, A., MACLAURIN, J. G., CALLAGHAN, S. M., CECCONI, F., YU, S. W., DAWSON, T. M., DAWSON, V. L., PARK, D. S., KROEMER, G. & SLACK, R. S. (2002) Apoptosis-inducing factor is involved in the regulation of caspase-independent neuronal cell death. *J Cell Biol,* 158, 507-17.

CROMPTON, M. (1999) The mitochondrial permeability transition pore and its role in cell death. *Biochem J,* 341 (Pt 2), 233-49.

CROSS, H. R., CLARKE, K., OPIE, L. H. & RADDA, G. K. (1995) Is lactate-induced myocardial ischaemic injury mediated by decreased pH or increased intracellular lactate? *J Mol Cell Cardiol,* 27, 1369-81.

CROW, M. T. (2006) Revisiting p53 and its effectors in ischemic heart injury. *Cardiovasc Res,* 70, 401-3.

CUI, Y., GIBLIN, J. P., CLAPP, L. H. & TINKER, A. (2001) A mechanism for ATP-sensitive potassium channel diversity: Functional coassembly of two pore-forming subunits. *Proc Natl Acad Sci U S A,* 98, 729-34.

CUMMING, D. V., HEADS, R. J., WATSON, A., LATCHMAN, D. S. & YELLON, D. M. (1996) Differential protection of primary rat cardiocytes by transfection of specific heat stress proteins. *J Mol Cell Cardiol,* 28, 2343-9.

CZAR, M. J., OWENS-GRILLO, J. K., YEM, A. W., LEACH, K. L., DEIBEL, M. R., JR., WELSH, M. J. & PRATT, W. B. (1994) The hsp56 immunophilin component of untransformed steroid receptor complexes is localized both to microtubules in the cytoplasm and to the same nonrandom regions within the nucleus as the steroid receptor. *Mol Endocrinol,* 8, 1731-41.

DALTON, D. K., PITTS-MEEK, S., KESHAV, S., FIGARI, I. S., BRADLEY, A. & STEWART, T. A. (1993) Multiple defects of immune cell function in mice with disrupted interferon-gamma genes. *Science,* 259, 1739-42.

DARNELL, J. E., JR., KERR, I. M. & STARK, G. R. (1994) Jak-STAT pathways and transcriptional activation in response to IFNs and other extracellular signaling proteins. *Science,* 264, 1415-21.

DAVIDSON, S. M. & DUCHEN, M. R. (2007) Endothelial mitochondria: contributing to vascular function and disease. *Circ Res,* 100, 1128-41.

DAVIDSON, S. M., TOWNSEND, P. A., CARROLL, C., YUREK-GEORGE, A., BALASUBRAMANYAM, K., KUNDU, T. K., STEPHANOU, A., PACKHAM, G., GANESAN, A. & LATCHMAN, D. S. (2005) The transcriptional coactivator p300 plays a critical role in the hypertrophic and protective pathways induced by phenylephrine in cardiac cells but is specific to the hypertrophic effect of urocortin. *Chembiochem,* 6, 162-70.

DAVIES, T. H. & SANCHEZ, E. R. (2005) Fkbp52. *Int J Biochem Cell Biol,* 37, 42-7.

DE CHIARA, G., MARCOCCI, M. E., TORCIA, M., LUCIBELLO, M., ROSINI, P., BONINI, P., HIGASHIMOTO, Y., DAMONTE, G., ARMIROTTI, A., AMODEI, S., PALAMARA, A. T., RUSSO, T., GARACI, E. & COZZOLINO, F. (2006) Bcl-2 Phosphorylation by p38 MAPK: identification of target sites and biologic consequences. *J Biol Chem,* 281, 21353-61.

DE SOUZA, E. B. (1995) Corticotropin-releasing factor receptors: physiology, pharmacology, biochemistry and role in central nervous system and immune disorders. *Psychoneuroendocrinology,* 20, 789-819.

DECKER, M. L., BEHNKE-BARCLAY, M., COOK, M. G., LA PRES, J. J., CLARK, W. A. & DECKER, R. S. (1991) Cell shape and organization of the contractile apparatus in cultured adult cardiac myocytes. *J Mol Cell Cardiol,* 23, 817-32.

DECKER, T. & KOVARIK, P. (2000) Serine phosphorylation of STATs. *Oncogene,* 19, 2628-37.

DEPRE, C., SHIPLEY, G. L., CHEN, W., HAN, Q., DOENST, T., MOORE, M. L., STEPKOWSKI, S., DAVIES, P. J. & TAEGTMEYER, H. (1998) Unloaded heart in vivo replicates fetal gene expression of cardiac hypertrophy. *Nat Med,* 4, 1269-75.

DEVRIES, T. A., KALKOFEN, R. L., MATASSA, A. A. & REYLAND, M. E. (2004) Protein kinase Cdelta regulates apoptosis via activation of STAT1. *J Biol Chem,* 279, 45603-12.

DONALDSON, C. J., SUTTON, S. W., PERRIN, M. H., CORRIGAN, A. Z., LEWIS, K. A., RIVIER, J. E., VAUGHAN, J. M. & VALE, W. W. (1996) Cloning and characterization of human urocortin. *Endocrinology,* 137, 3896.

DUPUIS, S., DARGEMONT, C., FIESCHI, C., THOMASSIN, N., ROSENZWEIG, S., HARRIS, J., HOLLAND, S. M., SCHREIBER, R. D. & CASANOVA, J. L. (2001) Impairment of mycobacterial but not viral immunity by a germline human STAT1 mutation. *Science,* 293, 300-3.

DURBIN, J. E., HACKENMILLER, R., SIMON, M. C. & LEVY, D. E. (1996) Targeted disruption of the mouse Stat1 gene results in compromised innate immunity to viral disease. *Cell,* 84, 443-50.

EDDLESTONE, G. T. (1995) ATP-sensitive K channel modulation by products of PLA2 action in the insulin-secreting HIT cell line. *Am J Physiol,* 268, C181-90.

EEFTING, F., RENSING, B., WIGMAN, J., PANNEKOEK, W. J., LIU, W. M., CRAMER, M. J., LIPS, D. J. & DOEVENDANS, P. A. (2004) Role of apoptosis in reperfusion injury. *Cardiovasc Res,* 61, 414-26.

EFTHYMIOU, C. A., MOCANU, M. M., DE BELLEROCHE, J., WELLS, D. J., LATCHMANN, D. S. & YELLON, D. M. (2004) Heat shock protein 27 protects

ENARI, M., SAKAHIRA, H., YOKOYAMA, H., OKAWA, K., IWAMATSU, A. & NAGATA, S. (1998) A caspase-activated DNase that degrades DNA during apoptosis, and its inhibitor ICAD. *Nature,* 391, 43-50.

ERSPAMER, V., ERSPAMER, G. F., IMPROTA, G., NEGRI, L. & DE CASTIGLIONE, R. (1980) Sauvagine, a new polypeptide from Phyllomedusa sauvagei skin. Occurrence in various Phyllomedusa species and pharmacological actions on rat blood pressure and diuresis. *Naunyn Schmiedebergs Arch Pharmacol,* 312, 265-70.

ESPOSITO, L. A., MELOV, S., PANOV, A., COTTRELL, B. A. & WALLACE, D. C. (1999) Mitochondrial disease in mouse results in increased oxidative stress. *Proc Natl Acad Sci U S A,* 96, 4820-5.

FIORDALISO, F., LERI, A., CESSELLI, D., LIMANA, F., SAFAI, B., NADAL-GINARD, B., ANVERSA, P. & KAJSTURA, J. (2001) Hyperglycemia activates p53 and p53-regulated genes leading to myocyte cell death. *Diabetes,* 50, 2363-75.

FISHER, L. A., JESSEN, G. & BROWN, M. R. (1983) Corticotropin-releasing factor (CRF): mechanism to elevate mean arterial pressure and heart rate. *Regul Pept,* 5, 153-61.

FISHMAN, G. I., KAPLAN, M. L. & BUTTRICK, P. M. (1994) Tetracycline-regulated cardiac gene expression in vivo. *J Clin Invest,* 93, 1864-8.

FLISS, H. & GATTINGER, D. (1996) Apoptosis in ischemic and reperfused rat myocardium. *Circ Res,* 79, 949-56.

GAVRIELI, Y., SHERMAN, Y. & BEN-SASSON, S. A. (1992) Identification of programmed cell death in situ via specific labeling of nuclear DNA fragmentation. *J Cell Biol,* 119, 493-501.

GILL, C., MESTRIL, R. & SAMALI, A. (2002) Losing heart: the role of apoptosis in heart disease--a novel therapeutic target? *Faseb J,* 16, 135-46.

GORDON, J. M., DUSTING, G. J., WOODMAN, O. L. & RITCHIE, R. H. (2003) Cardioprotective action of CRF peptide urocortin against simulated ischemia in adult rat cardiomyocytes. *Am J Physiol Heart Circ Physiol,* 284, H330-6.

GOSSEN, M. & BUJARD, H. (1992) Tight control of gene expression in mammalian cells by tetracycline-responsive promoters. *Proc Natl Acad Sci U S A,* 89, 5547-51.

GOTTLIEB, R. A., BURLESON, K. O., KLONER, R. A., BABIOR, B. M. & ENGLER, R. L. (1994) Reperfusion injury induces apoptosis in rabbit cardiomyocytes. *J Clin Invest,* 94, 1621-8.

GREENHALGH, C. J. & HILTON, D. J. (2001) Negative regulation of cytokine signaling. *J Leukoc Biol,* 70, 348-56.

GREENLUND, A. C., FARRAR, M. A., VIVIANO, B. L. & SCHREIBER, R. D. (1994) Ligand-induced IFN gamma receptor tyrosine phosphorylation couples the receptor to its signal transduction system (p91). *Embo J,* 13, 1591-600.

GROSS, G. J. & FRYER, R. M. (1999) Sarcolemmal versus mitochondrial ATP-sensitive K+ channels and myocardial preconditioning. *Circ Res,* 84, 973-9.

GRUNT, M., GLASER, J., SCHMIDHUBER, H., PAUSCHINGER, P. & BORN, J. (1993) Effects of corticotropin-releasing factor on isolated rat heart activity. *Am J Physiol,* 264, H1124-9.

GRUNT, M., HAUG, C., DUNTAS, L., PAUSCHINGER, P., MAIER, V. & PFEIFFER, E. F. (1992) Dilatory and inotropic effects of corticotropin-releasing factor (CRF) on the isolated heart. Effects on atrial natriuretic peptide (ANP) release. *Horm Metab Res,* 24, 56-9.

GUSTERSON, R., BRAR, B., FAULKES, D., GIORDANO, A., CHRIVIA, J. & LATCHMAN, D. (2002) The transcriptional co-activators CBP and p300 are activated via phenylephrine through the p42/p44 MAPK cascade. *J Biol Chem,* 277, 2517-24.

GUSTERSON, R. J., JAZRAWI, E., ADCOCK, I. M. & LATCHMAN, D. S. (2003) The transcriptional co-activators CREB-binding protein (CBP) and p300 play a critical role in cardiac hypertrophy that is dependent on their histone acetyltransferase activity. *J Biol Chem,* 278, 6838-47.

HALESTRAP, A. P., CLARKE, S. J. & JAVADOV, S. A. (2004) Mitochondrial permeability transition pore opening during myocardial reperfusion--a target for cardioprotection. *Cardiovasc Res,* 61, 372-85.

HARVEY, M., SANDS, A. T., WEISS, R. S., HEGI, M. E., WISEMAN, R. W., PANTAZIS, P., GIOVANELLA, B. C., TAINSKY, M. A., BRADLEY, A. & DONEHOWER, L. A. (1993) In vitro growth characteristics of embryo fibroblasts isolated from p53-deficient mice. *Oncogene,* 8, 2457-67.

HAUNSTETTER, A. & IZUMO, S. (1998) Apoptosis: basic mechanisms and implications for cardiovascular disease. *Circ Res,* 82, 1111-29.

HAUSENLOY, D. J. & YELLON, D. M. (2004) New directions for protecting the heart against ischaemia-reperfusion injury: targeting the Reperfusion Injury Salvage Kinase (RISK)-pathway. *Cardiovasc Res,* 61, 448-60.

HEADS, R. J., LATCHMAN, D. S. & YELLON, D. M. (1994) Stable high level expression of a transfected human HSP70 gene protects a heart-derived muscle cell line against thermal stress. *J Mol Cell Cardiol,* 26, 695-9.

HEADS, R. J., YELLON, D. M. & LATCHMAN, D. S. (1995) Differential cytoprotection against heat stress or hypoxia following expression of specific stress protein genes in myogenic cells. *J Mol Cell Cardiol,* 27, 1669-78.

HEINEKE, J. & MOLKENTIN, J. D. (2006) Regulation of cardiac hypertrophy by intracellular signalling pathways. *Nat Rev Mol Cell Biol,* 7, 589-600.

HEINRICH, P. C., BEHRMANN, I., HAAN, S., HERMANNS, H. M., MULLER-NEWEN, G. & SCHAPER, F. (2003) Principles of interleukin (IL)-6-type cytokine signalling and its regulation. *Biochem J,* 374, 1-20.

HELDWEIN, K. A., REDICK, D. L., RITTENBERG, M. B., CLAYCOMB, W. C. & STENZEL-POORE, M. P. (1996) Corticotropin-releasing hormone receptor expression and functional coupling in neonatal cardiac myocytes and AT-1 cells. *Endocrinology,* 137, 3631-9.

HILL, J. A., KARIMI, M., KUTSCHKE, W., DAVISSON, R. L., ZIMMERMAN, K., WANG, Z., KERBER, R. E. & WEISS, R. M. (2000) Cardiac hypertrophy is not a required compensatory response to short-term pressure overload. *Circulation,* 101, 2863-9.

HIRANO, T., NAKAJIMA, K. & HIBI, M. (1997) Signaling mechanisms through gp130: a model of the cytokine system. *Cytokine Growth Factor Rev,* 8, 241-52.

HOCHHAUSER, E., KIVITY, S., OFFEN, D., MAULIK, N., OTANI, H., BARHUM, Y., PANNET, H., SHNEYVAYS, V., SHAINBERG, A., GOLDSHTAUB, V., TOBAR, A. & VIDNE, B. A. (2003) Bax ablation protects against myocardial ischemia-reperfusion injury in transgenic mice. *Am J Physiol Heart Circ Physiol,* 284, H2351-9.

HSU, S. Y. & HSUEH, A. J. (2001) Human stresscopin and stresscopin-related peptide are selective ligands for the type 2 corticotropin-releasing hormone receptor. *Nat Med,* 7, 605-11.

HUANG, S., HENDRIKS, W., ALTHAGE, A., HEMMI, S., BLUETHMANN, H., KAMIJO, R., VILCEK, J., ZINKERNAGEL, R. M. & AGUET, M. (1993) Immune response in mice that lack the interferon-gamma receptor. *Science,* 259, 1742-5.

IEMITSU, M., MIYAUCHI, T., MAEDA, S., SAKAI, S., KOBAYASHI, T., FUJII, N., MIYAZAKI, H., MATSUDA, M. & YAMAGUCHI, I. (2001) Physiological and pathological cardiac hypertrophy induce different molecular phenotypes in the rat. *Am J Physiol Regul Integr Comp Physiol,* 281, R2029-36.

IHLE, J. N. (1995) The Janus protein tyrosine kinases in hematopoietic cytokine signaling. *Semin Immunol,* 7, 247-54.

IKEDA, K., TOJO, K., SATO, S., EBISAWA, T., TOKUDOME, G., HOSOYA, T., HARADA, M., NAKAGAWA, O. & NAKAO, K. (1998) Urocortin, a newly identified corticotropin-releasing factor-related mammalian peptide, stimulates atrial

natriuretic peptide and brain natriuretic peptide secretions from neonatal rat cardiomyocytes. *Biochem Biophys Res Commun,* 250, 298-304.

IKEUCHI, M., MATSUSAKA, H., KANG, D., MATSUSHIMA, S., IDE, T., KUBOTA, T., FUJIWARA, T., HAMASAKI, N., TAKESHITA, A., SUNAGAWA, K. & TSUTSUI, H. (2005) Overexpression of mitochondrial transcription factor a ameliorates mitochondrial deficiencies and cardiac failure after myocardial infarction. *Circulation,* 112, 683-90.

ISHIKAWA, M., SAITO, Y., MIYAMOTO, Y., HARADA, M., KUWAHARA, K., OGAWA, E., NAKAGAWA, O., HAMANAKA, I., KAJIYAMA, N., TAKAHASHI, N., MASUDA, I., HASHIMOTO, T., SAKAI, O., HOSOYA, T. & NAKAO, K. (1999) A heart-specific increase in cardiotrophin-1 gene expression precedes the establishment of ventricular hypertrophy in genetically hypertensive rats. *J Hypertens,* 17, 807-16.

JAMSHIDI, Y., ZOURLIDOU, A., CARROLL, C. J., SINCLAIR, J. & LATCHMAN, D. S. (2004) Signal-transduction pathways involved in the hypertrophic effect of hsp56 in neonatal cardiomyocytes. *J Mol Cell Cardiol,* 36, 381-92.

JANJUA, S., LAWRENCE, K. M., NG, L. L. & LATCHMAN, D. S. (2003) The cardioprotective agent urocortin induces expression of CT-1. *Cardiovasc Toxicol,* 3, 255-62.

JANJUA, S., STEPHANOU, A. & LATCHMAN, D. S. (2002) The C-terminal activation domain of the STAT-1 transcription factor is necessary and sufficient for stress-induced apoptosis. *Cell Death Differ,* 9, 1140-6.

JAVADOV, S. & KARMAZYN, M. (2007) Mitochondrial permeability transition pore opening as an endpoint to initiate cell death and as a putative target for cardioprotection. *Cell Physiol Biochem,* 20, 1-22.

JIN, H., LI, W., YANG, R., OGASAWARA, A., LU, H. & PAONI, N. F. (2005) Inhibitory effects of interferon-gamma on myocardial hypertrophy. *Cytokine,* 31, 405-14.

JIN, H., YANG, R., KELLER, G. A., RYAN, A., KO, A., FINKLE, D., SWANSON, T. A., LI, W., PENNICA, D., WOOD, W. I. & PAONI, N. F. (1996) In vivo effects of cardiotrophin-1. *Cytokine,* 8, 920-6.

JOUANGUY, E., ALTARE, F., LAMHAMEDI, S., REVY, P., EMILE, J. F., NEWPORT, M., LEVIN, M., BLANCHE, S., SEBOUN, E., FISCHER, A. & CASANOVA, J. L. (1996) Interferon-gamma-receptor deficiency in an infant with fatal bacille Calmette-Guerin infection. *N Engl J Med,* 335, 1956-61.

JOUGASAKI, M., LESKINEN, H., LARSEN, A. M., LUCHNER, A., CATALIOTTI, A., TACHIBANA, I. & BURNETT, J. C., JR. (2003) Ventricular cardiotrophin-1 activation precedes BNP in experimental heart failure. *Peptides,* 24, 889-92.

JOUGASAKI, M., TACHIBANA, I., LUCHNER, A., LESKINEN, H., REDFIELD, M. M. & BURNETT, J. C., JR. (2000) Augmented cardiac cardiotrophin-1 in experimental congestive heart failure. *Circulation,* 101, 14-7.

JOZA, N., SUSIN, S. A., DAUGAS, E., STANFORD, W. L., CHO, S. K., LI, C. Y., SASAKI, T., ELIA, A. J., CHENG, H. Y., RAVAGNAN, L., FERRI, K. F., ZAMZAMI, N., WAKEHAM, A., HAKEM, R., YOSHIDA, H., KONG, Y. Y., MAK, T. W., ZUNIGA-PFLUCKER, J. C., KROEMER, G. & PENNINGER, J. M. (2001) Essential role of the mitochondrial apoptosis-inducing factor in programmed cell death. *Nature,* 410, 549-54.

KAGEYAMA, K., GAUDRIAULT, G. E., BRADBURY, M. J. & VALE, W. W. (2000) Regulation of corticotropin-releasing factor receptor type 2 beta messenger ribonucleic acid in the rat cardiovascular system by urocortin, glucocorticoids, and cytokines. *Endocrinology,* 141, 2285-93.

KAGEYAMA, K., HANADA, K., NIGAWARA, T., MORIYAMA, T., TERUI, K., SAKIHARA, S. & SUDA, T. (2006) Urocortin induces interleukin-6 gene expression via cyclooxygenase-2 activity in aortic smooth muscle cells. *Endocrinology,* 147, 4454-62.

KAJSTURA, J., MANSUKHANI, M., CHENG, W., REISS, K., KRAJEWSKI, S., REED, J. C., QUAINI, F., SONNENBLICK, E. H. & ANVERSA, P. (1995) Programmed cell death and expression of the protooncogene bcl-2 in myocytes during postnatal maturation of the heart. *Exp Cell Res,* 219, 110-21.

KANG, P. M., HAUNSTETTER, A., AOKI, H., USHEVA, A. & IZUMO, S. (2000) Morphological and molecular characterization of adult cardiomyocyte apoptosis during hypoxia and reoxygenation. *Circ Res,* 87, 118-25.

KAPLAN, D. H., SHANKARAN, V., DIGHE, A. S., STOCKERT, E., AGUET, M., OLD, L. J. & SCHREIBER, R. D. (1998) Demonstration of an interferon gamma-dependent tumor surveillance system in immunocompetent mice. *Proc Natl Acad Sci U S A,* 95, 7556-61.

KERR, J. F., WYLLIE, A. H. & CURRIE, A. R. (1972) Apoptosis: a basic biological phenomenon with wide-ranging implications in tissue kinetics. *Br J Cancer,* 26, 239-57.

KIM, H. S. & LEE, M. S. (2007) STAT1 as a key modulator of cell death. *Cell Signal,* 19, 454-65.

KIMURA, Y., TAKAHASHI, K., TOTSUNE, K., MURAMATSU, Y., KANEKO, C., DARNEL, A. D., SUZUKI, T., EBINA, M., NUKIWA, T. & SASANO, H. (2002) Expression of urocortin and corticotropin-releasing factor receptor subtypes in the human heart. *J Clin Endocrinol Metab,* 87, 340-6.

KING, P. & GOODBOURN, S. (1998) STAT1 is inactivated by a caspase. *J Biol Chem,* 273, 8699-704.

KISHIMOTO, T., PEARSE, R. V., 2ND, LIN, C. R. & ROSENFELD, M. G. (1995) A sauvagine/corticotropin-releasing factor receptor expressed in heart and skeletal muscle. *Proc Natl Acad Sci U S A,* 92, 1108-12.

KISHIMOTO, T. (2006) Interleukin-6: discovery of a pleiotropic cytokine. *Arthritis Res Ther,* 8 Suppl 2, S2.

KISTLER, J., STROUD, R. M., KLYMKOWSKY, M. W., LALANCETTE, R. A. & FAIRCLOUGH, R. H. (1982) Structure and function of an acetylcholine receptor. *Biophys J,* 37, 371-83.

KLEIN, J. A., LONGO-GUESS, C. M., ROSSMANN, M. P., SEBURN, K. L., HURD, R. E., FRANKEL, W. N., BRONSON, R. T. & ACKERMAN, S. L. (2002) The harlequin mouse mutation downregulates apoptosis-inducing factor. *Nature,* 419, 367-74.

KLONER, R. A. & JENNINGS, R. B. (2001) Consequences of brief ischemia: stunning, preconditioning, and their clinical implications: part 1. *Circulation,* 104, 2981-9.

KOMAROV, P. G., KOMAROVA, E. A., KONDRATOV, R. V., CHRISTOV-TSELKOV, K., COON, J. S., CHERNOV, M. V. & GUDKOV, A. V. (1999) A chemical inhibitor of p53 that protects mice from the side effects of cancer therapy. *Science,* 285, 1733-7.

KOMAROVA, E. A., KRIVOKRYSENKO, V., WANG, K., NEZNANOV, N., CHERNOV, M. V., KOMAROV, P. G., BRENNAN, M. L., GOLOVKINA, T. V., ROKHLIN, O. W., KUPRASH, D. V., NEDOSPASOV, S. A., HAZEN, S. L., FEINSTEIN, E. & GUDKOV, A. V. (2005) p53 is a suppressor of inflammatory response in mice. *Faseb J,* 19, 1030-2.

KOTHAKOTA, S., AZUMA, T., REINHARD, C., KLIPPEL, A., TANG, J., CHU, K., MCGARRY, T. J., KIRSCHNER, M. W., KOTHS, K., KWIATKOWSKI, D. J. & WILLIAMS, L. T. (1997) Caspase-3-generated fragment of gelsolin: effector of morphological change in apoptosis. *Science,* 278, 294-8.

KOVARIK, P., STOIBER, D., EYERS, P. A., MENGHINI, R., NEININGER, A., GAESTEL, M., COHEN, P. & DECKER, T. (1999) Stress-induced phosphorylation of STAT1 at Ser727 requires p38 mitogen-activated protein kinase whereas IFN-gamma uses a different signaling pathway. *Proc Natl Acad Sci U S A,* 96, 13956-61.

KUIDA, K., HAYDAR, T. F., KUAN, C. Y., GU, Y., TAYA, C., KARASUYAMA, H., SU, M. S., RAKIC, P. & FLAVELL, R. A. (1998) Reduced apoptosis and cytochrome c-mediated caspase activation in mice lacking caspase 9. *Cell,* 94, 325-37.

KUKIELKA, G. L., SMITH, C. W., MANNING, A. M., YOUKER, K. A., MICHAEL, L. H. & ENTMAN, M. L. (1995) Induction of interleukin-6 synthesis in the myocardium. Potential role in postreperfusion inflammatory injury. *Circulation,* 92, 1866-75.

KUWAHARA, K., SAITO, Y., KISHIMOTO, I., MIYAMOTO, Y., HARADA, M., OGAWA, E., HAMANAKA, I., KAJIYAMA, N., TAKAHASHI, N., IZUMI, T., KAWAKAMI, R. & NAKAO, K. (2000) Cardiotrophin-1 phosphorylates akt and BAD, and prolongs cell survival via a PI3K-dependent pathway in cardiac myocytes. *J Mol Cell Cardiol,* 32, 1385-94.

LASSUS, P., OPITZ-ARAYA, X. & LAZEBNIK, Y. (2002) Requirement for caspase-2 in stress-induced apoptosis before mitochondrial permeabilization. *Science,* 297, 1352-4.

LATCHMAN, D. S. (2000) Cardiotrophin-1: a novel cytokine and its effects in the heart and other tissues. *Pharmacol Ther,* 85, 29-37.

LATCHMAN, D. S. (2001a) Heat shock proteins and cardiac protection. *Cardiovasc Res,* 51, 637-46.

LATCHMAN, D. S. (2001b) Urocortin protects against ischemic injury via a MAPK-dependent pathway. *Trends Cardiovasc Med,* 11, 167-9.

LAWRENCE, K. M., CHANALARIS, A., SCARABELLI, T., HUBANK, M., PASINI, E., TOWNSEND, P. A., COMINI, L., FERRARI, R., TINKER, A., STEPHANOU, A., KNIGHT, R. A. & LATCHMAN, D. S. (2002) K(ATP) channel gene expression is induced by urocortin and mediates its cardioprotective effect. *Circulation,* 106, 1556-62.

LAWRENCE, K. M., KABIR, A. M., BELLAHCENE, M., DAVIDSON, S., CAO, X. B., MCCORMICK, J., MESQUITA, R. A., CARROLL, C. J., CHANALARIS, A., TOWNSEND, P. A., HUBANK, M., STEPHANOU, A., KNIGHT, R. A., MARBER, M. S. & LATCHMAN, D. S. (2005) Cardioprotection mediated by urocortin is dependent on PKCepsilon activation. *Faseb J,* 19, 831-3.

LAWRENCE, K. M. & LATCHMAN, D. S. (2006) The Urocortins: mechanisms of cardioprotection and therapeutic potential. *Mini Rev Med Chem,* 6, 1119-26.

LAWRENCE, K. M., SCARABELLI, T. M., TURTLE, L., CHANALARIS, A., TOWNSEND, P. A., CARROLL, C. J., HUBANK, M., STEPHANOU, A., KNIGHT, R. A. & LATCHMAN, D. S. (2003) Urocortin protects cardiac myocytes from ischemia/reperfusion injury by attenuating calcium-insensitive phospholipase A2 gene expression. *Faseb J,* 17, 2313-5.

LAWRENCE, K. M., TOWNSEND, P. A., DAVIDSON, S. M., CARROLL, C. J., EATON, S., HUBANK, M., KNIGHT, R. A., STEPHANOU, A. & LATCHMAN, D. S. (2004) The cardioprotective effect of urocortin during ischaemia/reperfusion involves the prevention of mitochondrial damage. *Biochem Biophys Res Commun,* 321, 479-86.

LAZEBNIK, Y. A., KAUFMANN, S. H., DESNOYERS, S., POIRIER, G. G. & EARNSHAW, W. C. (1994) Cleavage of poly(ADP-ribose) polymerase by a proteinase with properties like ICE. *Nature,* 371, 346-7.

LEBEAU, M. C., MYAGKIKH, I., ROUVIERE-FOURMY, N., BAULIEU, E. E. & KLEE, C. B. (1994) Rabbit FKBP-59/HBI does not inhibit calcineurin activity in vitro. *Biochem Biophys Res Commun,* 203, 750-5.

LEE, P., SATA, M., LEFER, D. J., FACTOR, S. M., WALSH, K. & KITSIS, R. N. (2003) Fas pathway is a critical mediator of cardiac myocyte death and MI during ischemia-reperfusion in vivo. *Am J Physiol Heart Circ Physiol,* 284, H456-63.

LEIST, M. & NICOTERA, P. (1997) The shape of cell death. *Biochem Biophys Res Commun,* 236, 1-9.

LENZ, H. J., FISHER, L. A., VALE, W. W. & BROWN, M. R. (1985) Corticotropin-releasing factor, sauvagine, and urotensin I: effects on blood flow. *Am J Physiol,* 249, R85-90.

LERI, A., LIU, Y., MALHOTRA, A., LI, Q., STIEGLER, P., CLAUDIO, P. P., GIORDANO, A., KAJSTURA, J., HINTZE, T. H. & ANVERSA, P. (1998) Pacing-induced heart failure in dogs enhances the expression of p53 and p53-dependent genes in ventricular myocytes. *Circulation,* 97, 194-203.

LESINSKI, G. B., ANGHELINA, M., ZIMMERER, J., BAKALAKOS, T., BADGWELL, B., PARIHAR, R., HU, Y., BECKNELL, B., ABOOD, G., CHAUDHURY, A. R., MAGRO, C., DURBIN, J. & CARSON, W. E., 3RD (2003) The antitumor effects of IFN-alpha are abrogated in a STAT1-deficient mouse. *J Clin Invest,* 112, 170-80.

LEWANDOSKI, M. (2001) Conditional control of gene expression in the mouse. *Nat Rev Genet,* 2, 743-55.

LEWIS, K., LI, C., PERRIN, M. H., BLOUNT, A., KUNITAKE, K., DONALDSON, C., VAUGHAN, J., REYES, T. M., GULYAS, J., FISCHER, W., BILEZIKJIAN, L., RIVIER, J., SAWCHENKO, P. E. & VALE, W. W. (2001) Identification of urocortin III, an additional member of the corticotropin-releasing factor (CRF) family with high affinity for the CRF2 receptor. *Proc Natl Acad Sci U S A,* 98, 7570-5.

LI, E. & HRISTOVA, K. (2006) Role of receptor tyrosine kinase transmembrane domains in cell signaling and human pathologies. *Biochemistry,* 45, 6241-51.

LI, L., ZHANG, J., JIN, B., BLOCK, E. R. & PATEL, J. M. (2007) Nitric oxide upregulation of caspase-8 mRNA expression in lung endothelial cells: role of JAK2/STAT-1 signaling. *Mol Cell Biochem.*

LI, P., NIJHAWAN, D., BUDIHARDJO, I., SRINIVASULA, S. M., AHMAD, M., ALNEMRI, E. S. & WANG, X. (1997) Cytochrome c and dATP-dependent formation of Apaf-1/caspase-9 complex initiates an apoptotic protease cascade. *Cell,* 91, 479-89.

LIAO, Z., BRAR, B. K., CAI, Q., STEPHANOU, A., O'LEARY, R. M., PENNICA, D., YELLON, D. M. & LATCHMAN, D. S. (2002) Cardiotrophin-1 (CT-1) can protect the adult heart from injury when added both prior to ischaemia and at reperfusion. *Cardiovasc Res,* 53, 902-10.

LILLEMEIER, B. F., KOSTER, M. & KERR, I. M. (2001) STAT1 from the cell membrane to the DNA. *Embo J,* 20, 2508-17.

LISTER, K., AUTELITANO, D. J., JENKINS, A., HANNAN, R. D. & SHEPPARD, K. E. (2006) Cross talk between corticosteroids and alpha-adrenergic signalling augments cardiomyocyte hypertrophy: a possible role for SGK1. *Cardiovasc Res,* 70, 555-65.

LIU, G. S., COHEN, M. V., MOCHLY-ROSEN, D. & DOWNEY, J. M. (1999) Protein kinase C-epsilon is responsible for the protection of preconditioning in rabbit cardiomyocytes. *J Mol Cell Cardiol,* 31, 1937-48.

LIU, B., LIAO, J., RAO, X., KUSHNER, S. A., CHUNG, C. D., CHANG, D. D. & SHUAI, K. (1998) Inhibition of Stat1-mediated gene activation by PIAS1. *Proc Natl Acad Sci U S A,* 95, 10626-31.

LIU, J., FARMER, J. D., JR., LANE, W. S., FRIEDMAN, J., WEISSMAN, I. & SCHREIBER, S. L. (1991) Calcineurin is a common target of cyclophilin-cyclosporin A and FKBP-FK506 complexes. *Cell,* 66, 807-15.

LIU, P., XU, B., CAVALIERI, T. A. & HOCK, C. E. (2006) Pifithrin-alpha attenuates p53-mediated apoptosis and improves cardiac function in response to myocardial ischemia/reperfusion in aged rats. *Shock,* 26, 608-14.

LIVAK, K. J. & SCHMITTGEN, T. D. (2001) Analysis of relative gene expression data using real-time quantitative PCR and the 2(-Delta Delta C(T)) Method. *Methods,* 25, 402-8.

LONG, X., BOLUYT, M. O., HIPOLITO, M. L., LUNDBERG, M. S., ZHENG, J. S., O'NEILL, L., CIRIELLI, C., LAKATTA, E. G. & CROW, M. T. (1997) p53 and the hypoxia-induced apoptosis of cultured neonatal rat cardiac myocytes. *J Clin Invest,* 99, 2635-43.

LOVENBERG, T. W., CHALMERS, D. T., LIU, C. & DE SOUZA, E. B. (1995) CRF2 alpha and CRF2 beta receptor mRNAs are differentially distributed between the rat central nervous system and peripheral tissues. *Endocrinology,* 136, 4139-42.

LUKASHCHUK, N. & VOUSDEN, K. H. (2007) Ubiquitination And Degradation Of Mutant P53. *Mol Cell Biol.*

MA, X. L., KUMAR, S., GAO, F., LOUDEN, C. S., LOPEZ, B. L., CHRISTOPHER, T. A., WANG, C., LEE, J. C., FEUERSTEIN, G. Z. & YUE, T. L. (1999) Inhibition of p38 mitogen-activated protein kinase decreases cardiomyocyte apoptosis and improves cardiac function after myocardial ischemia and reperfusion. *Circulation,* 99, 1685-91.

MACLELLAN, W. R. & SCHNEIDER, M. D. (1997) Death by design. Programmed cell death in cardiovascular biology and disease. *Circ Res,* 81, 137-44.

MAGINOT, K. R., KLITZNER, T. S., FRIEDMAN, W. F. & WETZEL, G. T. (1998) The relationship between temperature and calcium in acute cell damage after exposure to radiofrequency or thermal energy in isolated neonatal and adult rabbit cardiac myocytes. *Pediatr Res,* 43, 527-31.

MARBER, M. S., MESTRIL, R., CHI, S. H., SAYEN, M. R., YELLON, D. M. & DILLMANN, W. H. (1995) Overexpression of the rat inducible 70-kD heat stress protein in a transgenic mouse increases the resistance of the heart to ischemic injury. *J Clin Invest,* 95, 1446-56.

MARBER, M. S. & YELLON, D. M. (1996) Myocardial adaptation, stress proteins, and the second window of protection. *Ann N Y Acad Sci,* 793, 123-41.

MARG, A., SHAN, Y., MEYER, T., MEISSNER, T., BRANDENBURG, M. & VINKEMEIER, U. (2004) Nucleocytoplasmic shuttling by nucleoporins Nup153 and Nup214 and CRM1-dependent nuclear export control the subcellular distribution of latent Stat1. *J Cell Biol,* 165, 823-33.

MARUYAMA, R., TAKEMURA, G., AOYAMA, T., HAYAKAWA, K., KODA, M., KAWASE, Y., QIU, X., OHNO, Y., MINATOGUCHI, S., MIYATA, K., FUJIWARA, T. &

FUJIWARA, H. (2001) Dynamic process of apoptosis in adult rat cardiomyocytes analyzed using 48-hour videomicroscopy and electron microscopy: beating and rate are associated with the apoptotic process. *Am J Pathol,* 159, 683-91.

MATE, M. J., ORTIZ-LOMBARDIA, M., BOITEL, B., HAOUZ, A., TELLO, D., SUSIN, S. A., PENNINGER, J., KROEMER, G. & ALZARI, P. M. (2002) The crystal structure of the mouse apoptosis-inducing factor AIF. *Nat Struct Biol,* 9, 442-6.

MATSUI, H., IHARA, Y., FUJIO, Y., KUNISADA, K., AKIRA, S., KISHIMOTO, T. & YAMAUCHI-TAKIHARA, K. (1999) Induction of interleukin (IL)-6 by hypoxia is mediated by nuclear factor (NF)-kappa B and NF-IL6 in cardiac myocytes. *Cardiovasc Res,* 42, 104-12.

MATSUI, T., LI, L., DEL MONTE, F., FUKUI, Y., FRANKE, T. F., HAJJAR, R. J. & ROSENZWEIG, A. (1999) Adenoviral gene transfer of activated phosphatidylinositol 3'-kinase and Akt inhibits apoptosis of hypoxic cardiomyocytes in vitro. *Circulation,* 100, 2373-9.

MATSUI, T., TAO, J., DEL MONTE, F., LEE, K. H., LI, L., PICARD, M., FORCE, T. L., FRANKE, T. F., HAJJAR, R. J. & ROSENZWEIG, A. (2001) Akt activation preserves cardiac function and prevents injury after transient cardiac ischemia in vivo. *Circulation,* 104, 330-5.

MATSUSAKA, H., IDE, T., MATSUSHIMA, S., IKEUCHI, M., KUBOTA, T., SUNAGAWA, K., KINUGAWA, S. & TSUTSUI, H. (2006) Targeted deletion of p53 prevents cardiac rupture after myocardial infarction in mice. *Cardiovasc Res.*

MATSUSHITA, K., IWANAGA, S., ODA, T., KIMURA, K., SHIMADA, M., SANO, M., UMEZAWA, A., HATA, J. & OGAWA, S. (2005) Interleukin-6/soluble interleukin-6 receptor complex reduces infarct size via inhibiting myocardial apoptosis. *Lab Invest,* 85, 1210-23.

MAULIK, N., SASAKI, H., ADDYA, S. & DAS, D. K. (2000) Regulation of cardiomyocyte apoptosis by redox-sensitive transcription factors. *FEBS Lett,* 485, 7-12.

MAUNEY, M. C. & KRON, I. L. (1995) The physiologic basis of warm cardioplegia. *Ann Thorac Surg,* 60, 819-23.

MCBRIDE, K. M., MCDONALD, C. & REICH, N. C. (2000) Nuclear export signal located within theDNA-binding domain of the STAT1transcription factor. *Embo J,* 19, 6196-206.

MCCORMICK, J., BARRY, S. P., SIVARAJAH, A., STEFANUTTI, G., TOWNSEND, P. A., LAWRENCE, K. M., EATON, S., KNIGHT, R. A., THIEMERMANN, C., LATCHMAN, D. S. & STEPHANOU, A. (2006) Free radical scavenging inhibits STAT phosphorylation following in vivo ischemia/reperfusion injury. *Faseb J,* 20, 2115-7.

MEISTER, N., SHALABY, T., VON BUEREN, A. O., RIVERA, P., PATTI, R., OEHLER, C., PRUSCHY, M. & GROTZER, M. A. (2007) Interferon-gamma mediated up-

regulation of caspase-8 sensitises medulloblastoma cells to radio- and chemotherapy. *Eur J Cancer.*

MELOV, S., COSKUN, P., PATEL, M., TUINSTRA, R., COTTRELL, B., JUN, A. S., ZASTAWNY, T. H., DIZDAROGLU, M., GOODMAN, S. I., HUANG, T. T., MIZIORKO, H., EPSTEIN, C. J. & WALLACE, D. C. (1999) Mitochondrial disease in superoxide dismutase 2 mutant mice. *Proc Natl Acad Sci U S A,* 96, 846-51.

MERAZ, M. A., WHITE, J. M., SHEEHAN, K. C., BACH, E. A., RODIG, S. J., DIGHE, A. S., KAPLAN, D. H., RILEY, J. K., GREENLUND, A. C., CAMPBELL, D., CARVER-MOORE, K., DUBOIS, R. N., CLARK, R., AGUET, M. & SCHREIBER, R. D. (1996) Targeted disruption of the Stat1 gene in mice reveals unexpected physiologic specificity in the JAK-STAT signaling pathway. *Cell,* 84, 431-42.

MEYER, T., BEGITT, A., LODIGE, I., VAN ROSSUM, M. & VINKEMEIER, U. (2002) Constitutive and IFN-gamma-induced nuclear import of STAT1 proceed through independent pathways. *Embo J,* 21, 344-54.

MILLER, R., TONEFF, T., VISHNUVARDHAN, D., BEINFELD, M. & HOOK, V. Y. (2003) Selective roles for the PC2 processing enzyme in the regulation of peptide neurotransmitter levels in brain and peripheral neuroendocrine tissues of PC2 deficient mice. *Neuropeptides,* 37, 140-8.

MITCHESON, J. S., HANCOX, J. C. & LEVI, A. J. (1998) Cultured adult cardiac myocytes: future applications, culture methods, morphological and electrophysiological properties. *Cardiovasc Res,* 39, 280-300.

MIURA, M., ZHU, H., ROTELLO, R., HARTWIEG, E. A. & YUAN, J. (1993) Induction of apoptosis in fibroblasts by IL-1 beta-converting enzyme, a mammalian homolog of the C. elegans cell death gene ced-3. *Cell,* 75, 653-60.

MOLKENTIN, J. D., LU, J. R., ANTOS, C. L., MARKHAM, B., RICHARDSON, J., ROBBINS, J., GRANT, S. R. & OLSON, E. N. (1998) A calcineurin-dependent transcriptional pathway for cardiac hypertrophy. *Cell,* 93, 215-28.

MUGLIA, L. J., JENKINS, N. A., GILBERT, D. J., COPELAND, N. G. & MAJZOUB, J. A. (1994) Expression of the mouse corticotropin-releasing hormone gene in vivo and targeted inactivation in embryonic stem cells. *J Clin Invest,* 93, 2066-72.

MULLER-NEWEN, G. (2003) The cytokine receptor gp130: faithfully promiscuous. *Sci STKE,* 2003, PE40.

MURATA, M., AKAO, M., O'ROURKE, B. & MARBAN, E. (2001) Mitochondrial ATP-sensitive potassium channels attenuate matrix Ca(2+) overload during simulated ischemia and reperfusion: possible mechanism of cardioprotection. *Circ Res,* 89, 891-8.

MURRAY, P. J. (2007) The JAK-STAT signaling pathway: input and output integration. *J Immunol,* 178, 2623-9.

MURRY, C. E., JENNINGS, R. B. & REIMER, K. A. (1986) Preconditioning with ischemia: a delay of lethal cell injury in ischemic myocardium. *Circulation,* 74, 1124-36.

NAKAGAWA, R., NAKA, T., TSUTSUI, H., FUJIMOTO, M., KIMURA, A., ABE, T., SEKI, E., SATO, S., TAKEUCHI, O., TAKEDA, K., AKIRA, S., YAMANISHI, K., KAWASE, I., NAKANISHI, K. & KISHIMOTO, T. (2002) SOCS-1 participates in negative regulation of LPS responses. *Immunity,* 17, 677-87.

NAKAJIMA, T., KINOSHITA, S., SASAGAWA, T., SASAKI, K., NARUTO, M., KISHIMOTO, T. & AKIRA, S. (1993) Phosphorylation at threonine-235 by a ras-dependent mitogen-activated protein kinase cascade is essential for transcription factor NF-IL6. *Proc Natl Acad Sci U S A,* 90, 2207-11.

NAKAO, K., MYERS, J. E. & FABER, L. E. (1985) Development of a monoclonal antibody to the rabbit 8.5S uterine progestin receptor. *Can J Biochem Cell Biol,* 63, 33-40.

NEWPORT, M. J., HUXLEY, C. M., HUSTON, S., HAWRYLOWICZ, C. M., OOSTRA, B. A., WILLIAMSON, R. & LEVIN, M. (1996) A mutation in the interferon-gamma-receptor gene and susceptibility to mycobacterial infection. *N Engl J Med,* 335, 1941-9.

NICHOLSON, D. W. & THORNBERRY, N. A. (1997) Caspases: killer proteases. *Trends Biochem Sci,* 22, 299-306.

NICKSON, P., TOTH, A. & ERHARDT, P. (2007) PUMA is critical for neonatal cardiomyocyte apoptosis induced by endoplasmic reticulum stress. *Cardiovasc Res,* 73, 48-56.

NICOL, R. L., FREY, N., PEARSON, G., COBB, M., RICHARDSON, J. & OLSON, E. N. (2001) Activated MEK5 induces serial assembly of sarcomeres and eccentric cardiac hypertrophy. *Embo J,* 20, 2757-67.

NISHIKIMI, T., MIYATA, A., HORIO, T., YOSHIHARA, F., NAGAYA, N., TAKISHITA, S., YUTANI, C., MATSUO, H., MATSUOKA, H. & KANGAWA, K. (2000) Urocortin, a member of the corticotropin-releasing factor family, in normal and diseased heart. *Am J Physiol Heart Circ Physiol,* 279, H3031-9.

NISHIZAWA, J., NAKAI, A., HIGASHI, T., TANABE, M., NOMOTO, S., MATSUDA, K., BAN, T. & NAGATA, K. (1996) Reperfusion causes significant activation of heat shock transcription factor 1 in ischemic rat heart. *Circulation,* 94, 2185-92.

NOORDZIJ, J. G., HARTWIG, N. G., VERRECK, F. A., DE BRUIN-VERSTEEG, S., DE BOER, T., DISSEL, J. T., DE GROOT, R., OTTENHOFF, T. H. & VAN DONGEN, J. J. (2007) Two Patients with Complete Defects in Interferon Gamma Receptor-Dependent Signaling. *J Clin Immunol.*

OHIRO, Y., GARKAVTSEV, I., KOBAYASHI, S., SREEKUMAR, K. R., NANTZ, R., HIGASHIKUBO, B. T., DUFFY, S. L., HIGASHIKUBO, R., USHEVA, A., GIUS, D., KLEY, N. & HORIKOSHI, N. (2002) A novel p53-inducible apoptogenic gene, PRG3, encodes a homologue of the apoptosis-inducing factor (AIF). *FEBS Lett,* 524, 163-71.

OKOSI, A., BRAR, B. K., CHAN, M., D'SOUZA, L., SMITH, E., STEPHANOU, A., LATCHMAN, D. S., CHOWDREY, H. S. & KNIGHT, R. A. (1998) Expression and

protective effects of urocortin in cardiac myocytes. *Neuropeptides,* 32, 167-71.

OLAFSSON, B., FORMAN, M. B., PUETT, D. W., POU, A., CATES, C. U., FRIESINGER, G. C. & VIRMANI, R. (1987) Reduction of reperfusion injury in the canine preparation by intracoronary adenosine: importance of the endothelium and the no-reflow phenomenon. *Circulation,* 76, 1135-45.

OPIE, L. H. (1989) Reperfusion injury and its pharmacologic modification. *Circulation,* 80, 1049-62.

OPIE, L. H. (2004) *Heart Physiology: From Cell to Circulation.* ISBN-13: 978-0-7817-4278-8.

OUCHI, T., LEE, S. W., OUCHI, M., AARONSON, S. A. & HORVATH, C. M. (2000) Collaboration of signal transducer and activator of transcription 1 (STAT1) and BRCA1 in differential regulation of IFN-gamma target genes. *Proc Natl Acad Sci U S A,* 97, 5208-13.

PAULE, B., BELOT, J., RUDANT, C., COULOMBEL, C. & ABBOU, C. C. (2000) The importance of IL-6 protein expression in primary human renal cell carcinoma: an immunohistochemical study. *J Clin Pathol,* 53, 388-90.

PARKES, D. G., VAUGHAN, J., RIVIER, J., VALE, W. & MAY, C. N. (1997) Cardiac inotropic actions of urocortin in conscious sheep. *Am J Physiol,* 272, H2115-22.

PASSMAN, R. S. & FISHMAN, G. I. (1994) Regulated expression of foreign genes in vivo after germline transfer. *J Clin Invest,* 94, 2421-5.

PEATTIE, D. A., HARDING, M. W., FLEMING, M. A., DECENZO, M. T., LIPPKE, J. A., LIVINGSTON, D. J. & BENASUTTI, M. (1992) Expression and characterization of human FKBP52, an immunophilin that associates with the 90-kDa heat shock protein and is a component of steroid receptor complexes. *Proc Natl Acad Sci U S A,* 89, 10974-8.

PENNICA, D., KING, K. L., SHAW, K. J., LUIS, E., RULLAMAS, J., LUOH, S. M., DARBONNE, W. C., KNUTZON, D. S., YEN, R., CHIEN, K. R. & ET AL. (1995) Expression cloning of cardiotrophin 1, a cytokine that induces cardiac myocyte hypertrophy. *Proc Natl Acad Sci U S A,* 92, 1142-6.

PENNICA, D., SWANSON, T. A., SHAW, K. J., KUANG, W. J., GRAY, C. L., BEATTY, B. G. & WOOD, W. I. (1996) Human cardiotrophin-1: protein and gene structure, biological and binding activities, and chromosomal localization. *Cytokine,* 8, 183-9.

PERRIN, M., DONALDSON, C., CHEN, R., BLOUNT, A., BERGGREN, T., BILEZIKJIAN, L., SAWCHENKO, P. & VALE, W. (1995) Identification of a second corticotropin-releasing factor receptor gene and characterization of a cDNA expressed in heart. *Proc Natl Acad Sci U S A,* 92, 2969-73.

PETRAGLIA, F., FLORIO, P., GALLO, R., SIMONCINI, T., SAVIOZZI, M., DI BLASIO, A. M., VAUGHAN, J. & VALE, W. (1996) Human placenta and fetal

membranes express human urocortin mRNA and peptide. *J Clin Endocrinol Metab,* 81, 3807-10.

PICQ, M., DUBOIS, M., GRYNBERG, A., LAGARDE, M. & PRIGENT, A. F. (1995) Developmental differences in distribution of cyclic nucleotide phosphodiesterase isoforms in cardiomyocytes and the ventricular tissue from newborn and adult rats. *J Cardiovasc Pharmacol,* 26, 742-50.

PLUMIER, J. C., ROSS, B. M., CURRIE, R. W., ANGELIDIS, C. E., KAZLARIS, H., KOLLIAS, G. & PAGOULATOS, G. N. (1995) Transgenic mice expressing the human heat shock protein 70 have improved post-ischemic myocardial recovery. *J Clin Invest,* 95, 1854-60.

PRZYKLENK, K., ZHAO, L., KLONER, R. A. & ELLIOTT, G. T. (1996) Cardioprotection with ischemic preconditioning and MLA: role of adenosine-regulating enzymes? *Am J Physiol,* 271, H1004-14.

RAILSON, J. E., LAWRENCE, K., BUDDLE, J. C., PENNICA, D. & LATCHMAN, D. S. (2001) Heat shock protein-56 is induced by cardiotrophin-1 and mediates its hypertrophic effect. *J Mol Cell Cardiol,* 33, 1209-21.

RAILSON, J. E., LIAO, Z., BRAR, B. K., BUDDLE, J. C., PENNICA, D., STEPHANOU, A. & LATCHMAN, D. S. (2002) Cardiotrophin-1 and urocortin cause protection by the same pathway and hypertrophy via distinct pathways in cardiac myocytes. *Cytokine,* 17, 243-53.

RAVAGNAN, L., GURBUXANI, S., SUSIN, S. A., MAISSE, C., DAUGAS, E., ZAMZAMI, N., MAK, T., JAATTELA, M., PENNINGER, J. M., GARRIDO, C. & KROEMER, G. (2001) Heat-shock protein 70 antagonizes apoptosis-inducing factor. *Nat Cell Biol,* 3, 839-43.

READ, S. H., BALIGA, B. C., EKERT, P. G., VAUX, D. L. & KUMAR, S. (2002) A novel Apaf-1-independent putative caspase-2 activation complex. *J Cell Biol,* 159, 739-45.

REDFERN, C. H., DEGTYAREV, M. Y., KWA, A. T., SALOMONIS, N., COTTE, N., NANEVICZ, T., FIDELMAN, N., DESAI, K., VRANIZAN, K., LEE, E. K., COWARD, P., SHAH, N., WARRINGTON, J. A., FISHMAN, G. I., BERNSTEIN, D., BAKER, A. J. & CONKLIN, B. R. (2000) Conditional expression of a Gi-coupled receptor causes ventricular conduction delay and a lethal cardiomyopathy. *Proc Natl Acad Sci U S A,* 97, 4826-31.

RENOIR, J. M., RADANYI, C., FABER, L. E. & BAULIEU, E. E. (1990) The non-DNA-binding heterooligomeric form of mammalian steroid hormone receptors contains a hsp90-bound 59-kilodalton protein. *J Biol Chem,* 265, 10740-5.

REYES, T. M., LEWIS, K., PERRIN, M. H., KUNITAKE, K. S., VAUGHAN, J., ARIAS, C. A., HOGENESCH, J. B., GULYAS, J., RIVIER, J., VALE, W. W. & SAWCHENKO, P. E. (2001) Urocortin II: a member of the corticotropin-releasing factor (CRF) neuropeptide family that is selectively bound by type 2 CRF receptors. *Proc Natl Acad Sci U S A,* 98, 2843-8.

ROBERTSON, J. D., ENOKSSON, M., SUOMELA, M., ZHIVOTOVSKY, B. & ORRENIUS, S. (2002) Caspase-2 acts upstream of mitochondria to promote cytochrome c release during etoposide-induced apoptosis. *J Biol Chem,* 277, 29803-9.

ROBLEDO, O., FOURCIN, M., CHEVALIER, S., GUILLET, C., AUGUSTE, P., POUPLARD-BARTHELAIX, A., PENNICA, D. & GASCAN, H. (1997) Signaling of the cardiotrophin-1 receptor. Evidence for a third receptor component. *J Biol Chem,* 272, 4855-63.

ROSE-JOHN, S. & SCHOOLTINK, H. (2007) Cytokines are a therapeutic target for the prevention of inflammation-induced cancers. *Recent Results Cancer Res,* 174, 57-66.

ROSS, R. (1999) Atherosclerosis--an inflammatory disease. *N Engl J Med,* 340, 115-26.

ROSSANT, C. J., PINNOCK, R. D., HUGHES, J., HALL, M. D. & MCNULTY, S. (1999) Corticotropin-releasing factor type 1 and type 2alpha receptors regulate phosphorylation of calcium/cyclic adenosine 3',5'-monophosphate response element-binding protein and activation of p42/p44 mitogen-activated protein kinase. *Endocrinology,* 140, 1525-36.

ROTHEN-RUTISHAUSER, B. M., EHLER, E., PERRIARD, E., MESSERLI, J. M. & PERRIARD, J. C. (1998) Different behaviour of the non-sarcomeric cytoskeleton in neonatal and adult rat cardiomyocytes. *J Mol Cell Cardiol,* 30, 19-31.

ROTONDA, J., NICHOLSON, D. W., FAZIL, K. M., GALLANT, M., GAREAU, Y., LABELLE, M., PETERSON, E. P., RASPER, D. M., RUEL, R., VAILLANCOURT, J. P., THORNBERRY, N. A. & BECKER, J. W. (1996) The three-dimensional structure of apopain/CPP32, a key mediator of apoptosis. *Nat Struct Biol,* 3, 619-25.

RUDEL, T. & BOKOCH, G. M. (1997) Membrane and morphological changes in apoptotic cells regulated by caspase-mediated activation of PAK2. *Science,* 276, 1571-4.

RUFF, V. A., YEM, A. W., MUNNS, P. L., ADAMS, L. D., REARDON, I. M., DEIBEL, M. R., JR. & LEACH, K. L. (1992) Tissue distribution and cellular localization of hsp56, an FK506-binding protein. Characterization using a highly specific polyclonal antibody. *J Biol Chem,* 267, 21285-8.

RUWHOF, C. & VAN DER LAARSE, A. (2000) Mechanical stress-induced cardiac hypertrophy: mechanisms and signal transduction pathways. *Cardiovasc Res,* 47, 23-37.

SAMARDZIC, T., JANKOVIC, V., STOSIC-GRUJICIC, S. & TRAJKOVIC, V. (2001) STAT1 is required for iNOS activation, but not IL-6 production in murine fibroblasts. *Cytokine,* 13, 179-82.

SANCEAU, J., KAISHO, T., HIRANO, T. & WIETZERBIN, J. (1995) Triggering of the human interleukin-6 gene by interferon-gamma and tumor necrosis factor-alpha in monocytic cells involves cooperation between interferon regulatory factor-1, NF kappa B, and Sp1 transcription factors. *J Biol Chem,* 270, 27920-31.

SANCHEZ, E. R., FABER, L. E., HENZEL, W. J. & PRATT, W. B. (1990) The 56-59-kilodalton protein identified in untransformed steroid receptor complexes is a unique protein that exists in cytosol in a complex with both the 70- and 90-kilodalton heat shock proteins. *Biochemistry,* 29, 5145-52.

SANTHANAM, U., RAY, A. & SEHGAL, P. B. (1991) Repression of the interleukin 6 gene promoter by p53 and the retinoblastoma susceptibility gene product. *Proc Natl Acad Sci U S A,* 88, 7605-9.

SARKAR, S., LEAMAN, D. W., GUPTA, S., SIL, P., YOUNG, D., MOREHEAD, A., MUKHERJEE, D., RATLIFF, N., SUN, Y., RAYBORN, M., HOLLYFIELD, J. & SEN, S. (2004) Cardiac overexpression of myotrophin triggers myocardial hypertrophy and heart failure in transgenic mice. *J Biol Chem,* 279, 20422-34.

SCAFFIDI, C., SCHMITZ, I., KRAMMER, P. H. & PETER, M. E. (1999) The role of c-FLIP in modulation of CD95-induced apoptosis. *J Biol Chem,* 274, 1541-8.

SCARABELLI, T. M., PASINI, E., FERRARI, G., FERRARI, M., STEPHANOU, A., LAWRENCE, K., TOWNSEND, P., CHEN-SCARABELLI, C., GITTI, G., SARAVOLATZ, L., LATCHMAN, D., KNIGHT, R. A. & GARDIN, J. M. (2004) Warm blood cardioplegic arrest induces mitochondrial-mediated cardiomyocyte apoptosis associated with increased urocortin expression in viable cells. *J Thorac Cardiovasc Surg,* 128, 364-71.

SCARABELLI, T. M., PASINI, E., STEPHANOU, A., COMINI, L., CURELLO, S., RADDINO, R., FERRARI, R., KNIGHT, R. & LATCHMAN, D. S. (2002) Urocortin promotes hemodynamic and bioenergetic recovery and improves cell survival in the isolated rat heart exposed to ischemia/reperfusion. *J Am Coll Cardiol,* 40, 155-61.

SCHIENE, C. & FISCHER, G. (2000) Enzymes that catalyse the restructuring of proteins. *Curr Opin Struct Biol,* 10, 40-5.

SCHINDLER, C., FU, X. Y., IMPROTA, T., AEBERSOLD, R. & DARNELL, J. E., JR. (1992) Proteins of transcription factor ISGF-3: one gene encodes the 91-and 84-kDa ISGF-3 proteins that are activated by interferon alpha. *Proc Natl Acad Sci U S A,* 89, 7836-9.

SCHULMAN, D., LATCHMAN, D. S. & YELLON, D. M. (2002) Urocortin protects the heart from reperfusion injury via upregulation of p42/p44 MAPK signaling pathway. *Am J Physiol Heart Circ Physiol,* 283, H1481-8.

SCHURINGA, J. J., SCHEPERS, H., VELLENGA, E. & KRUIJER, W. (2001) Ser727-dependent transcriptional activation by association of p300 with STAT3 upon IL-6 stimulation. *FEBS Lett,* 495, 71-6.

SEARLE, J., KERR, J. F. & BISHOP, C. J. (1982) Necrosis and apoptosis: distinct modes of cell death with fundamentally different significance. *Pathol Annu,* 17 Pt 2, 229-59.

SEKIMOTO, T., NAKAJIMA, K., TACHIBANA, T., HIRANO, T. & YONEDA, Y. (1996) Interferon-gamma-dependent nuclear import of Stat1 is mediated by the GTPase activity of Ran/TC4. *J Biol Chem,* 271, 31017-20.

SEOL, D. W. & BILLIAR, T. R. (1999) A caspase-9 variant missing the catalytic site is an endogenous inhibitor of apoptosis. *J Biol Chem,* 274**,** 2072-6.

SHALL, S. & DE MURCIA, G. (2000) Poly(ADP-ribose) polymerase-1: what have we learned from the deficient mouse model? *Mutat Res,* 460**,** 1-15.

SHENG, Z., PENNICA, D., WOOD, W. I. & CHIEN, K. R. (1996) Cardiotrophin-1 displays early expression in the murine heart tube and promotes cardiac myocyte survival. *Development,* 122**,** 419-28.

SHIMOYAMA, M., HAYASHI, D., TAKIMOTO, E., ZOU, Y., OKA, T., UOZUMI, H., KUDOH, S., SHIBASAKI, F., YAZAKI, Y., NAGAI, R. & KOMURO, I. (1999) Calcineurin plays a critical role in pressure overload-induced cardiac hypertrophy. *Circulation,* 100**,** 2449-54.

SHUAI, K., ZIEMIECKI, A., WILKS, A. F., HARPUR, A. G., SADOWSKI, H. B., GILMAN, M. Z. & DARNELL, J. E. (1993) Polypeptide signalling to the nucleus through tyrosine phosphorylation of Jak and Stat proteins. *Nature,* 366**,** 580-3.

SIGMUND, C. D. (1993) Major approaches for generating and analyzing transgenic mice. An overview. *Hypertension,* 22**,** 599-607.

SINN, P. L., DAVIS, D. R. & SIGMUND, C. D. (1999) Highly regulated cell type-restricted expression of human renin in mice containing 140- or 160-kilobase pair P1 phage artificial chromosome transgenes. *J Biol Chem,* 274**,** 35785-93.

SIRONI, J. J. & OUCHI, T. (2004) STAT1-induced apoptosis is mediated by caspases 2, 3, and 7. *J Biol Chem,* 279**,** 4066-74.

SKRZYPIEC-SPRING, M., GROTTHUS, B., SZELAG, A. & SCHULZ, R. (2007) Isolated heart perfusion according to Langendorff---still viable in the new millennium. *J Pharmacol Toxicol Methods,* 55**,** 113-26.

SPEECHLY-DICK, M. E., GROVER, G. J. & YELLON, D. M. (1995) Does ischemic preconditioning in the human involve protein kinase C and the ATP-dependent K+ channel? Studies of contractile function after simulated ischemia in an atrial in vitro model. *Circ Res,* 77**,** 1030-5.

SPINA, M., MERLO-PICH, E., CHAN, R. K., BASSO, A. M., RIVIER, J., VALE, W. & KOOB, G. F. (1996) Appetite-suppressing effects of urocortin, a CRF-related neuropeptide. *Science,* 273**,** 1561-4.

SRINIVASULA, S. M., AHMAD, M., GUO, Y., ZHAN, Y., LAZEBNIK, Y., FERNANDES-ALNEMRI, T. & ALNEMRI, E. S. (1999) Identification of an endogenous dominant-negative short isoform of caspase-9 that can regulate apoptosis. *Cancer Res,* 59**,** 999-1002.

STEER, S. A., WIRSIG, K. C., CREER, M. H., FORD, D. A. & MCHOWAT, J. (2002) Regulation of membrane-associated iPLA2 activity by a novel PKC isoform in ventricular myocytes. *Am J Physiol Cell Physiol,* 283**,** C1621-6.

STENZEL, P., KESTERSON, R., YEUNG, W., CONE, R. D., RITTENBERG, M. B. & STENZEL-POORE, M. P. (1995) Identification of a novel murine receptor for corticotropin-releasing hormone expressed in the heart. *Mol Endocrinol,* 9**,** 637-45.

STEPHANOU, A. (2004) Role of STAT-1 and STAT-3 in ischaemia/reperfusion injury. *J Cell Mol Med,* 8, 519-25.

STEPHANOU, A., BRAR, B., HEADS, R., KNIGHT, R. D., MARBER, M. S., PENNICA, D. & LATCHMAN, D. S. (1998) Cardiotrophin-1 induces heat shock protein accumulation in cultured cardiac cells and protects them from stressful stimuli. *J Mol Cell Cardiol,* 30, 849-55.

STEPHANOU, A., BRAR, B., LIAO, Z., SCARABELLI, T., KNIGHT, R. A. & LATCHMAN, D. S. (2001a) Distinct initiator caspases are required for the induction of apoptosis in cardiac myocytes during ischaemia versus reperfusion injury. *Cell Death Differ,* 8, 434-5.

STEPHANOU, A., BRAR, B. K., SCARABELLI, T. M., JONASSEN, A. K., YELLON, D. M., MARBER, M. S., KNIGHT, R. A. & LATCHMAN, D. S. (2000) Ischemia-induced STAT-1 expression and activation play a critical role in cardiomyocyte apoptosis. *J Biol Chem,* 275, 10002-8.

STEPHANOU, A. & LATCHMAN, D. S. (2003) STAT-1: a novel regulator of apoptosis. *Int J Exp Pathol,* 84, 239-44.

STEPHANOU, A., OKOSI, A., KNIGHT, R. A., CHOWDREY, H. S. & LATCHMAN, D. S. (1997) C/EBP activates the human corticotropin-releasing hormone gene promoter. *Mol Cell Endocrinol,* 134, 41-50.

STEPHANOU, A., SCARABELLI, T. M., BRAR, B. K., NAKANISHI, Y., MATSUMURA, M., KNIGHT, R. A. & LATCHMAN, D. S. (2001b) Induction of apoptosis and Fas receptor/Fas ligand expression by ischemia/reperfusion in cardiac myocytes requires serine 727 of the STAT-1 transcription factor but not tyrosine 701. *J Biol Chem,* 276, 28340-7.

STEPHANOU, A., SCARABELLI, T. M., KNIGHT, R. A. & LATCHMAN, D. S. (2002) Antiapoptotic activity of the free caspase recruitment domain of procaspase-9: a novel endogenous rescue pathway in cell death. *J Biol Chem,* 277, 13693-9.

STEPHANOU, A., SCARABELLI, T. M., TOWNSEND, P. A., BELL, R., YELLON, D., KNIGHT, R. A. & LATCHMAN, D. S. (2002) The carboxyl-terminal activation domain of the STAT-1 transcription factor enhances ischemia/reperfusion-induced apoptosis in cardiac myocytes. *Faseb J,* 16, 1841-3.

SUSIN, S. A., LORENZO, H. K., ZAMZAMI, N., MARZO, I., SNOW, B. E., BROTHERS, G. M., MANGION, J., JACOTOT, E., COSTANTINI, P., LOEFFLER, M., LAROCHETTE, N., GOODLETT, D. R., AEBERSOLD, R., SIDEROVSKI, D. P., PENNINGER, J. M. & KROEMER, G. (1999) Molecular characterization of mitochondrial apoptosis-inducing factor. *Nature,* 397, 441-6.

SUZUKI, M., KOTAKE, K., FUJIKURA, K., INAGAKI, N., SUZUKI, T., GONOI, T., SEINO, S. & TAKATA, K. (1997) Kir6.1: a possible subunit of ATP-sensitive K+ channels in mitochondria. *Biochem Biophys Res Commun,* 241, 693-7.

TAI, P. K., MAEDA, Y., NAKAO, K., WAKIM, N. G., DUHRING, J. L. & FABER, L. E. (1986) A 59-kilodalton protein associated with progestin, estrogen, androgen, and glucocorticoid receptors. *Biochemistry,* 25, 5269-75.

TAKAHASHI, A., ALNEMRI, E. S., LAZEBNIK, Y. A., FERNANDES-ALNEMRI, T., LITWACK, G., MOIR, R. D., GOLDMAN, R. D., POIRIER, G. G., KAUFMANN, S. H. & EARNSHAW, W. C. (1996) Cleavage of lamin A by Mch2 alpha but not CPP32: multiple interleukin 1 beta-converting enzyme-related proteases with distinct substrate recognition properties are active in apoptosis. *Proc Natl Acad Sci U S A,* 93, 8395-400.

TAKANO, H., TANG, X. L. & BOLLI, R. (2000) Differential role of K(ATP) channels in late preconditioning against myocardial stunning and infarction in rabbits. *Am J Physiol Heart Circ Physiol,* 279, H2350-9.

TAKASHI, E., WANG, Y. & ASHRAF, M. (1999) Activation of mitochondrial K(ATP) channel elicits late preconditioning against myocardial infarction via protein kinase C signaling pathway. *Circ Res,* 85, 1146-53.

TAKEDA, K., YU, Z. X., NISHIKAWA, T., TANAKA, M., HOSODA, S., FERRANS, V. J. & KASAJIMA, T. (1996) Apoptosis and DNA fragmentation in the bulbus cordis of the developing rat heart. *J Mol Cell Cardiol,* 28, 209-15.

TALWAR, S., DOWNIE, P. F., SQUIRE, I. B., BARNETT, D. B., DAVIES, J. D. & NG, L. L. (1999) An immunoluminometric assay for cardiotrophin-1: a newly identified cytokine is present in normal human plasma and is increased in heart failure. *Biochem Biophys Res Commun,* 261, 567-71.

TANAKA, M., ITO, H., ADACHI, S., AKIMOTO, H., NISHIKAWA, T., KASAJIMA, T., MARUMO, F. & HIROE, M. (1994) Hypoxia induces apoptosis with enhanced expression of Fas antigen messenger RNA in cultured neonatal rat cardiomyocytes. *Circ Res,* 75, 426-33.

TEN HOEVE, J., DE JESUS IBARRA-SANCHEZ, M., FU, Y., ZHU, W., TREMBLAY, M., DAVID, M. & SHUAI, K. (2002) Identification of a nuclear Stat1 protein tyrosine phosphatase. *Mol Cell Biol,* 22, 5662-8.

TERUI, K., HIGASHIYAMA, A., HORIBA, N., FURUKAWA, K. I., MOTOMURA, S. & SUDA, T. (2001) Coronary vasodilation and positive inotropism by urocortin in the isolated rat heart. *J Endocrinol,* 169, 177-83.

THOMAS, M., FINNEGAN, C. E., ROGERS, K. M., PURCELL, J. W., TRIMBLE, A., JOHNSTON, P. G. & BOLAND, M. P. (2004) STAT1: a modulator of chemotherapy-induced apoptosis. *Cancer Res,* 64, 8357-64.

THORNBERRY, N. A., BULL, H. G., CALAYCAY, J. R., CHAPMAN, K. T., HOWARD, A. D., KOSTURA, M. J., MILLER, D. K., MOLINEAUX, S. M., WEIDNER, J. R., AUNINS, J. & ET AL. (1992) A novel heterodimeric cysteine protease is required for interleukin-1 beta processing in monocytes. *Nature,* 356, 768-74.

THORNBERRY, N. A. & LAZEBNIK, Y. (1998) Caspases: enemies within. *Science,* 281, 1312-6.

TOTH, A., JEFFERS, J. R., NICKSON, P., MIN, J. Y., MORGAN, J. P., ZAMBETTI, G. P. & ERHARDT, P. (2006a) Targeted deletion of Puma attenuates cardiomyocyte death and improves cardiac function during ischemia-reperfusion. *Am J Physiol Heart Circ Physiol,* 291**,** H52-60.

TOTH, A., NICKSON, P., QIN, L. L. & ERHARDT, P. (2006b) Differential regulation of cardiomyocyte survival and hypertrophy by MDM2, an E3 ubiquitin ligase. *J Biol Chem,* 281**,** 3679-89.

TOWNSEND, P. A., DAVIDSON, S. M., CLARKE, S. J., KHALIULIN, I., CARROLL, C. J., SCARABELLI, T. M., KNIGHT, R. A., STEPHANOU, A., LATCHMAN, D. S. & HALESTRAP, A. P. (2007) Urocortin prevents mitochondrial permeability transition in response to reperfusion injury indirectly, by reducing oxidative stress. *Am J Physiol Heart Circ Physiol.*

TOWNSEND, P. A., SCARABELLI, T. M., DAVIDSON, S. M., KNIGHT, R. A., LATCHMAN, D. S. & STEPHANOU, A. (2004a) STAT-1 interacts with p53 to enhance DNA damage-induced apoptosis. *J Biol Chem,* 279**,** 5811-20.

TOWNSEND, P. A., SCARABELLI, T. M., PASINI, E., GITTI, G., MENEGAZZI, M., SUZUKI, H., KNIGHT, R. A., LATCHMAN, D. S. & STEPHANOU, A. (2004b) Epigallocatechin-3-gallate inhibits STAT-1 activation and protects cardiac myocytes from ischemia/reperfusion-induced apoptosis. *Faseb J,* 18**,** 1621-3.

TRANGUCH, S., CHEUNG-FLYNN, J., DAIKOKU, T., PRAPAPANICH, V., COX, M. B., XIE, H., WANG, H., DAS, S. K., SMITH, D. F. & DEY, S. K. (2005) Cochaperone immunophilin FKBP52 is critical to uterine receptivity for embryo implantation. *Proc Natl Acad Sci U S A,* 102**,** 14326-31.

TURNBULL, A. V., VALE, W. & RIVIER, C. (1996) Urocortin, a corticotropin-releasing factor-related mammalian peptide, inhibits edema due to thermal injury in rats. *Eur J Pharmacol,* 303**,** 213-6.

UDDIN, S., SASSANO, A., DEB, D. K., VERMA, A., MAJCHRZAK, B., RAHMAN, A., MALIK, A. B., FISH, E. N. & PLATANIAS, L. C. (2002) Protein kinase C-delta (PKC-delta) is activated by type I interferons and mediates phosphorylation of Stat1 on serine 727. *J Biol Chem,* 277**,** 14408-16.

VALE, W., SPIESS, J., RIVIER, C. & RIVIER, J. (1981) Characterization of a 41-residue ovine hypothalamic peptide that stimulates secretion of corticotropin and beta-endorphin. *Science,* 213**,** 1394-7.

VARFOLOMEEV, E. E., SCHUCHMANN, M., LURIA, V., CHIANNILKULCHAI, N., BECKMANN, J. S., METT, I. L., REBRIKOV, D., BRODIANSKI, V. M., KEMPER, O. C., KOLLET, O., LAPIDOT, T., SOFFER, D., SOBE, T., AVRAHAM, K. B., GONCHAROV, T., HOLTMANN, H., LONAI, P. & WALLACH, D. (1998) Targeted disruption of the mouse Caspase 8 gene ablates cell death induction by the TNF receptors, Fas/Apo1, and DR3 and is lethal prenatally. *Immunity,* 9**,** 267-76.

VAUGHAN, J., DONALDSON, C., BITTENCOURT, J., PERRIN, M. H., LEWIS, K., SUTTON, S., CHAN, R., TURNBULL, A. V., LOVEJOY, D., RIVIER, C. & ET AL. (1995) Urocortin, a mammalian neuropeptide related to fish urotensin I and to corticotropin-releasing factor. *Nature,* 378**,** 287-92.

VENKATAPURAM, S., WANG, C., KROLIKOWSKI, J. G., WEIHRAUCH, D., KERSTEN, J. R., WARLTIER, D. C., PRATT, P. F., JR. & PAGEL, P. S. (2006) Inhibition of apoptotic protein p53 lowers the threshold of isoflurane-induced cardioprotection during early reperfusion in rabbits. *Anesth Analg,* 103, 1400-5.

VERMES, I., HAANEN, C., STEFFENS-NAKKEN, H. & REUTELINGSPERGER, C. (1995) A novel assay for apoptosis. Flow cytometric detection of phosphatidylserine expression on early apoptotic cells using fluorescein labelled Annexin V. *J Immunol Methods,* 184, 39-51.

WAIBOCI, L. W., AHMED, C. M., MUJTABA, M. G., FLOWERS, L. O., MARTIN, J. P., HAIDER, M. I. & JOHNSON, H. M. (2007) Both the suppressor of cytokine signaling 1 (SOCS-1) kinase inhibitory region and SOCS-1 mimetic bind to JAK2 autophosphorylation site: implications for the development of a SOCS-1 antagonist. *J Immunol,* 178, 5058-68.

WANG, P., CHEN, H., QIN, H., SANKARAPANDI, S., BECHER, M. W., WONG, P. C. & ZWEIER, J. L. (1998) Overexpression of human copper, zinc-superoxide dismutase (SOD1) prevents postischemic injury. *Proc Natl Acad Sci U S A,* 95, 4556-60.

WATERHOUSE, N. J. & TRAPANI, J. A. (2002) CTL: Caspases Terminate Life, but that's not the whole story. *Tissue Antigens,* 59, 175-83.

WEBSTER, K. A., DISCHER, D. J., KAISER, S., HERNANDEZ, O., SATO, B. & BISHOPRIC, N. H. (1999) Hypoxia-activated apoptosis of cardiac myocytes requires reoxygenation or a pH shift and is independent of p53. *J Clin Invest,* 104, 239-52.

WESTPHAL, N. J. & SEASHOLTZ, A. F. (2006) CRH-BP: the regulation and function of a phylogenetically conserved binding protein. *Front Biosci,* 11, 1878-91.

WHITEHURST, R. M., JR., ZHANG, M., BHATTACHARJEE, A. & LI, M. (1999) Dexamethasone-induced hypertrophy in rat neonatal cardiac myocytes involves an elevated L-type Ca(2+)current. *J Mol Cell Cardiol,* 31, 1551-8.

WIDSCHWENDTER, A., TONKO-GEYMAYER, S., WELTE, T., DAXENBICHLER, G., MARTH, C. & DOPPLER, W. (2002) Prognostic significance of signal transducer and activator of transcription 1 activation in breast cancer. *Clin Cancer Res,* 8, 3065-74.

WILLIAMS, R. S. & WAGNER, P. D. (2000) Transgenic animals in integrative biology: approaches and interpretations of outcome. *J Appl Physiol,* 88, 1119-26.

WOLLERT, K. C., TAGA, T., SAITO, M., NARAZAKI, M., KISHIMOTO, T., GLEMBOTSKI, C. C., VERNALLIS, A. B., HEATH, J. K., PENNICA, D., WOOD, W. I. & CHIEN, K. R. (1996) Cardiotrophin-1 activates a distinct form of cardiac muscle cell hypertrophy. Assembly of sarcomeric units in series VIA gp130/leukemia inhibitory factor receptor-dependent pathways. *J Biol Chem,* 271, 9535-45.

WOO, M., HAKEM, R., SOENGAS, M. S., DUNCAN, G. S., SHAHINIAN, A., KAGI, D., HAKEM, A., MCCURRACH, M., KHOO, W., KAUFMAN, S. A., SENALDI, G.,

HOWARD, T., LOWE, S. W. & MAK, T. W. (1998) Essential contribution of caspase 3/CPP32 to apoptosis and its associated nuclear changes. *Genes Dev,* 12, 806-19.

WOZNIAK, R. W., ROUT, M. P. & AITCHISON, J. D. (1998) Karyopherins and kissing cousins. *Trends Cell Biol,* 8, 184-8.

WU, M., XU, L. G., LI, X., ZHAI, Z. & SHU, H. B. (2002) AMID, an apoptosis-inducing factor-homologous mitochondrion-associated protein, induces caspase-independent apoptosis. *J Biol Chem,* 277, 25617-23.

XIE, Z., KOYAMA, T., ABE, K., FUJI, Y., SAWA, H. & NAGTASHIMA, K. (2000) Upregulation of P53 protein in rat heart subjected to a transient occlusion of the coronary artery followed by reperfusion. *Jpn J Physiol,* 50, 159-62.

YAMADA, S., SHIONO, S., JOO, A. & YOSHIMURA, A. (2003) Control mechanism of JAK/STAT signal transduction pathway. *FEBS Lett,* 534, 190-6.

YAMAUCHI-TAKIHARA, K., IHARA, Y., OGATA, A., YOSHIZAKI, K., AZUMA, J. & KISHIMOTO, T. (1995) Hypoxic stress induces cardiac myocyte-derived interleukin-6. *Circulation,* 91, 1520-4.

YAN, S. F., ZOU, Y. S., MENDELSOHN, M., GAO, Y., NAKA, Y., DU YAN, S., PINSKY, D. & STERN, D. (1997) Nuclear factor interleukin 6 motifs mediate tissue-specific gene transcription in hypoxia. *J Biol Chem,* 272, 4287-94.

YAOITA, H., OGAWA, K., MAEHARA, K. & MARUYAMA, Y. (1998) Attenuation of ischemia/reperfusion injury in rats by a caspase inhibitor. *Circulation,* 97, 276-81.

YASUKAWA, H., SASAKI, A. & YOSHIMURA, A. (2000) Negative regulation of cytokine signaling pathways. *Annu Rev Immunol,* 18, 143-64.

YE, H., CANDE, C., STEPHANOU, N. C., JIANG, S., GURBUXANI, S., LAROCHETTE, N., DAUGAS, E., GARRIDO, C., KROEMER, G. & WU, H. (2002) DNA binding is required for the apoptogenic action of apoptosis inducing factor. *Nat Struct Biol,* 9, 680-4.

YELLON, D. M. & BAXTER, G. F. (1995) A "second window of protection" or delayed preconditioning phenomenon: future horizons for myocardial protection? *J Mol Cell Cardiol,* 27, 1023-34.

YEM, A. W., TOMASSELLI, A. G., HEINRIKSON, R. L., ZURCHER-NEELY, H., RUFF, V. A., JOHNSON, R. A. & DEIBEL, M. R., JR. (1992) The Hsp56 component of steroid receptor complexes binds to immobilized FK506 and shows homology to FKBP-12 and FKBP-13. *J Biol Chem,* 267, 2868-71.

YOSHIMURA, A., NAKA, T. & KUBO, M. (2007) SOCS proteins, cytokine signalling and immune regulation. *Nat Rev Immunol,* 7, 454-65.

YU, S. W., WANG, H., POITRAS, M. F., COOMBS, C., BOWERS, W. J., FEDEROFF, H. J., POIRIER, G. G., DAWSON, T. M. & DAWSON, V. L. (2002) Mediation of poly(ADP-ribose) polymerase-1-dependent cell death by apoptosis-inducing factor. *Science,* 297, 259-63.

YUE, T. L., WANG, C., GU, J. L., MA, X. L., KUMAR, S., LEE, J. C., FEUERSTEIN, G. Z., THOMAS, H., MALEEFF, B. & OHLSTEIN, E. H. (2000) Inhibition of extracellular signal-regulated kinase enhances Ischemia/Reoxygenation-induced apoptosis in cultured cardiac myocytes and exaggerates reperfusion injury in isolated perfused heart. *Circ Res,* 86, 692-9.

ZEBROWSKI, D. C., ALCENDOR, R. R., KIRSHENBAUM, L. A. & SADOSHIMA, J. (2006) Caspase-3 mediated cleavage of MEKK1 promotes p53 transcriptional activity. *J Mol Cell Cardiol,* 40, 605-618.

ZHANG, C. L., MCKINSEY, T. A., CHANG, S., ANTOS, C. L., HILL, J. A. & OLSON, E. N. (2002) Class II histone deacetylases act as signal-responsive repressors of cardiac hypertrophy. *Cell,* 110, 479-88.

ZHANG, J. J., VINKEMEIER, U., GU, W., CHAKRAVARTI, D., HORVATH, C. M. & DARNELL, J. E., JR. (1996) Two contact regions between Stat1 and CBP/p300 in interferon gamma signaling. *Proc Natl Acad Sci U S A,* 93, 15092-6.

ZHANG, J. J., ZHAO, Y., CHAIT, B. T., LATHEM, W. W., RITZI, M., KNIPPERS, R. & DARNELL, J. E., JR. (1998) Ser727-dependent recruitment of MCM5 by Stat1alpha in IFN-gamma-induced transcriptional activation. *Embo J,* 17, 6963-71.

ZOLK, O., NG, L. L., O'BRIEN, R. J., WEYAND, M. & ESCHENHAGEN, T. (2002) Augmented expression of cardiotrophin-1 in failing human hearts is accompanied by diminished glycoprotein 130 receptor protein abundance. *Circulation,* 106, 1442-6.